HIGHWAY SIGN SUPPORT STRUCTURES

VOLUME 2

WIND LOADS ON ROADSIDE SIGNS

Final Report

of

PROJECT HPR-2(104), CONTRACT NO. CPR-11-3550
HIGHWAY SIGN SUPPORT RESEARCH

AREA III REDUCTION OF WIND LOADS

TEXAS TRANSPORTATION INSTITUTE
TEXAS A&M UNIVERSITY
COLLEGE STATION, TEXAS

JULY 1967

FOREWORD

The information contained herein was developed on Research Project HPR-2(104), entitled "Highway Sign Support Research," which was a pooled fund research project sponsored jointly by the U. S. Department of Transportation, Federal Highway Administration, Bureau of Public Roads, and the following highway departments: Alabama, California, Illinois, Kansas, Louisiana, Minnesota, Mississippi, Nebraska, North Dakota, Oklahoma, South Dakota, Tennessee, Texas, and the District of Columbia.

The results of this Research Project have been reported in three separate volumes, each concerning itself with a specific area of investigation as follows:

VOLUME 1	BREAK-AWAY ROADSIDE SIGN SUPPORT STRUCTURES
VOLUME 2	WIND LOADS ON ROADSIDE SIGNS
VOLUME 3	FEASIBILITY STUDY OF IMPACT ATTENUATION OR PROTECTIVE DEVICES FOR FIXED HIGHWAY OBSTACLES

Each volume is complete within itself, presenting the objectives, work done, conclusions, and recommendations.

The Contract Manager of this project was R. F. Baker of the Office of Research and Development, Bureau of Public Roads. A Policy Committee composed of engineers from the various participating highway departments and the Bureau of Public Roads was established to represent the participating agencies to (1) insure that the contractor would be responsive to the desires of the cooperating highway agencies, (2) provide a means for keeping all parties informed of progress and action on the subject, and

(3) provide adequate liaison between the technical personnel on the project and those of the technical staff of the Bureau of Public Roads and the participating agencies to insure the success of the work and its early acceptance.

This Policy Committee was composed of the following members and alternates.

Chairman: T. S. Huff

Vice Chairman: J. E. Wilson

Secretary: M. D. Shelby (ex officio)

STATE	MEMBER	ALTERNATE
Alabama	J. F. Tribble	F. L. Holman
California	J. E. Wilson	J. L. Beaton
Illinois	J. E. Burke	V. E. Staff
Kansas	R. L. Anderson	J. D. McNeal
Louisiana	V. Adam	W. T. Taylor, Jr.
Minnesota	F. C. Marshall	G. Carlson
Mississippi	A. M. White	S. Q. Kidd
Nebraska	A. H. Dederman	R. L. Meyer
North Dakota	V. Zink	G. J. Stelzmiller
Oklahoma	B. C. Hartronft	
South Dakota	P. A. Hoffman	R. S. O'Neill
Tennessee	L. E. Hinds	H. M. Brooks
Texas	T. S. Huff	R. L. Lewis
District of Columbia	F. W. Ellerman	
Bureau of Public Roads	A. Taragin	C. F. Scheffey

In addition, a Technical Subcommittee was established to provide continuous and critical review of the progress of the work. This committee was selected by the Policy Committee and was composed of engineers with special technical competence and ability to contribute to the success of the project and implementation of its findings. The members of the Technical Subcommittee were as follows:

Chairman: T. S. Huff

Secretary: M. D. Shelby (ex officio)

STATE	MEMBER
California	J. L. Beaton
Kansas	R. L. Anderson
Louisiana	W. T. Taylor, Jr.
Tennessee	L. E. Hinds
Texas	T. S. Huff

The opinions, findings and conclusions expressed in this report are those of the authors and not necessarily those of the Bureau of Public Roads.

ACKNOWLEDGEMENTS

This project was conducted by the Texas Transportation Institute, C. J. Keese, Director, through the Texas A&M Research Foundation, Fred J. Benson, Vice President. The work was accomplished through combined efforts of the Structural Research Department, T. J. Hirsch, Head, and the Highway Design and Traffic Department, Charles Pinnell, Head.

The organization of the research team in responsible charge for accomplishing the objectives of the research was under the Co-Directorship of R. M. Olson (Structures) and Neilon J. Rowan (Highway Design and Traffic). The three specific research efforts were under the supervision of three research area supervisors as follows:

Area I	Sign Support Structures Thomas C. Edwards, Supervisor
Area II	Protective Devices Peter D. Weiner, Supervisor
Area III	Reduction of Wind Loads Hayes E. Ross, Jr. , Supervisor

In addition to the research area supervisors, a support group under the supervision of Thomas Williams and James Mahle provided purchasing, procurement, fabrication, and test installation services.

James Bradley supervised the photographic coverage of all crash tests and assisted Rowan and Olson in the preparation of the 16 mm sound movie summarizing the results of the Break-Away Roadside Sign Research.

Mrs. Diantha Langley was in charge of data reduction and processing from the high speed movie film records and oscillogram records from all

crash tests. Mrs. Langley also made significant contributions in preparing this final report by documenting crash tests with selected photographs and tabulated data.

Electronic instrumentation, including transducers, recorders, and other devices was accomplished by A. M. Gaddis, Gerald Clark, James Byram, and Monroe White.

The typing and preparation of the manuscript for this report was accomplished by Mrs. Ruth DeShaw and Mrs. Sylvia Velasco.

M. D. Shelby, Research Engineer of TTI, was Secretary (ex officio) of both the Project Policy Committee and Technical Subcommittee and worked tirelessly in coordinating the efforts of the researchers in response to the requirements of the sponsoring agencies.

Charles F. Scheffey, Chief of Structures and Applied Mechanics Division, Office of Research and Development, BPR, is due particular acknowledgement for the many hours spent in counseling the researchers concerning the technical aspects of this research. His advice and counsel based on many years of experience were invaluable to the researchers.

The suggestions and encouragement of A. C. Taylor, Regional Engineer, Bureau of Public Roads, were a continuing source of inspiration which are sincerely and gratefully acknowledged.

Last, but not least, the significant contributions of Leon Hawkins, Texas Highway Department Engineer, are acknowledged. Mr. Hawkins deserves credit for developing the original concept and design of the break-away base for use on cantilever type roadside signs. From the beginning and throughout this project, Mr. Hawkins has worked closely with the researchers of TTI offering his technical and practical advice concerning the development

and implementation of the break-away design concept. He supervised the preparation and revision of standards for design and installation of the many break-away signs now installed along Texas highways. He has worked tirelessly in collecting information concerning the behavior and performance of sign installations in Texas.

A distinguishing characteristic of this research study has been the activities of the Project Policy Committee, whose interest in the primary objective of eliminating roadside hazards, and whose examination of the detailed information developed in this investigation, has proven invaluable to the research staff. It is believed that the liaison between the practicing engineers and the researchers during this investigation has resulted in a clearer understanding of the nature of the hazard and its elimination through a cooperative research effort. It is apparent that the elapsed time between research investigation and field application has been substantially reduced by the continuing deliberations of the Project Policy Committee.

TABLE OF CONTENTS

TABLE OF CONTENTS (Continued)

TABLE OF CONTENTS (Continued)

LIST OF FIGURES

LIST OF TABLES

NOTATION

A = Useful life (years)

A_c = Cross-sectional area ($in.^2$)

AR = Aspect ratio

A_s = Area of sign ($ft.^2$)

B = Replacement factor

C_I = Initial cost of sign (general) (dollars)

C_{Ip} = Initial cost, present sign (dollars)

C_L = Lift-force coefficient

C_{MP} = Pitching-moment coefficient

C_{mp} = Maintenance cost (dollars)

C_{MR} = Rolling-moment coefficient

C_{MT} = Twisting-moment coefficient

C_N = Normal-force coefficient

C_R = Replacement cost of sign (general) (dollars)

C_{RP} = Replacement cost, present sign (dollars)

C_s = Salvage value of sign (general) (dollars)

C_{sp} = Salvage value, present sign (dollars)

C_T = Side-force coefficient

C_t = Total cost of sign (general) (dollars)

C_{tp} = Total cost, present sign (dollars)

D = Drag force in "wind tunnel" axes, (lb.)

f = Load characteristic factor

F_L = Lift force in "sign" axes (lb.)

F_N = Normal force in "sign" axes (lb.)

F_T = Side force in "sign" axes (lb.)

F(X) = Probability factor

I = Interest rate (percent)

K_1 = Salvage factor of sign (general)

K_2 = Salvage factor, present sign

K_P = Maintenance factor

L = Lift force in "wind tinnel" axes, (lb.)

L_Y = Horizontal location of normal force, (in.)

L_Z = Vertical location of normal force, (in.)

M_P = Pitching moment in "sign" axes, (in.-lb.)

M_p = Pitching moment in "wind tunnel" axes, (in.-lb.)

M_R = Rolling moment in "sign" axes (in.-lb.)

M_r = Rolling moment in "wind tunnel" axes (in.-lb.)

M_T = Twisting moment in "sign" axes (in.-lb.)

M_y = Yawing moment in "wind tunnel" axes (in.-lb.)

q = Impact pressure ($lb./ft.^2$)

R = Design life (general) (years)

r = Reduction in size (percent)

R_E = Reynolds number

R_P = Present design life (years)

S = Side force in "wind tunnel" axes, (lb.)

V = Wind velocity (mph)

V_1 = Mean 2-year wind speed (mph)

V_2 = Mean 50-year wind speed (mph)

Z = Ratio of reduced design cost to present design cost

z = Section modulus ($in.^3$)

Z_r = Reduction in present design cost (percent)

α = Angle of attack (degrees)

θ = Louver angle (degrees)

θ' = Effective louver angle (degrees)

θ_S = Sign angle (degrees)

θ_W = Wind angle (degrees)

ν = Kinematic viscosity ($ft.^2/sec.$)

ϕ = Cost function

ψ = Rotation angle (degrees)

ρ = Mass density of air ($lb.\text{-}sec.^2/ft.^4$)

CHAPTER 1

GENERAL DESCRIPTION OF STUDY

1.1 Need for the Study

The development of the modern interstate freeway system has been accompanied by the need for an adequate signing system to warn and inform the motorist. The dimension of the sign, its message, and location must be such that the motorist will have time to take necessary actions. Often a large sign is required and massive supports are needed to resist wind loads. The large supports, in turn, present a hazard to the motorist since the sign is usually placed in close proximity to the road's edge.

An obvious means of reducing this hazard would be the relocation of the sign at a safer distance from the roadway. The "break-away" post[1*] that disengages from its foundation upon impact also offers a safe configuration.

The two means just indicated of reducing this roadside hazard cannot always be employed. In any case, if the wind loads used in designing a sign are excessive and can be reduced, the stiffness and mass of the structure can be reduced. Such changes in the sign structure could prove beneficial to the travelling public from the viewpoint of safety.

1.2 Objectives

The basic objectives of this study were as follows:

1. To substantiate existing wind load design criteria[2] on conventional highway signs, or provide a basis for revisions to the criteria.

---

*Superscripts indicate corresponding items in the References.

2. To establish design criteria for sign backgrounds having reduced wind resistance characteristics.

3. To investigate the economic and safety aspects of a sign as a function of the frequency of occurrence of design winds.

4. To compare the economic and safety aspects of the conventional solid background sign with the experimental non-solid background sign and arrive at a recommended design.

1.3 Literature Review

Wind load studies of flat plates have been conducted since the middle of the 19th Century. Some of the earlier methods used in testing the plates were rather crude by present standards. For example, Eiffel,[3] during the initial stages of his tests, dropped plates from towers and observed the changes in velocity and forces on the plates. Other investigators mounted the plates on moving vehicles.

Eiffel was also among the first to conduct wind tunnel tests on flat plates. Stanton[4] utilized a wind tunnel for most of his wind load studies of plates. He was the first to take accurate pressure readings across a plate. He also gave a firm proof that the maximum resultant force on a plate does not always occur when the plate is normal to the direction of flow. Winter[5] and Tidwell[6] are two of the more recent investigators of wind loads on plates.

Figure 1.3.1 shows the results of some of the above mentioned studies for a plate with a height to width ratio equal to 1 (square plate). It is obvious that differences exist in the results. These differences are attributed to several factors, some of which are:

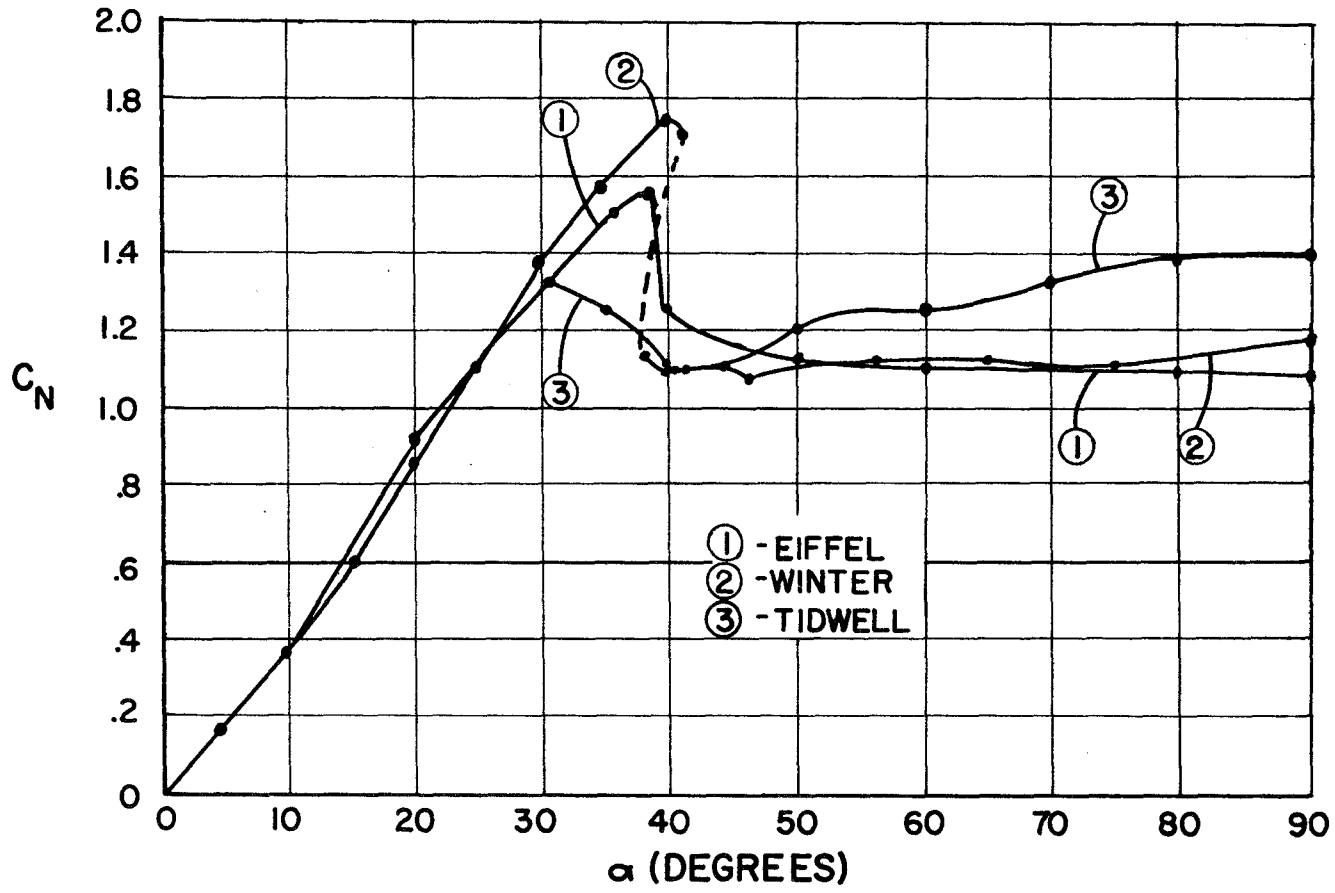

FIGURE 1.3.1 NORMAL FORCE COEFFICIENT VERSUS ANGLE OF ATTACK FOR A SQUARE FLAT PLATE

1. Model size - The area of the models used in these tests ranged from three square inches to four square feet.

2. Method of testing - As mentioned previously, some of the earlier methods were crude, which would include the earlier wind tunnel tests.

3. Manner in which the model was supported - The methods used to support these models during wind load tests varied. Some were supported by wires, while others were mounted on rigid fixtures.

However, regardless of the differences in these tests, the fact remains that practically all of the plates tested were small in area. The majority of the tests were also conducted under ideal conditions, i.e., a controlled environment, such as uniform flow in a wind tunnel. These questions then arise: (1) Are the wind loads on plates (or signs) a function of size? (2) To what extent does the natural environment influence the wind loads as opposed to an ideal one? (3) Can wind tunnel tests of sign models be used to determine wind loads on larger signs?

In searching the literature only one instance of tests on large plates was found, that by Stanton[7] in 1907. Stanton tested three plates which had height to width dimensions of ten feet by ten feet, ten feet by five feet, and five feet by five feet. His method of testing these plates, although good for that time period, are now considered to be inadequate and the validity of his results is in question.

The criteria now being used for wind loads on signs were deter-

mined by use of the previously referenced material and by wind tunnel tests similar to those mentioned in the references. It is therefore desirable that more accurate and up-to-date information be gained on this subject.

Research in the area of non-solid signs has been very limited. The only literature available on non-solid sign backgrounds specifically is that of Tidwell and Samson.[8] In their study, several types of non-solid configurations were tested, e.g., expanded metals, honeycomb materials and louvered signs. Of the types tested, the "louvered" configuration appeared to offer the greatest promise from the standpoint of wind load reducing capabilities and visibility. The louvered model was constructed with 0.052 inch thick louvers spaced at one-inch intervals at an angle of 30 degrees with the horizontal. When compared with a flat plate, the louvered model showed a 57% reduction in maximum force and an 83% reduction in twisting moment. It also provides a solid appearance when the louvers are properly spaced.

A literature survey of topics within the aerodynamics field revealed that a very limited amount of information exists which could be applied to the investigation of wind loads on flat plate louvers. Previous work in the area of louvers (or cascaded airfoils) has, for the most part, been directed toward turbine or axial compressor applications.[9] In most of these cases, the cascades were smooth airfoil shapes and were orientated at small angles of attack (less than 10^{o}), in which case the air flow over and under the cascade does not separate. For the flat plate cascades (as in the louvered sign) the air flow will separate for all but the smaller angles of attack (about 15^{o} or less).

When the flow separates a region of low pressure air forms behind the plate and the drag force, which is parallel to the direction of flow, increases appreciably. The theoretical and empirical equations which describe the forces on a body subjected to non-separated flow are not applicable to the separated case. In fact, no theory exists which does justice to experimental results of drag on a body subjected to separated flow.

Following a literature survey, it became apparent that little has been done in the area of optimal sign design as a function of the frequency of occurrence of design winds. The lack of research in this field is attributed to the heretofore absence of reliable extreme wind velocity distribution data. In the past, methods used by the United States Weather Bureau in recording wind data were inconsistent. Many of the stations were located in cities where the surrounding buildings greatly influenced the recorded data. In more recent years, the stations have been moved to areas of more uniform exposures, usually airports. As a result, more reliable wind data is now available.

Thom[10] has made use of the more recent wind velocity data in arriving at distributions of extreme winds in the United States. In his study, information was gleaned from 141 open-country stations, with a cumulative total of about 1700 years of records averaging about 15 years per station, and, through statistical analysis, extreme wind velocity distributions were determined.

1.4 Methods of Research

In order to meet the objectives outlined, the following general

procedures were followed.

Wind loads on conventional signs. A full-scale sign, ten feet by ten feet in size was built and instrumented for use in determining wind loads on a typical sign when subjected to field conditions, i.e., its natural environment. The details of the sign appear in Figures 2.1.1 and 2.1.2. Some of the more important features of this sign are described below.

(a) In general, six actions are necessary to describe the effects of wind acting on a body. These actions are shown in Figure 1.4.1. However, for a flat, rectangular, solid background sign, three of these actions will sufficiently describe the wind effects, namely, side and normal force and twisting moment. The other three actions are negligible. Thus, the support was instrumented with five full electric strain gage bridges for use in determining the side and normal forces and the twisting moment on the sign.

(b) The single tubular support was a statically determinate structure. This feature was advantageous from an instrumentation standpoint since the loads have but one path after entering the support. Initially in the full-scale studies, an attempt was made to use a two-post, statically indeterminant, cantilevered, instrumented sign mounted on a trailer for movement to and from the test site. However, it was discovered that any movement of the sign and trailer caused an unknown amount of load shift within the instrumented supports, resulting in a loss of the zero or no load reference on the instrumentation. With the single support this problem was eliminated.

(c) With the flanged connection at the base of the tubular support

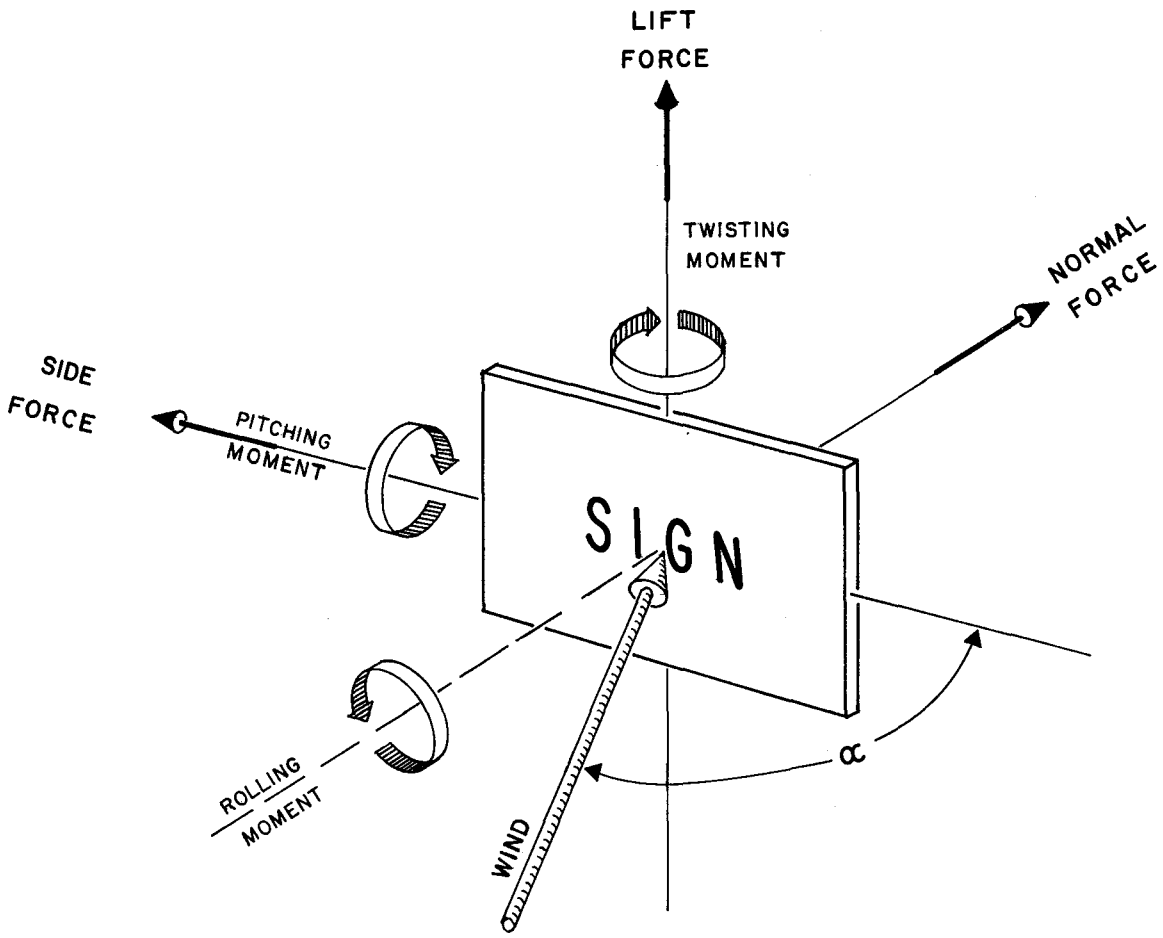

FIGURE 1.4.1 **WIND ACTIONS ON SIGN**

the sign could be rotated in 22.5 degree increments allowing for a semi-controlled environment.

(d) The wind loads on a sign with a single tubular support are believed to be of the same order of magnitude as those on signs with two or more supports. The test results would, therefore, be applicable to other support configurations.

The sign was placed on a remote site of the Texas Transportation Institute's Safety Proving Grounds, as shown in Figure 1.4.2. The site was free of any large obstructions for several hundred feet in all directions, allowing the wind a relatively undisturbed path to the sign.

The twisting moment was measured directly with the strain gage instrumentation used. However, in determining the normal force a basic principle of beam theory was used, i.e., the shear in a beam at a point equals the change in moment with respect to a differential length. If the shear is constant, the change in moment can be measured over a finite length, and in the present case it was assumed that the shear is constant after entering the instrumented portion of the tubular support. The bending moment at two different elevations of the tubular support was measured directly by strain gages. The normal force was then computed by dividing the difference in the two moments by the length between the two gages. The side force was determined in the same fashion.

Figure 1.4.3 shows the basic equipment employed in conducting the tests, i.e., the instrumented sign, the wind speed and direction indicators, a mobile instrumentation laboratory, and a portable generator for supplying the electrical power. The mobile instrumentation laboratory

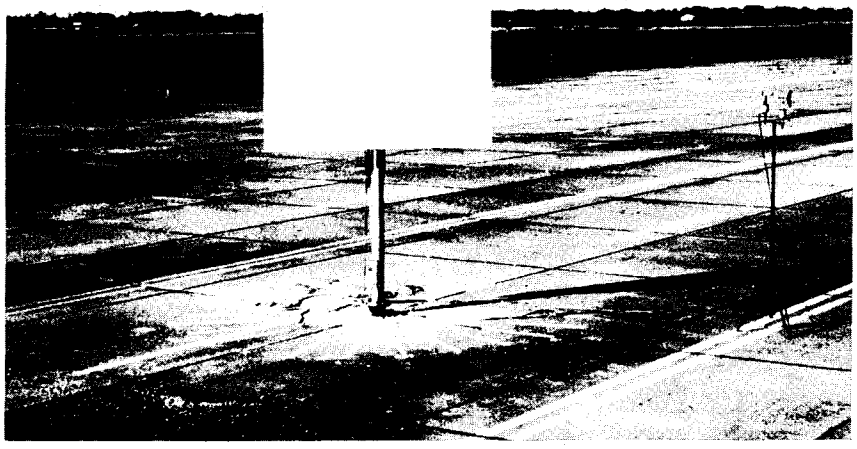

FIGURE 1.4.2 FULL-SCALE SIGN ON TEST SITE

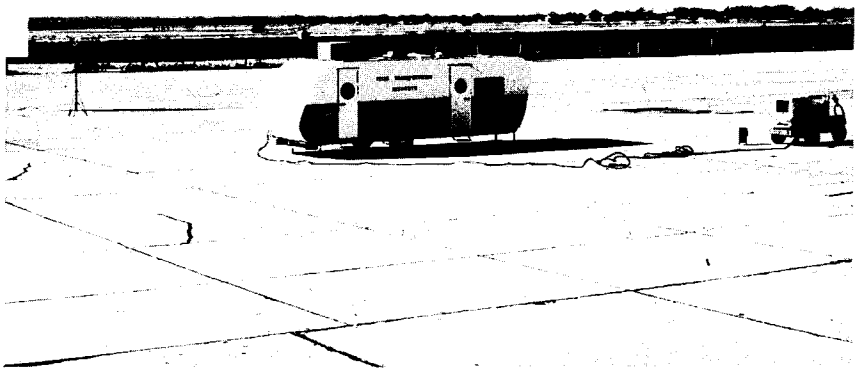

FIGURE 1.4.3 BASIC TEST EQUIPMENT

housed the instruments used in recording the data.

Tests were made as wind conditions dictated. When possible, the tests were made with wind velocities above 20 miles per hour. The highest sustained winds during any particular day of testing were about 35 miles per hour.

Simultaneous readings of strain, wind speed, and wind direction were made for a given sign angle of attack, α (refer to Figure 1.4.1 for α). The readings were made continuously for about five minutes, which constituted a "run." The sign was then rotated to a different angle and the readings resumed. Data were obtained on seven different days of testing. An average of nine runs were made each day.

The anemometer, used to measure the wind velocity, and the wind direction indicator (shown in Figure 1.4.2) were placed at an elevation equal to approximately that of the sign's center. In plan, they were about 20 feet from the center of the sign in a direction perpendicular to the direction of the wind. The latter location was used so that the instruments would not disturb the wind into the sign.

After completion of the full-scale tests, the raw data were reduced, aided by a 7094 electronic computer, to dimensionless force and moment coefficients.

In addition to the full-scale tests, a scale model of the full size sign, 1.84 feet by 1.84 feet in size, was tested in Texas A&M University's 7 by 10 foot Low Speed Wind Tunnel, shown in Figure 1.4.4. A front view of the model in the tunnel appears in Figure 1.4.5. The model is oriented so that the direction of flow is 45 degrees to the plan of the sign face.

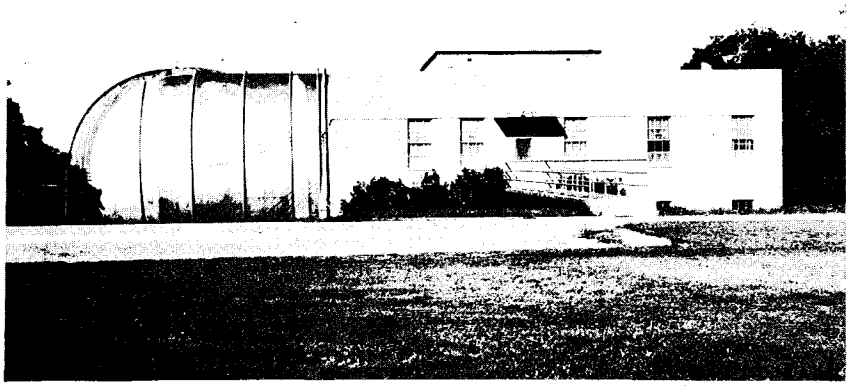

FIGURE 1.4.4 WIND-TUNNEL FACILITY

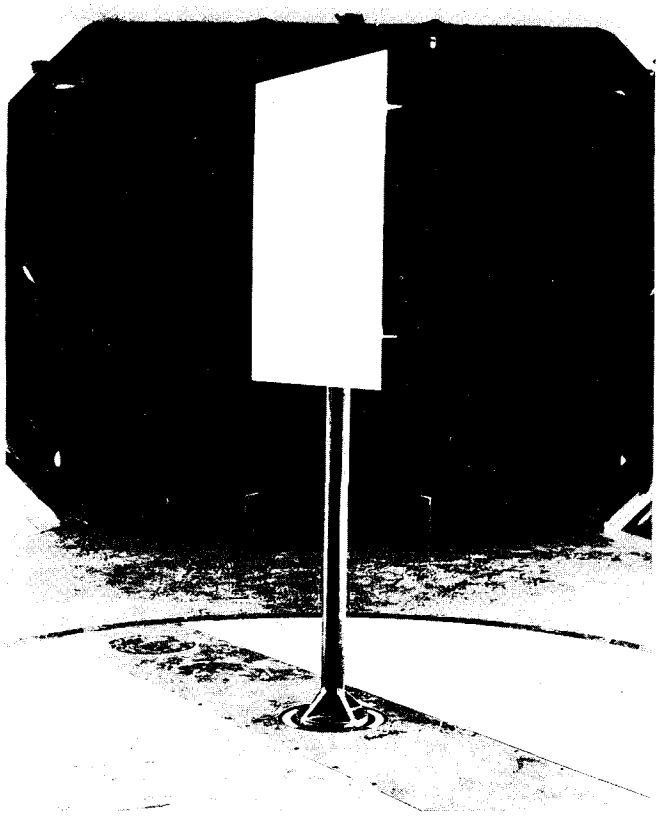

FIGURE 1.4.5 FLAT-PLATE MODEL MOUNTED IN WIND TUNNEL

The model was supported in a method similar to that used in the full-scale sign, i.e., angle chaped windbeams and a single tubular support, with the exception of the number of windbeams used. The model had two windbeams and the full-scale sign had four. The effect this difference had on the relative wind loads was assumed to be small.

The model was subjected to wind velocities ranging from 25 miles per hour to 164 miles per hour. The higher velocities were necessary in order to obtain a Reynolds number for the model equivalent to the Reynolds number for the full-scale sign.

Forces and moments on the sign model were measured directly with respect to the wind tunnel instrumentation axis for a given sign angle of attack. They were then resolved into the "sign axis" system as shown in Figure 1.4.1, by use of a 7094 electronic computer, and reduced to dimensionless coefficients.

In addition to the model test just described, two other flat plate sign models were tested in the wind tunnel. The dimensions of these two models were 1.3 feet in width by 2.6 feet high, and 2.2 feet in width by 1.6 feet high. These models were tested in order to determine the variations in wind load as the height to width ratio (aspect ratio) varied.

Wind loads on non-solid signs. After considering many non-solid background configurations, it appeared that the "louvered" configuration offered the greatest possibility for meeting the visibility requirements and reducing the wind loads. Although no known criteria exist on the use of non-solid sign backgrounds it was the opinion of the Texas Transportation Institute staff that the sign background should appear solid when viewed within the normal range of sight for which the sign's message

was intended to be read.

Previous work in the area of louvered sign backgrounds was limited to one particular test.[11] More information was needed on the variations in wind loads as the louver angle and width changed and as the overall sign height and width varied. To determine these variations, thirteen louvered sign models were built as shown in Figure 2.1.17 and 2.1.18.

The methods used in assembling the models were very basic. The flat plate louvers were fillet welded to the vertical sideplate. The windbeams were welded to the sideplates, and the mounting gussets were bolted to the windbeams and welded to the support pole.

The models were tested in the wind tunnel (Figure 1.4.4). Models 1 through 3 were used to determine the effects of the wind tunnel wall interference on the measured wind loads. For any given wind tunnel there is a limit to the model size that can be tested before appreciable errors occur in the measured wind loads. These errors are due to the influence of the wall. Models 3 through 11 were used to obtain a relation between the wind loads and the louver width and louver angle. Three louver angles were considered, i.e., 45°, 30°, and 15°. For each louver angle, three louver widths were considered, i.e., 2.8 inches, 2.3 inches, and 2.0 inches. Models 12 and 13 were used to obtain a relation between the wind loads and the louvered model height to width ratio. Figure 1.4.6 shows a front and rear view of model number 5 in the wind tunnel.

Upon completion of the tests, sign model number 8 was equipped with a typical message and again subjected to wind tunnel tests in order to

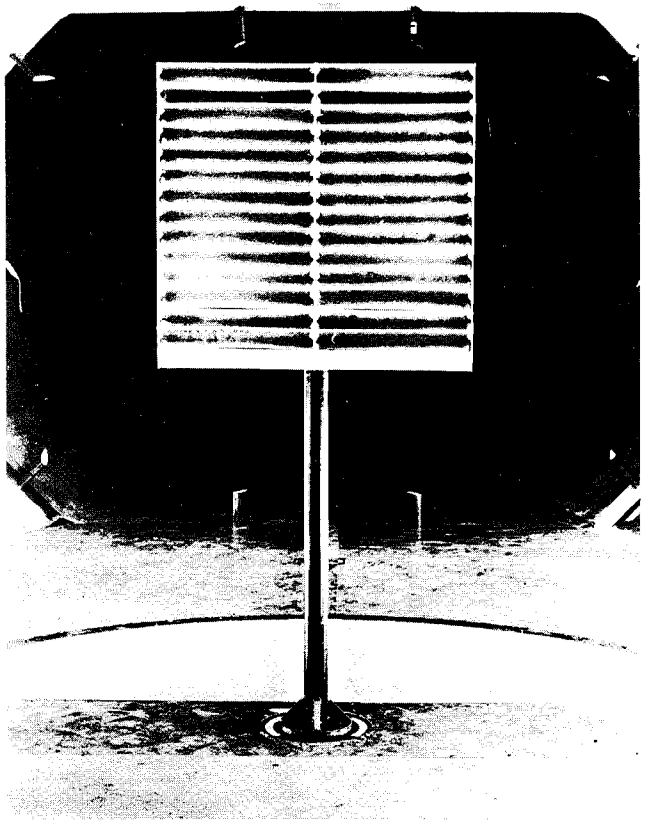

(a) FRONT VIEW

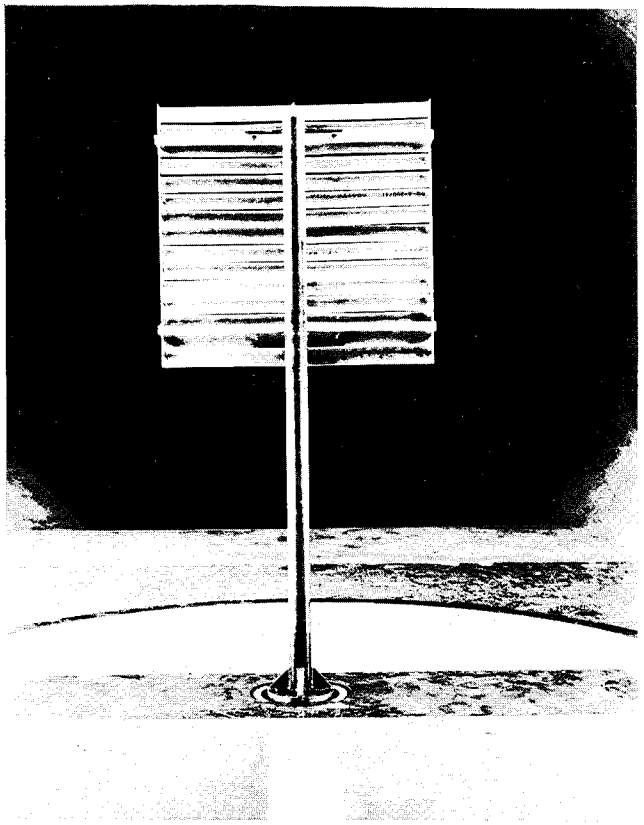

(b) REAR VIEW

FIGURE I.4.6 LOUVERED MODEL NO. 5 MOUNTED IN WIND TUNNEL

determine the message's effect on the wind loads. Each letter of the message was fastened by metal screws to two 1/4 inch wide by 1/8 inch thick by 2 foot long strips of sheet aluminum, which, in turn, were welded to the model's sideplate. Sign model 8 with the message attached, is shown in Figure 1.4.7.

After completing the tests and analyzing the data, certain conclusions were drawn. These results and conclusions are described in detail later in the report. The results indicated that an even greater reduction in wind loads could likely be realized in louvered signs if the louvers were curved rather than straight, as had been tested. Therefore, three curved louver sign models, numbered 14, 15, and 16, were built and wind tunnel tested. The geometry of the curved louvers is shown in Figure 2.1.19. The frame for the curved louvered models was similar to that used for the straight louvers with the exception of the number of sideplates. The methods of fabrication were similar. In the curved louver models, only the two outer sideplates were used. The omission of the interior sideplates was made possible by the increased stiffness of the curved louvers. Refer to Figure 1.4.8 for a view of curved louver model 14.

In addition to the sixteen louvered models just described, three models consisting of a commercially available non-solid aluminum material were tested in the wind tunnel. The material was essentially expanded metal composed of a series of short, both in length and width, louvers. The three models consisted of different combinations of louver angle, width, and length. Figure 1.4.9 shows one of the models. Further details of this material will not be given since the test results indicated that it had

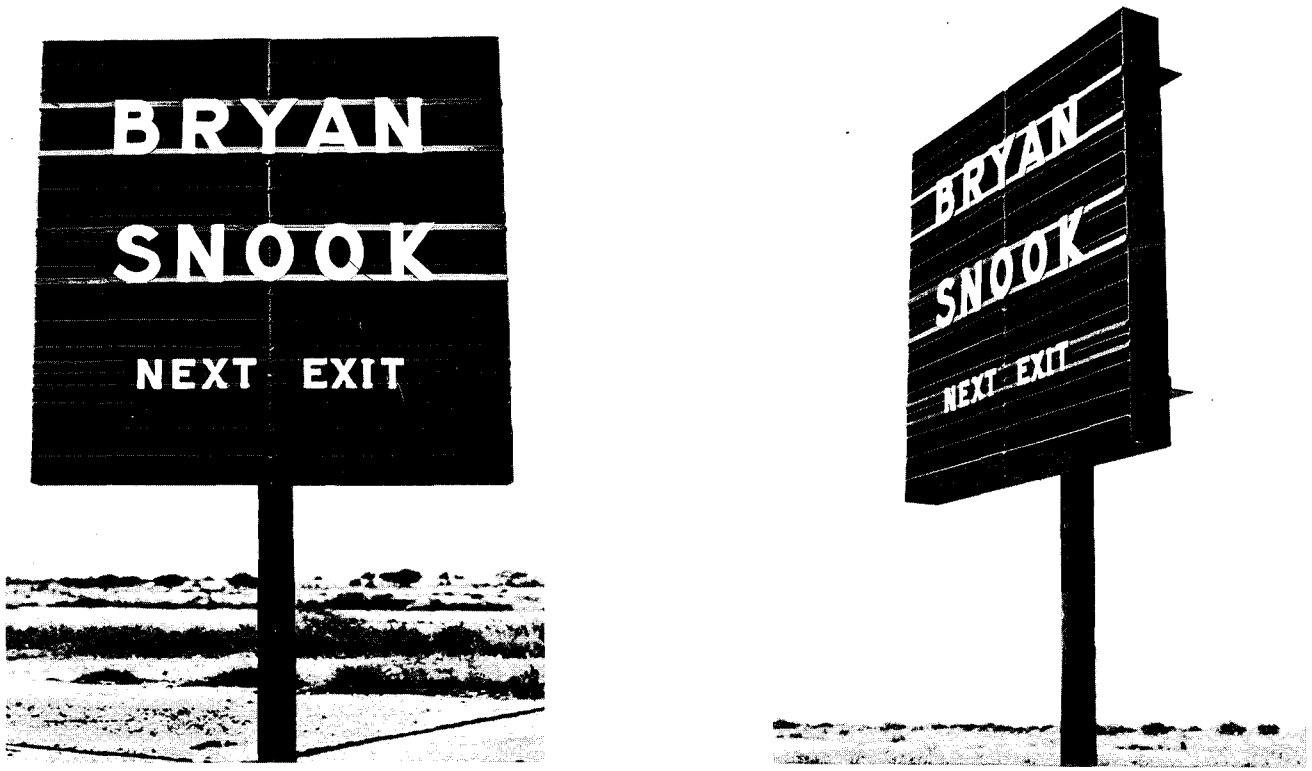

(a) NORMAL VIEW (b) SIDE VIEW

FIGURE 1.4.7 LOUVERED MODEL NO. 8 WITH MESSAGE

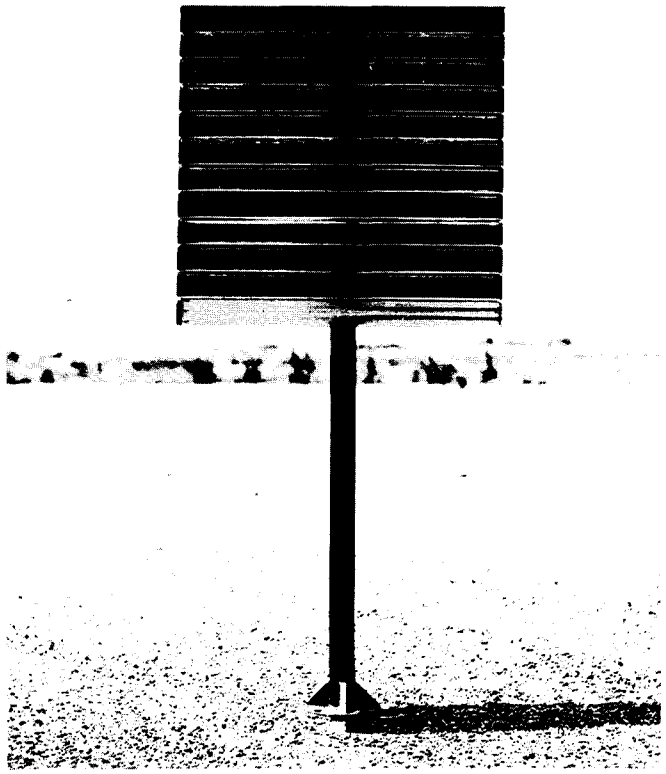

FIGURE 1.4.8 CURVED LOUVER MODEL NO. 14

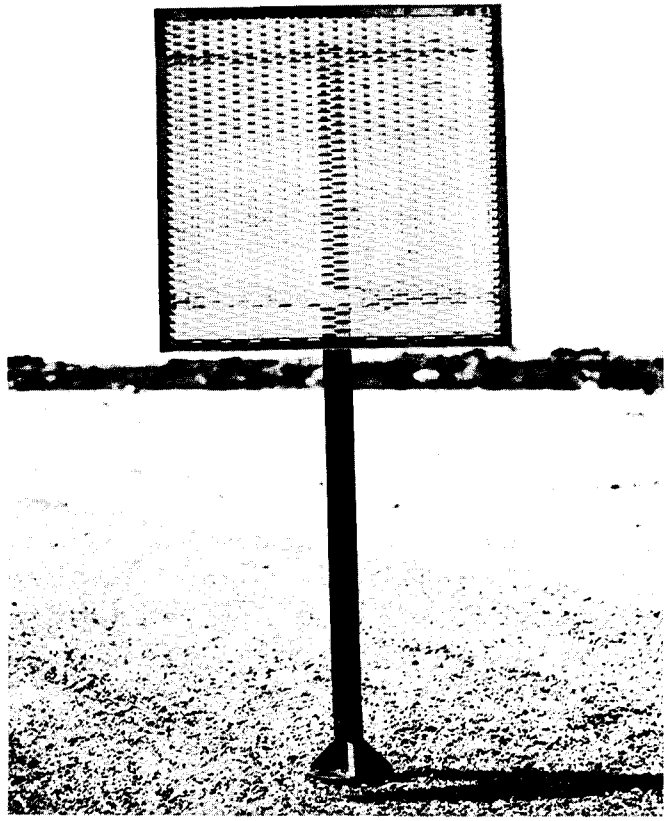

FIGURE 1.4.9 EXPANDED METAL MODEL

little ability to reduce wind loads.

Economic and safety aspects as a function of the frequency of occurrence of design winds. The methods used in this investigation were analytical in nature. No experimental work was done.

Two mathematical relationships were derived. The first relationship expressed the change (in percentage) in a sign's size as a function of the sign's design life for certain parameters (assumed to be known). Design life is defined as the recurrence interval of the design wind velocity. The second relationship expressed the change (in percentage) in a sign's cost as a function of the sign's design life for certain parameters. The parameters referred to include factors such as the ratio of the average two-year velocity to the 50-year wind velocity, the replacement cost of a blown-down sign, the useful life of a sign, and others.

Two basic equations were utilized in deriving the above mentioned relations. The first of these two equations was an expression presented by Thom,[12] which can be used to determine the probability of any given wind speed occurring in any given location in the United States. The second equation was the general relationship between the wind load on a structure and the corresponding wind velocity.

A computer program was written for use in evaluating the derived equations since they were lengthy and rather cumbersome to handle. Examples of each equation were evaluated for selected parameters.

A detailed account of this investigation including the mathematical formulation is included in Chapter 3.

Economics of conventional and non-solid signs. An extensive economic evaluation of the two types of signs was not possible within the scope of this study. The problems one faces in this type of study are great. It was especially difficult in the case of the non-solid signs, mainly because none have ever been fabricated on a full-scale basis.

Several industrial firms were contacted and asked to submit estimates on the cost involved in manufacturing the non-solid louvered sign. Both steel and aluminum fabricators were contacted. These estimates were then used as a basis for the economic evaluation of the louvered sign.

The economics of the conventional sign were obtained from local sources, i.e., the Texas Transportation Institute staff and Texas Highway Department officials. The values used are based on local prices and do not necessarily represent any type of national average.

1.5 Results

The detailed results of this study are presented in Section 2.3. A general discussion of the results follows.

Wind loads on conventional signs. There was very close agreement between the results of the full-scale wind load study and the wind tunnel test (see Figure 2.3.11) of the conventional sign model. This is fortunate because it permits the use of scale model data from wind tunnel tests on full-scale signs. It is much more economical to test models than to test full-scale structures.

The results of the full-scale tests and wind tunnel tests on conventional flat plate signs clearly indicate that the current wind load

design criteria,[13] with regard to wind pressure, are not excessive. In fact, the results show the criteria to be unconservative.

The currently used equation for wind pressure in psf on a sign is as follows:

$$p = 0.00256\ (C_g V)^2\ (C_s) \qquad (1.5.1)$$

where

V = wind speed (mph)

C_g = gust factor = 1.3

C_s = shape coefficient = 1.3

$0.00256 = 1/2\ \rho\ (K_v)$

where

ρ = mass density of air at sea level = .00238 lb.-sec./ft.^{4}

K_v = conversion factor for converting V in mph to ft./sec.

$K_v = (1.467)^2 = 2.15$

In Equation 1.5.1 the shape coefficient is equal to 1.3 for all conventional signs, regardless of its shape, i.e., its height to width ratio (or its aspect ratio). The results of this study show this to be inconsistent. The values of the shape coefficient C_s (also termed C_n) were found to vary from 1.7 for an aspect ratio of 0.5 to 1.5 for an aspect ratio of 1.4. It is noted that the aspect ratios of most highway signs are within this range.

In addition to the above inconsistencies in normal loads or pressures, there also exists a difference in the value of the twisting moment on a sign. The current criteria does not specify a twisting moment for signs with more than one support. This is likely due to the belief that a conventional sign is subjected to the most critical wind loads when the wind direction is normal to the face of the sign, i.e., when the angle of attack is 90°, in which case the twisting moment is zero. However, this is not always the case. In some instances the critical condition will occur at angles of attack less than 90°. Consider the following example.

Given:

A sign with dimensions as shown in Figure 1.5.1(a) subjected to 100 mph winds.

Required:

Compute the critical support loads by:

(a) current criteria

(b) results of this study

Solution:

By (a), current criteria:

Normal wind pressure p, (from Equation 1.5.1)

$$p = 0.00256\ (1.3V)^2\ (1.3)$$

$$p = 0.00256\ [(1.3)\ (100)]^2\ (1.3)$$

$$p = 56.25\ \text{lbs./ft.}^2$$

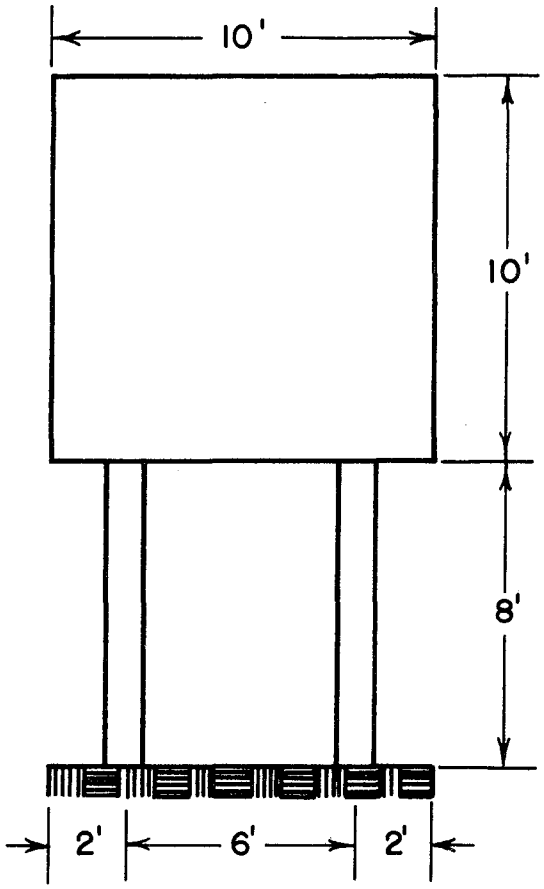

(a) GIVEN SIGN CONFIGURATION

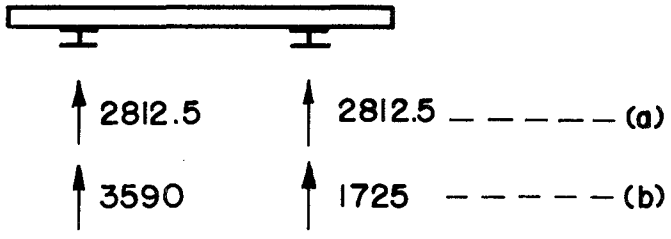

(b) LOAD COMPARISON

FIGURE 1.5.1 COMPARATIVE LOAD STUDY OF A TYPICAL SIGN

Load per support P_S,

$$P_S = pA_s/2$$

where

A_s = area of sign = 100 ft.^{2}

therefore

$$P_S = 56.25\ (100)/2 = \underline{2812.5\ \text{lbs}}.$$

By (b), results of this study:

The results of this study show that the critical load condition for an aspect ratio of 1.0 occurs when the angle of attack is 30° to the face of the sign, as shown in Figure 1.5.2. For this direction, the combination of normal force and twisting moment gives a more critical load condition on the support than any other wind angle.

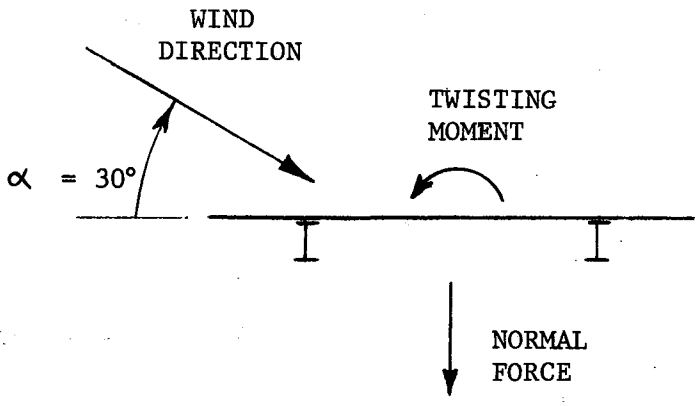

FIGURE 1.5.2 CRITICAL LOAD ORIENTATION

The normal wind pressure p, in lbs./ft.^{2} computed by the use of the

equation,

$$p = 0.00256\ (1.3V)^2\ (C_N)$$

where

$C_N = 1.23$ at $\alpha = 30°$ (Reference Figure 2.3.5)

Therefore,

$$p = 0.00256\ [(1.3)\ (100)]^2\ (1.23)$$

$$p = 53.2\ \text{lbs./ft.}^2$$

The total normal force N is computed by

$$N = pA_s = 53.2\ (100) = 5320\ \text{lbs.}$$

The twisting moment M_T is computed by use of Equation 2.2.4 as follows:

$$M_T = (C_{MT})\ (1/2)\ (p)\ (V)^2\ (A_s)\ (W)$$

where

C_{MT} = moment coefficient

W = width of sign (feet)

and all other terms are as previously defined.

If a gust factor of 1.3 is multiplied by V and if V is in mph, the equation for M_T in ft.-lbs. reduces to

$$M_T = 0.00256\ (1.3V)^2\ (A_s)\ (W)\ (C_{MT})$$

For the given sign,

C_{MT} = 0.13 (Reference Figure 2.3.7, α = 30°)

W = 10 ft.

Thus,

$$M_T = 0.00256\ [(1.3)\ (100)]^2\ (100)(10)(0.13)$$

M_T = 5605 ft.-lbs.

The total load per support P_S is computed by,

$$P_S = N/2 \pm M_T/a$$

where,

a = support spacing = 6 ft.

Therefore,

$P_S = 5320/2 \pm 5605/6$

P_S = 3590 lbs. & 1725 lbs.

The results of the comparison are shown in Figure 1.5.1(b). It is evident that differences exist between the current criteria and the results of this study. It is also evident that the critical load condition does not necessarily occur when the wind direction is normal to the sign's face. To determine the critical condition, one must therefore take into consideration not only the shape of the sign (aspect ratio) but also the twisting moment and normal force at all angles of attack and the support spacing.

Only small variations in the coefficients were noted as the Reynolds number varied in both the full-scale and model tests. The

characteristic length used in the Reynolds number was the sign's horizontal width. Independence of the Reynolds number makes it possible to apply the model test results to large signs.

The values recommended in the current criteria for the side (or transverse) force were essentially verified in this study.

Wind loads on non-solid signs. As described previously, three non-solid background configurations were tested. These three consisted of the straight louver, curved louver, and the expanded metal.

Of the three, the expanded metal was found to possess very little ability to reduce wind loads when compared with the conventional sign. A reduction of approximately 10 percent was the highest value obtained for the three models tested.

In order to present a summary of the straight louvered test results, a comparison was made between the wind loads that would exist on a straight louvered sign and a geometrically similar conventional sign. The wind load values for both cases are based on the results of this study. In the louvered case, the wind loads include the effects of a typical message on the sign, assuming the message is attached similarly to the method used in this investigation. A sign with 100 square feet in area and whose aspect ratio equals 1.0 was chosen as a typical example. The comparative summary is presented in Tables 1.5.1, 1.5.2, and 1.5.3, for louver angles of 15^{o}, 30^{o}, and 45^{o}, respectively.

As evident, the smaller the louver angle (θ) the greater the reduction in wind loads. It is also evident that for a given louver angle, the normal force did not vary appreciably as the louver width

TABLE 1.5.1 COMPARATIVE SUMMARY OF STRAIGHT LOUVER MODEL RESULTS, $\theta = 15°$

	LOUVER WIDTH (INCHES)			
	2.0	2.3	2.8	FLAT PLATE
MAXIMUM NORMAL FORCE F_N (POUNDS)	1377.0	1388.0	1288.0	3841.0
PERCENT REDUCTION IN FLAT PLATE NORMAL FORCE	64.0%	64.0%	66.0%	
MAXIMUM SIDE FORCE F_T (POUNDS)	805.0	884.0	1039.0	256.0
PERCENT INCREASE IN FLAT PLATE SIDE FORCE	214.0%	245.0%	306.0%	
MAXIMUM LIFT FORCE F_L (POUNDS)	821.0	838.0	818.0	
WEIGHT OF SIGN (POUNDS)	450.0	450.0	450.0	300.0
PERCENT INCREASE IN FLAT PLATE WEIGHT	50.0%	50.0%	50.0%	

TABLE 1.5.2 COMPARATIVE SUMMARY OF STRAIGHT LOUVER MODEL RESULTS, $\theta = 30°$

	LOUVER WIDTH (INCHES)			
	2.0	2.3	2.8	FLAT PLATE
MAXIMUM NORMAL FORCE F_N (POUNDS)	2347.0	2209.0	2109.0	3841.0
PERCENT REDUCTION IN FLAT PLATE NORMAL FORCE	39.0%	43.0%	45.0%	
MAXIMUM SIDE FORCE F_T (POUNDS)	551.0	699.0	845.0	256.0
PERCENT INCREASE IN FLAT PLATE SIDE FORCE	116.0%	173.0%	230.0%	
MAXIMUM LIFT FORCE F_L (POUNDS)	2044.0	1967.0	1993.0	
WEIGHT OF SIGN (POUNDS)	290.0	290.0	290.0	300.0
PERCENT DECREASE IN FLAT PLATE WEIGHT	3.3%	3.3%	3.3%	

TABLE 1.5.3 COMPARATIVE SUMMARY OF STRAIGHT LOUVER MODEL RESULTS, $\theta = 45°$

	LOUVER WIDTH (INCHES)			
	2.0	2.3	2.8	FLAT PLATE
MAXIMUM NORMAL FORCE F_N (POUNDS)	2945.0	2919.0	2867.0	3841.0
PERCENT REDUCTION IN FLAT PLATE NORMAL FORCE	23.4%	24.0%	25.4%	
MAXIMUM SIDE FORCE F_T (POUNDS)	507.0	587.0	707.0	256.0
PERCENT INCREASE IN FLAT PLATE SIDE FORCE	98.0%	129.0%	176.0%	
MAXIMUM LIFT FORCE F_L (POUNDS)	1516.0	1582.0	1507.0	
WEIGHT OF SIGN (POUNDS)	210.0	210.0	210.0	300.0
PERCENT DECREASE IN FLAT PLATE WEIGHT	30.0%	30.0%	30.0%	

varied. However, the side force was found to be influenced considerably by the louver width. This was obviously due to the increased width of the sideplates.

An additional force component must be considered in the louvered sign when compared to the conventional sign. That component is the lift force, which can act in either the upward or downward direction, depending upon the wind direction. However, its effect on the structural designs of the sign would be small.

The sign weights are based on an aluminum louvered sign and a plywood conventional sign. The weights include the windbeams but exclude the sign supports.

Not shown in the summary are the twisting moment comparisons. The twisting moment on the straight louvered signs was found to be much less than the twisting moment on the flat plate.

The value of the maximum normal force shown in Tables 1.5.1, 1.5.2, and 1.5.3 was also the maximum resultant force, i.e., the maximum resultant of the side and normal forces. The maximum normal forces all occurred at an angle of attack of 90^{o}. The maximum side forces occurred at angles of attack between 30^{o} and 45^{o}. The maximum lift forces all occurred at an angle of attack of 90^{o}.

No extreme flutter problems were encountered during the straight louvered test. All models were tested up to 100 miles per hour. The longest unsupported louver length was 15.5 inches on model number 12. The top and bottom louvers of all models experienced varying degrees of flutter, depending upon the louver configuration, sign angles of attack, and wind velocity. In general, the flutter was more pronounced in the

models with the larger louver angles, at a sign angle of attack of 90^{o}, and for wind velocities from 80 to 100 miles per hour. The flutter did not become catastrophic in any case and is not believed to be a serious problem. A plate over the top and bottom louvers, making in effect a box-frame for the sign, would likely eliminate the flutter, at the expense of a slight increase in the normal wind force.

Very small variations in the force and moment coefficients were found as the aspect ratio of the straight louvered models varied. Also, the normal force coefficient remained practically constant as the Reynolds number varied.

The curved louver results are presented in a manner similar to the straight louver results, i.e., they are applied to a 100 square foot size sign and compared to a similar conventional sign. This comparison is presented in Table 1.5.4.

The results of the curved louver tests were comparable to the straight louver test for a straight louver angle of 15^{o}. Curved louver model number 16 ($\theta'=14.1°$) did exhibit a greater ability to reduce the normal force than did the straight louver models. Its weight was greater than any of the straight louvered models, however.

In addition to the normal, side, and lift force, and the twisting moment, there was also a pitching moment (refer to Figure 1.4.1) on the curved louver models. This pitching moment was caused by the geometry of the louvers. The values were such that consideration would have to be given to the pitching moment in the support member design.

The curved louvers experienced a greater degree of flutter than the straight louvers. The flutter was evident at a wind speed of approx-

TABLE 1.5.4 COMPARATIVE SUMMARY OF CURVED LOUVER MODEL RESULTS

	LOUVER ANGLE (θ')			
	14.1°	20.6°	26.6°	FLAT PLATE
MAXIMUM NORMAL FORCE F_N (POUNDS)	1067	1259	1654	3841
PERCENT REDUCTION IN FLAT PLATE NORMAL FORCE	72%	67%	57%	
MAXIMUM SIDE FORCE F_T (POUNDS)	960	975	991	256
PERCENT INCREASE IN FLAT PLATE SIDE FORCE	275%	281%	287%	
MAXIMUM LIFT FORCE F_L (POUNDS)	358	851	1609	0
WEIGHT OF SIGN (POUNDS)	500	370	320	300
PERCENT INCREASE IN FLAT PLATE WEIGHT	67%	23%	7%	

imately 75 miles per hour and increased in intensity as the wind speed increased. The top louver of model number 16 broke loose at a wind speed of approximately 80 miles per hour when excessive flutter caused a weld failure.

As in the straight louvers, the flutter was much more pronounced in the upper and lower louvers. The corrective action recommended in the straight louver flutter problem should also reduce the curved louver flutter problem.

The curved louver test results also indicated that the force and moment coefficients were independent of the Reynolds number. No data are available on the variations in the coefficients with aspect ratio, since the three models tested all had the same aspect ratio (1.0). However, it is unlikely that appreciable variations would exist, at least within the range of aspect ratios of most highway signs, since the variations were negligible in the straight louvered models.

Economic and safety aspects as a function of the frequency of occurrence of design winds. The results of this investigation indicated that in some cases the recommended recurrence interval for design winds on highway signs is excessive. In these cases both the economic and safety aspects of the sign can be improved by reducing the recurrence interval. In any case the safety aspects can always be improved by designing to lower recurrence interval winds.

Several parameters were considered in the formulation of the study. Some of the parameters were the useful life of the sign, the replacement cost for the blown-down sign, discount rates, etc. In order to

arrive at any conclusions it was necessary to assign values to these parameters. In some cases this was difficult. Defining the actual useful life of a sign, for example, was subject to conjecture, opinion, and other conditions. However, based on a best engineering judgment approach, an "average" situation was considered and certain conclusions were drawn.

It appears that only small reductions in cost can be realized by reducing the recurrence interval. A 7% reduction in the present 50-year design cost was found to be the maximum under ideal conditions.

The safety aspects are more encouraging, however. For an "average" situation it appears that the sign's mass can be reduced 30% without any increase in present cost by designing to a lower recurrence interval wind.

Economics of Conventional and non-solid signs. Evaluating the economic aspects of the louvered sign proved to be a difficult task. Cost estimates obtained from different commercial firms varied somewhat. After considering the estimates it appears that the cost of a straight louvered aluminum background would be roughly as follows:

Louver Angle	Cost
15^{o}	\$5.00 to \$6.00 per square foot
30^{o}	\$4.50 to \$5.50 per square foot
45^{o}	\$4.00 to \$5.00 per square foot

These values include the material and fabrication cost of the background but exclude the material and attachment cost of the windbeams, supports, and message. The geometry of the background, for which these prices are based, was similar to that of the models, i.e., a series of

0.0625 inch thick louvers, 12 inches in length, interlocked by vertical plates (called sideplates in the models).

No prices were available on the cost of materials other than aluminum. The use of steel may be feasible. However, the mass of the sign background would be increased. This could present problems in the dynamic stability of the sign since the larger sign background mass would tend to reduce the sign's natural frequencies.

Curved louver background costs are also unavailable. However, it is likely that their cost would be comparable to the straight louver, using the louver angle (θ) in the straight louvers and the effective louver angle (θ') in the curved louvers as a basis for comparison. The curved louver could probably be extruded for a cost not greatly exceeding the straight louver. The wider unsupported lengths allowable in the stiffer curved louvers would tend to offset the cost differences between the two configurations.

The cost of a plywood background for the conventional signs was estimated to be seventy-five cents per square foot. This price would include the cost of the plywood, splice plates, fasteners, and labor to assemble. All other costs are excluded. This price can then be compared with the previously quoted prices for louvered sign backgrounds.

Reduction in the material cost of the windbeams, supports, and foundation on the louvered sign could be realized. The amount of reduction would be roughly proportional to the wind load reductions. However, these reductions would likely be offset by the increased cost of the message attachment.

The cost of a paneled aluminum background is estimated to be two dollars per square foot. Again, this price includes material cost and labor cost to assemble the background.

Visibility aspects of a non-solid sign. The visibility aspects of the louvered sign, both curved and straight louvers, were found to be adequate. With the background of the model painted green, the white painted message was clearly visible from the usual viewing angles. Refer to Figure 1.4.7 for two views of a straight louver model (louver angle = 30°) with a message attached.

The method of attachment, described previously, also proved to be adequate from both a functional and structural standpoint. The model with message was subjected to 100 mile per hour winds.

CHAPTER 2

DETAILED ACCOUNT OF RESEARCH PROCEDURE

2.1 Data Acquisition

Full-scale conventional sign. A sign ten feet by ten feet in size was built and instrumented for use in determining wind loads on a typical sign when subjected to field conditions, i.e., its natural environment. The details of the sign appear in Figures 2.1.1 and 2.1.2. Figure 1.4.2 shows the sign as built, on the test site.

The actions exerted on a sign by wind forces are shown in Figure 1.4.1. Three actions are sufficient to describe the wind loads on a conventional sign, namely, normal force, side force and twisting moment. In order to measure these actions five full electric strain gage bridges were used. The bridge locations and the arms of each bridge are shown in Figure 2.1.3.

Bridge 5 was used to measure the twisting moment, or torsion, on the sign. With the arms of the bridge oriented 45° to the horizontal, the twisting moment could be measured directly. The bridge measures strain caused by torsional shearing stresses only.

Bridges 1 and 2 were used to measure bending moments in the support, at their respective positions, caused by the normal force on the sign. A basic principle of beam theory was then applied to determine the normal force, i.e., the transverse shear in a beam at a point equals the change in moment at the point with respect to a differential length. If constant, the shear can be measured over a finite length. In this case, the shear

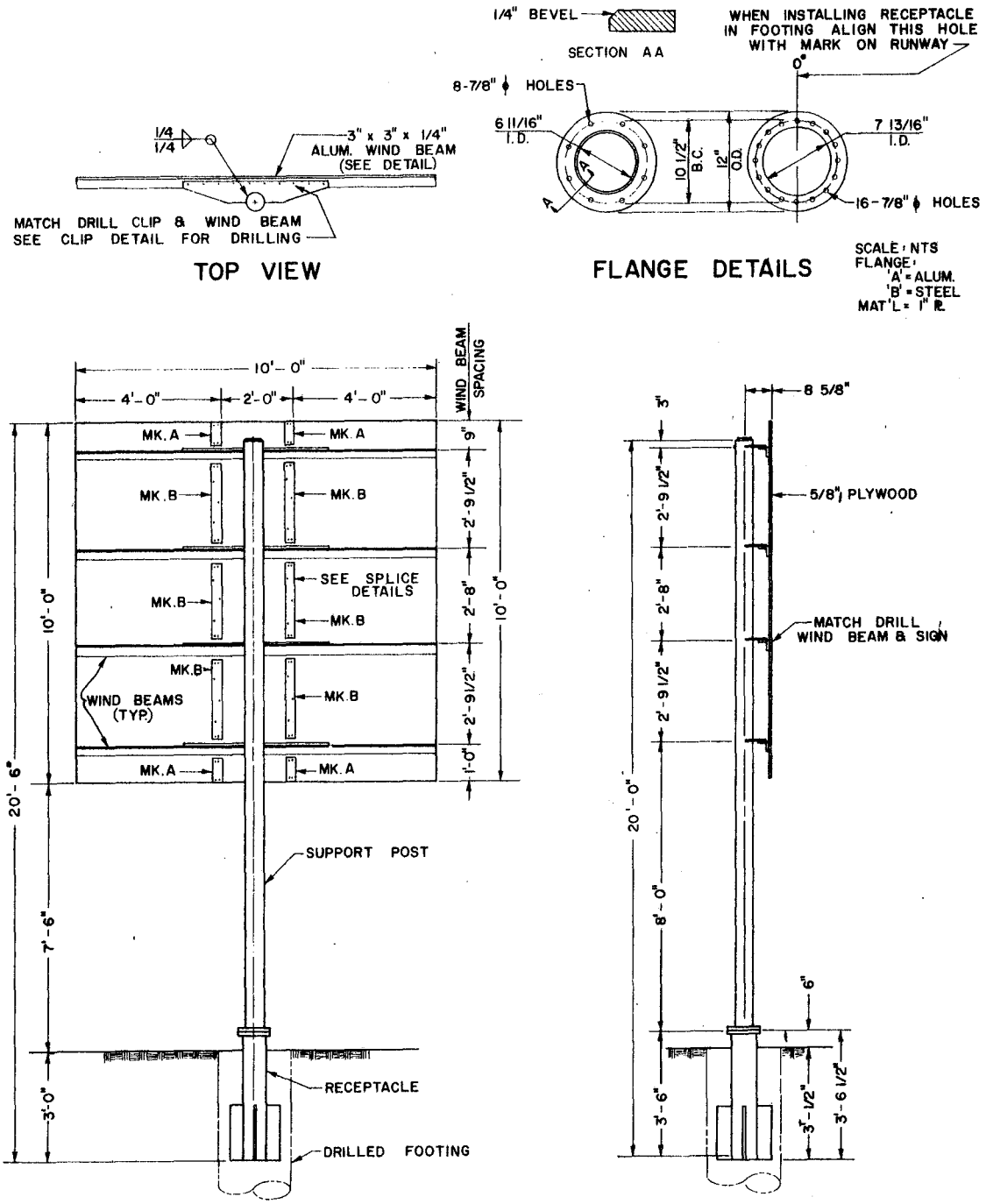

FIGURE 2.1.1 FULL-SCALE SIGN DETAILS, PART 1

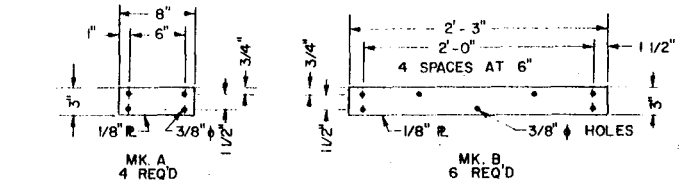

SPLICE DETAILS

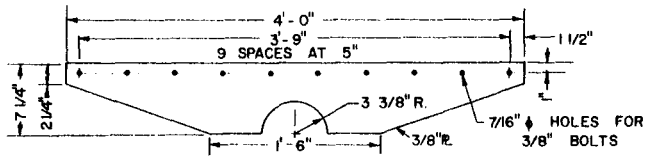

CLIP DETAILS

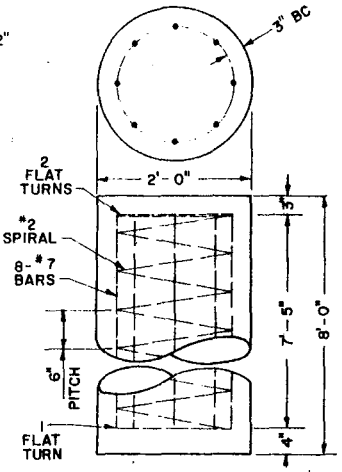

CONCRETE FILLED
DRILLED FOOTING

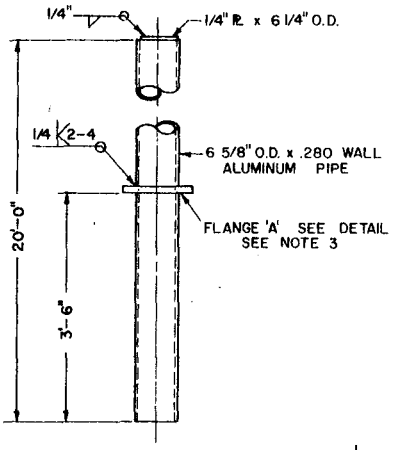

SIGN SUPPORT POST
N.T.S.

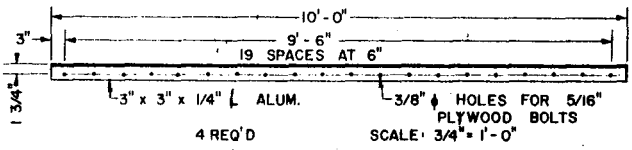

WIND BEAM DETAILS

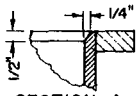

SECTION A

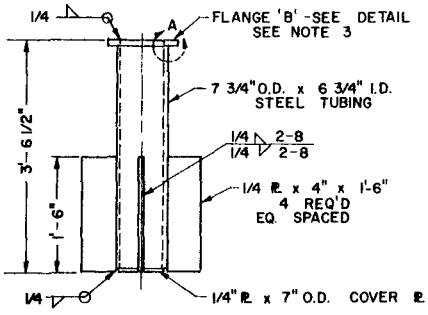

RECEPTACLE DETAIL
N.T.S.

GENERAL NOTES

1. ORDER OF ASSEMBLY
   1. DRILL 1/4" ϕ PILOT HOLES IN CLIPS
   2. MATCH DRILL CLIPS & WIND BEAMS
   3. WELD CLIPS TO SIGN SUPPORT POST
   4. WELD FLANGE 'A' TO SIGN SUPPORT POST
   5. WELD COVER R. ON SIGN SUPPORT POST

- BEFORE CONTINING ASSEMBLY THE SUPPORT POST IS TO BE INSTRUMENTED & CALIBRATED

   6. WITH WIND BEAMS ATTACHED TO CLIPS, MATCH DRILL WIND & PLYWOOD.
   7. DRILL 1/8" ϕ PILOT HOLES IN SPLICE R'S
   8. MATCH DRILL SPLICE R'S & PLYWOOD
   9. FABRICATE RECEPTACLE

2. REMOVE BURRS & SHARP EDGES
3. BOLT HOLES TO BE ON ℄'S
4. MATERIAL
   1. ALUMINUM - 6061 - T6
   2. STEEL - STRUCTURAL STEEL

FIGURE 2.1.2 FULL-SCALE SIGN DETAILS, PART 2

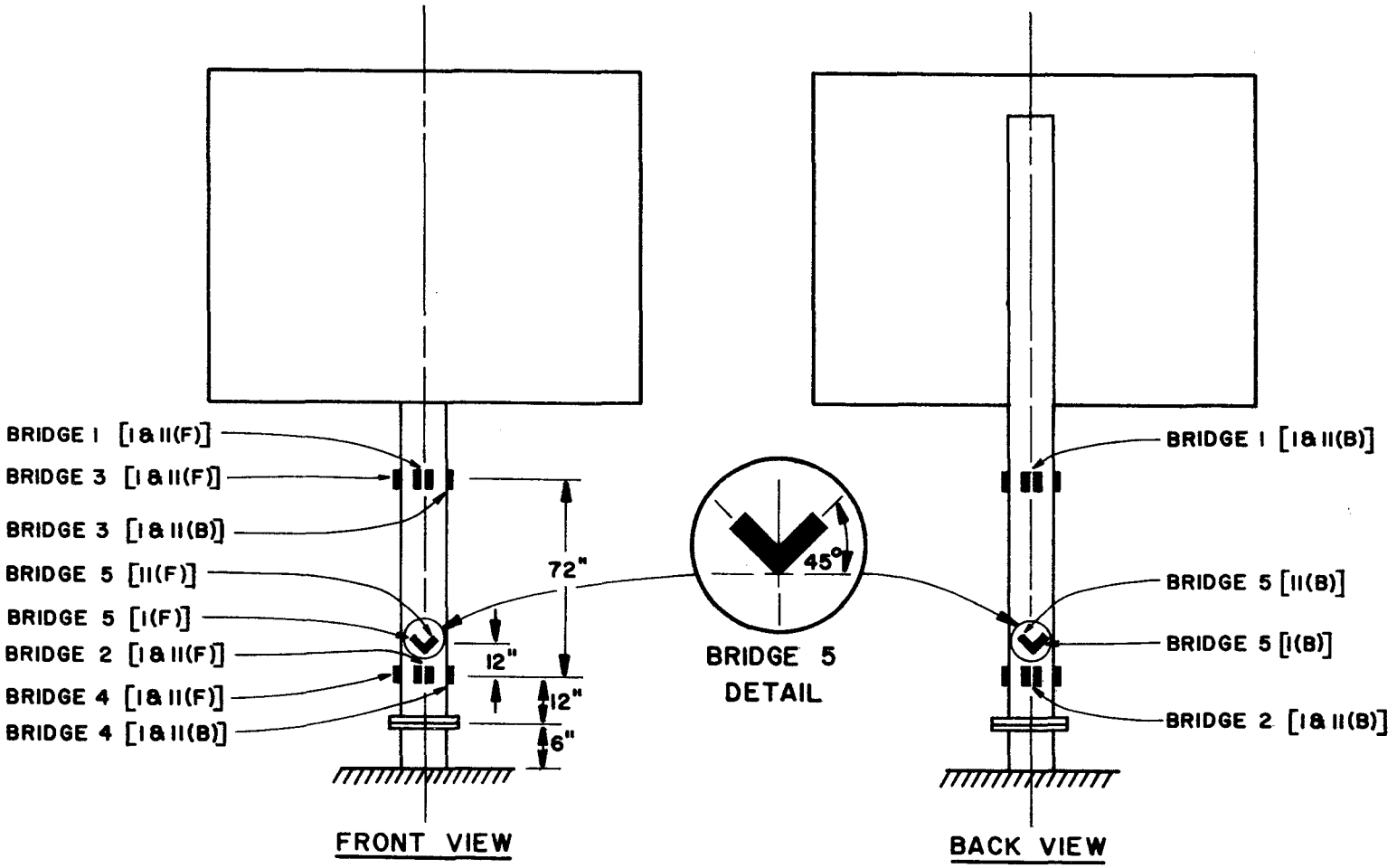

FIGURE 2.1.3 LOCATION OF STRAIN GAGE BRIDGES ON FULL-SCALE SIGN

or normal force is essentially constant after entering the instrumented portion of the support. The shear at bridge 2 was slightly higher than at bridge 1 due to the wind pressure on the support between these two locations. However, this difference is accounted for in the data reduction by use of accepted wind load data for cylindrical shapes.

Bridges 3 and 4 were used to measure the bending moments, at their respective positions, caused by the side force on the sign. The procedure for obtaining the actual side force was identical to that just described.

Figure 2.1.4 shows the bridge diagram used in bridges 1 through 4. With this arrangement, only strain due to bending stresses will cause a bridge unbalance. The axial and temperature strains are cancelled. The bridge diagram for torsion, bridge 5, was as shown in Figure 2.1.5. This bridge will become unbalanced by torsional shearing stresses only. Bending, axial, and temperature strains are cancelled.

A "dead weight" method was used to calibrate the strain gage bridges. With the instrumented pole supported in the horizontal direction, known weights were placed at known distances from the bridges. The instrumented support is shown in Figure 2.1.6(a) in a position for applying moments to bridges 3 and 4. Figure 2.1.6(b) shows the support being loaded for calibration of bridges 1 and 2. The load locations are shown in Figure 2.1.7. With known loads at known distances from the bridges, a relation was obtained between indicated strain and the corresponding moments on the support. The results of the dead weight

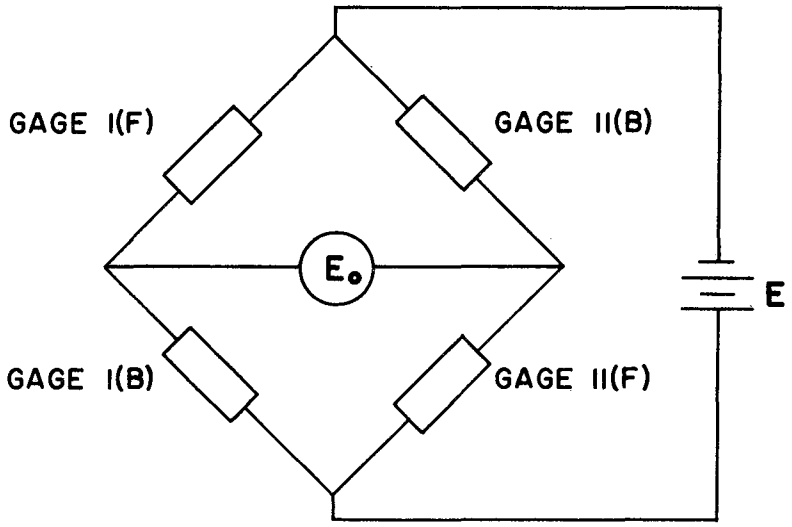

FIGURE 2.1.4 BRIDGE DIAGRAM FOR BENDING MOMENT

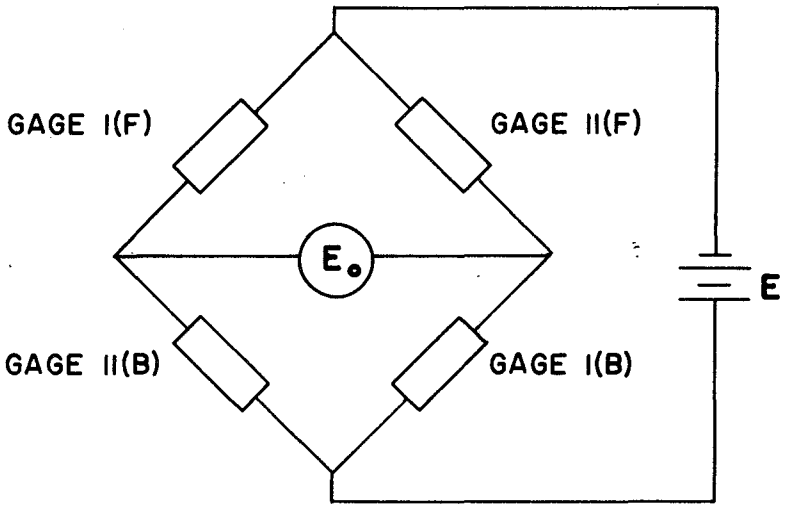

FIGURE 2.1.5 BRIDGE DIAGRAM FOR TORSION

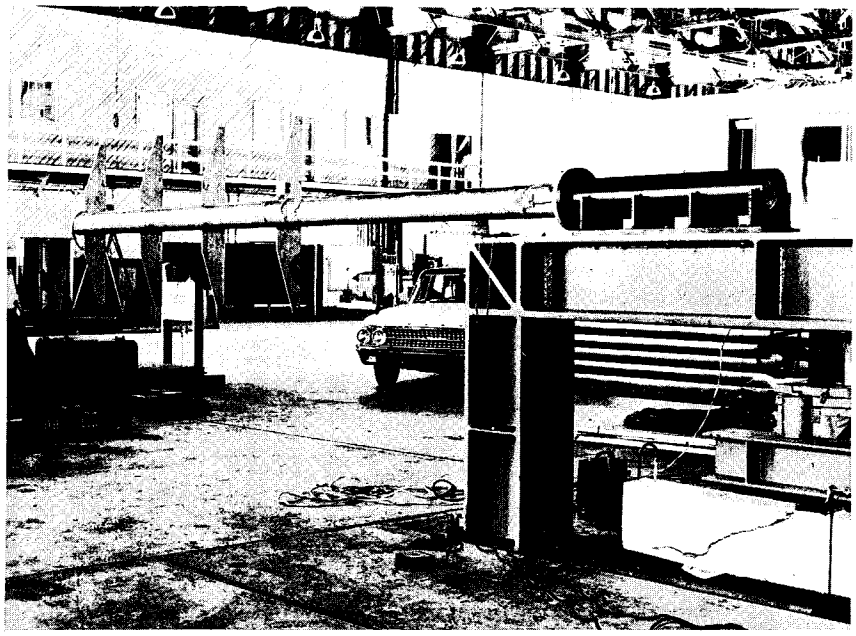

(a) BRIDGES 3 AND 4

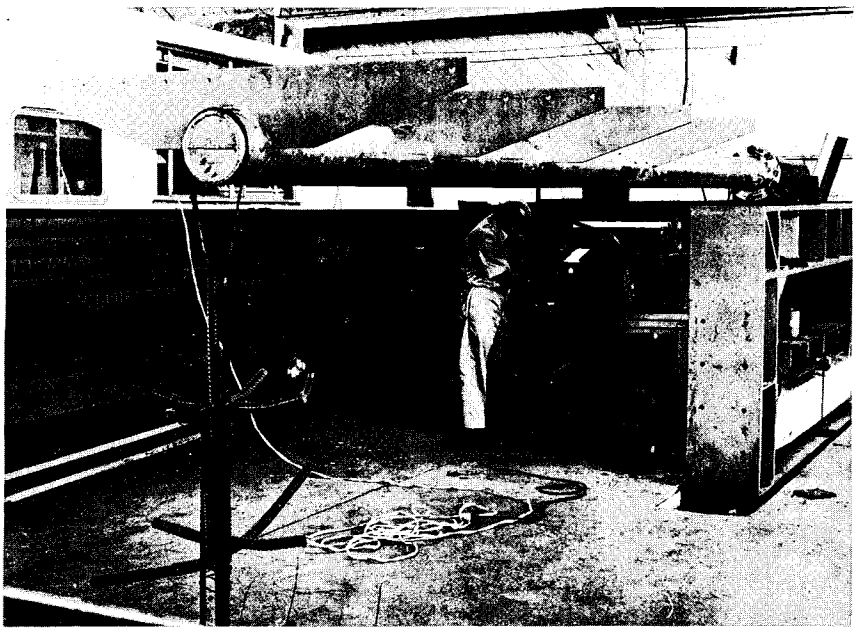

(b) BRIDGES 1 AND 2

FIGURE 2.1.6 CALIBRATION POSITIONS

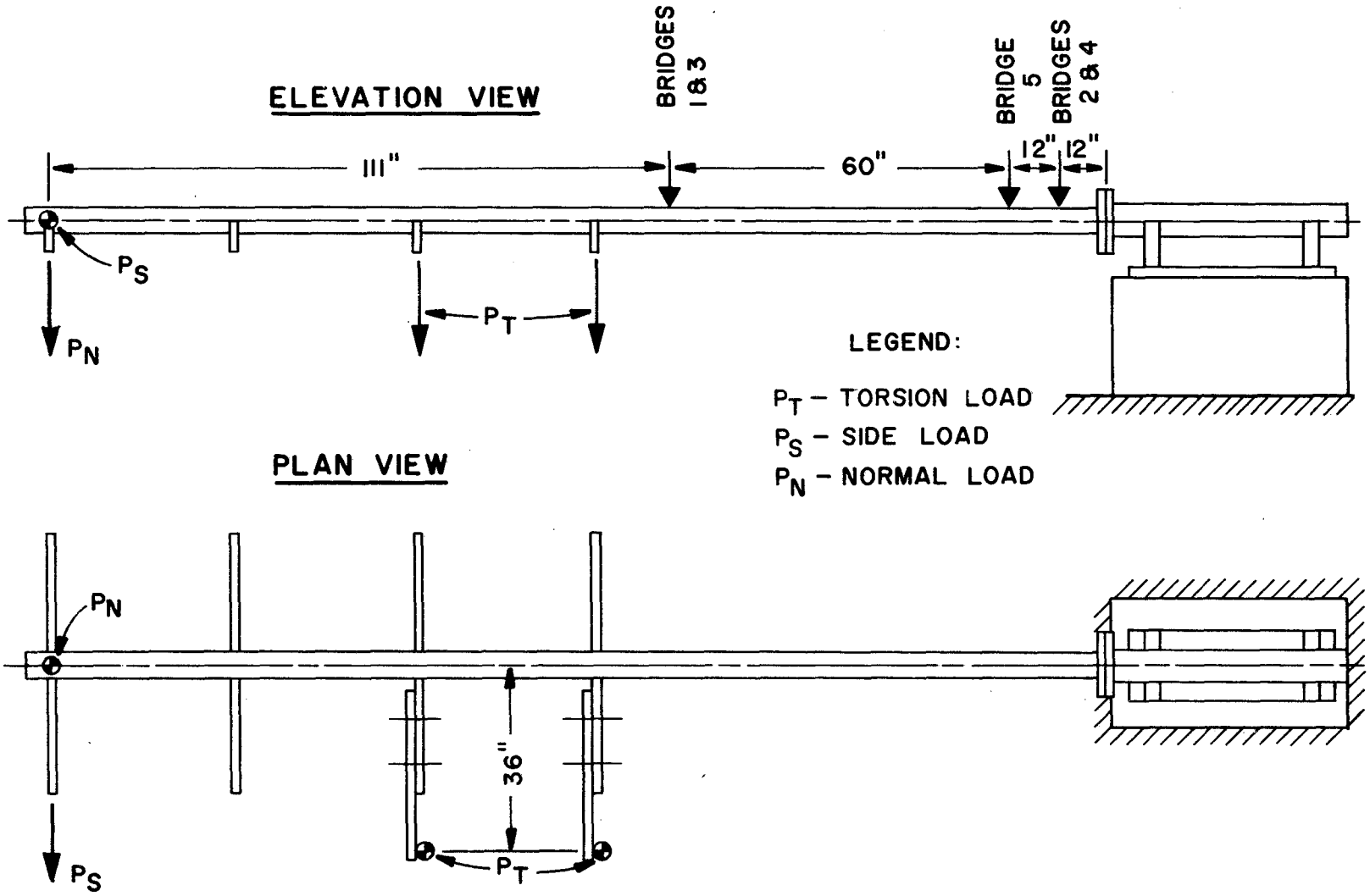

FIGURE 2.1.7 DEAD WEIGHT CALIBRATION TECHNIQUE

calibration of bridge no. 2 are shown in Figure 2.1.8 for exemplary purposes.

A load bank consisting of several different size resistors was used to simulate load on each bridge. A 100,000 ohm resistor shunted across one arm of bridge 2 produced an apparent strain reading of 595 micro inches per inch of strain, which represents a 12,500 inch-pound moment, as shown in Figure 2.1.8. Similarly, a 50,000 ohm resistor produced the equivalent of a 24,750 inch-pound moment. With this method a relation between bridge resistance and load was obtained for each of the five bridges.

The sign and instrumented supports were mounted in the upright position, in a protective hangar, as shown in Figure 2.1.9. This was done in order to obtain the no-load balance for the amplifiers used in the strain gage recording equipment. The load bank just described was then used to simulate load on each bridge. In this manner, the ± B-step for the oscillograph recorders was determined, i.e., a relation between the recorded deflections of the oscillograph trace and the load (moment, in this case) was determined.

The electronic recording equipment used in the full-scale wind load studies was contained in a mobile instrumentation laboratory, a converted 8' x 24' house trailer, as shown in Figure 2.1.10.

Two oscillograph recorders were used to record the information collected from the strain gage bridges. One of the recorders is shown in Figure 2.1.11. Galvanometers, contained in the recorders, respond to strain gage signals, reflecting a beam of light from a mercury

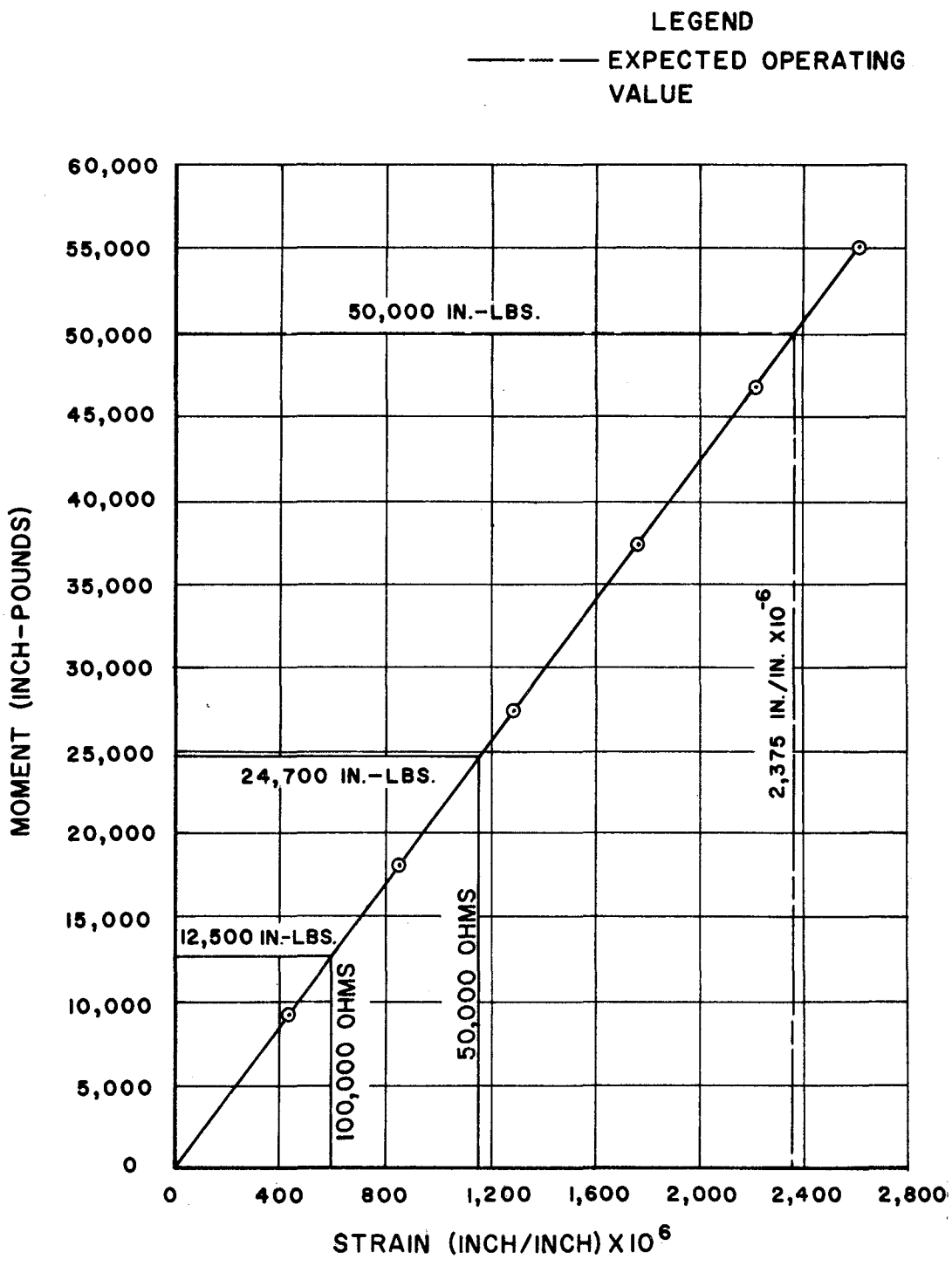

FIGURE 2.1.8 BRIDGE NO. 2 CALIBRATION CURVE

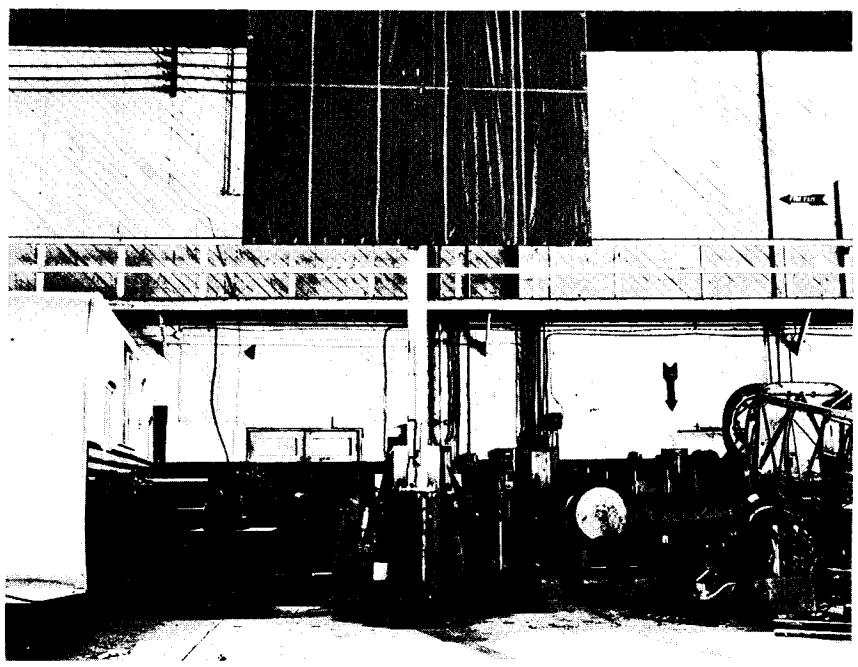

FIGURE 2.1.9 FULL-SCALE SIGN IN UPRIGHT POSITION

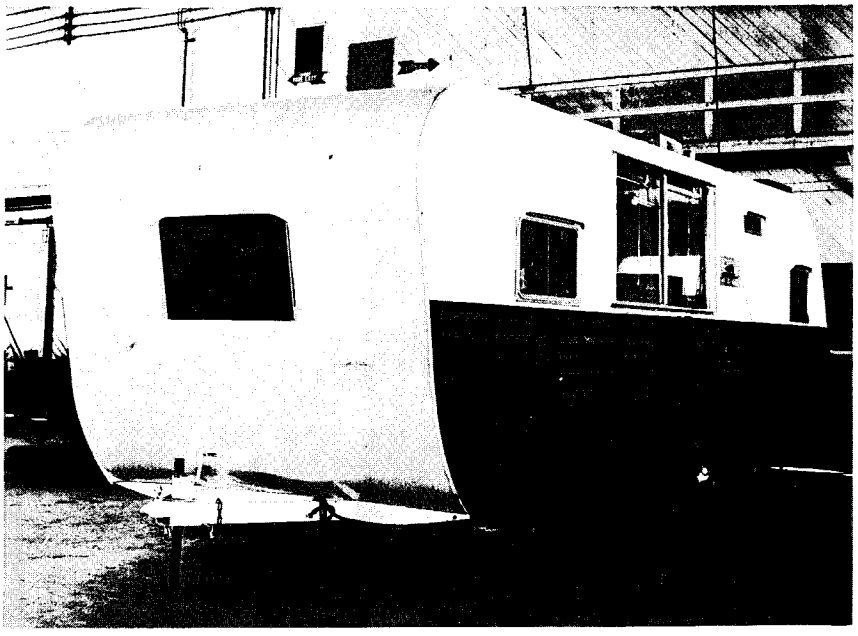

FIGURE 2.1.10 MOBILE INSTRUMENTATION LABORATORY

vapor lamp onto light-sensitive paper. The paper speed was set at 0.15 inches per second during data acquisition.

Two carrier amplifiers were used to excite the strain gages with a five-volt peak to peak signal at a frequency of 5000 cycles per second. One of the amplifiers is shown in Figure 2.1.12.

The transducers used to measure the wind speed and direction are shown in Figure 2.1.13(a). The signal from these instruments was fed to an amplifier which conditioned and fed the signal to the ink recorders shown in Figure 2.1.13(b). The ink recorders were operated at a speed of 0.1 inch per second. Simultaneous readings of strain, wind speed, and wind direction were made at a given sign angle of attack. The readings were made continuously for about five minutes which constituted a "run." The sign was then rotated to a different angle and the readings resumed. The recording instruments were sequenced with a common timing input in order to correlate the data.

The temperature, atmospheric pressure, and the relative humidity of the air were measured at regular intervals during each test in order to determine standard day information.

Sign angle of attack, α, is defined as the angle between the plane of the sign face and the direction of the wind. Refer to Figure 2.1.14 for the sign convention chosen for the angle of attack. The sign has a positive angle of attack for winds approaching from quadrants I and II and a negative angle of attack for wind approaching through quadrants III and IV.

To determine the angle of attack, the wind direction angle, θ_w,

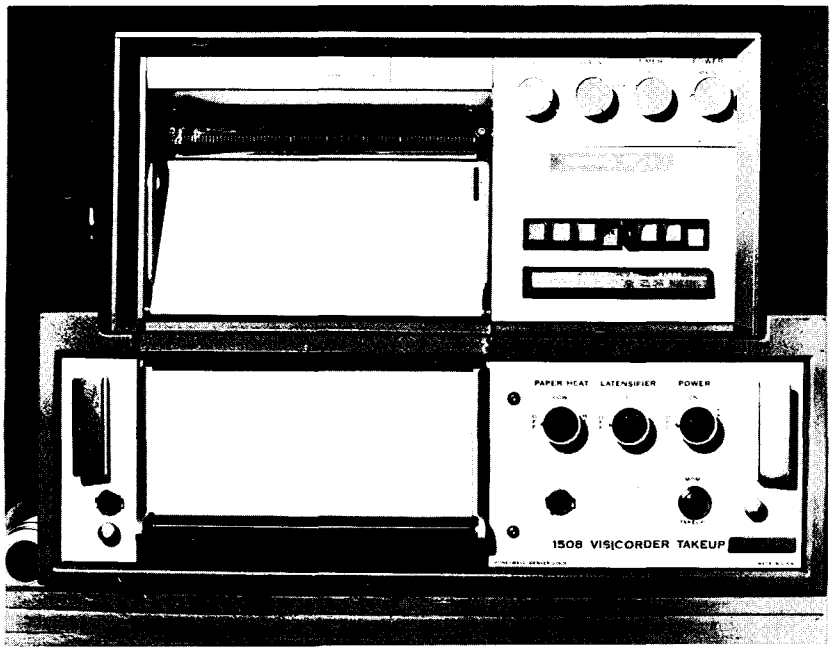

FIGURE 2.1.11 OSCILLOGRAPH RECORDER AND TAKEUP UNIT

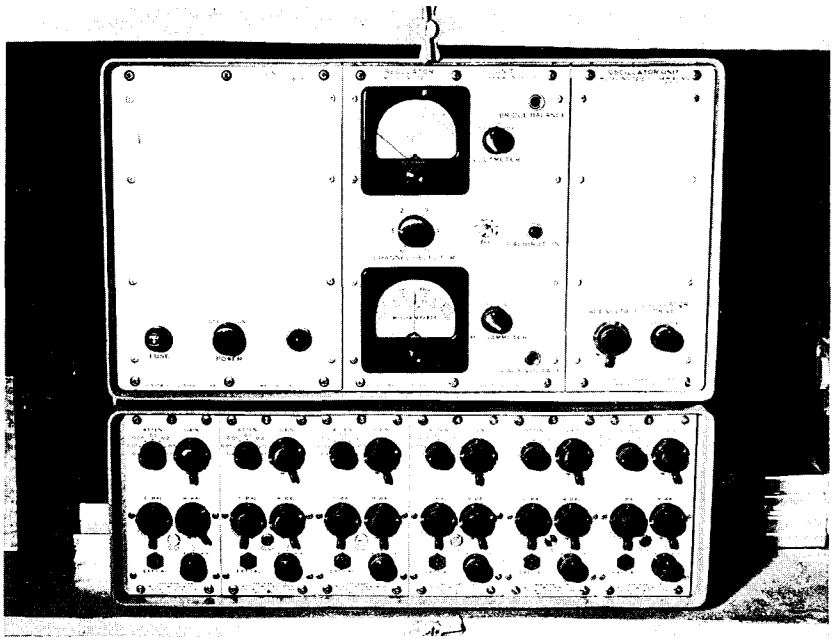

FIGURE 2.1.12 OSCILLOGRAPH AMPLIFIER AND POWER SUPPLY

(a) TRANSDUCERS

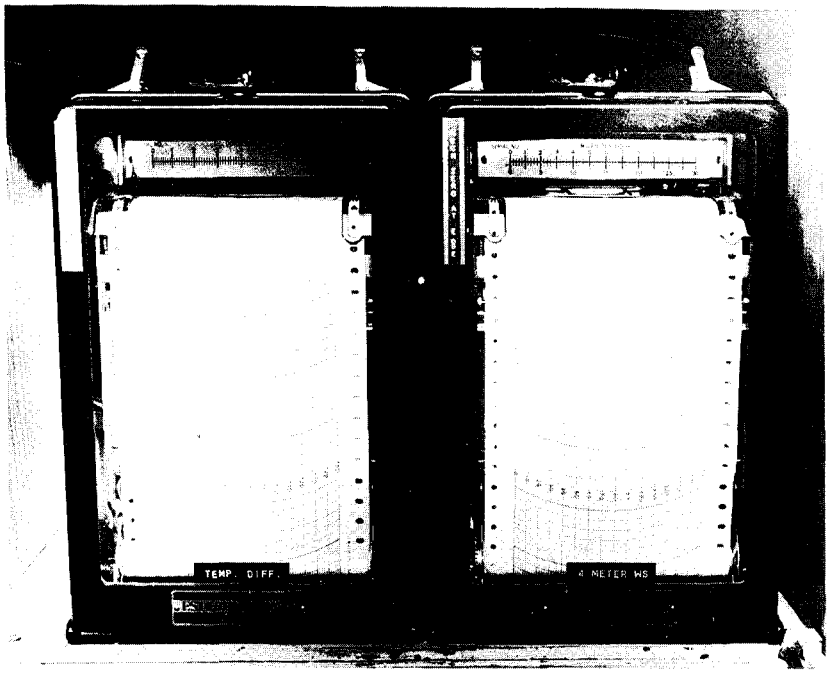

(b) RECORDERS

FIGURE 2.1.13 WIND SPEED AND DIRECTION EQUIPMENT

and sign direction angle, θ_s, were recorded with respect to the 0° (or north) direction as shown in Figure 2.1.15. The sign direction was arbitrarily chosen to be the direction in which the right hand side of the sign pointed when viewed from the front. Relations were then derived between the angle of attack, α , and the various combinations of sign and wind direction angles.

In order to rotate the sign, a very simple scheme was devised. A rope tied around the lower part of the sign in the form of a harness proved to be adequate. Refer to Figure 2.1.16.

Wind tunnel tests of sign models. As mentioned earlier, four different types of sign models were subjected to wind tunnel tests, namely, (a) flat plate, solid background, conventional sign models, (b) straight louver sign models, (c) curved louver models, and (d) commercially available non-solid background material. The flat plate models simply consisted of a 1/4 inch aluminum plate. Two angle windbeams were welded to the plate for attachment to the support pole.

Details of the 13 straight louvered models are shown in Figures 2.1.17 and 2.1.18. The construction of the three curved louver models was similar to the straight louvered models. The interior sideplate was eliminated in the curved louver models. The details of the curved louvers appear in Figure 2.1.19. Each model was supported by a single tubular support. A flange, welded to the base of the support, provided a convenient interface between the model support and the tunnel balance located at the base of the test section. The pole and flange can be seen in Figure 2.1.22.

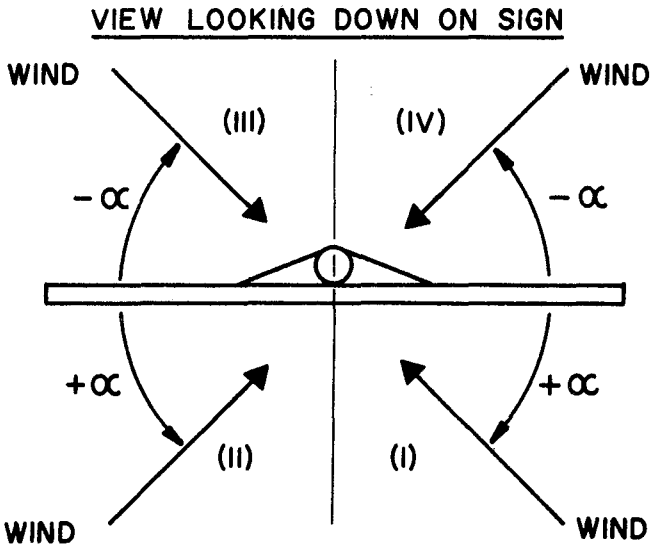

α = ANGLE OF ATTACK

FIGURE 2.1.14 SIGN CONVENTION FOR ANGLE OF ATTACK

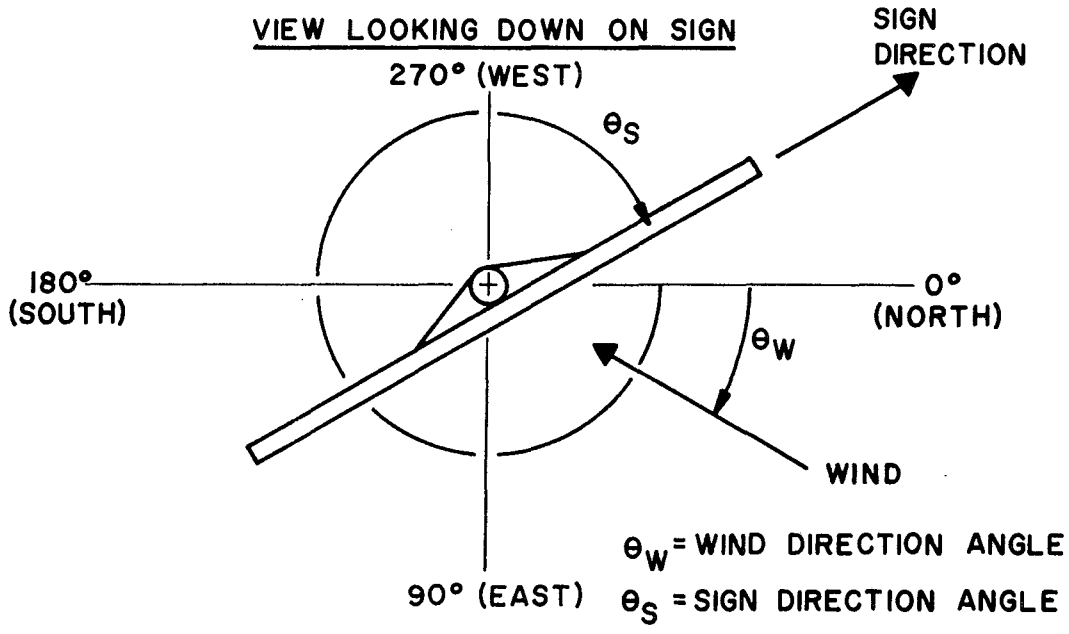

FIGURE 2.1.15 SIGN AND WIND DIRECTION ANGLES

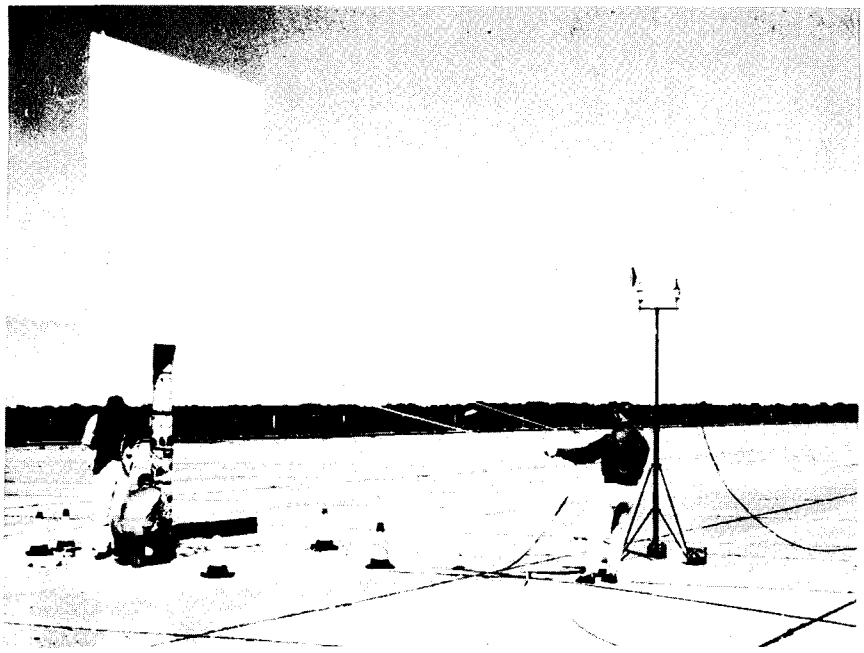

FIGURE 2.1.16 SIGN-ROTATION SCHEME

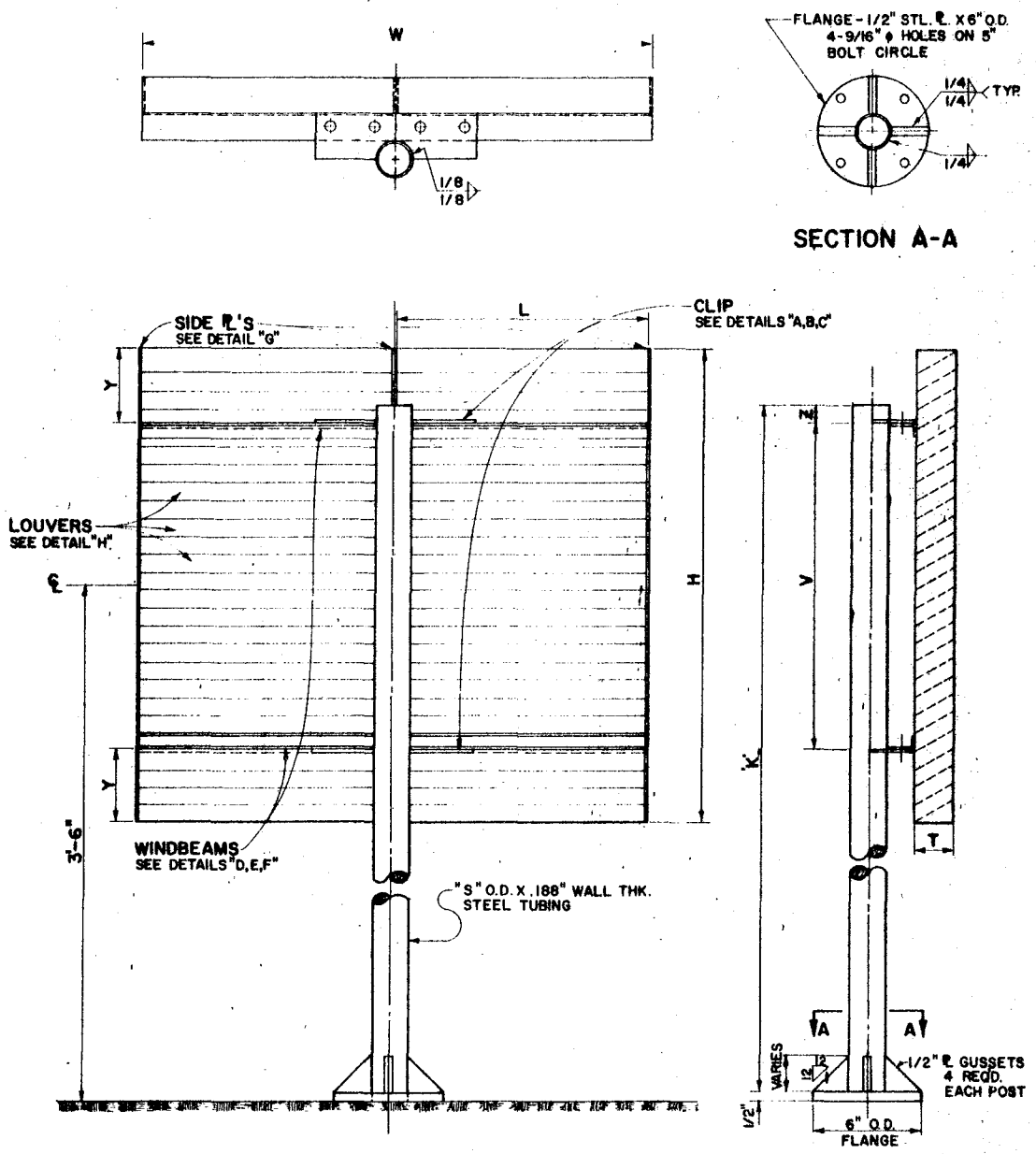

FIGURE 2.1.17 STRAIGHT LOUVER SIGN MODELS, PART I

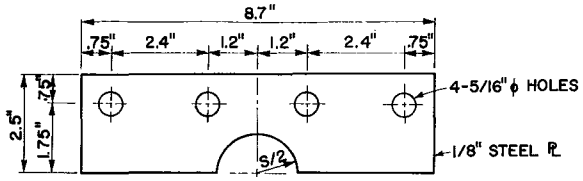

CLIP DETAIL "A"
TWO (2) REQ'D.

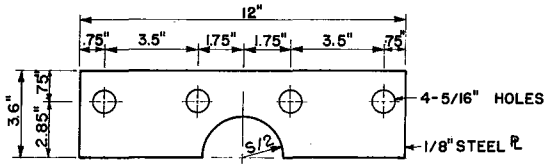

CLIP DETAIL "B"
TWO (2) REQ'D.

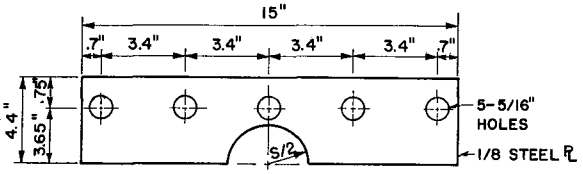

CLIP DETAIL "C"
TWO(2) REQ.D

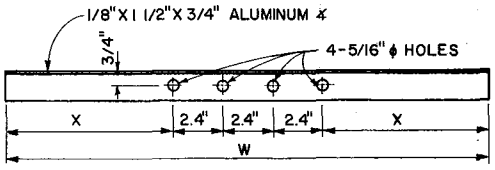

WINDBEAM DETAIL "D"
TWO (2) REQ'D EACH SIGN

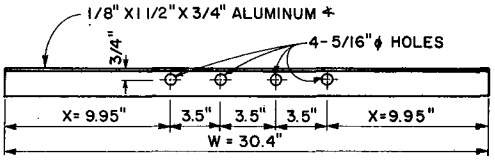

WINDBEAM DETAIL "E"
TWO (2) REQ'D

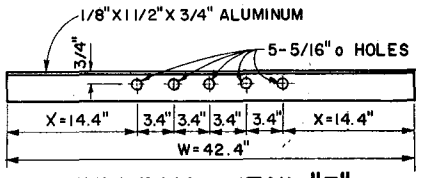

WINDBEAM DETAIL "F"
TWO (2) REQ'D

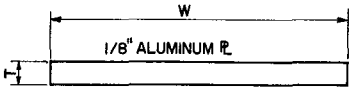

SIDE PL DETAIL "G"
THREE (3) REQ'D EACH SIGN

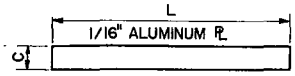

LOUVER DETAIL "H"
SEE SCHEDULE FOR NUMBER REQ'D

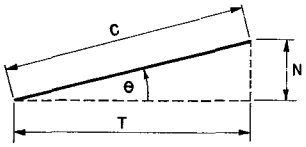

LOUVER ANGLE
SEE SCHEDULE FOR θ

MODEL SCHEDULE

	LOUVER					SIDE PLATE		MISCELLANEOUS							CLIP	WIND BEAM
MOD. NO.	L	C	NO REQ'D	θ	N	H	T	W	K	X	Y	V	S	Z	DET.	DET.
1	21	2.8	42	45°	2	42.0	2	42.4	60.5	14.4	7.0	28	3.5	5	"C"	"F"
2	15	2.8	30	45°	2	30.0	2	30.4	54.5	9.95	5.0	20	2.5	3	"B"	"E"
3	12	2.8	24	45°	2	24.0	2	24.4	51.5	8.6	3.0	18	2.0	1	"A"	"D"
4	12	2	34	45°	1.4	23.8	1.4	24.4	51.5	8.6	2.9	18	2.0	1	"A"	"D"
5	12.1	2.3	30	45°	1.6	24.0	1.6	24.6	51.5	8.7	3.0	18	2.0	1	"A"	"D"
6	12	2	48	30°	1.0	24.0	1.7	24.4	51.5	8.6	3.0	18	2.0	1	"A"	"D"
7	11.9	2.3	44	30°	1.1	24.2	2.0	24.2	51.5	8.5	3.1	18	2.0	1	"A"	"D"
8	12	2.8	34	30°	1.4	23.8	2.4	24.4	51.5	8.6	2.9	18	2.0	1	"A"	"D"
9	11.9	2	92	15°	.52	23.9	2.0	24.2	51.5	8.5	3.0	18	2.0	1	"A"	"D"
10	12.1	2.3	82	15°	.59	24.2	2.2	24.6	51.5	8.7	3.1	18	2.0	1	"A"	"D"
11	12	2.8	66	15°	.73	24.1	2.7	24.4	51.5	8.6	3.1	18	2.0	1	"A"	"D"
12	15.5	2.3	28	30°	1.1	15.3	2.0	31.4	47.0	13.1	3.2	8.9	2.0	1	"A"	"D"
13	8.9	2.3	48	30°	1.1	27.0	2.0	18.2	53.0	5.5	3.0	21	2.0	1	"A"	"D"

NOTES:

1. SEE DESIGNER FOR WELDING DETAILS OF LOUVER TO SIDE PLATE, SIDE PLATE TO WINDBEAM, AND CLIPS TO TUBE.
2. MATERIALS:
   a. ALUMINUM - 6061-T6
   b. STEEL - STRUCTURAL STEEL

FIGURE 2.1.18 STRAIGHT LOUVER SIGN MODELS, PART 2

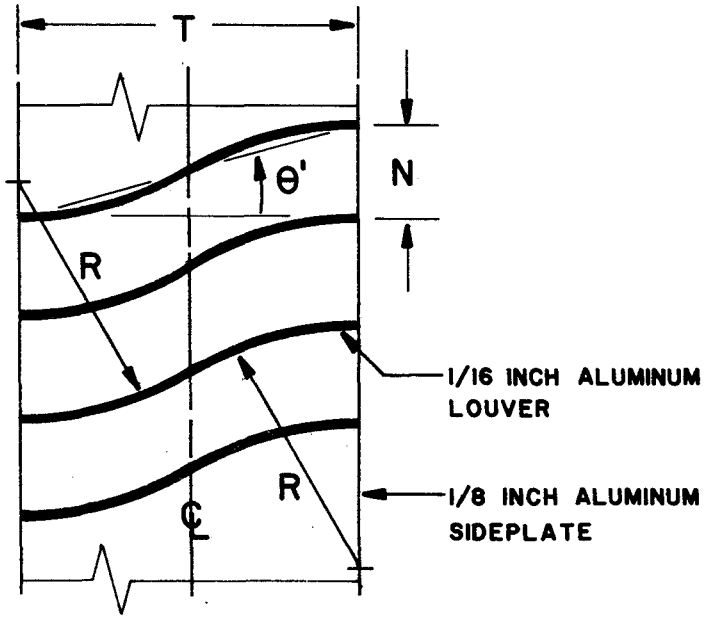

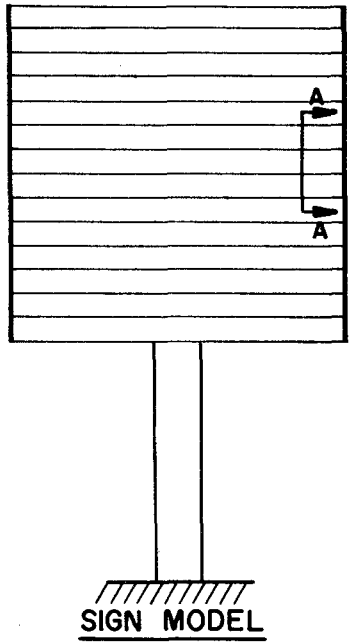

MODEL SCHEDULE

MOD. NO.	LOUVER L*	C**	R	θ'	N	NO. REQD	SIDE PLATE H*	T	MISCELLANEOUS W*	K*	X*	Y*	V*	S*	U*	Z*	CLIP DET.*	WIND BEAM DET.*
14	24.0	4.60	2.50	26.6°	2.0	12	24.0	4.0	24.4	51.5	8.6	3.0	18.0	2.0	2.0	1.0	"A"	"D"
15	24.0	4.37	3.05	20.6°	1.5	16	24.0	4.0	24.4	51.5	8.6	3.0	18.0	2.0	2.0	1.0	"A"	"D"
16	24.0	4.17	4.26	14.1°	1.0	24	24.0	4.0	24.4	51.5	8.6	3.0	18.0	2.0	2.0	1.0	"A"	"D"

* REFER TO FIGURES 2.1.17 AND 2.1.18 FOR GEOMETRIC DESCRIPTION
** ARC LENGTH

FIGURE 2.1.19 CURVED LOUVER GEOMETRY

The Texas A&M University's 7 by 10 foot Low Speed Wind Tunnel (Fig. 1.4.4) was used to test these models. The tunnel is capable of producing wind velocities up to approximately 200 miles per hour. The test section of the tunnel contains 65 square feet of plate glass assuring adequate visual access to a model undergoing test. The wind tunnel operator's control console, shown in Figure 2.1.20, is located in a room adjacent to the test section and is placed so that the operator has full view of the model during testing.

The tunnel is equipped with a six-component mechanical balance which measures six wind actions on the model. These six actions, shown in the positive "wind tunnel" axes in Figure 2.1.21, are the drag force D, lift force L, side force S, yaw moment M_y (also called twisting moment), pitch moment M_p, and roll moment M_r. The six actions were displayed by digital readout dials. The dials are shown on the right of the console in Figure 2.1.20.

The six actions were recorded for each model as the angle of attack was varied in 15° increments from 0° to +90°, and from 0° to -90°. Figure 2.1.22 shows the square, flat plate model mounted in the test section (the view shown is looking upstream), at angles of attack of +90°, +45°, and 0°.

The range of wind velocities to which the models were subjected was as follows:

(a) Flat plates - 0 to 165 miles per hour

(b) Straight louvers - 0 to 100 miles per hour

(c) Curved louvers - 0 to 100 miles per hour

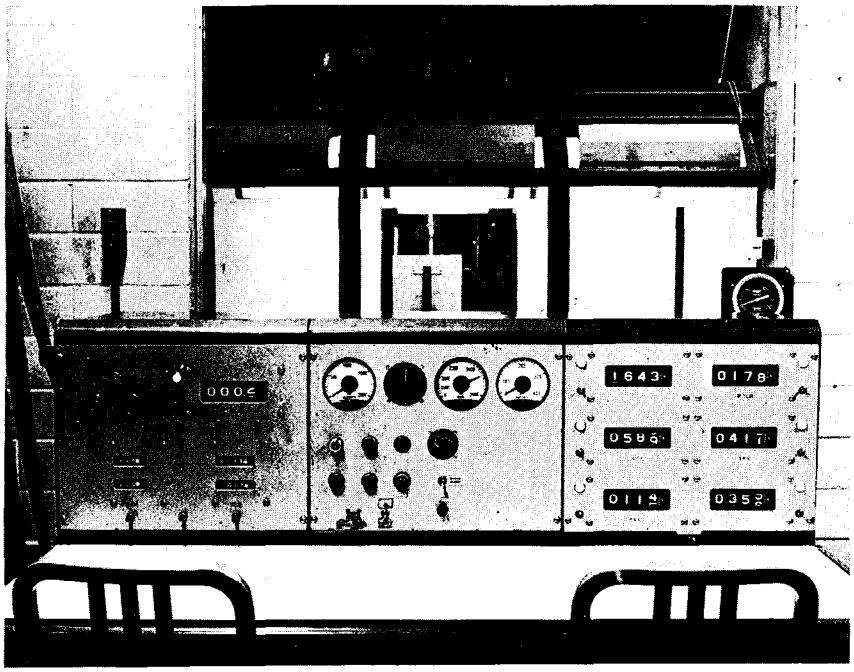

FIGURE 2.1.20 WIND-TUNNEL CONTROL CONSOLE

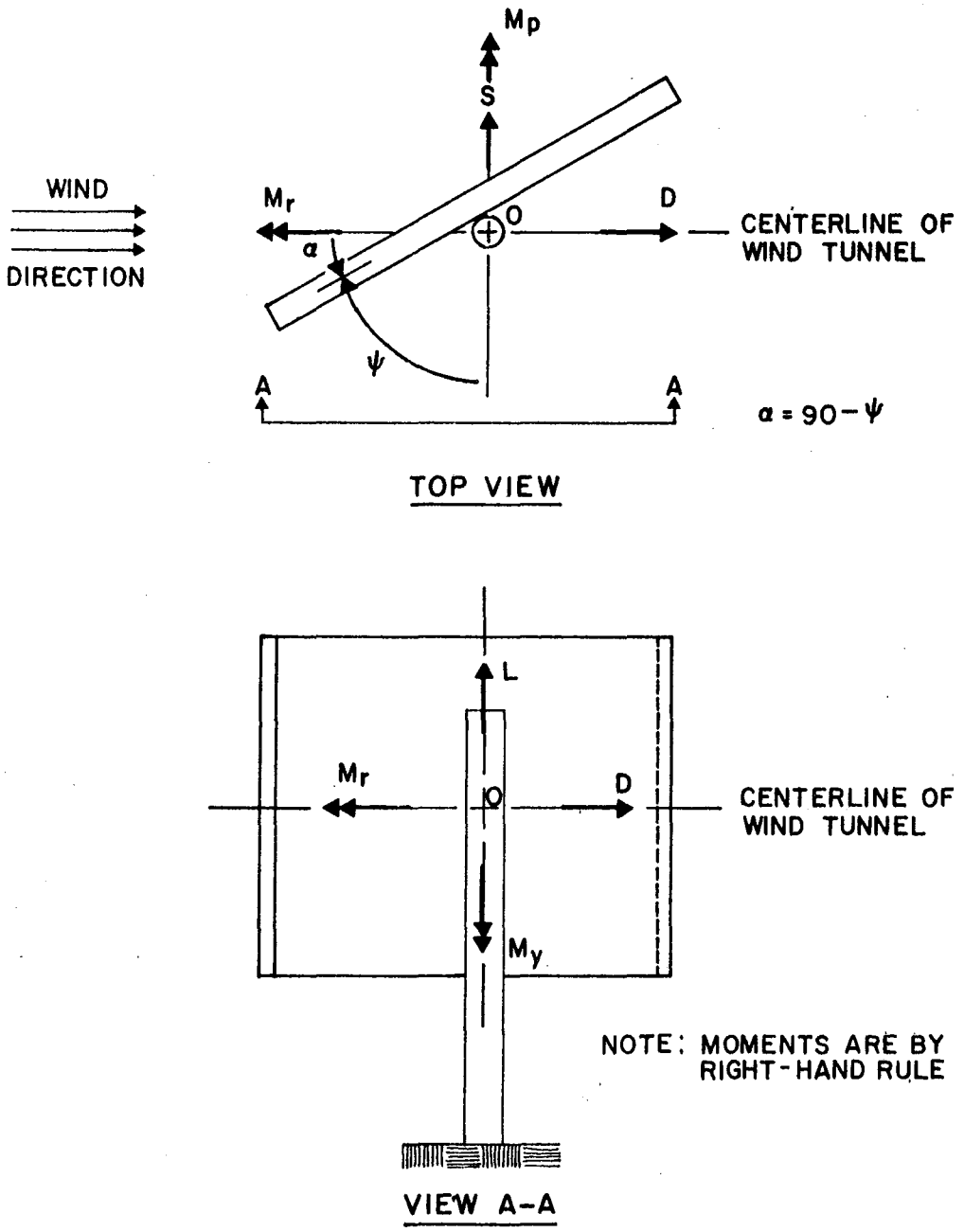

FIGURE 2.1.21 POSITIVE SIGN CONVENTION FOR WIND TUNNEL AXIS SYSTEM

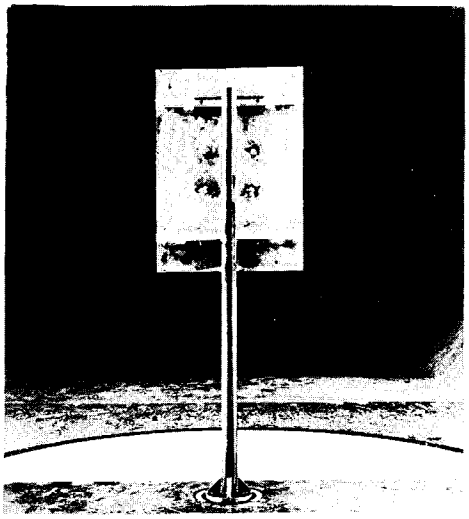

(a) $\alpha = +90°$

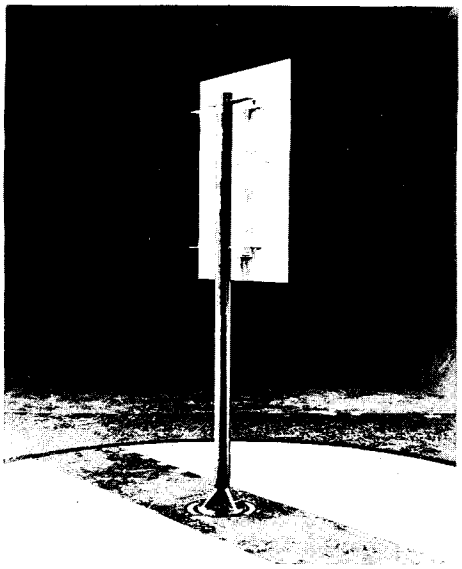

(b) $\alpha = +45°$

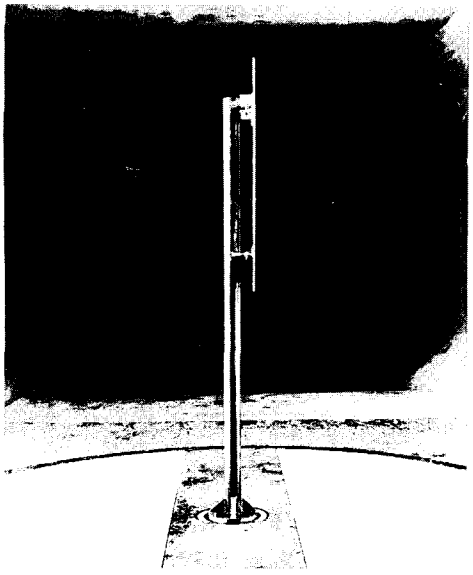

(c) $\alpha = 0°$

FIGURE 2.1.22 SQUARE, FLAT-PLATE MODEL MOUNTED IN WIND TUNNEL

(d) Expanded metal - 0 to 100 miles per hour

The flat plates were subjected to the higher wind speeds in order to obtain a Reynolds number equivalent to that of the instrumented full-scale sign. For the full-scale sign, the Reynolds number R_E was determined by

$$R_E = \frac{Vd\ (1.467)}{\nu}$$

where

V = average wind speed = 30 miles per hour

d = characteristic length = sign width = 10 ft.

ν = kinematic viscosity of air = 1.576×10^{-4} ft.^{2}/sec.

Substituting these values in the above equation yields

$$R_E = 2.793 \times 10^6$$

To obtain the same Reynolds number for the model, the necessary wind velocity was determined as follows:

$$R_E = \frac{V_m\ d_m}{\nu}$$

where

V_m = required wind velocity on model

d_m = model width = 1.845 ft.

Therefore

$$V_m = \frac{R_E \nu}{d_m} = \frac{(2.793 \times 10^6)\ (1.576 \times 10^{-4})}{(1.467)\ (1.845)}$$

V_m = 163 miles per hour

2.2 Data Reduction

In analyzing the effects of wind on a body, it is usually convenient to reduce the experimental, or theoretical results to dimensionless coefficient form, i.e., express the forces and moments acting on the body in dimensionless form. It is convenient in many cases because the coefficients are independent of the Reynolds number, whereas the forces and moments are dependent on the Reynolds number. Being independent of the Reynolds number means the coefficient is not a function of either the body's size or the wind velocity.

The experimental results of this study, both the full-scale and the wind tunnel tests, were reduced to dimensionless coefficient form for analysis. These coefficients are defined as follows:

Normal force coefficient, C_N

$$C_N = \frac{F_N}{qA_s} \qquad (2.2.1)$$

Side force coefficient, C_T

$$C_T = \frac{F_T}{qA_s} \qquad (2.2.2)$$

Lift force coefficient, C_L

$$C_L = \frac{F_L}{qA_s} \qquad (2.2.3)$$

Twisting moment coefficient, C_{MT}

$$C_{MT} = \frac{M_T}{qA_sW} \qquad (2.2.4)$$

Pitching moment coefficient, C_{MP}

$$C_{MP} = \frac{M_P}{qA_sW} \qquad (2.2.5)$$

Rolling moment coefficient, C_{MR}

$$C_{MR} = \frac{M_R}{qA_sW} \qquad (2.2.6)$$

where

F_N = normal force
F_T = side force
F_L = lift force
M_T = twisting moment
M_P = pitching moment
M_R = rolling moment

} These actions are shown in Figure 2.2.1 in their positive directions.

and

A_s = frontal area of sign

q = impact pressure

$= 1/2\ \rho V^2$

and,

ρ = mass density of air

V = velocity of air

W = width of sign

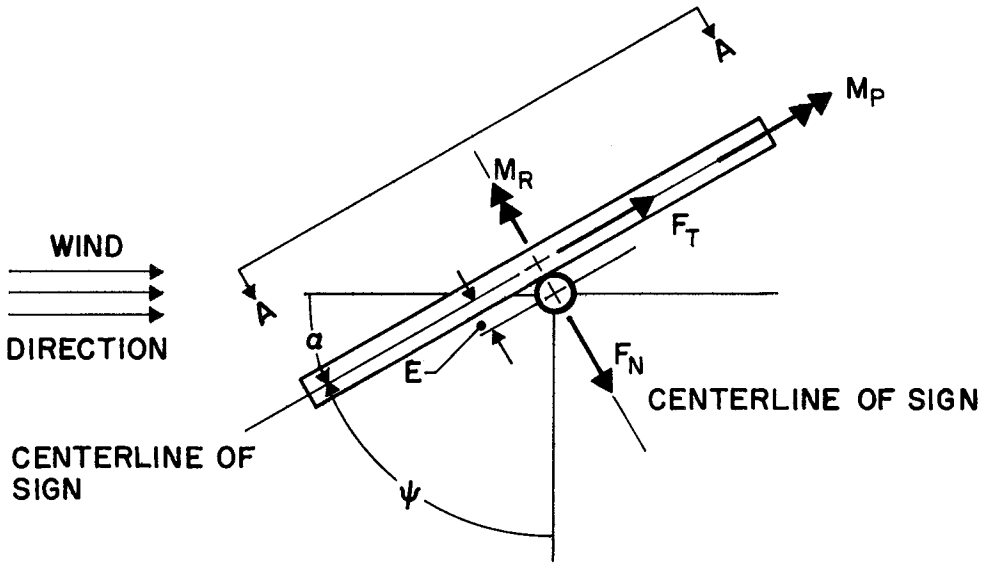

TOP VIEW

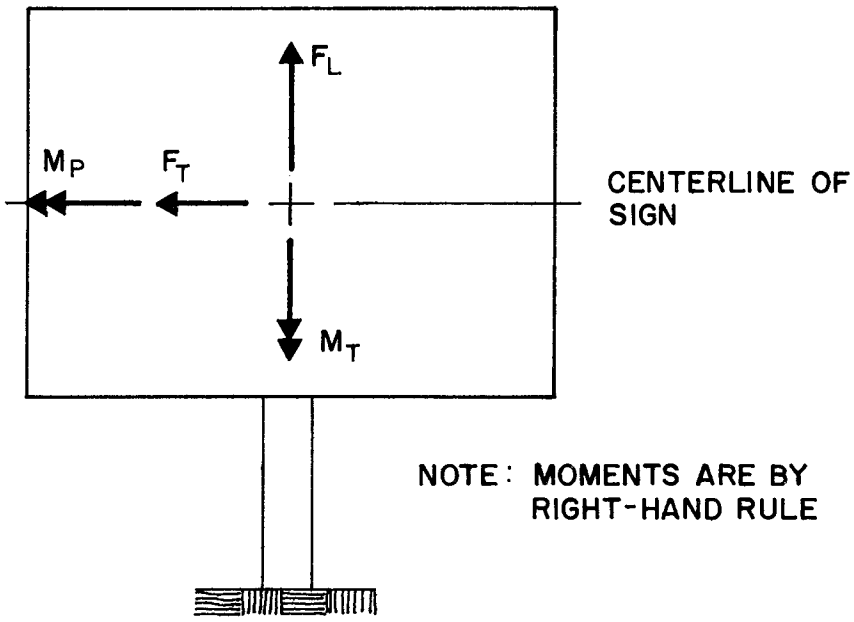

VIEW A-A

FIGURE 2.2.1 POSITIVE SIGN CONVENTION FOR SIGN AXIS SYSTEM

Full-scale tests. For a flat plate, solid background sign, three coefficients are sufficient to describe the effects of wind forces at various angles of attack. These are the side and normal force coefficient, C_T and C_N, and the twisting moment coefficient, C_{MT}. The lift force and the pitching and rolling moment are essentially zero. There may be some pitching moment on signs due to the wind velocity gradient that occurs in the vertical direction. However, this effect was found to be negligible.

In addition to the three coefficients, C_N, C_T, and C_{MT}, it is sometimes useful to know the location of the resultant normal force. With the instrumentation used on the full-scale sign it was possible to determine this location.

A computer program was written to assist in reducing the data obtained in the full-scale test. Input to the program consisted of the strain gage data, wind velocity and direction, sign direction and atmospheric conditions. Output consisted of three coefficients, C_N, C_T, and C_{MT}, and the resultant normal force location. The program and a description of its formulation are included in Appendix D.

A Gerber Digital Data Reduction System, shown in Figure 2.2.2, was used to reduce the oscillograph records. It was interconnected with an IBM 026 key punch machine for automatic card punching.

Information of wind speed and direction was recorded on strip charts, scaled such that the values could be read directly.

Wind tunnel tests. Six actions were measured and recorded for each model at a given angle of attack and wind velocity. These actions were in the "wind tunnel" axis system and had to be transformed into

FIGURE 2.2.2 GERBER DIGITAL

DATA REDUCTION SYSTEM

the "sign" axis system. After transformation the actions were reduced to dimensionless coefficients.

A computer program was written to assist in reducing the wind tunnel data. Input to the program consisted of the model geometry, impact pressure of wind, sign angle of attack, and the six actions in the "wind tunnel" axis system. The program transformed the actions to the "sign" axis system. Output consisted of six coefficients, C_N, C_T, C_L, C_{MT}, C_{MP}, and C_{MR}, and the location of the resultant normal force. The program and a description of its formulation are included in Appendix E.

2.3 Data Analysis

Full-scale tests. A total of eight tests were completed on the full-scale instrumented sign. A summary of these tests appears in Table 2.3.1. The information gained from these tests was considered to be sufficient to adequately describe the wind loads on the sign.

The test results contained a considerable amount of scatter. The scatter was attributed to several factors. One of the main contributing factors was the difference in response time of the two types of instrumentation used in obtaining the data. The instrumentation used in measuring the forces and twisting moment on the sign consists of strain gages and an oscillograph recorder. This type of instrumentation is, for all practical purposes, instantaneous. A cup type anemometer and a vane type wind direction indicator, together with pen type ink recorders, were used to obtain the wind velocity and direction. The response of this type of instrumentation is something less than

TABLE 2.3.1 SUMMARY OF FULL-SCALE TESTS

TEST	DATE	NO. OF RUNS	AVERAGE VELOCITY (ESTIMATED) (mph)	COMMENTS
1	10/ 5/66	8	15	Relatively low wind velocity. All instrumentation functioning properly.
2	10/14/66	11	20	All O.K.
3	10/15/66	9	20	All O.K.
4	10/19/66	9	25	Instrumentation problem with Channel (or Bridge) Number 3. Other measurements O.K.
5	11/ 4/66	9	25	All O.K.
6	11/10/66	8	NO WIND	Test used to check zero balance on instrumentation (no-load condition).
7	12/ 7/66	10	30	All O.K.
8	1/16/67	9	25	Wind speed and direction amplifer malfunction. Some of data O.K.

instantaneous.

This difference in response time obviously presents problems when correlating the forces on the sign with the corresponding wind velocity and wind direction. However, steps were taken to cope with this problem. The first corrective action taken was to locate the anemometer several feet upstream from the sign. This met with limited success.

Better results were obtained by a closer examination of the data. For each test, an attempt was made to compute the actual lag time, i.e., the amount of time by which the wind velocity and direction data lagged the strain gage data. In this manner a better correlation of the data was realized. Another means used in reducing the data was to take advantage of recorded periods of time in which the wind velocity was relatively steady. These periods, which were usually three or four seconds in duration, allowed the wind recording devices sufficient time to stabilize and "catch up" with the strain gage readings.

Another major factor which is believed to have contributed to the scatter was a difference in wind velocity and direction at the location of the wind instruments and the sign itself. As mentioned earlier, the wind instruments were located at the same elevation as the center of the sign, but approximately 20 feet from the center of the sign in a direction perpendicular to the wind direction. Velocity gradients as large as ±25% have been measured over a distance of 11 feet.[14] However, with the large number of data points recorded, the effects of this velocity gradient were assumed to be self-equilibrating, i.e., in some cases the recorded velocities were higher than the average velocity of wind on the sign, while in other cases the recorded velocities

were lower.

A multiple regression curve fitting computer program was used in analyzing the full-scale data due to the amount of scatter. Different degree polynomials were used in determining the best curve fit. Actual data prints are omitted on the plots to insure clarity. Each curve represents a best fit of approximately 500 data points.

For a normal force coefficient, a fifth degree polynomial through the test results represented the best fit. The normal force coefficient is shown in Figure 2.3.1, plotted against the angle of attack. A third degree polynomial appeared to represent the best fit curve for the side force coefficient and the moment coefficient data as shown in Figures 2.3.2 and 2.3.3, respectively.

No definite reasons can be given for the apparent values of side force and twisting moment at a sign angle of attach of 90 degrees. It is likely due to small discrepancies in the side force data. As shown in Appendix D, the measured value of the moment includes the effect of the side force acting at a known distance from the center of the instrumented pole. This effect has to be subtracted from the measured value of the moment in order to obtain the correct twisting moment. Therefore, if the side force measurements contain discrepancies, so will the calculated moment values. However, the magnitude of the error in the moment values will be, at most, equal to the error in the side force.

The difficulties in measuring the side force were mainly due to the relatively low sensitivity of the bridges used in determining the side forces. The mechanical section properties of the instrumented tubular support in bending were essentially the same in all directions.

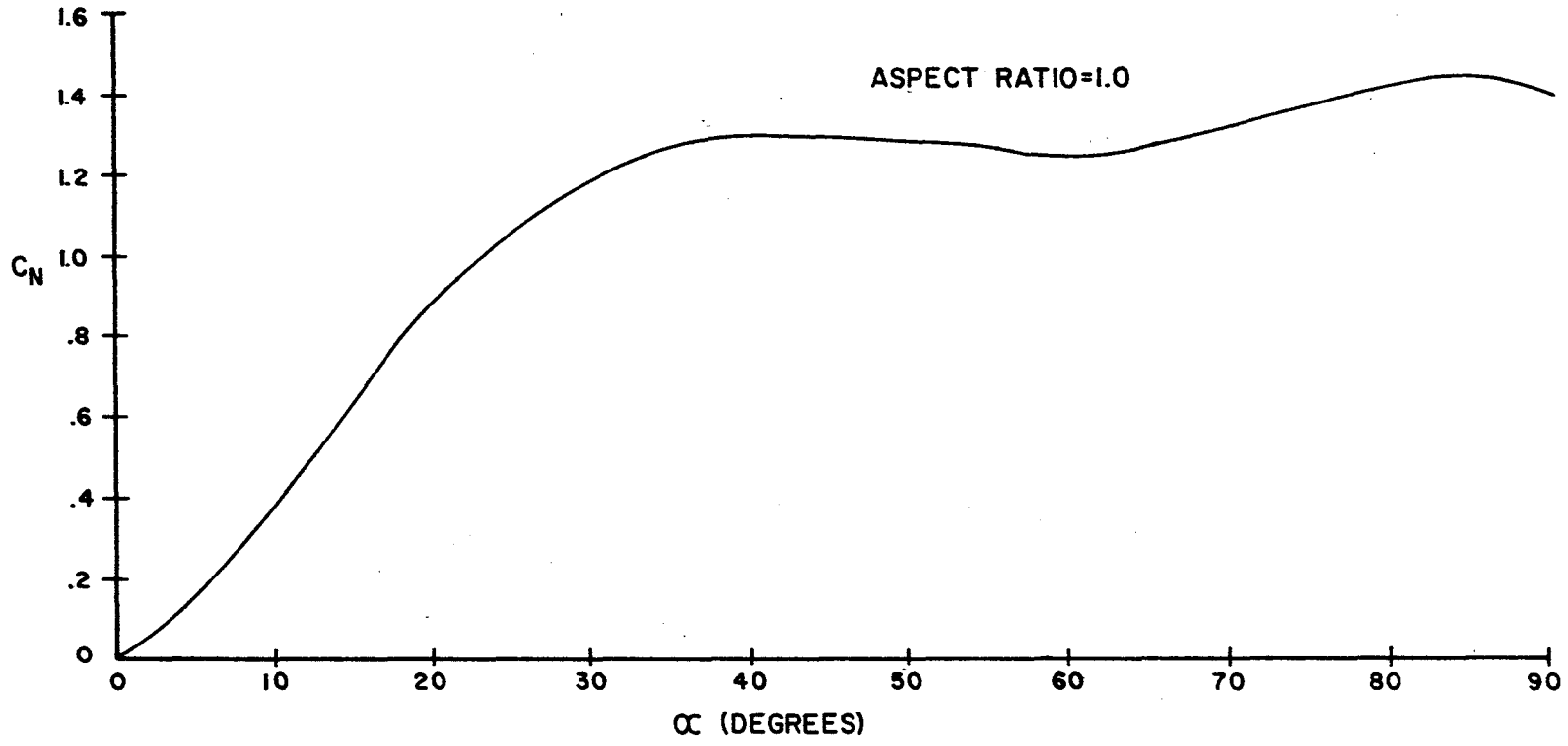

FIGURE 2.3.1 NORMAL-FORCE COEFFICIENT VERSUS ANGLE OF ATTACK, FULL-SCALE SIGN

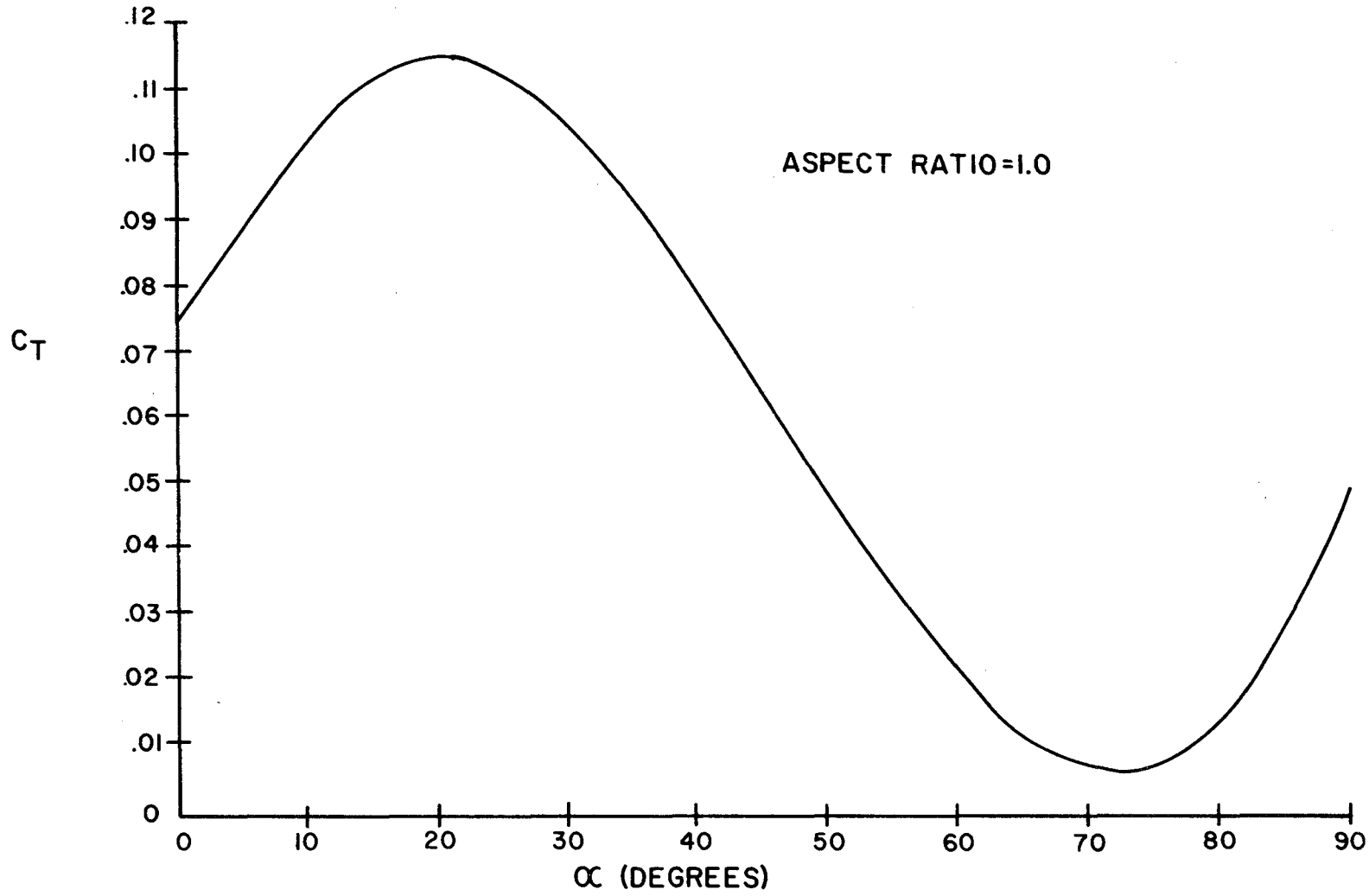

FIGURE 2.3.2 SIDE-FORCE COEFFICIENT VERSUS ANGLE OF ATTACK, FULL-SCALE SIGN

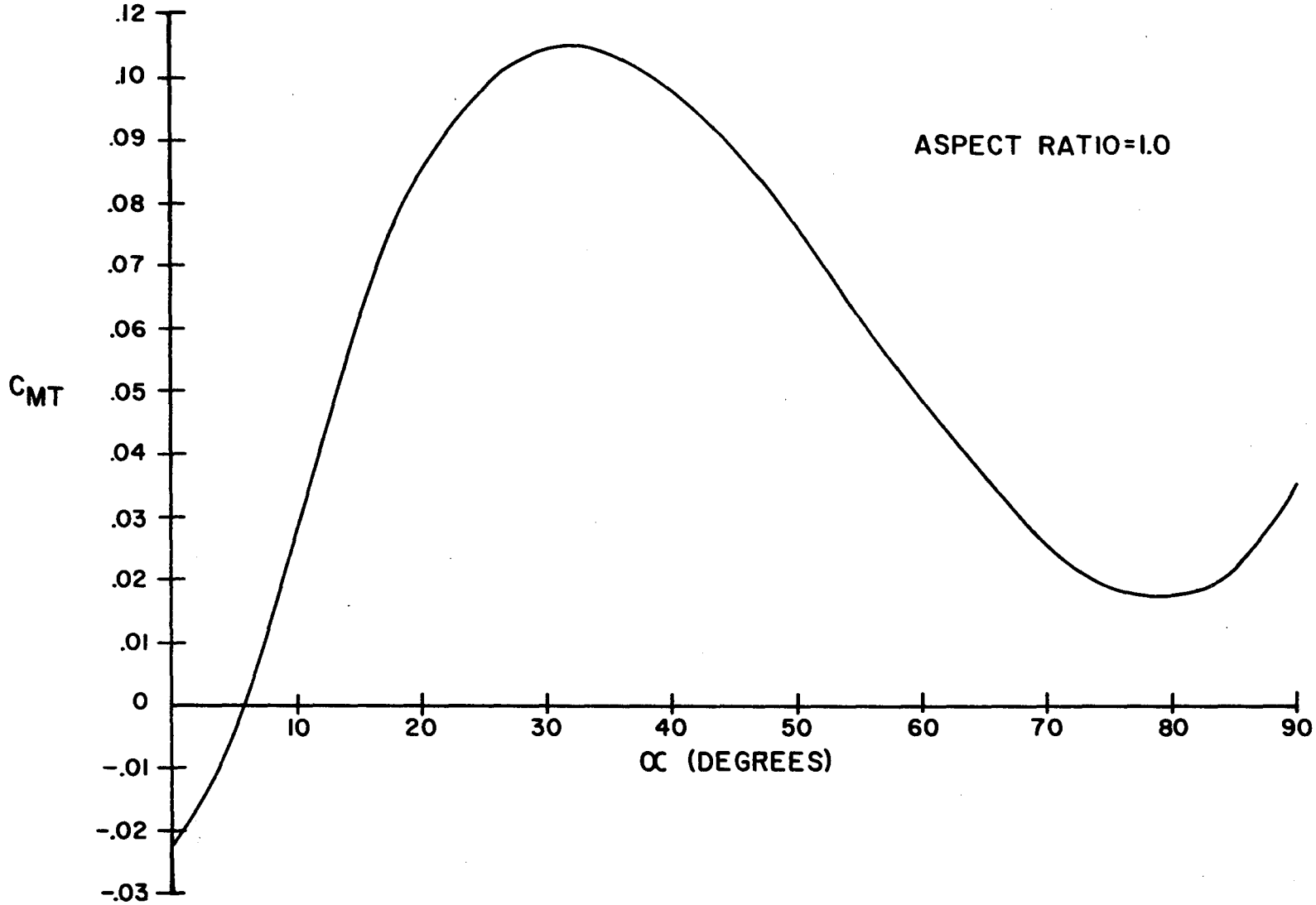

FIGURE 2.3.3 TWISTING-MOMENT COEFFICIENT VERSUS ANGLE OF ATTACK, FULL-SCALE SIGN

The small values of the side force, coupled with the large section properties of the pole, resulted in small signal outputs. High gain was then required of the amplifiers in order to obtain measurable deflections on the oscillograph records. In instances of low wind velocity, it was especially difficult to measure accutately the small deflections, even with maximum gain.

The natural vibrations of the sign structure were recorded by the oscillograph. (Reference Appendix C, Figure C-1.2.) This also contributed to the difficulties encountered in measuring the side force.

Values of the moment coefficient between approximately 15° and 75° are considered to be essentially accurate. The contribution of the side force to the measured moment in this range is small compared to the normal force contribution, i.e., if errors did exist in the side force data, they would not influence the values of the calculated moment to any extent.

The side force coefficients include the effects of wind on that part of the support which is directly behind the sign face. This explains the relatively large values of the side force coefficient at an angle of attack of 0°. It is also the main reason that the moment coefficients are not zero at the 0° angle of attack. At an angle of attack of approximately 30° or greater, the support had little influence on the side force. This was due to the separation of air behind the sign.

The location of the resultant normal force in the vertical direction was found to be, on the average, at the center of the sign. The

horizontal location is shown in Figure 2.3.4, plotted against the angle of attack. Again, the small discrepancies in the horizontal location between the angles of attack of 75° to 90° are attributed to the discrepancies in the side force data.

An extensive gust analysis of the wind was not undertaken. However, included in Appendix C is an observation of the wind speed measurements for a particular test in which the wind was rather gusty. Also included is an explanation of "fastest mile of wind" and how the gust factor is related to it.

No recommendations can be made with regard to gust factors on signs based on the results of the full-scale tests. The conditions under which the tests were made would not justify it, i.e., relatively low wind speeds and no storm conditions. The 1.3 gust factor recommended in the present criteria[13] seems to be in agreement with the general consensus.[15]

Wind tunnel tests of conventional sign models. The normal force coefficient, side force coefficient, and twisting moment coefficient of the three flat plate models are shown plotted against the angle of attack in Figures 2.3.5, 2.3.6 and 2.3.7, respectively.

As seen in Figures 2.3.5, the normal force coefficient increases as the aspect ratio decreases, at least for the range tested. This trend is in agreement with the results of Winter[5] and Tidwell[6] in their tests of flat plates for the same aspect ratio. The magnitudes of the maximum normal force coefficients obtained by Winter were somewhat higher than those shown here, with Tidwell's values being slightly lower. A

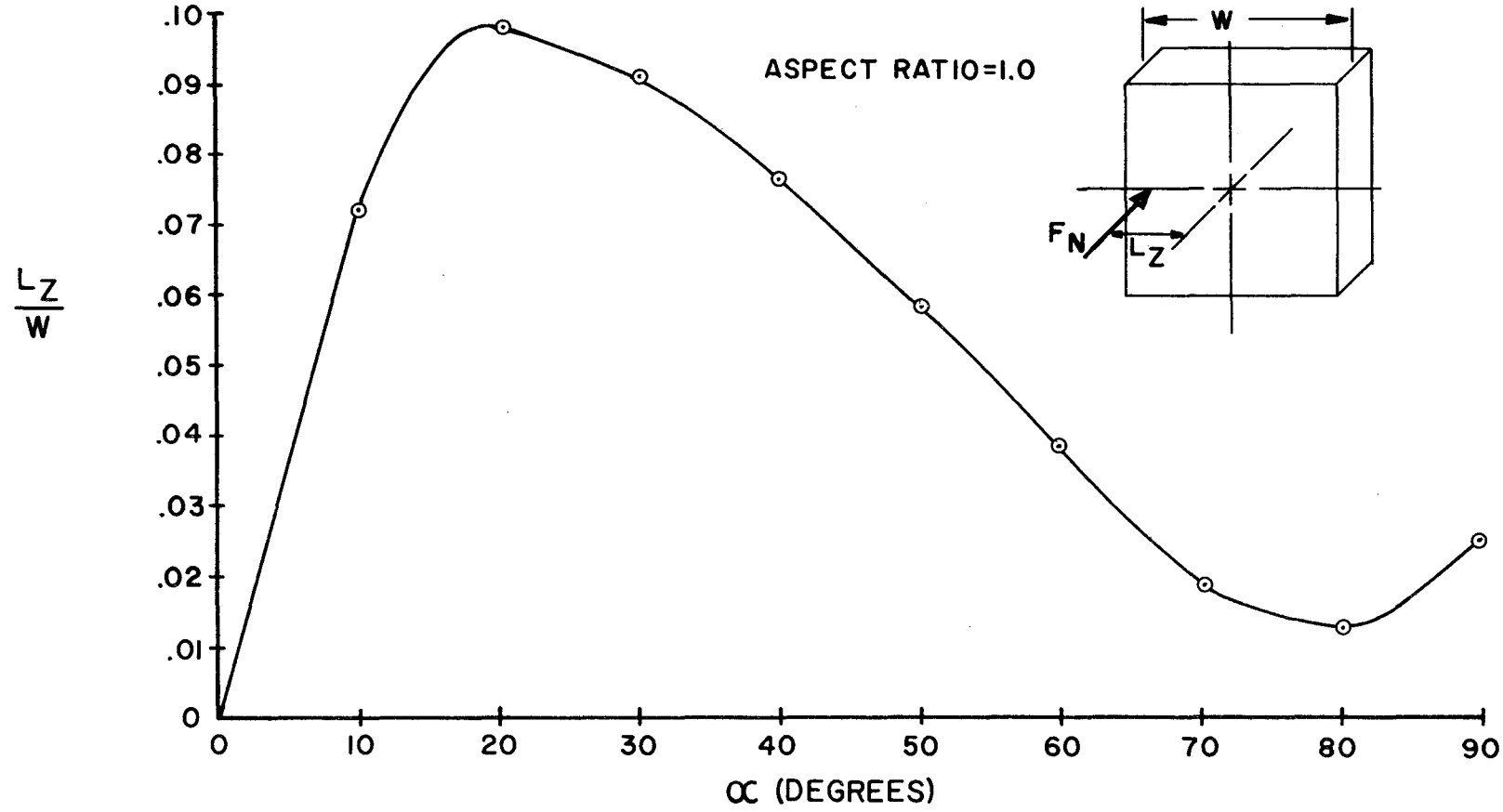

FIGURE 2.3.4 NORMAL-FORCE LOCATION VERSUS ANGLE OF ATTACK, FULL-SCALE SIGN

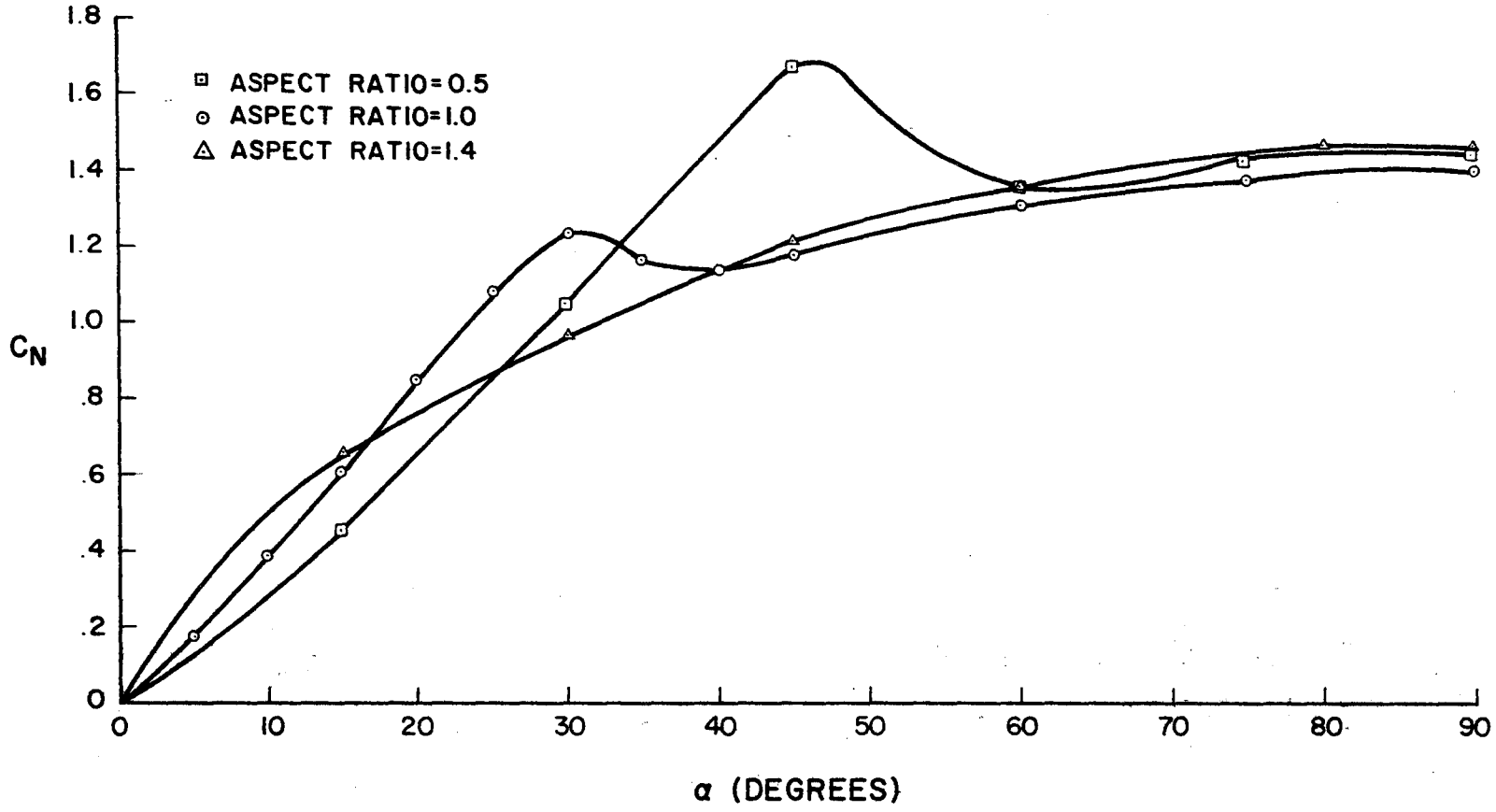

FIGURE 2.3.5 NORMAL-FORCE COEFFICIENT VERSUS ANGLE OF ATTACK, FLAT-PLATE MODELS

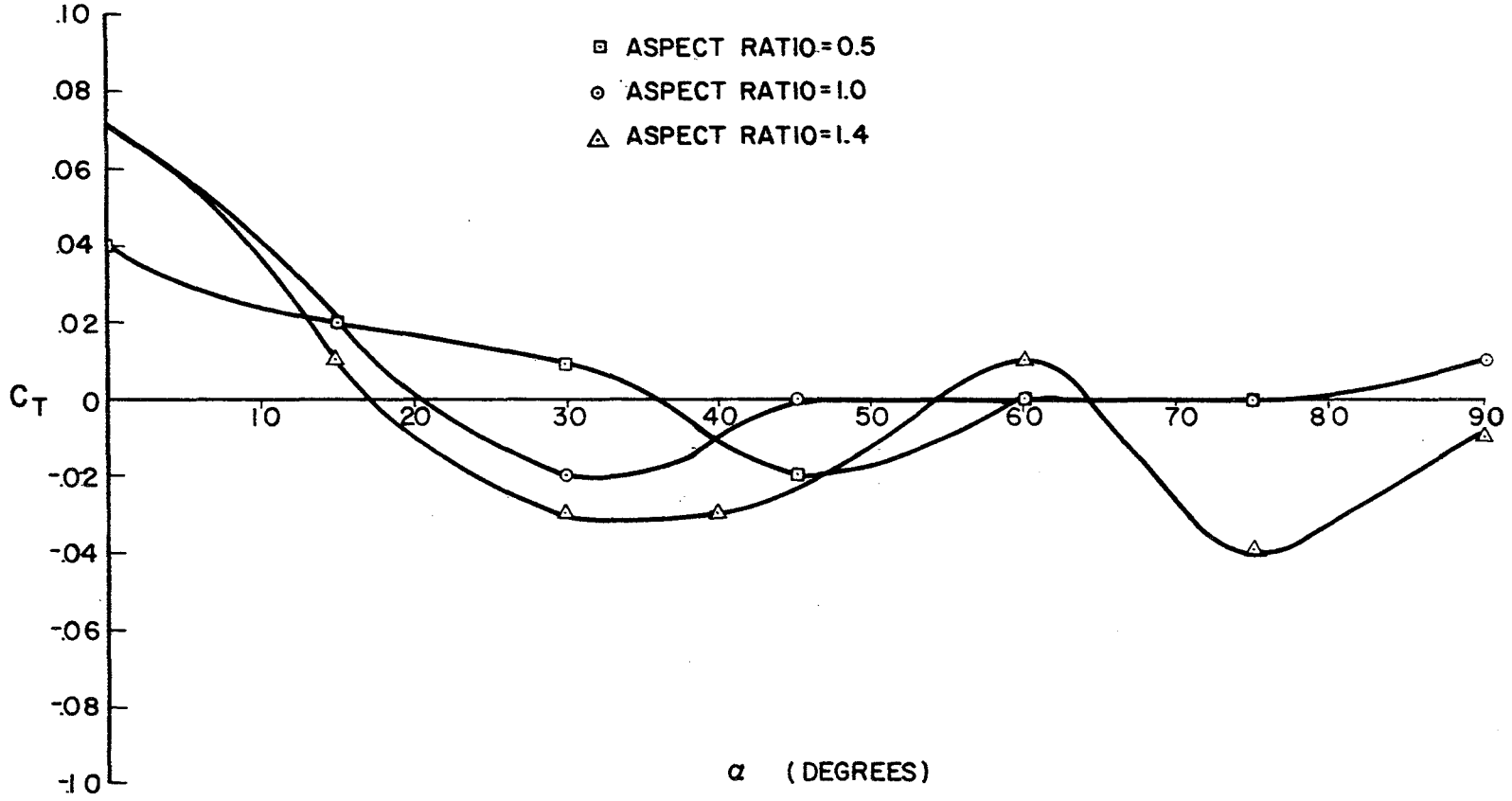

FIGURE 2.3.6 SIDE-FORCE COEFFICIENT VERSUS ANGLE OF ATTACK, FLAT-PLATE MODELS

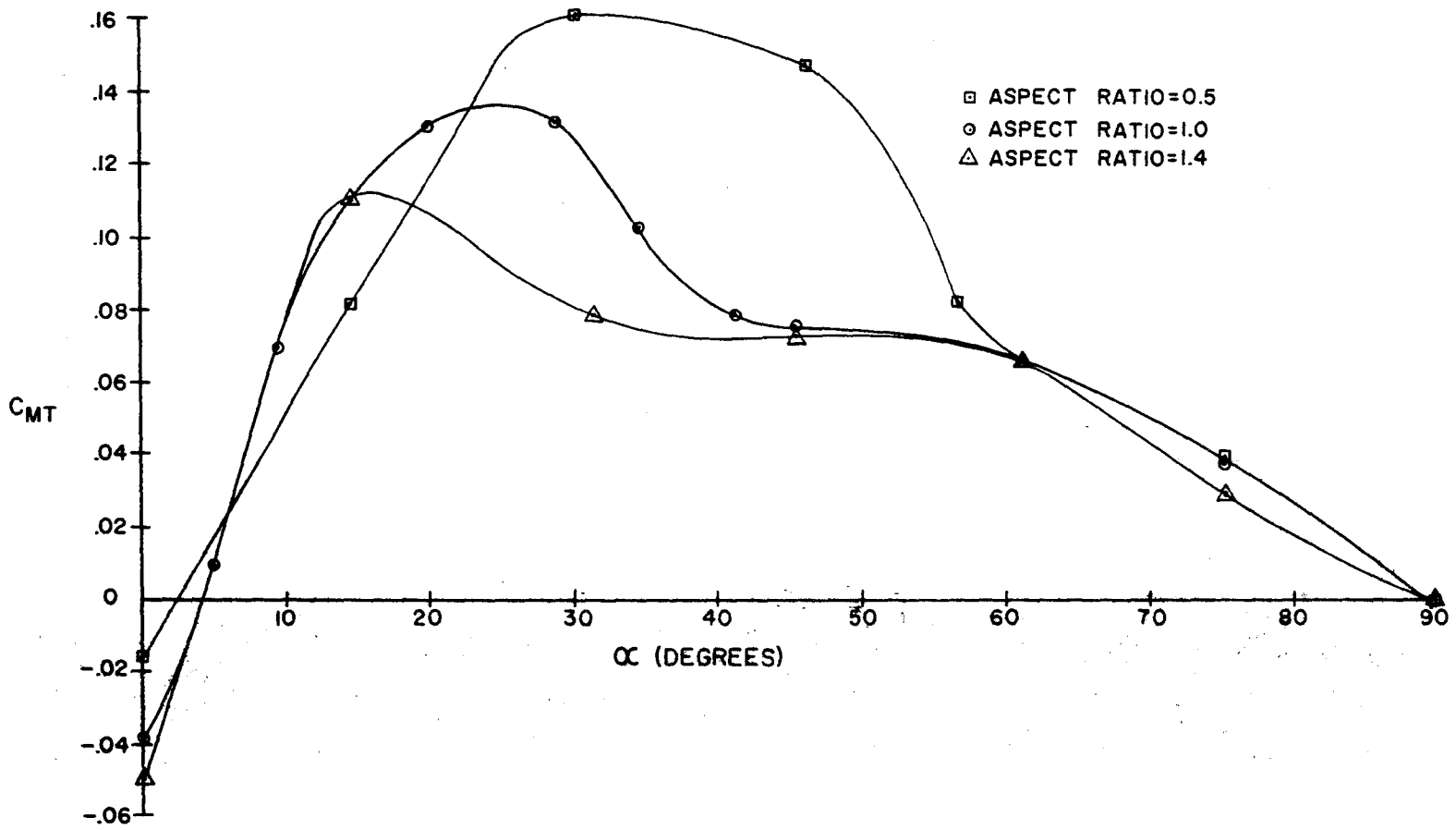

FIGURE 2.3.7 TWISTING-MOMENT COEFFICIENT VERSUS ANGLE OF ATTACK, FLAT-PLATE MODELS

plot of the normal force coefficient versus aspect ratio is shown in Figure 2.3.8 for various angle of attack values.

A plot of the normal force coefficient versus Reynolds number is shown in Figure 2.3.9. The values of the normal force coefficient at an angle of attack of 90° were practically the same for the three different aspect ratios. The variations of the coefficient with Reynolds number were about the same also. Hence the one plot in Figure 2.3.9.

The different Reynolds number values were obtained by varying the wind velocity. As shown, the coefficients are essentially independent of the Reynolds numbers.

The test results show the vertical location of the normal force as being at the center of the model, as was the case in the full-scale test. The results of the horizontal location are shown in Figure 2.3.10 plotted against the angle of attack.

Comparison of conventional sign data. In general, close agreement was obtained between full-scale tests and the wind tunnel tests.

Shown in Figure 2.3.11 is a comparison of the normal force coefficient results. The variation in the two curves at angles of attack between 30° and 45° is attributed to the different environments in which the tests were conducted. In the wind tunnel the air flow entering the test section is maintained at a constant velocity. It is also in a streamlined state with no turbulence. Under these conditions, a distinct drop in the normal force will occur after a certain angle of attack is reached. The point at which this occurs is termed the stall

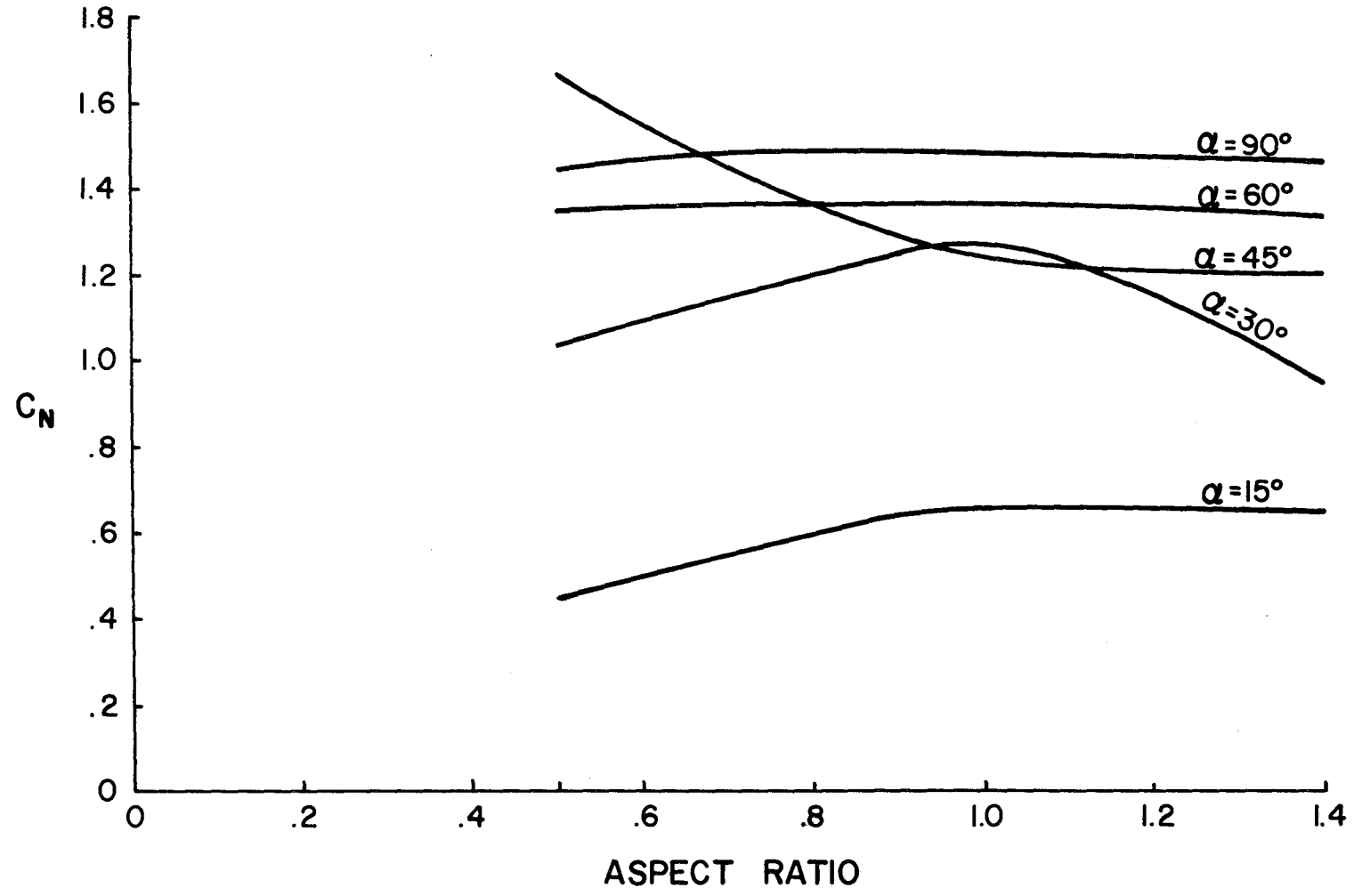

FIGURE 2.3.8 NORMAL-FORCE COEFFICIENT VERSUS ASPECT RATIO, FLAT-PLATE MODELS

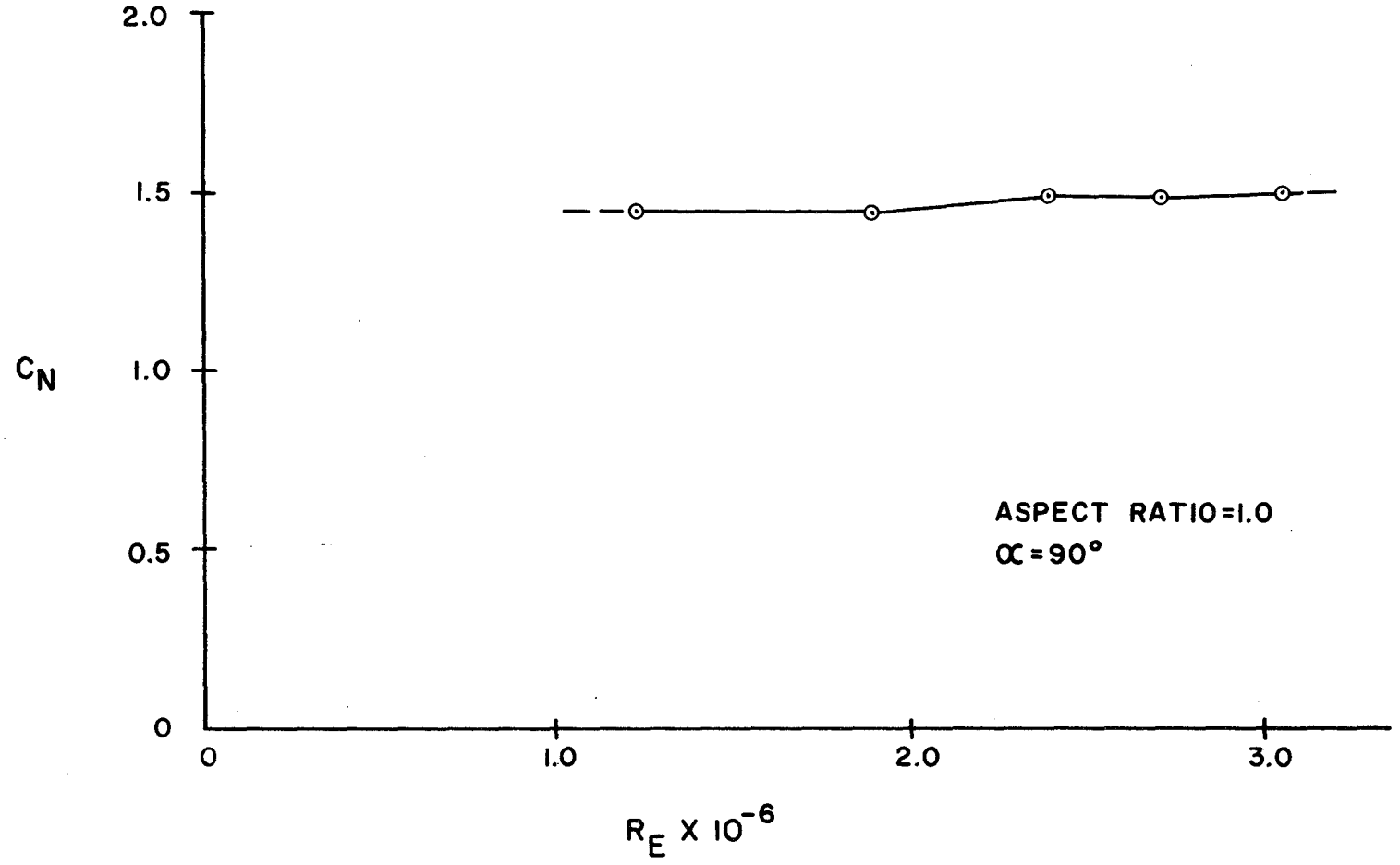

FIGURE 2.3.9 NORMAL-FORCE COEFFICIENT VERSUS REYNOLDS NUMBER, FLAT-PLATE MODEL

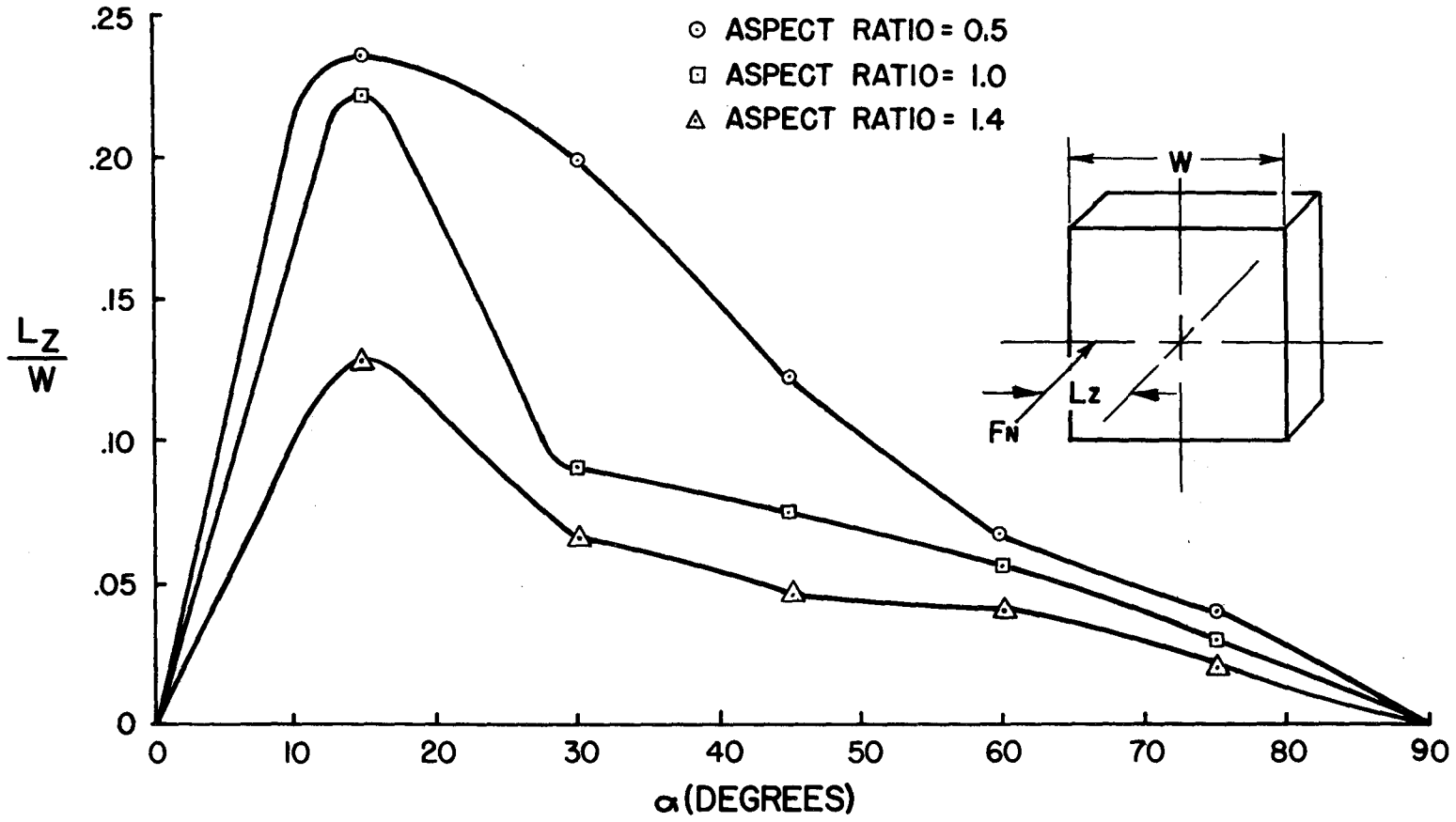

FIGURE 2.3.10 NORMAL-FORCE LOCATION VERSUS ANGLE OF ATTACK, FLAT-PLATE MODELS

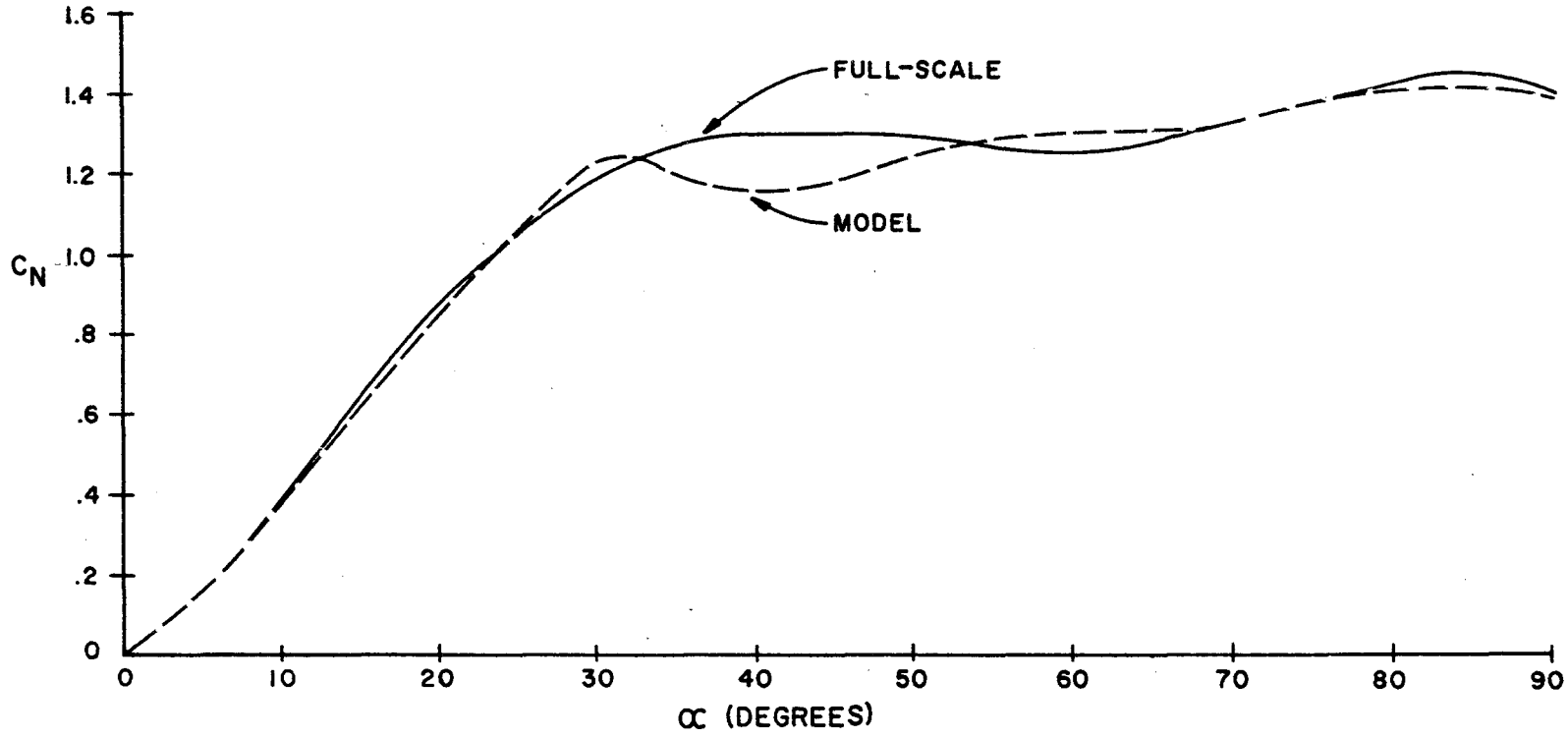

FIGURE 2.3.11 NORMAL-FORCE COEFFICIENT VERSUS ANGLE OF ATTACK, FULL-SCALE AND MODEL TESTS

point. In a sign's natural environment the air flow is usually turbulent. The general direction of the air flow is continuously changing, also. These conditions tend to prevent the formation of the stall.

In comparing the curves of Figures 2.3.3 and 2.3.7, for an aspect ratio equal to 1.0, it can be seen that favorable agreement was obtained between the twisting moments. As shown, the maximum value of the moment coefficient was larger in the model results. The difference is attributed to the different environments under which the tests were conducted, as just described, and difficulties experienced in the side force measurements, described in "Full scale tests" of Section 2.3.

The mathematical signs of the coefficients shown plotted in Figure 2.3.7 are opposite the actual measured values. The signs were changed in order to compare the data with the full-scale data of Figures 2.3.3

The orientation of the model in the wind tunnel was as shown in Figure 2.1.21. The models were rotated clockwise from an initial rotation angle Ψ equal to zero. From $\Psi = 0°$ to $\Psi = 90°$ (or from $\alpha = 90°$ to $\alpha = 0°$) it can be seen that the twisting moment, M_T, in the "sign" axis system (Figure 2.2.1), would be negative.

It should be noted that the mathematical sign of the coefficients is immaterial in conventional sign design. The sign in its field location is subjected to winds from all directions. Any combination of mathematical signs on the forces and moments can be obtained.

Some disagreement exists between the full-scale and model results of the side force measurements. The differences are seen in comparing Figures 2.3.2 and 2.3.6. As mentioned before, it was difficult to

measure the small values of side force in the full-scale studies. This accounts for some of the disagreement. The difference in the surface roughness of the full-scale sign and the flat plate models likely contributed to the disagreement, also.

All of the conventional sign data, both full-scale and model data, are shown at positive angles of attack, i.e., wind impinging on the front of the sign. Tests were conducted at negative angles of attack also. The results were similar to those at positive angles.

It is recommended that the wind tunnel results of the conventional sign models be used as design criteria for full-scale signs. The recommendation is based on the relative accuracies of the two methods of data acquisition. It was apparent that the accuracy of the wind tunnel measurements exceeded those of the full-scale tests, especially in the smaller side force values.

The close agreement between the normal force results of the full-scale and wind tunnel tests show the applicability of model tests. The coefficients were also shown to be essentially independent of the Reynolds number (Figure 2.3.9). This, in itself, indicates that the model data can be applied to larger signs.

Wind tunnel tests of straight louver models. The results of the wind tunnel wall interference tests are shown in Figure 2.3.12. The purpose of this test was to determine the amount by which the true wind loads are affected by the wall's influence. The wall interference may be defined as the distortion of the flow in the test section resulting from the constrainment of the air flow within the wind tunnel walls.

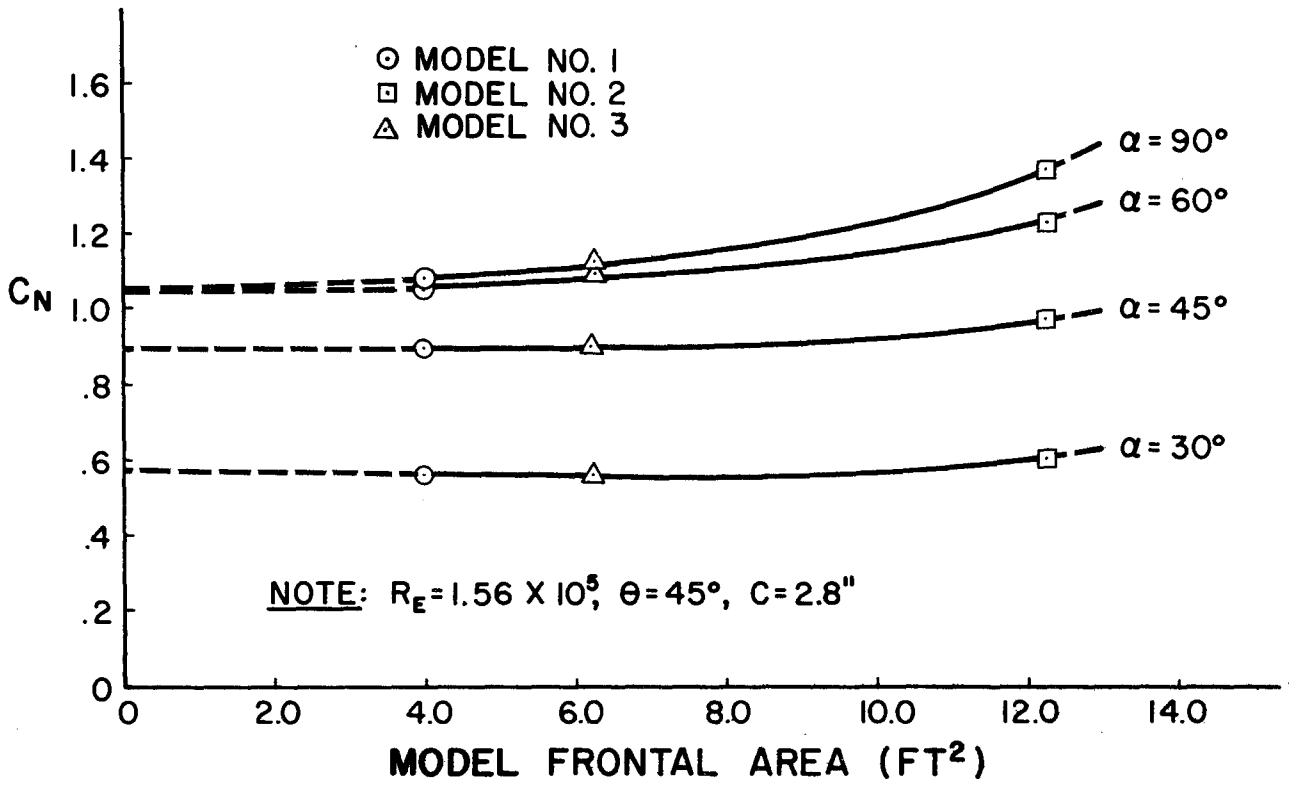

FIGURE 2.3.12 INTERFERENCE TEST

The three models used in the test had constant aspect ratios (AR = 1.0), constant louver angles (θ = 45°), and constant louver widths (C = 2.8 inches). The model frontal areas were 12.2, 6.4, and 4.1 square feet.

As shown in Figure 2.3.12, the interference effect was greatest at an angle of attack of 90°. This was the angle at which the model affected the greatest amount of air flowing through the test section. The value of C_N on model number 3 (frontal area of four square feet) appeared to be interference free. The slope of the curves at this point approach zero. The interference effect was therefore assumed to be negligible for the models with frontal areas of four square feet or less. All the remaining tests were conducted with models of approximately four square feet of frontal area.

Models 3 through 11 were used to determine the amount by which the wind loads were affected by variations in the louver angle, louver width, and Reynolds number. Models 7, 12, and 13 were used to determine the wind load variations due to aspect ratio changes.

In order to compare the results, the tests were all conducted at a constant Reynolds number ($R_E = 1.56 \times 10^5$), with the exception of the Reynolds number tests. The louver width was chosen as the characteristic length of the Reynolds number.

Curves of the normal force coefficient, side force coefficient, lift force coefficient, and twisting moment coefficient are shown in Figures 2.3.13 through 2.3.24, plotted against the angle of attack. Each figure contains three curves. The three curves represent the results of the three louver angle configurations for a particular louver width.

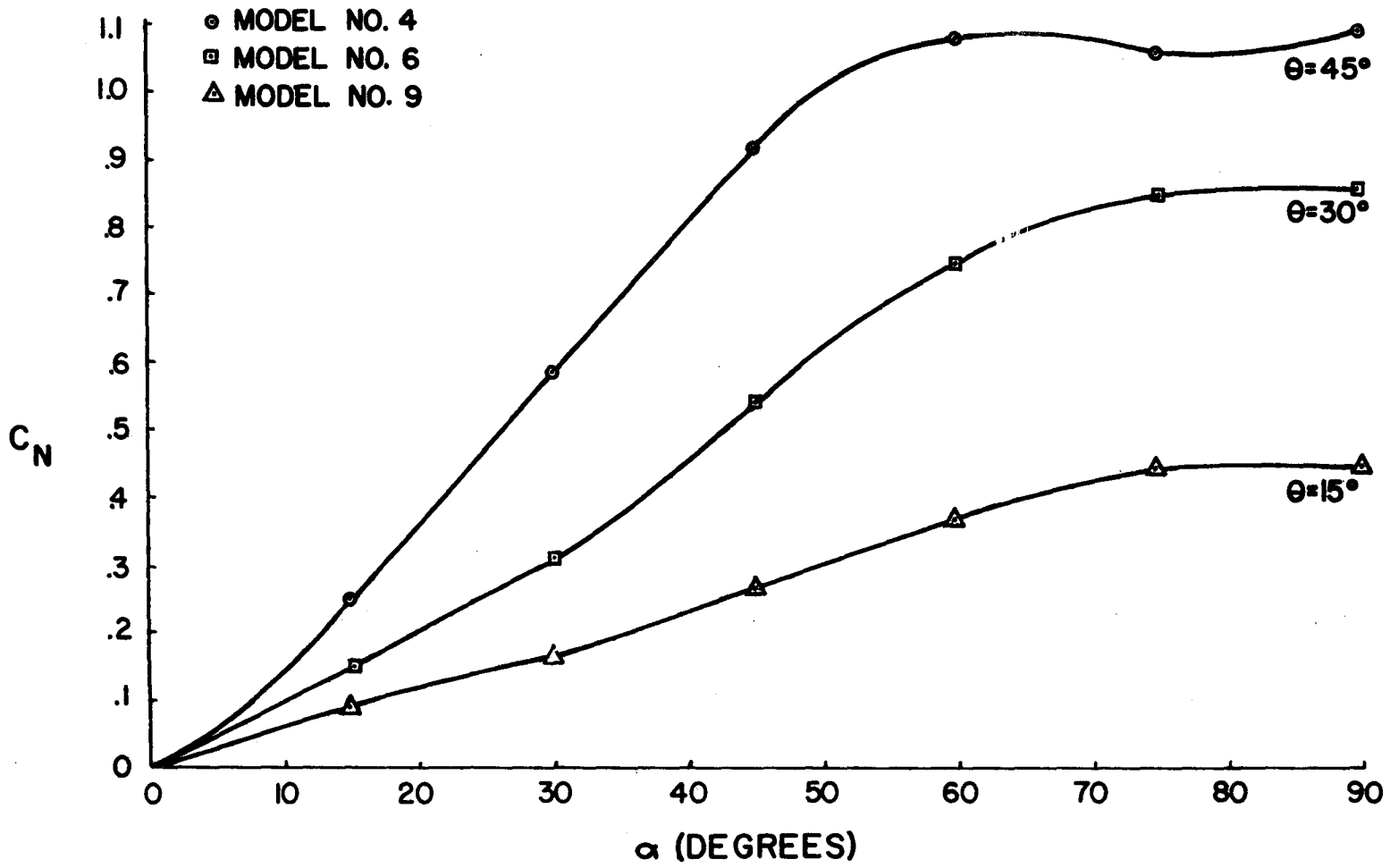

FIGURE 2.3.13 NORMAL-FORCE COEFFICIENT VERSUS ANGLE OF ATTACK FOR STRAIGHT LOUVER MODELS, LOUVER WIDTH=2.0 INCHES

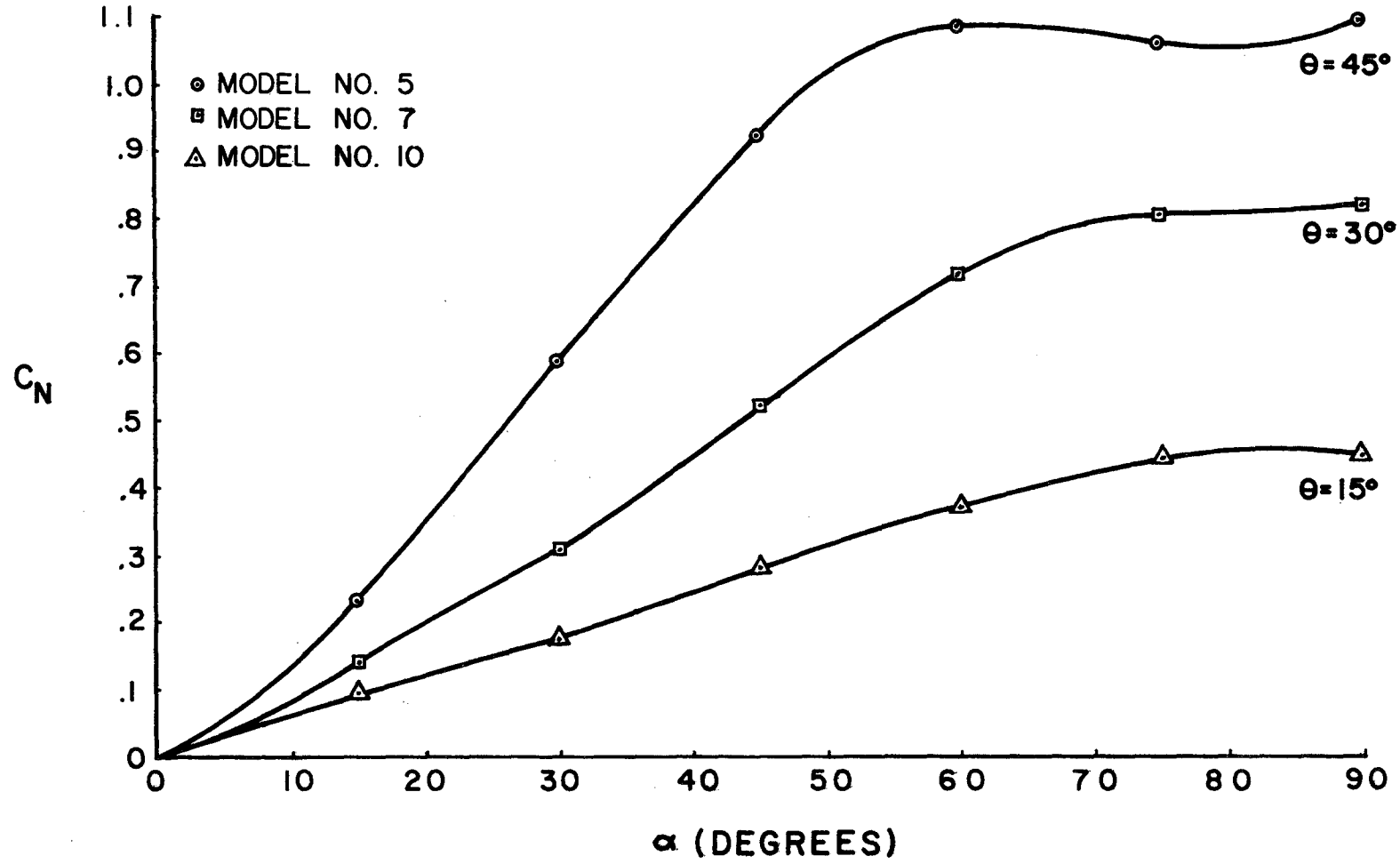

FIGURE 2.3.14 NORMAL-FORCE COEFFICIENT VERSUS ANGLE OF ATTACK FOR STRAIGHT LOUVER MODELS, LOUVER WIDTH=2.3 INCHES

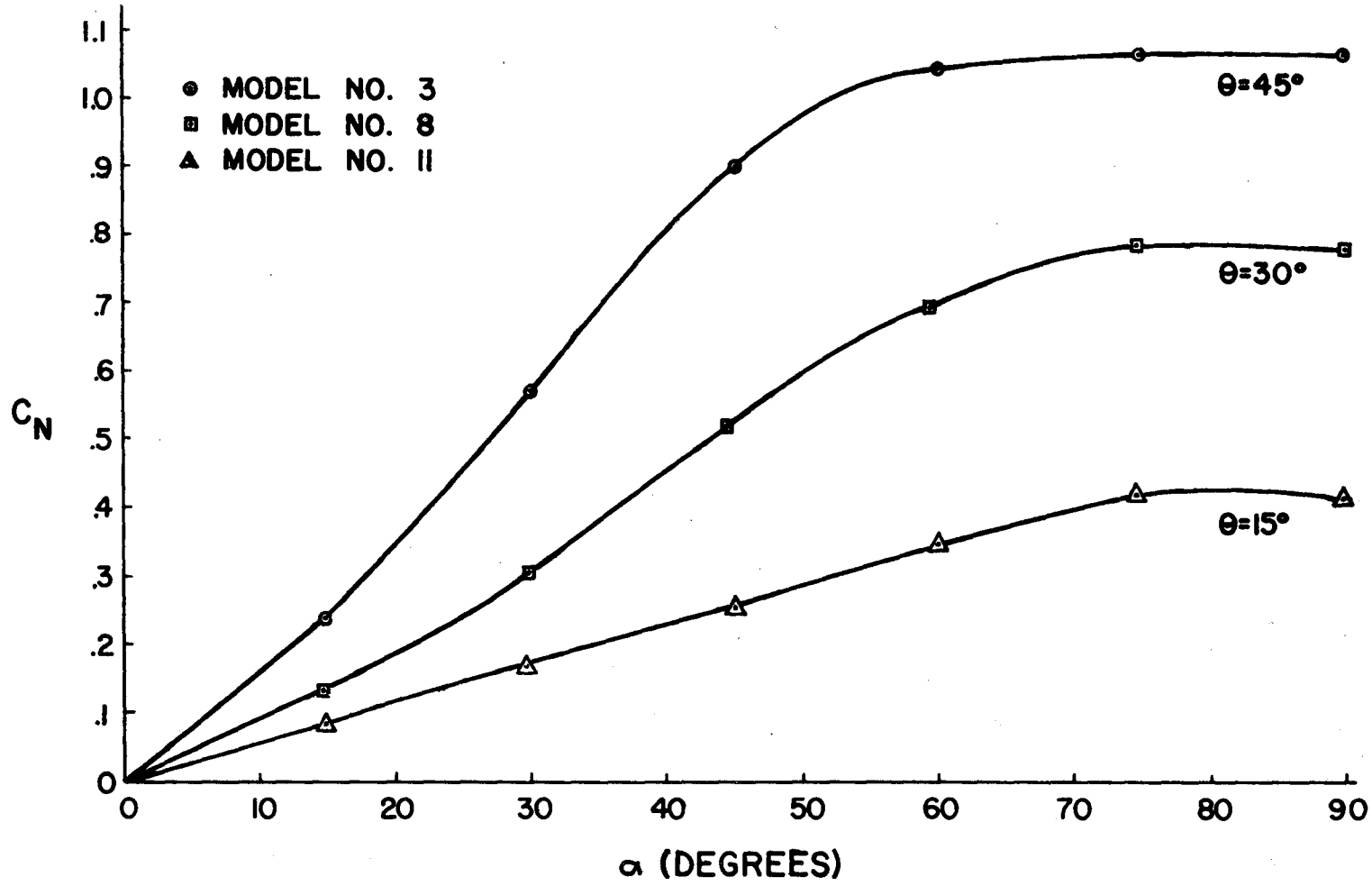

FIGURE 2.3.15 NORMAL-FORCE COEFFICIENT VERSUS ANGLE OF ATTACK FOR STRAIGHT LOUVER MODELS, LOUVER WIDTH=2.8 INCHES

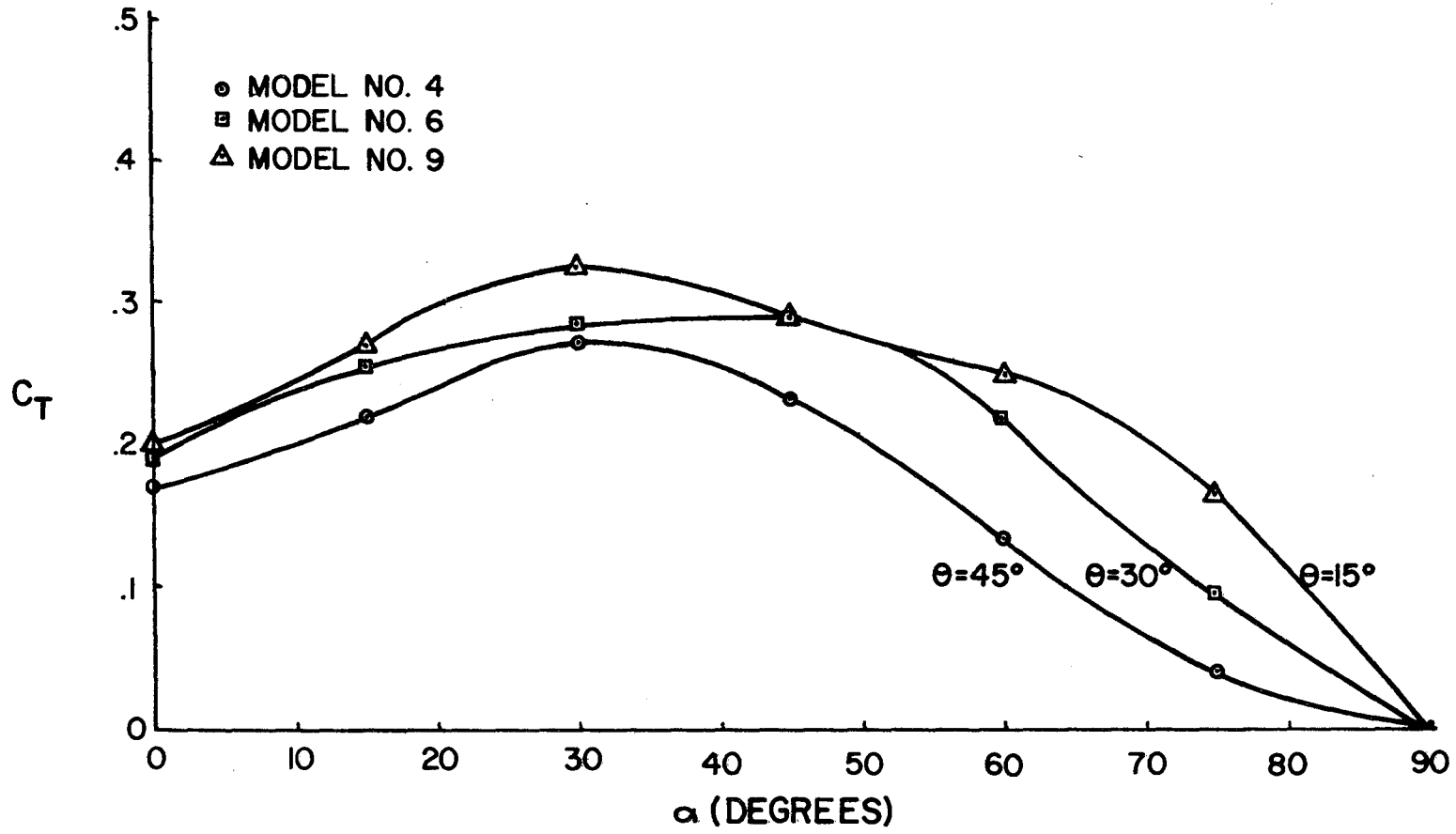

FIGURE 2.3.16 SIDE-FORCE COEFFICIENT VERSUS ANGLE OF ATTACK FOR STRAIGHT LOUVER MODELS, LOUVER WIDTH=2.0 INCHES

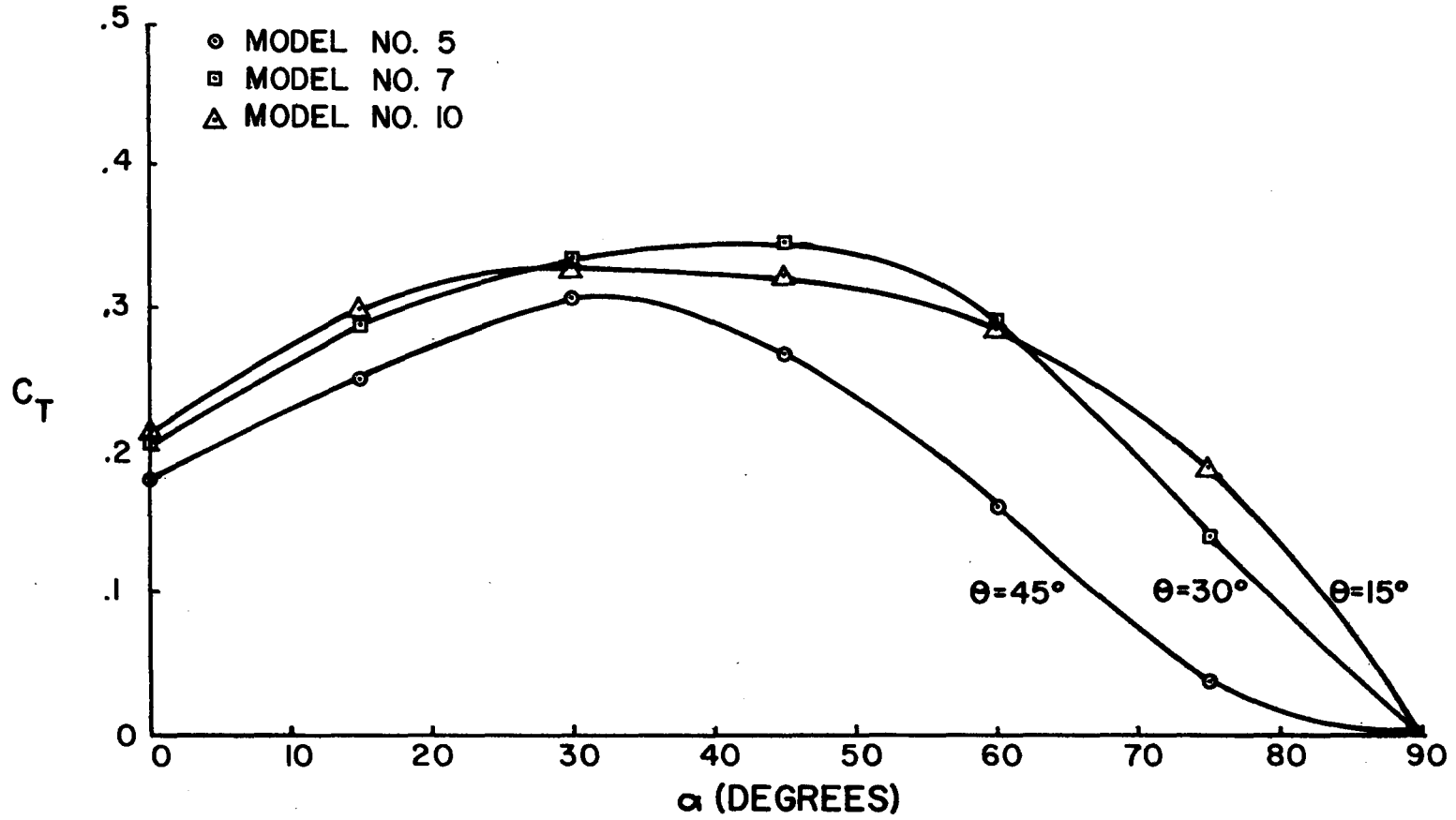

FIGURE 2.3.17 SIDE-FORCE COEFFICIENT VERSUS ANGLE OF ATTACK FOR STRAIGHT LOUVER MODELS, LOUVER WIDTH=2.3 INCHES

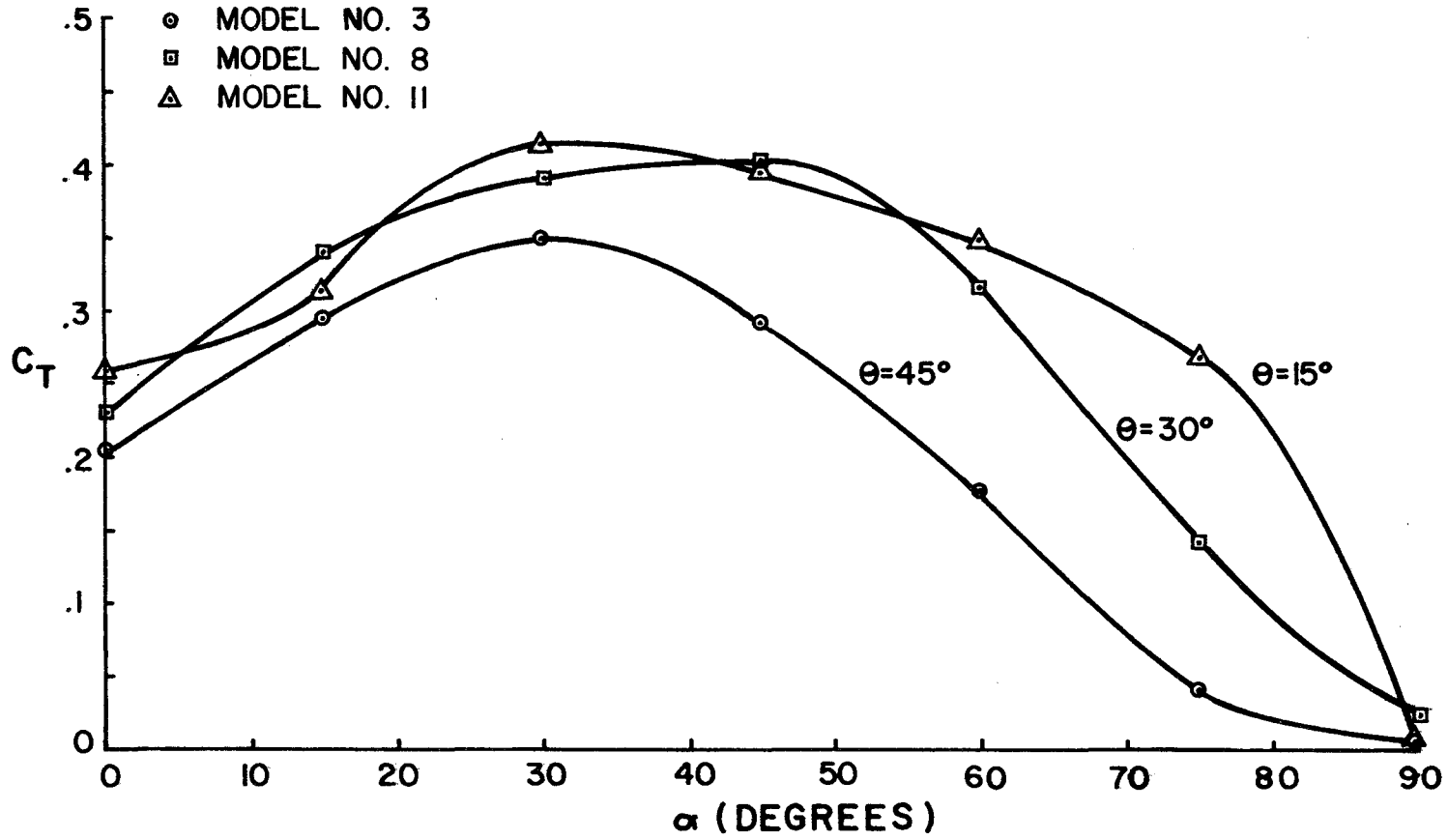

FIGURE 2.3.18 SIDE-FORCE COEFFICIENT VERSUS ANGLE OF ATTACK FOR STRAIGHT LOUVER MODELS, LOUVER WIDTH = 2.8 INCHES

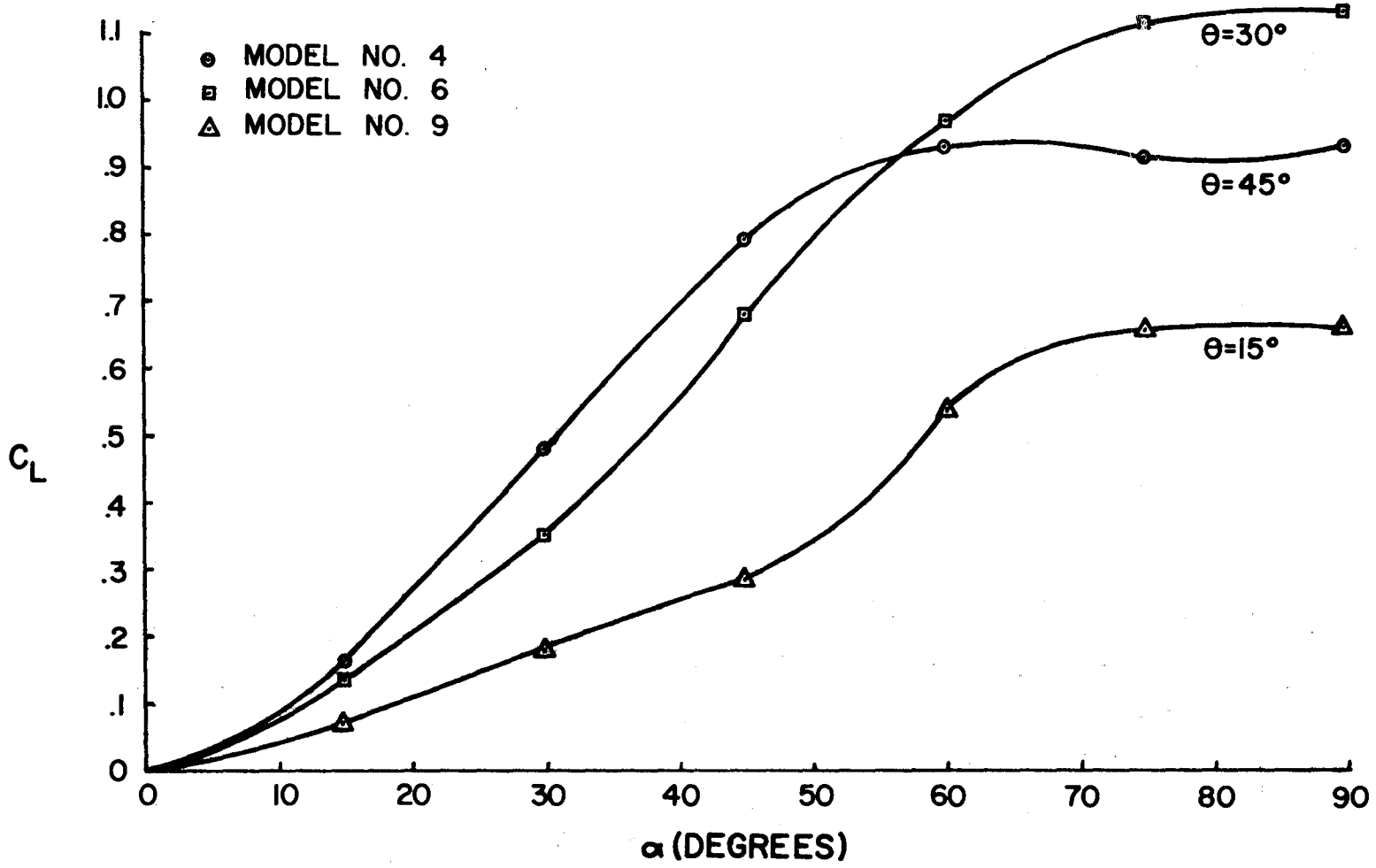

FIGURE 2.3.19 LIFT-FORCE COEFFICIENT VERSUS ANGLE OF ATTACK FOR STRAIGHT LOUVER MODELS, LOUVER WIDTH=2.0 INCHES

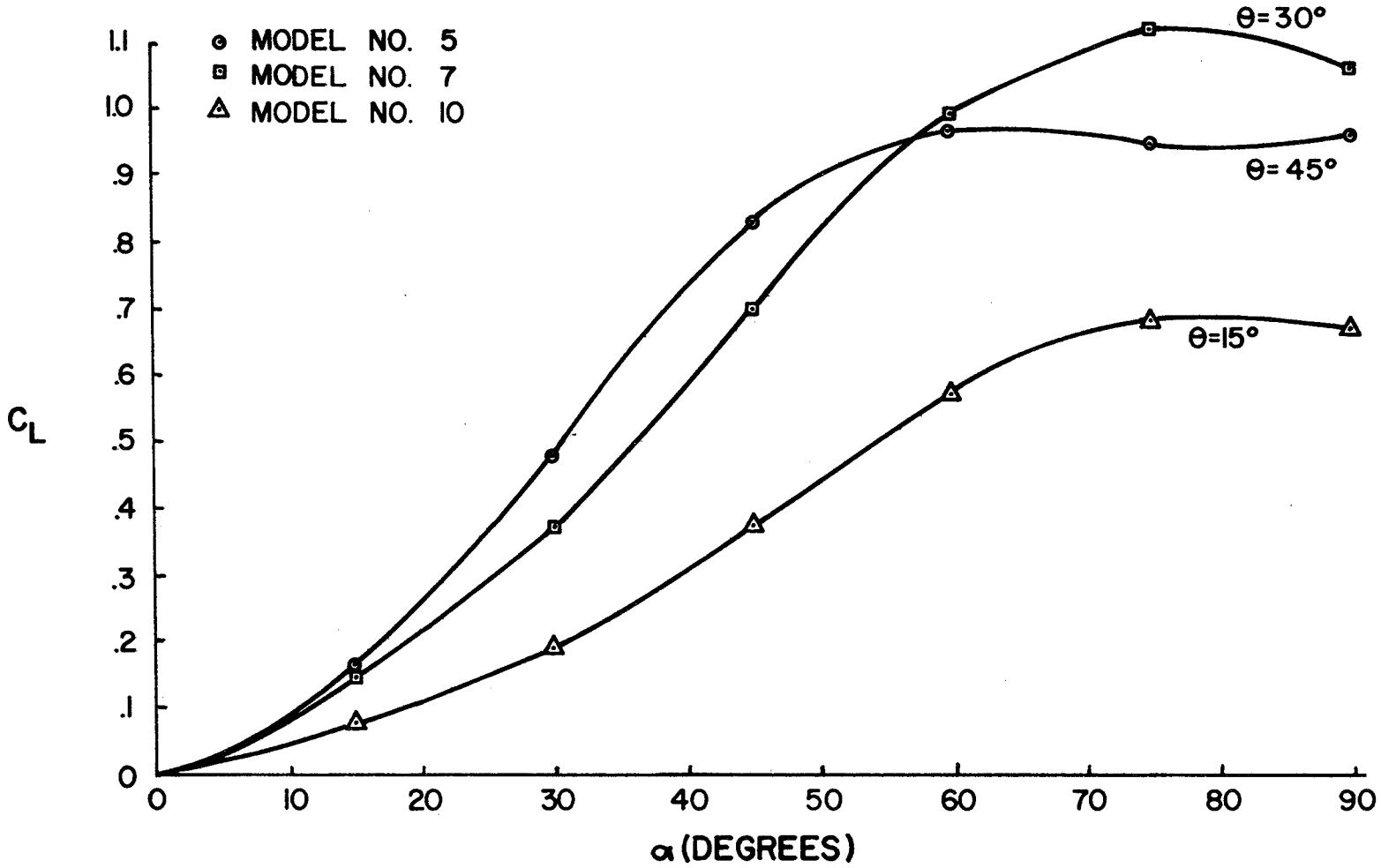

FIGURE 2.3.20 LIFT-FORCE COEFFICIENT VERSUS ANGLE OF ATTACK FOR STRAIGHT LOUVER MODELS, LOUVER WIDTH=2.3 INCHES

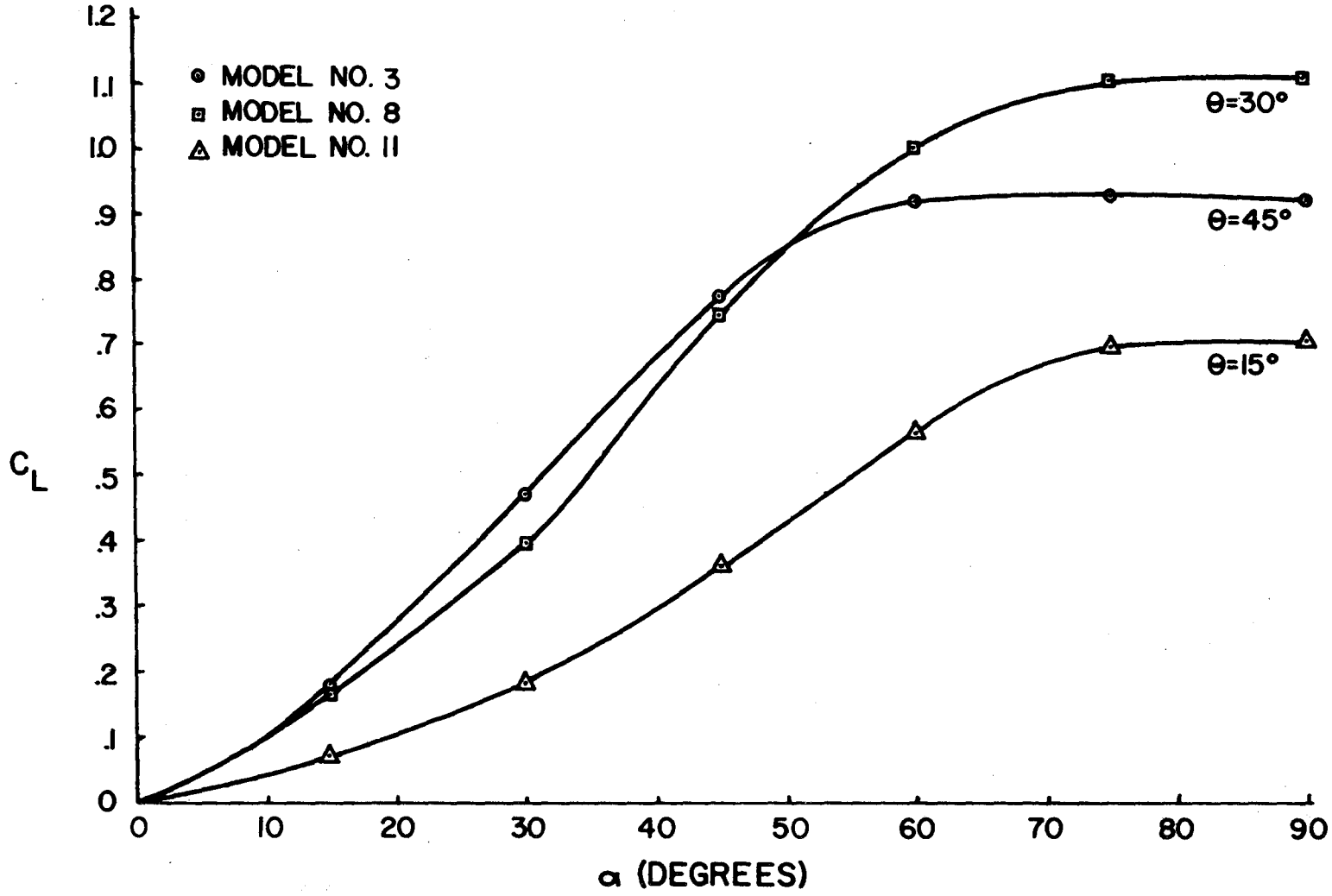

FIGURE 2.3.21 LIFT-FORCE COEFFICIENT VERSUS ANGLE OF ATTACK FOR STRAIGHT LOUVER MODELS, LOUVER WIDTH=2.8 INCHES

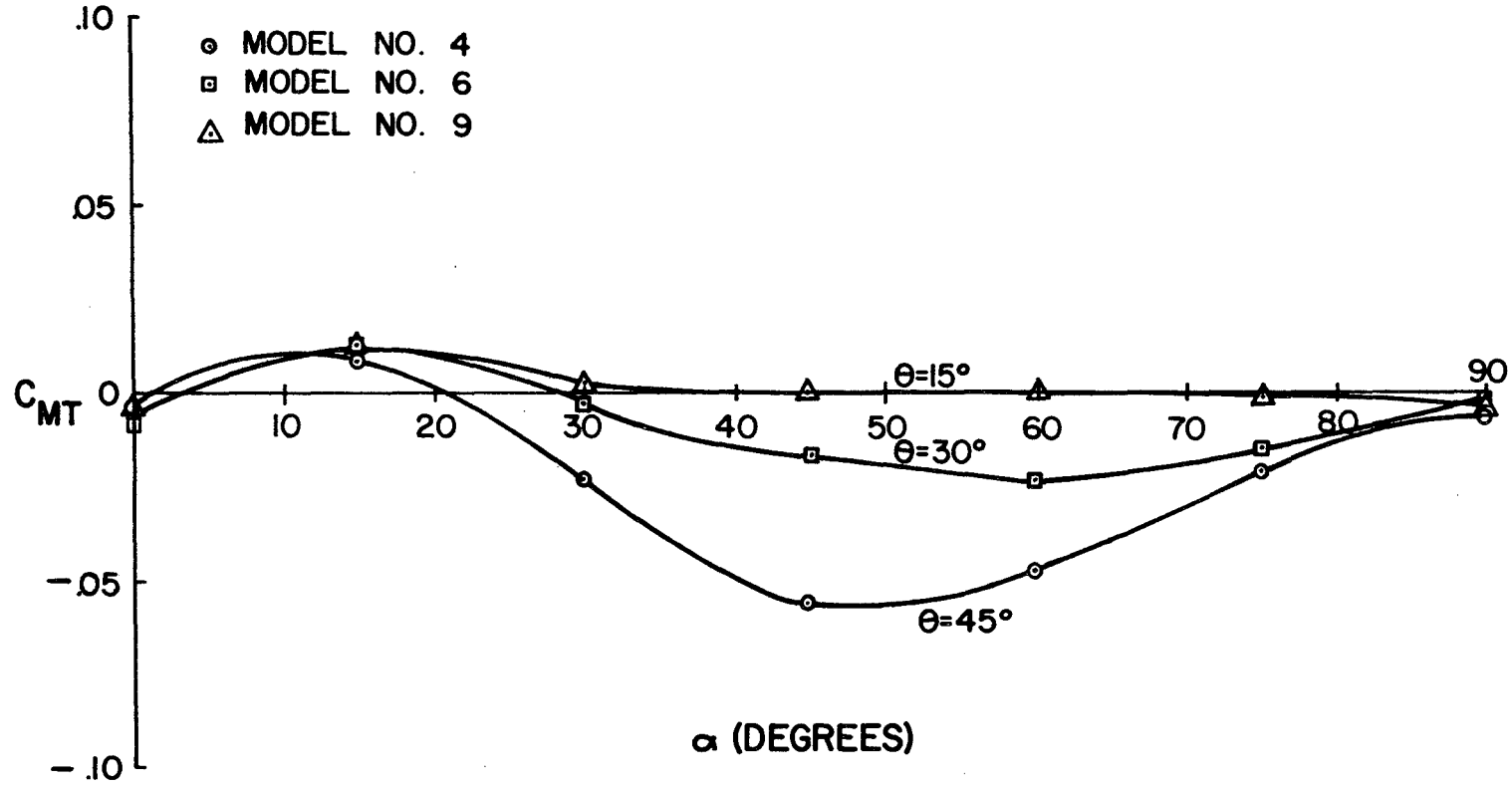

FIGURE 2.3.22 TWISTING-MOMENT COEFFICIENT VERSUS ANGLE OF ATTACK FOR STRAIGHT LOUVER MODELS, LOUVER WIDTH=2.0 INCHES

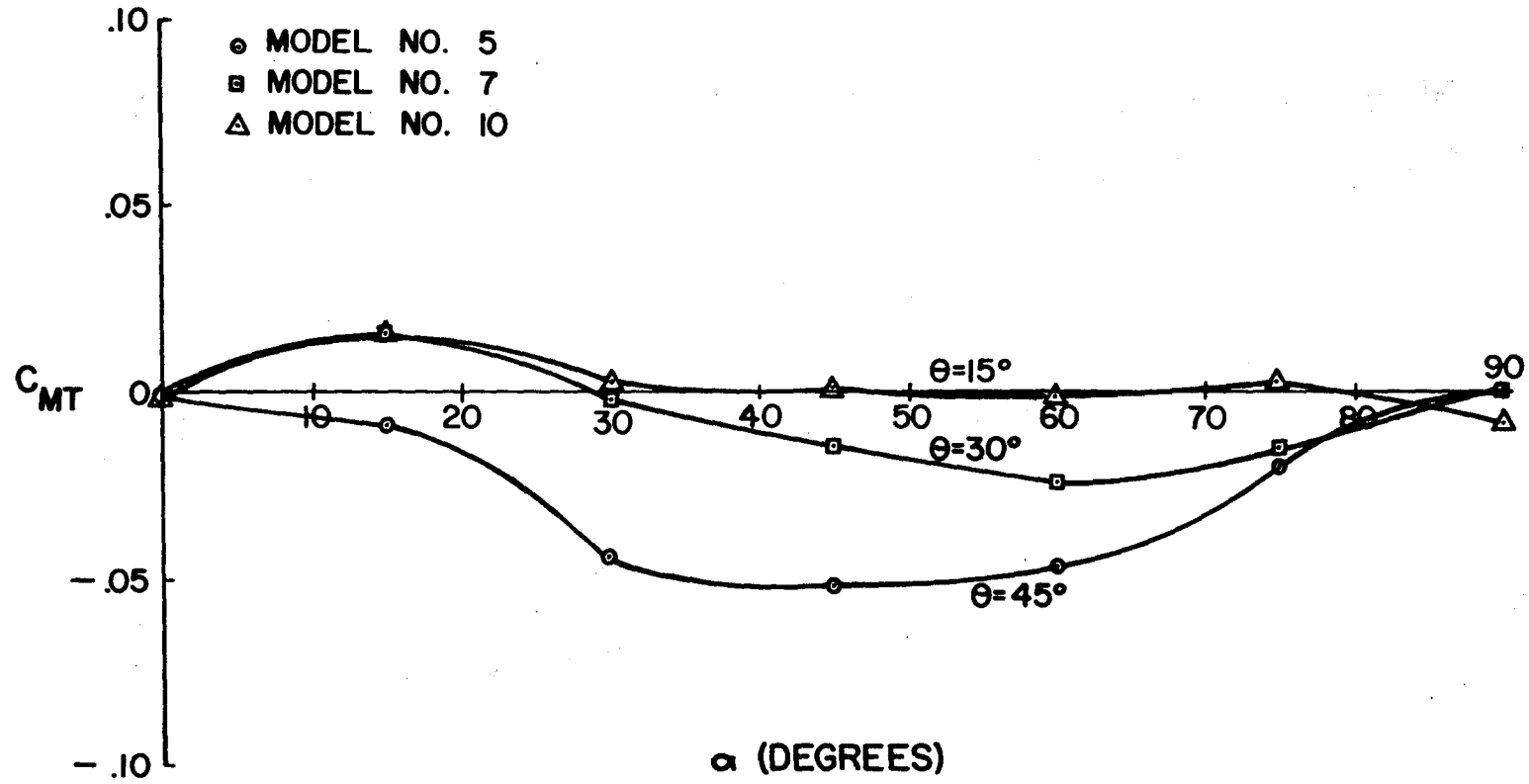

FIGURE 2.3.23 TWISTING-MOMENT COEFFICIENT VERSUS ANGLE OF ATTACK FOR STRAIGHT LOUVER MODELS, LOUVER WIDTH=2.3 INCHES

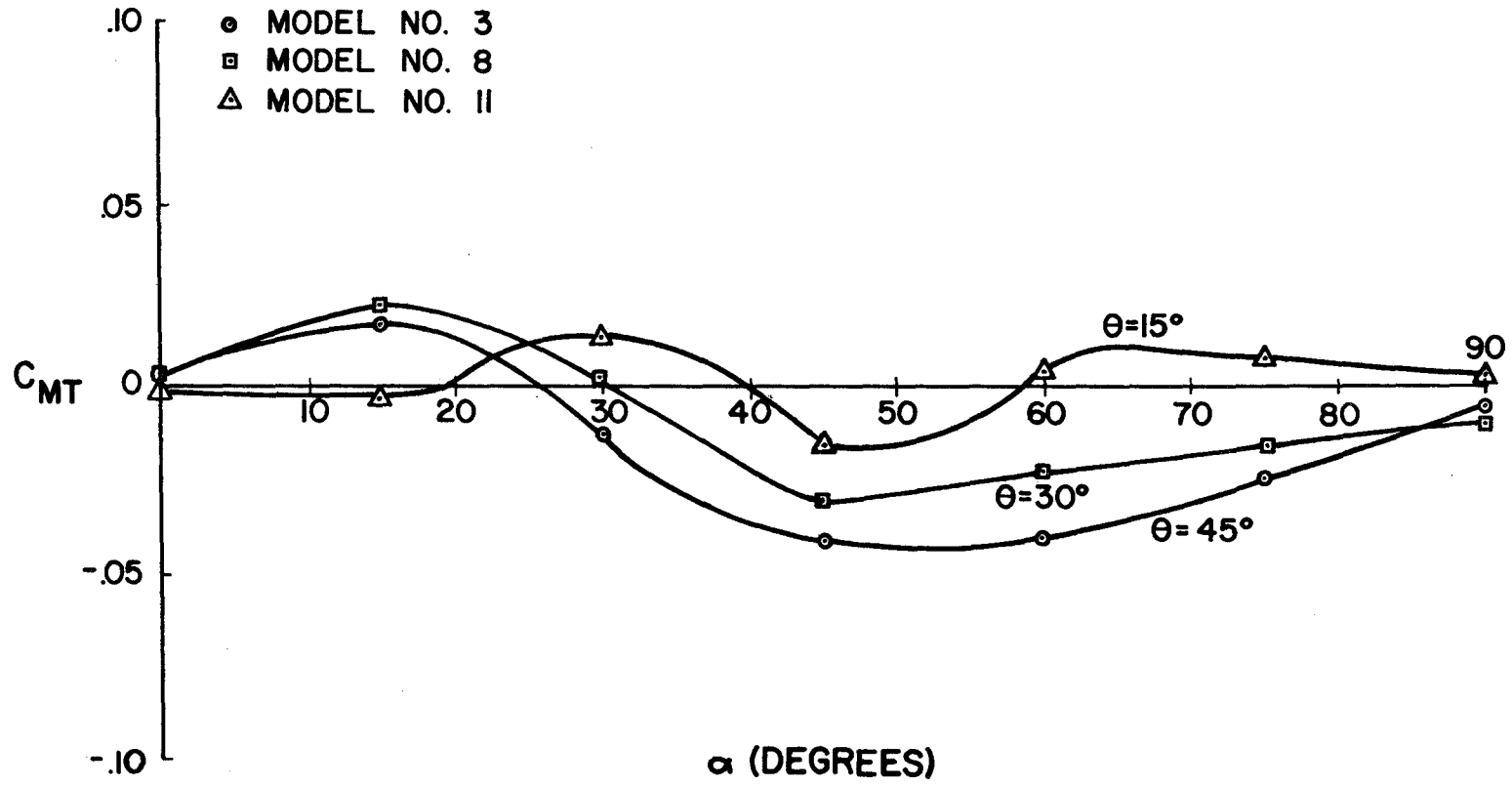

FIGURE 2.3.24 TWISTING-MOMENT COEFFICIENT VERSUS ANGLE OF ATTACK FOR STRAIGHT LOUVER MODELS, LOUVER WIDTH=2.8 INCHES

The pitching moment coefficient and the rolling moment coefficient were found to be negligible on all models.

Variations in the normal force coefficient with louver angle are shown in Figure 2.3.25 for the louver widths. The comparison is shown at an angle of attack of 90°. In most cases this was the angle at which the coefficient obtained its maximum value.

The variations in the normal force coefficient are not necessarily attributable to the difference in louver angles alone. The distance between the louvers is dependent on the louver angle and louver width of the model. The louver spacing was therefore different for any two louver angles. Hence, the variations in the coefficients may include the effect of the different louver spacings also.

The louver spacing on each model was such that a solid appearance was maintained without any louver overlap. As a result, the louver spacing was different on models 3 through 11. It is not suggested that an overlap would have been detrimental from either an aerodynamic standpoint or a visibility standpoint. The decision not to overlap was based on economic considerations. It seemed apparent that the cost would increase as the louver overlap increased.

Variations in the normal coefficient with louver width are shown in Figure 2.3.26. In this case the variations cannot be attributed to the difference in louver widths alone. The variations may include the effect of the different louver spacings, also. Regardless of the cause, it is apparent that the normal force was affected only slightly by the changes in louver width.

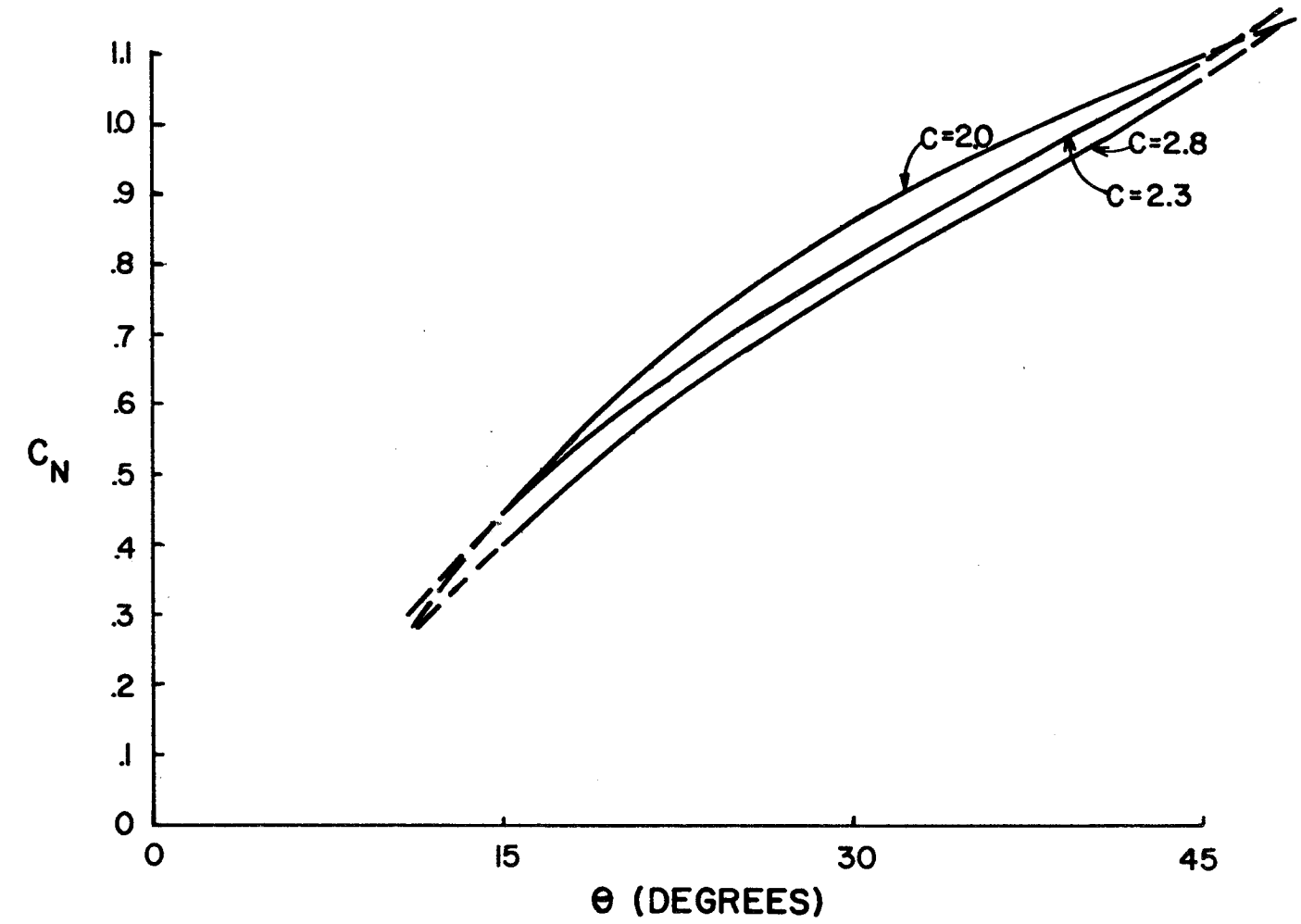

FIGURE 2.3.25 NORMAL-FORCE COEFFICIENT VERSUS LOUVER ANGLE FOR STRAIGHT LOUVER MODELS AT $\alpha = 90°$

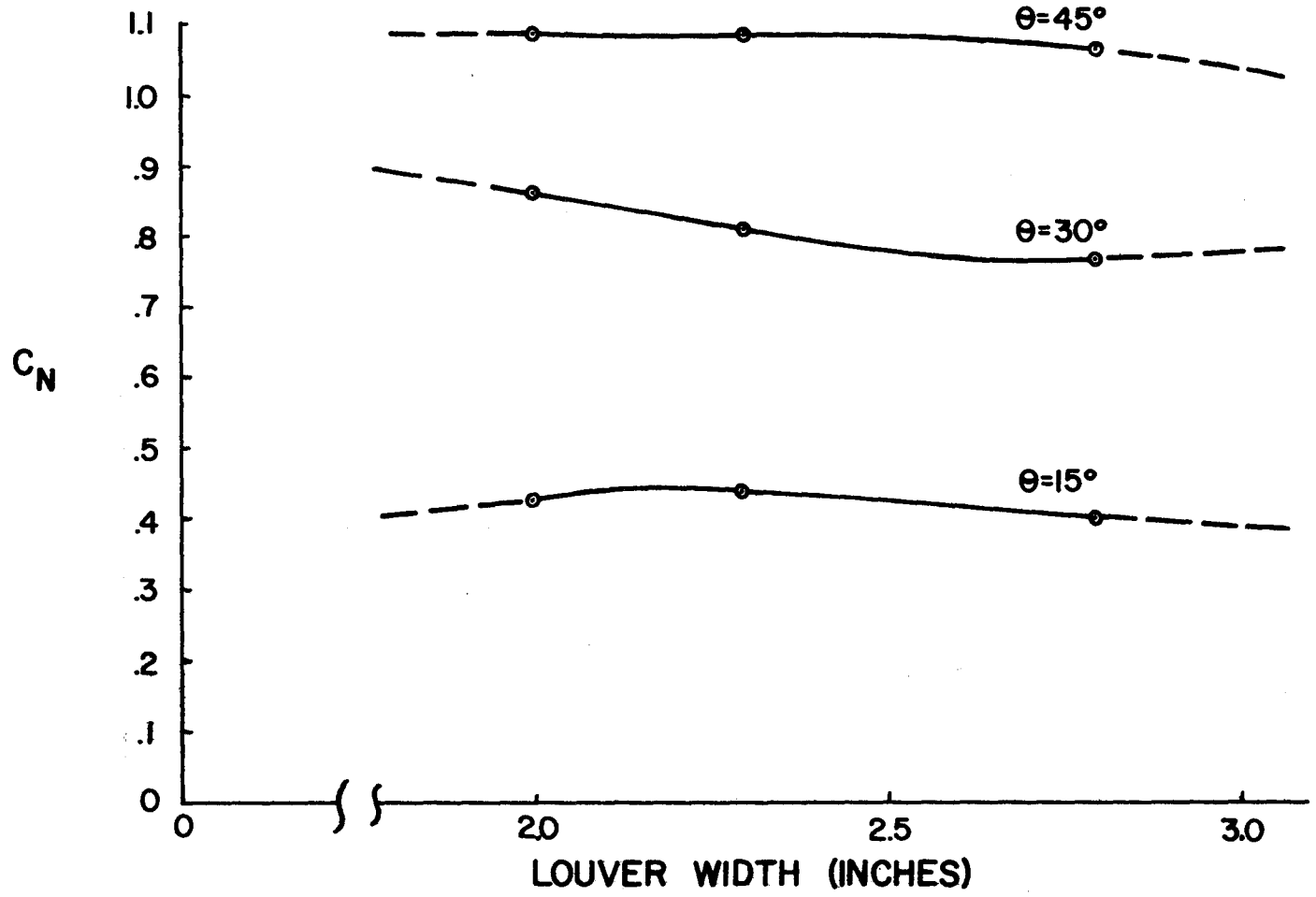

FIGURE 2.3.26 NORMAL-FORCE COEFFICIENT VERSUS LOUVER WIDTH FOR STRAIGHT LOUVER MODELS AT $\alpha = 90°$

Figure 2.3.27 shows the side force coefficient plotted against the louver width for three louver angles. The comparison was made at an angle of attack of 45°. In most cases the coefficient obtained its maximum value at this angle. The changes in louver width were found to affect the side force to a greater extent than the normal force (Figure 2.3.26). The increase in side force with increasing louver width is obviously due to the increase in sideplate area.

The normal force coefficient is shown plotted against the aspect ratio in Figure 2.3.28, for various angles of attack. These results were obtained from the tests on models 7, 12, and 13, having aspect ratios of 1.0, 0.5 and 1.5, respectively. All three models had equal louver angles, louver widths and frontal areas. Only small changes in the coefficient are evident between the different aspect ratios.

The normal force coefficient is shown plotted against the Reynolds number in Figure 2.3.29 for three different models. The coefficients appear to be independent of the Reynolds number, at least within the range tested.

Model number 8 was equipped with a typical message in order to determine its effects on the wind loads. The results are shown in Figures 2.3.30, 31, and 32. The message increased the coefficients by approximately 12% on this particular model.

Only model number 8 was tested for message effects. However, the information obtained in this test is considered to be applicable to the other configurations.

It is suggested that the message coefficients shown in Figures

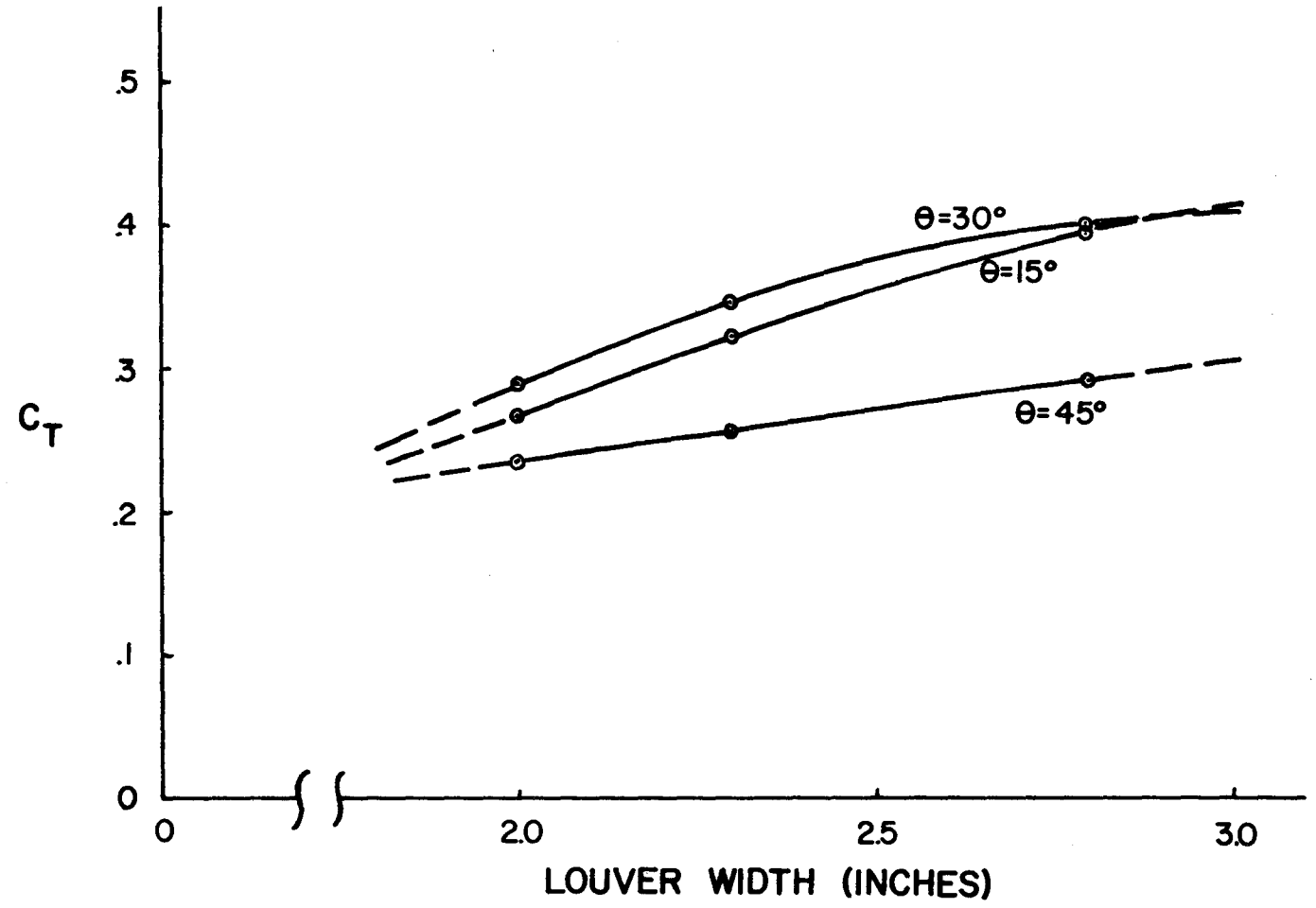

FIGURE 2.3.27 SIDE-FORCE COEFFICIENT VERSUS LOUVER WIDTH FOR STRAIGHT LOUVER MODELS AT $\alpha = 45°$

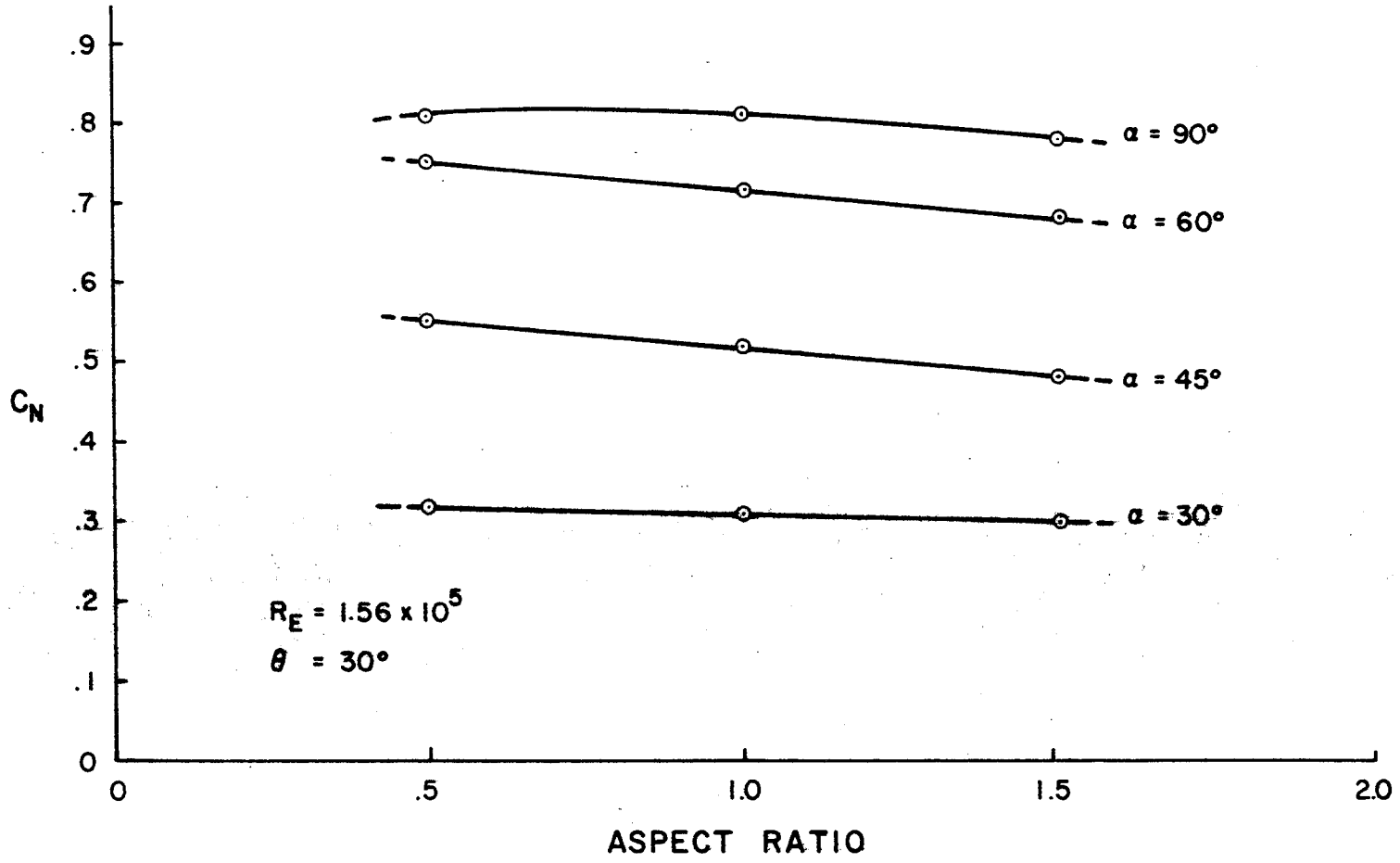

FIGURE 2.3.28 NORMAL-FORCE COEFFICIENT VERSUS ASPECT RATIO, STRAIGHT LOUVER MODELS

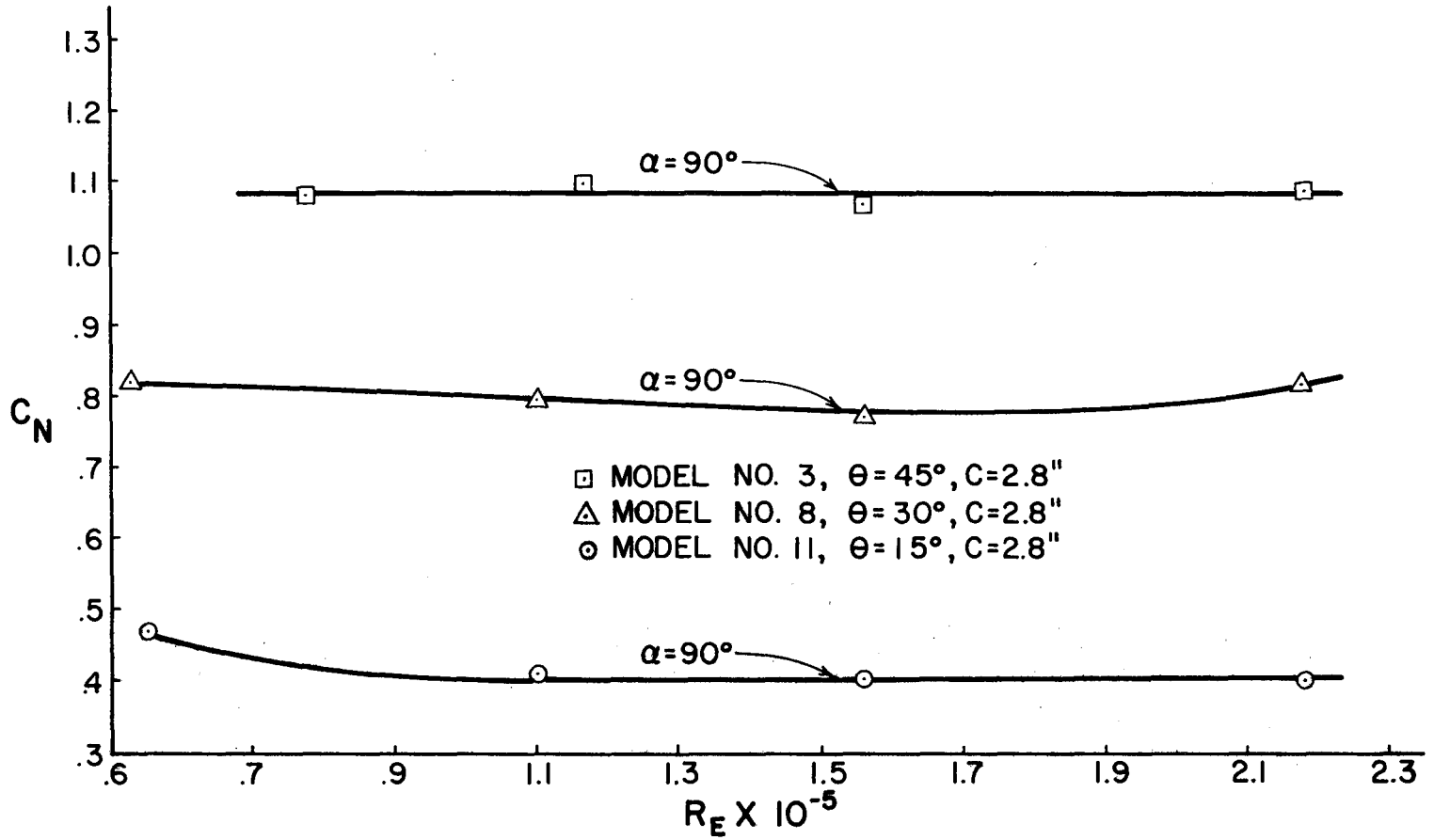

FIGURE 2.3.29 NORMAL-FORCE COEFFICIENT VERSUS REYNOLDS NUMBER, STRAIGHT LOUVER MODELS

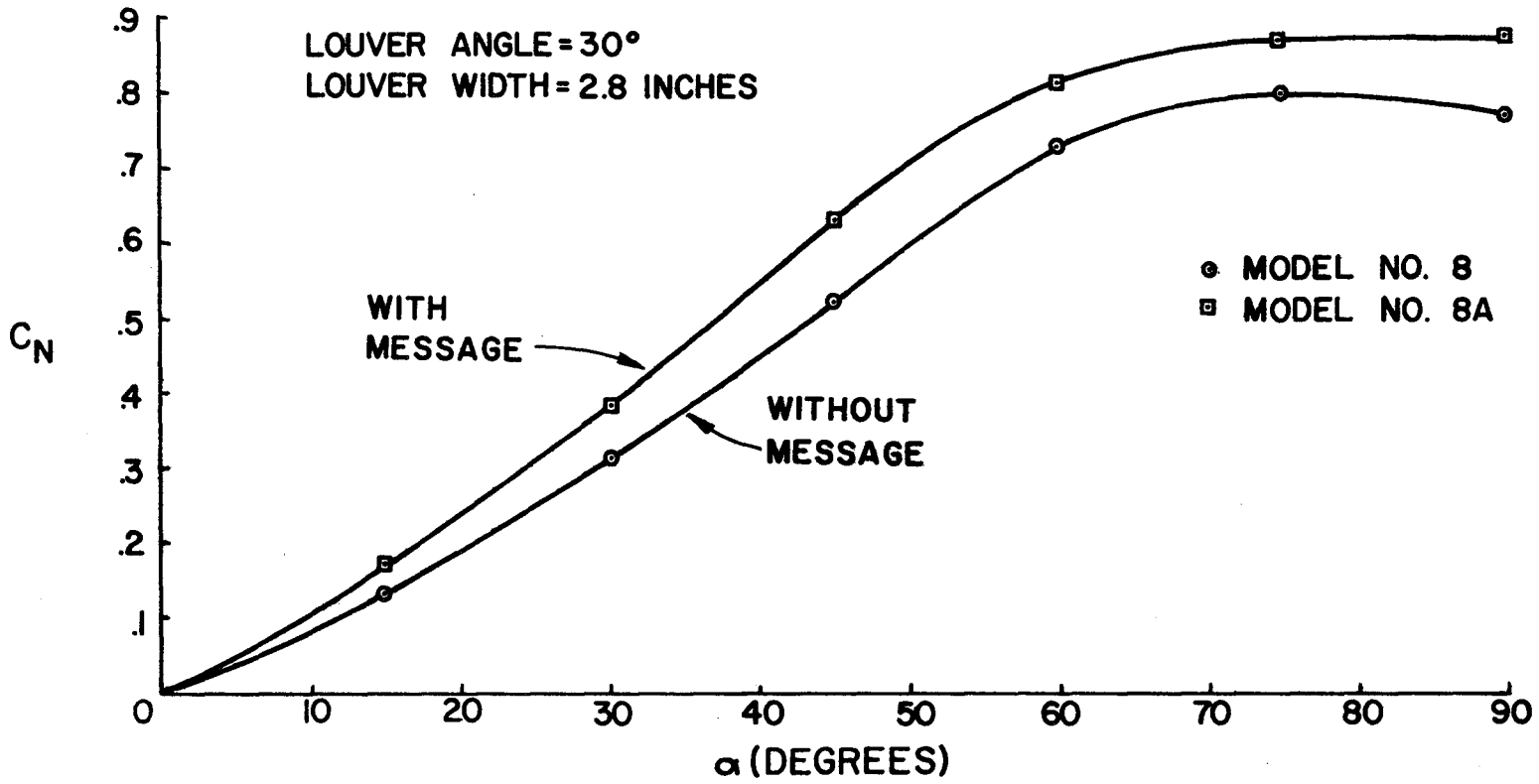

FIGURE 2.3.30 NORMAL-FORCE COEFFICIENT VERSUS ANGLE OF ATTACK FOR STRAIGHT LOUVER MODELS, WITH AND WITHOUT MESSAGE

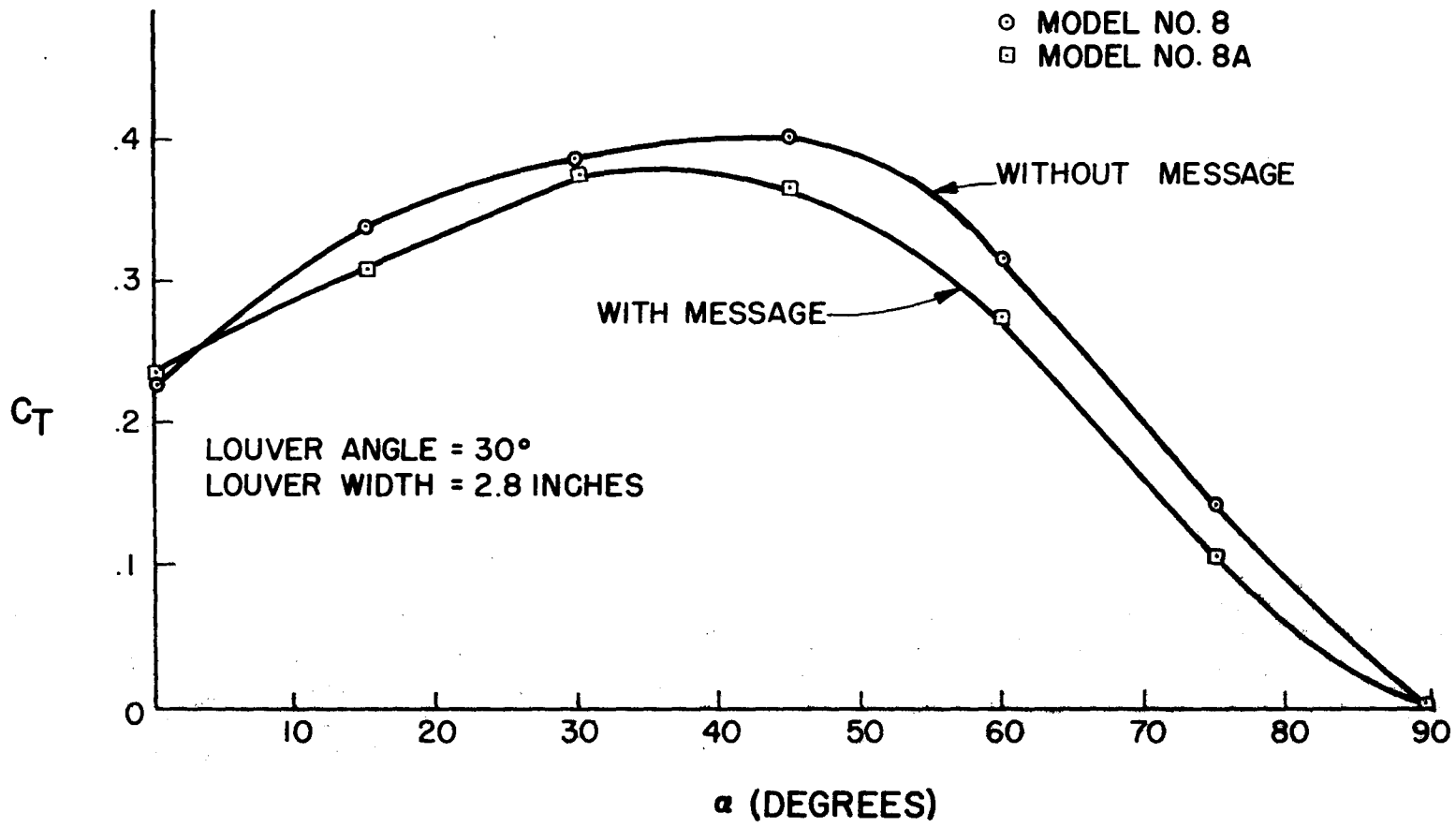

FIGURE 2.3.31 SIDE-FORCE COEFFICIENT VERSUS ANGLE OF ATTACK FOR STRAIGHT LOUVER MODELS, WITH AND WITHOUT MESSAGE

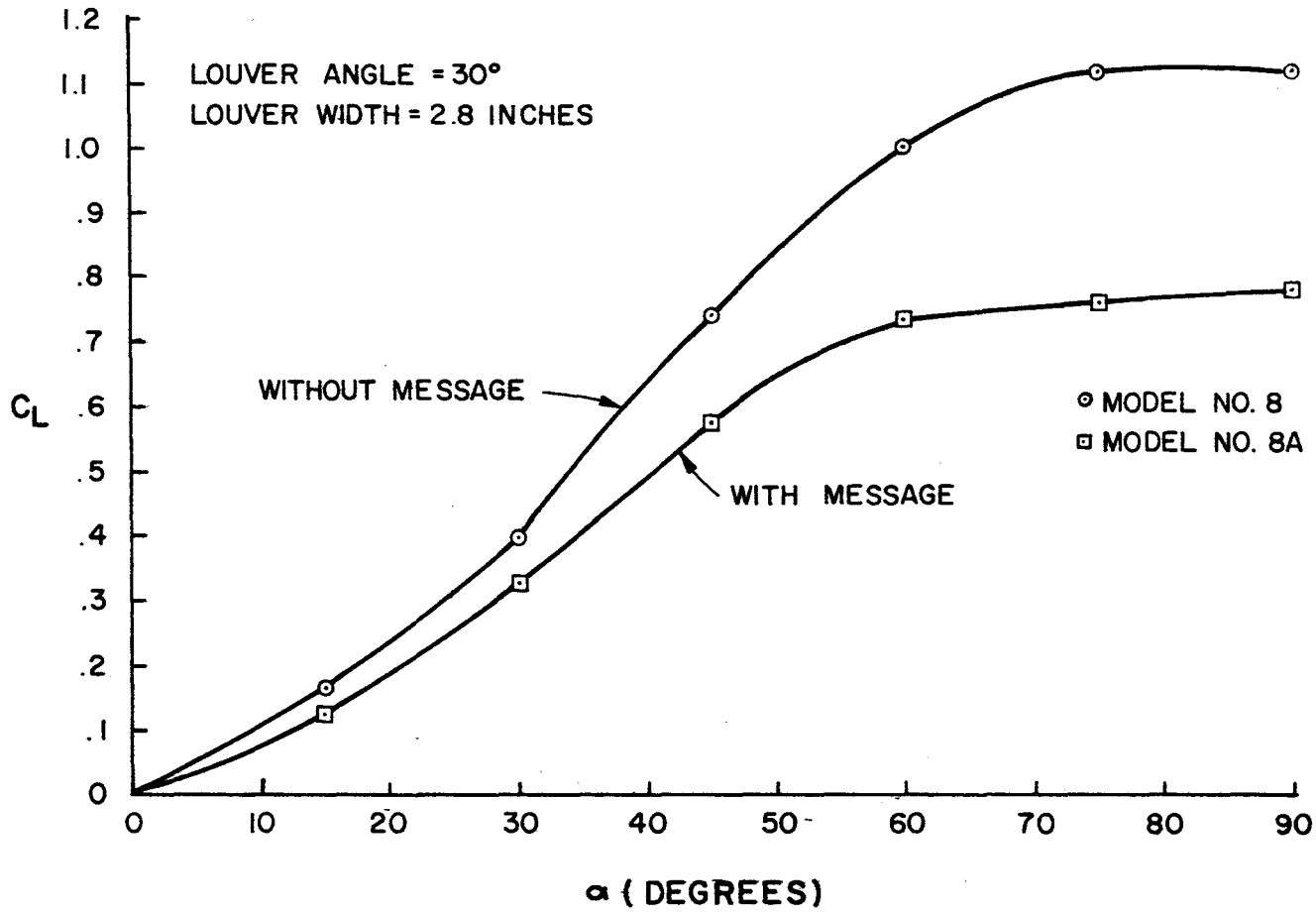

FIGURE 2.3.32 LIFT-FORCE COEFFICIENT VERSUS ANGLE OF ATTACK FOR STRAIGHT LOUVER MODELS, WITH AND WITHOUT MESSAGE

2.3.33, 34, and 35 be used in conjunction with the coefficients of Figures 2.3.13 through 2.3.21, since the latter were obtained without a message. No corrections are suggested in the twisting moment coefficients for message effects.

The message coefficients were obtained by the following general relation:

$$C_{i_m} = \frac{(F_{i_w} - F_{i_{w/o}})}{qA_L} \qquad (2.3.1)$$

where

i = N, T, or L (normal, side or lift)

F_{i_w} = Measured "i" force with message

$F_{i_{w/o}}$ = Measured "i" force without message

q = Impact pressure (defined previously)

A_L = Frontal area of message and its related supports

(A_L = 0.59 ft.^{2} for the message and attachment used in the test)

Thus, the equation for wind loads on a louvered sign with message is, as determined from Equation 2.3.1,

$$F_{i_w} = (C_{i_m})\ (q)\ (A_L) + F_{i_{w/o}} \qquad (2.3.2)$$

where

$$F_{i_{w/o}} = C_i qA \qquad (2.3.3)$$

The terms C_i and C_{i_m} are obtained from Figures 2.3.13 through 2.3.21

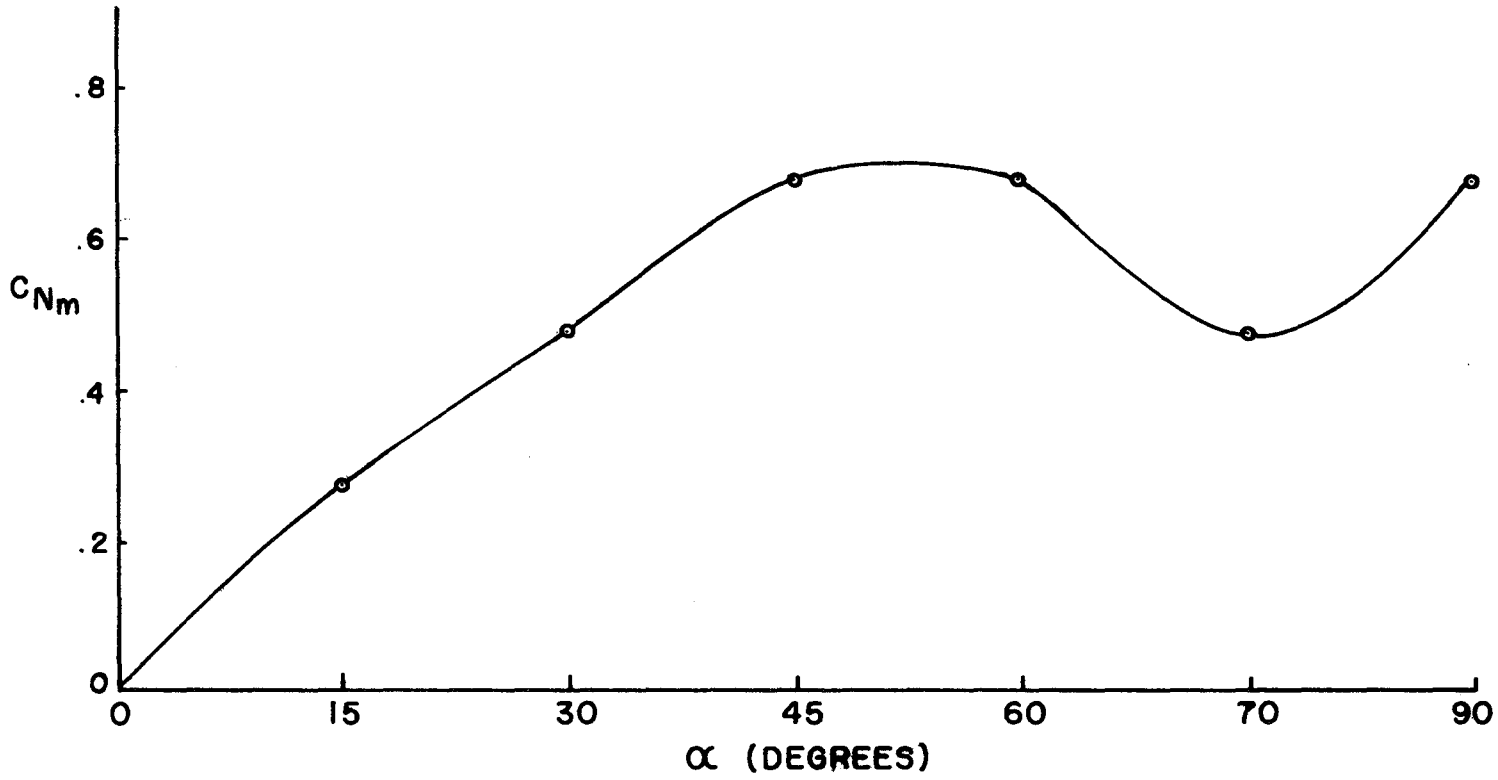

FIGURE 2.3.33 MESSAGE NORMAL-FORCE COEFFICIENT VERSUS ANGLE OF ATTACK, STRAIGHT LOUVER MODELS

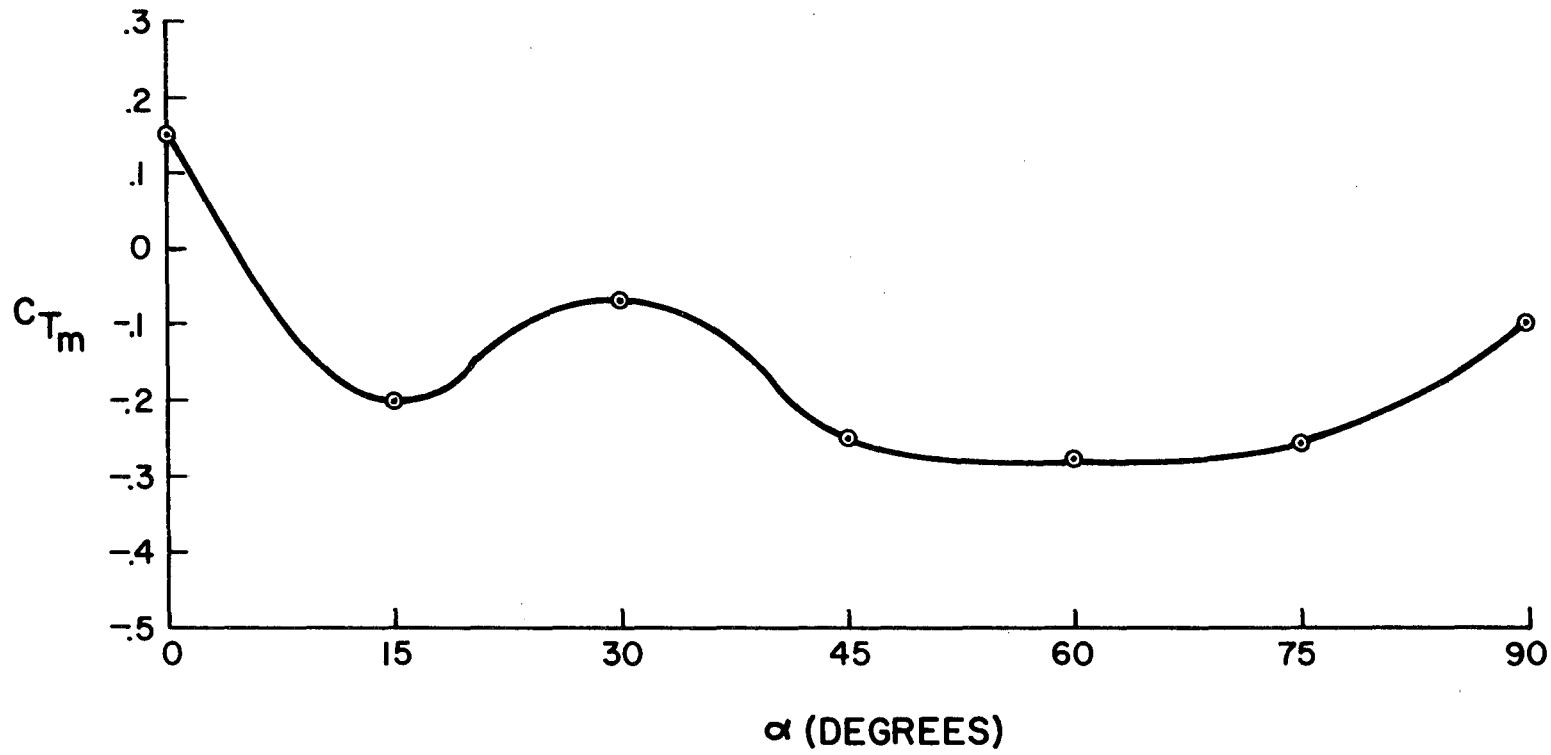

FIGURE 2.3.34 MESSAGE SIDE-FORCE COEFFICIENT VERSUS ANGLE OF ATTACK, STAIGHT LOUVER MODELS

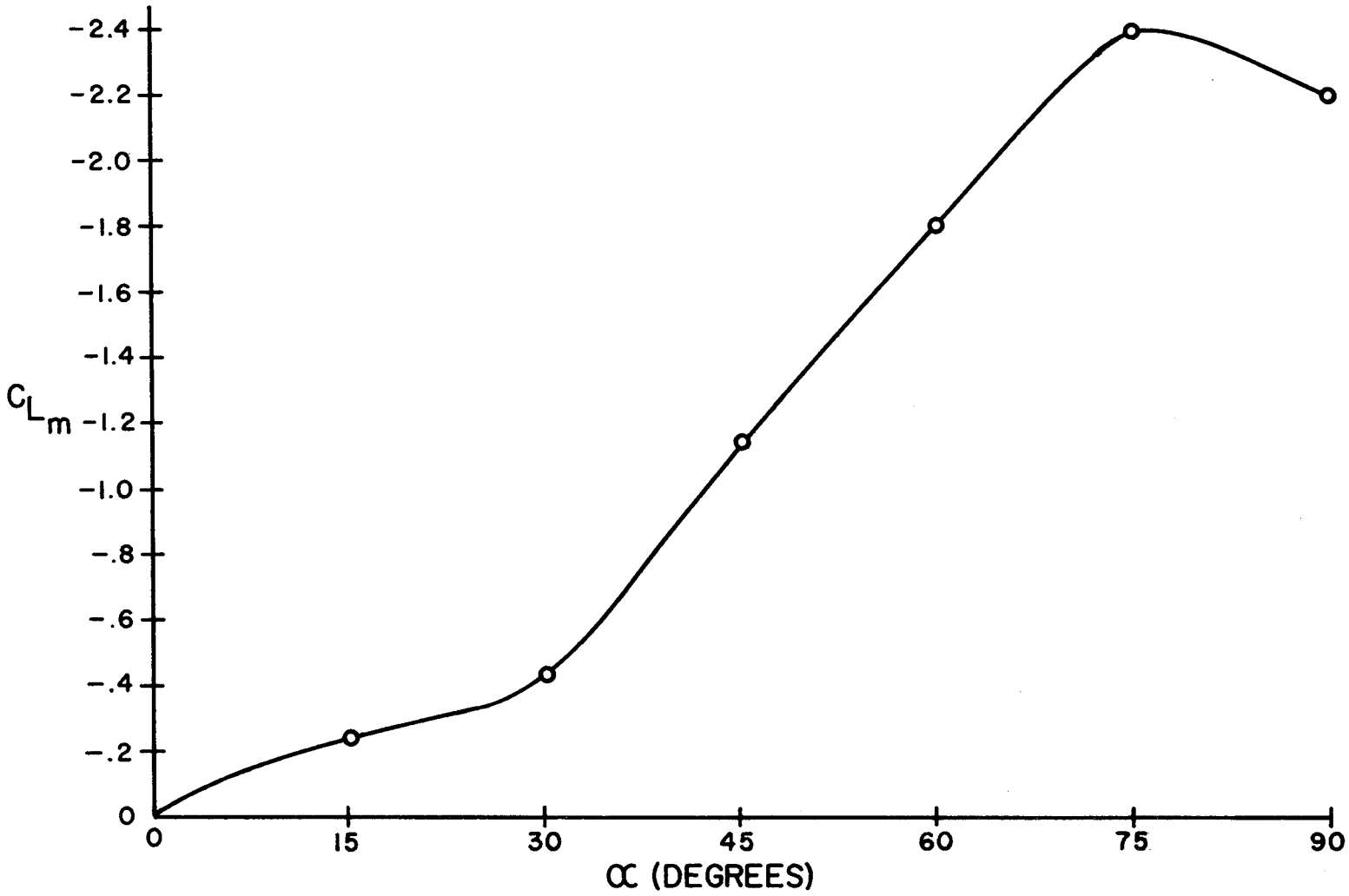

FIGURE 2.3.35 MESSAGE LIFT-FORCE COEFFICIENT VERSUS ANGLE OF ATTACK, STRAIGHT LOUVER MODELS

and Figures 2.3.33 through 2.3.35, respectively.

Although the message caused an increase in the normal force, it reduced the side and lift forces as shown in Figures 2.3.31 and 32. This is the reason for the negative message coefficients in Figures 2.3.34 and 35.

All of the louver model coefficients include the effects of the windbeams and that part of the supporting pole directly behind the model. The frontal area of the windbeams blocking the air flow totaled about 0.25 square feet. This comprised about 6.3% of the sign's frontal area. The total blockage by windbeams on full-scale signs would likely be about the same amount. Hence, the coefficients can be used in most cases without alterations due to account for windbeam effects.

It is recommended that the coefficients not be used to include the effects of the sign supports, although the coefficients included the effects of a portion of the model support. The single tubular support is not believed to have affected the wind loads on the models to any extent. In actual design, the wind loads on the sign supports should be computed separately and then added to the background wind loads.

All of the coefficients are shown for positive angles of attack, i.e., wind impinging on the front of the sign. However, the models were tested at negative angles of attack also. The results with negative angles were similar to those at positive angles, with one exception. Winds on the back side of the model caused a negative lift. In the design of the sign supports the negative lift would likely be more critical, since it would be a compressive load.

No serious flutter problems were encountered in the tests. The flutter observations are discussed in "Wind loads on non-solid signs," Section 1.5. The visibility observations of louvered signs were also discussed in this section.

The applicability of the presented data to full-scale signs is discussed in the "Louvered signs" portion of Section 2.4.

Wind tunnel tests of curved louver models. The results of the curved louver tests are shown in Figures 2.3.36 through 2.3.41. Because of time limitations only three curved louver configurations were tested. The results were encouraging, however.

The normal force coefficients were found to be similar in magnitude to those of the straight louvered models with a 15° louver angle. The minimum normal force coefficient obtained in the curved louver test was 0.3 (at $\theta' = 14.1°$) compared to a 0.4 (at $\theta = 15°$) in the straight louver test. Both values represent a considerable reduction in the corresponding flat plate value of 1.4.

The side force coefficients were slightly higher than the straight louvered values. The larger values are attributed in part to the wider side plates used in the curved louver models. The nature of the air flow through the curved louver models likely contributed to the side force differences.

The geometry of the curved louvers causes a momentum change in the air flow. This change produces a pitching moment on the background. The pitching moment coefficient is shown plotted in Figure 2.3.40. The mathematical sign of the pitching moment coefficient is important. As shown, it is positive for most of the positive angles of attack.

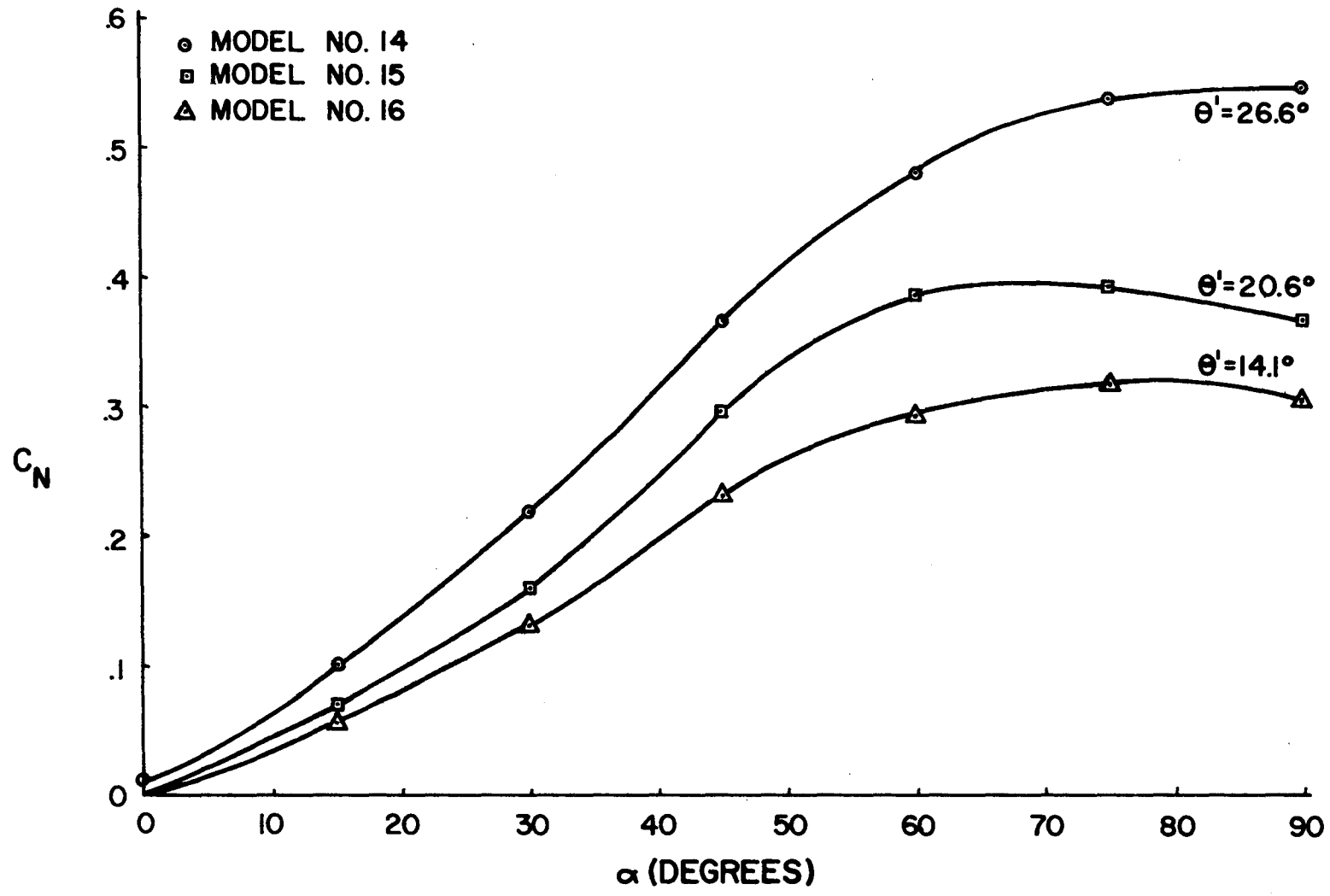

FIGURE 2.3.36 NORMAL-FORCE COEFFICIENT VERSUS ANGLE OF ATTACK FOR CURVED LOUVERS, SIDEPLATE WIDTH = 4.0 INCHES

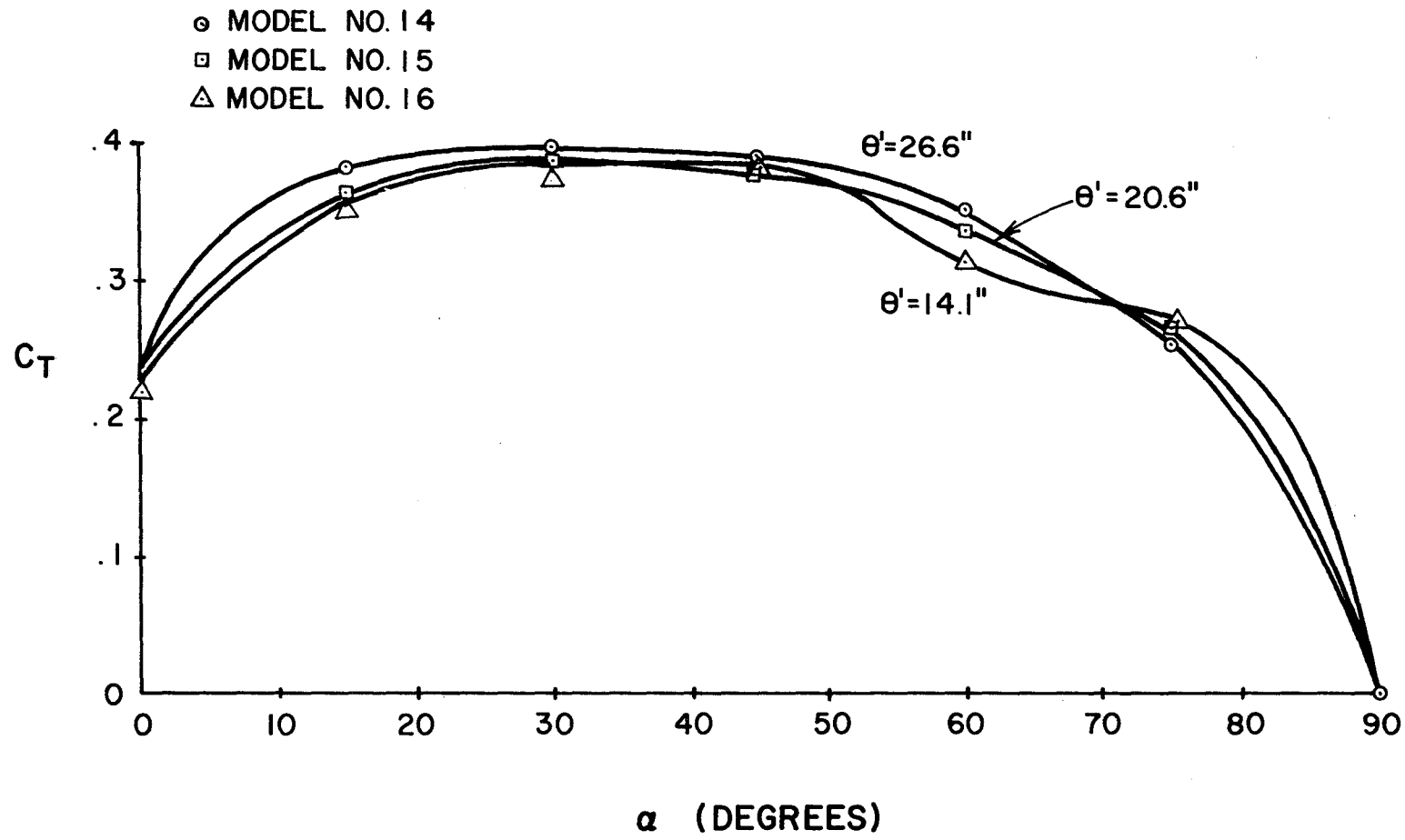

FIGURE 2.3.37 SIDE-FORCE COEFFICIENT VERSUS ANGLE OF ATTACK FOR CURVED LOUVERS, SIDEPLATE WIDTH=4.0 INCHES

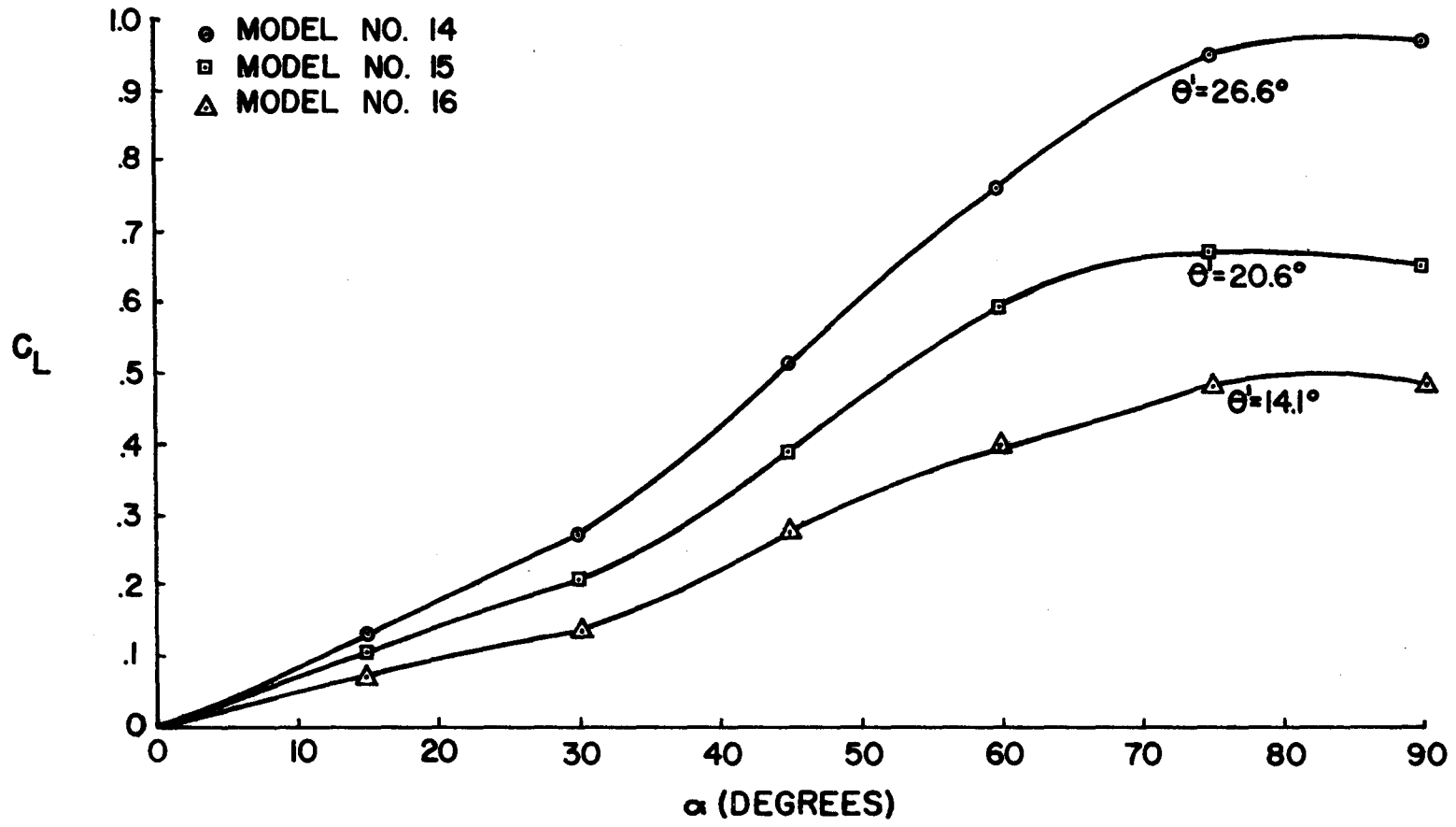

FIGURE 2.3.38 LIFT-FORCE COEFFICIENT VERSUS ANGLE OF ATTACK FOR CURVED LOUVERS, SIDEPLATE WIDTH=4.0 INCHES

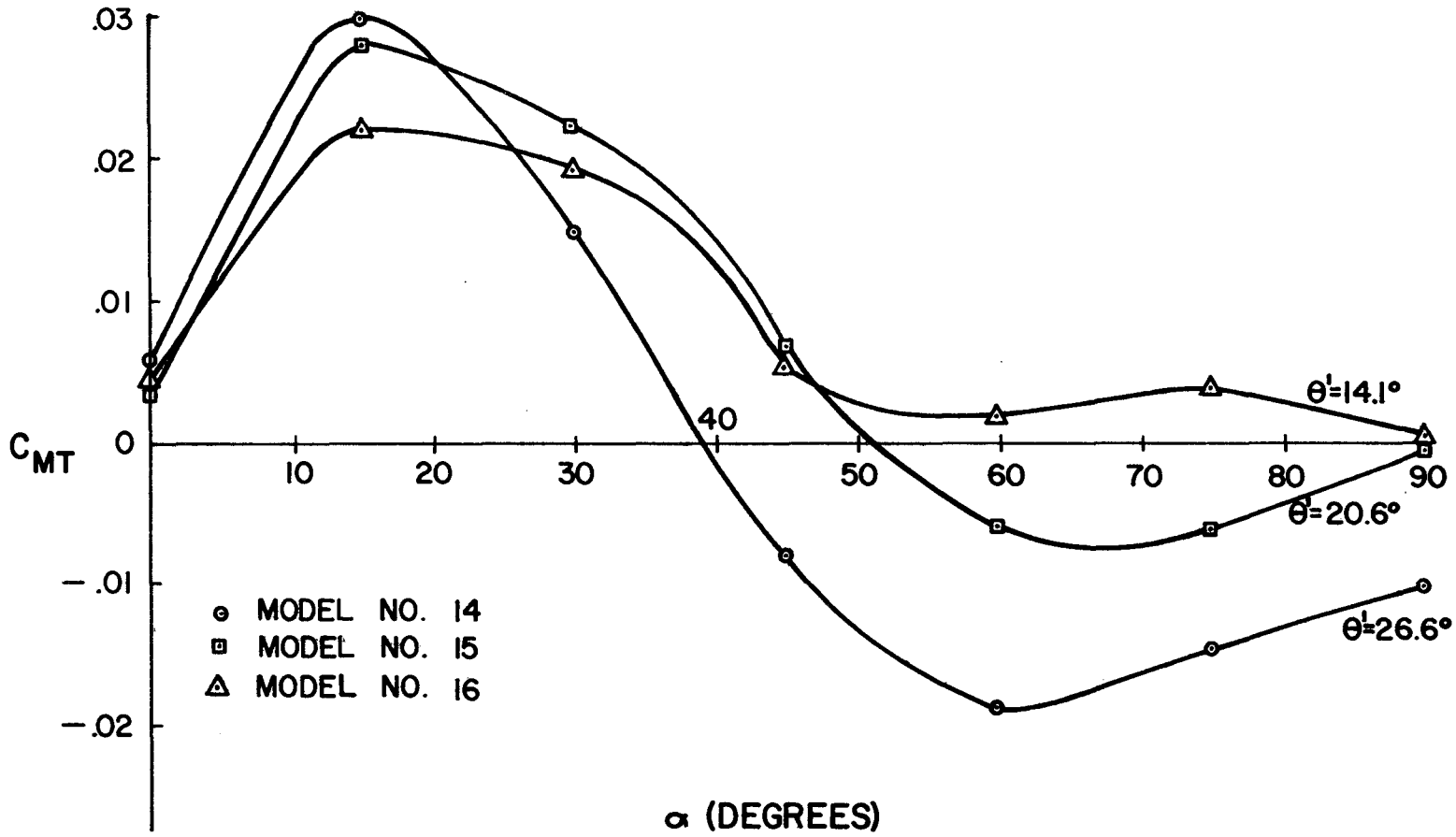

FIGURE 2.3.39 TWISTING-MOMENT COEFFICIENT VERSUS ANGLE OF ATTACK FOR CURVED LOUVERS, SIDEPLATE WIDTH = 4.0 INCHES

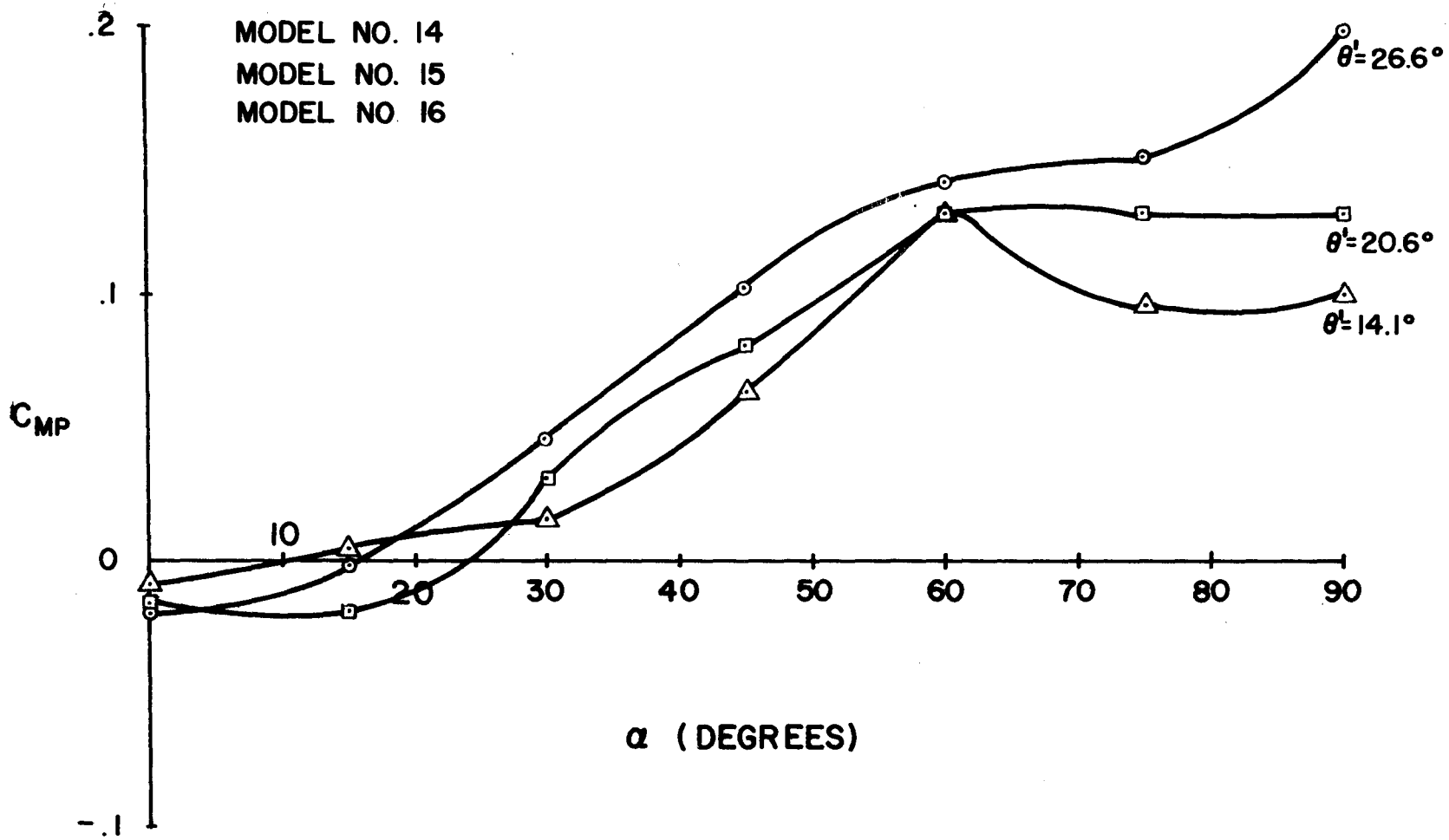

FIGURE 2.3.40 PITCHING-MOMENT COEFFICIENT VERSUS ANGLE OF ATTACK FOR CURVED LOUVERS, SIDEPLATE WIDTH=4.0 INCHES

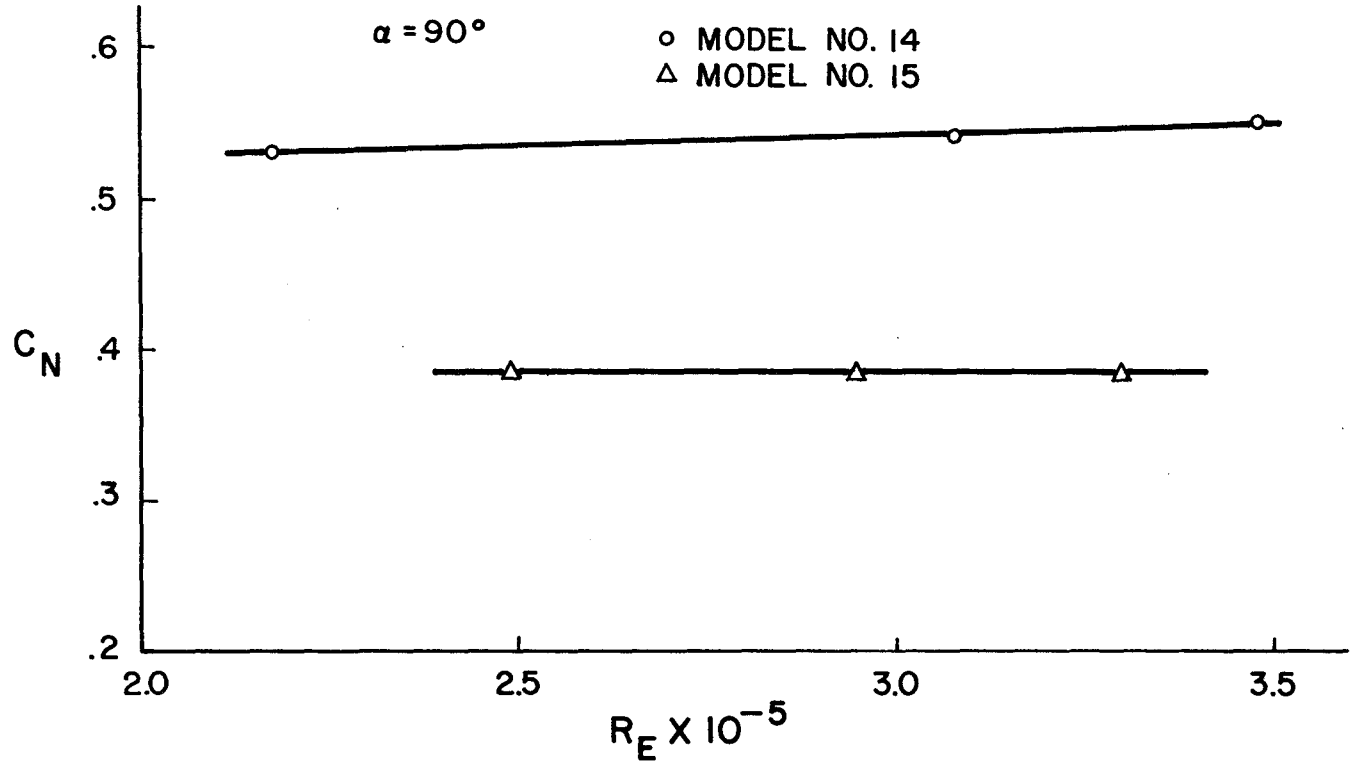

FIGURE 2.3.41 NORMAL-FORCE COEFFICIENT VERSUS REYNOLDS NUMBER, CURVED LOUVERS

This means that the pitching moment adds to that caused by the normal force on the sign supports (refer to Figure 2.2.1).

As an example, consider the summary shown in Table 1.5.4 for the θ' equal to 20.6° configuration. The normal force acts at the center of the sign. The center was assumed to be 14 feet above ground. The moment M at the base of the sign would be

$$M = 14(F_N) + (q)\ (A_s)\ (W)\ (C_{MP}) \qquad (2.3.4)$$

where

F_N = 1259 lbs.

q = 25 lbs./ft.^{2} (at 100 mph)

A_s = 100 ft.^{2}

W = 10 ft.

C_{MP} = 0.13 (from Figure 2.3.40 for α = 90°)

Thus,

$M = 14(1259) + (25)(100)(10)(0.13)$

$M = 17,600 + 3,250$

$M = 20,850$ ft.-lbs.

For a comparison consider the straight louvered configuration with a 15° louver angle and 2.3 inch louver width. The maximum value of F_N, from Table 1.5.1, is 1388 pounds. This value occurs at α = 90° also. The value of the support moment would be

$M = 1388\ (14) = 19,400$ ft.-lbs.

Although the normal force was less in the curved louver case (1259 lbs. to 1388 lbs.), the design moment was less for the straight louver case. The pitching moment must therefore be considered in curved louver signs.

The normal force coefficient versus Reynolds number is shown in Figure 2.3.41. A slight variation is noted in the $\theta' = 26.6°$ case. However, it is not considered significant. The Reynolds number variation for the $\theta' = 14.1°$ case is not available due to a weld failure that occurred on this model.

The characteristic length chosen for the Reynolds number was the distance between the forward and rear edge of the curved louver. It is the hypotenuse of the triangle having as sides the sideplate width and the louver spacing.

Wind tunnel tests of expanded metal models. Three models consisting of an aluminum expanded metal were tested in hopes of finding a commercially available non-solid background that would reduce wind loads. The material was chosen for its possibilities as an overhead sign. From an angle of approximately 20° to the horizontal and up it appeared solid. Its use as a roadside sign background was questionable, however, due to the size of louver openings (see Figure 1.4.9).

The results of the tests were not encouraging. Figure 2.3.42 shows the normal force coefficient plotted against the angle of attack. Reasons for the lack of any appreciable wind load reductions are presented in Section 2.4.

All three models had an aspect ratio equal to 1.0. The maximum normal force coefficient for a flat plate with the same aspect ratio is

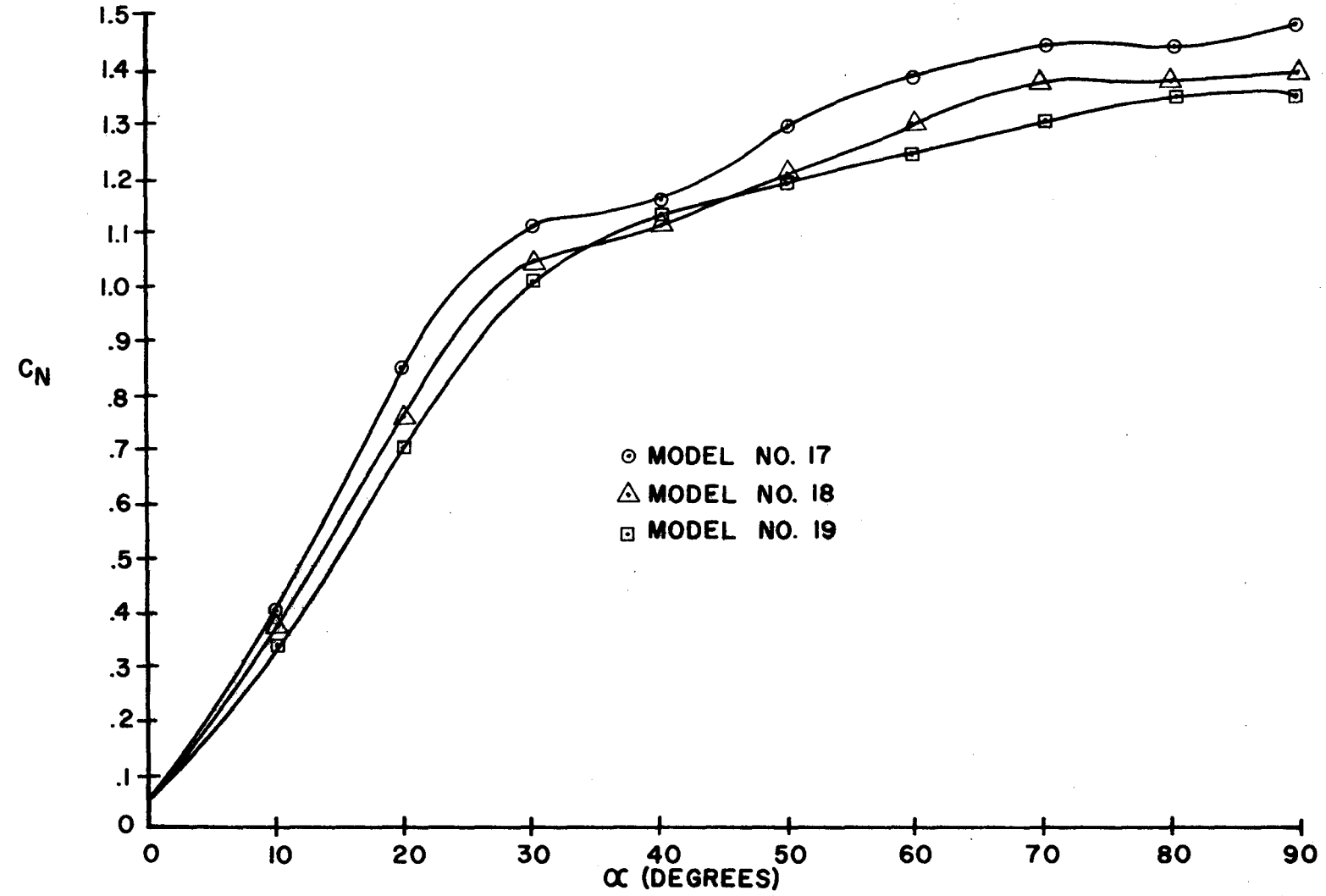

FIGURE 2.3.42 NORMAL-FORCE COEFFICIENT VERSUS ANGLE OF ATTACK, EXPANDED-METAL MODELS

1.4. As shown, the maximum for the expanded metal was practically the same.

No problems were encountered with the structural adequacy of this material under wind loads. It appeared very steady at all wind speeds including the maximum 100 mile per hour winds.

General comparison of data. Figures 2.3.43 and 44 are included for comparative purposes. The curves were derived from the wind tunnel tests conducted in this study. Both figures represent data for an aspect ratio of 1.0.

The louvered configurations chosen for this comparison are not necessarily the optimum design in all cases. It was felt these represented, in general, typical results of the straight and curved louver tests.

2.4 Theoretical Considerations

The total resistance of a body with fluid flowing against it is the resultant of two sets of forces; the viscous forces developed along the boundary which act tangetial to the surface and the pressure forces which act normal to the surface. For high viscous fluids and/or low fluid velocities the viscous forces are usually predominate. When the fluid is air the pressure forces are usually predominate. This is especially true of bodies with sharp edges where the fluid breaks away at definite points, such as a flat plate.

In general, the resistance depends on the shape and position of the body, its size, the properties of the fluid, and the fluid's velocity. The problems that arise in theoretically relating these parameters with resistance are usually immense. Experimental results must be relied

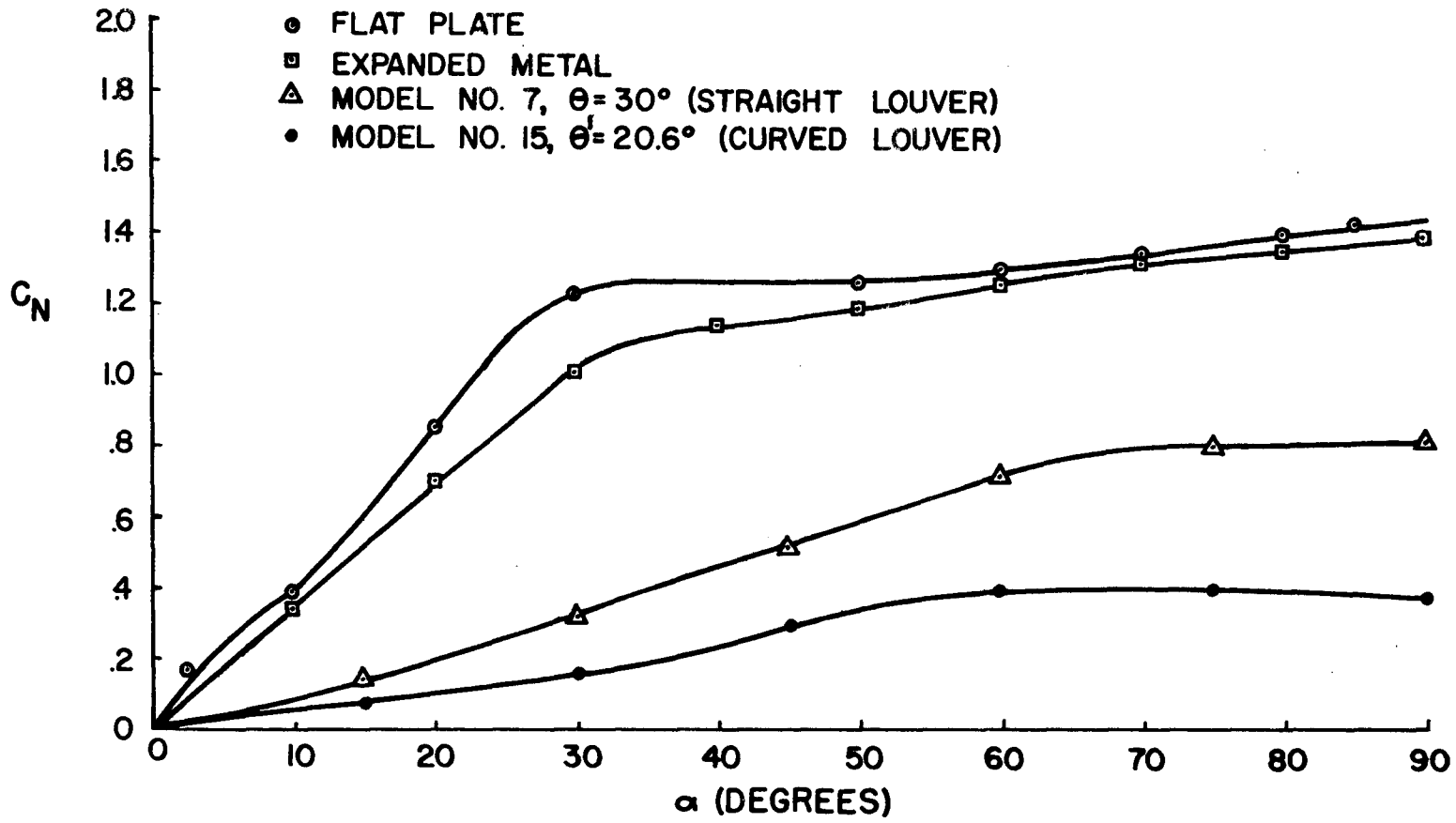

FIGURE 2.3.43 NORMAL-FORCE COEFFICIENT VERSUS ANGLE OF ATTACK FOR FOUR BACKGROUND CONFIGURATIONS

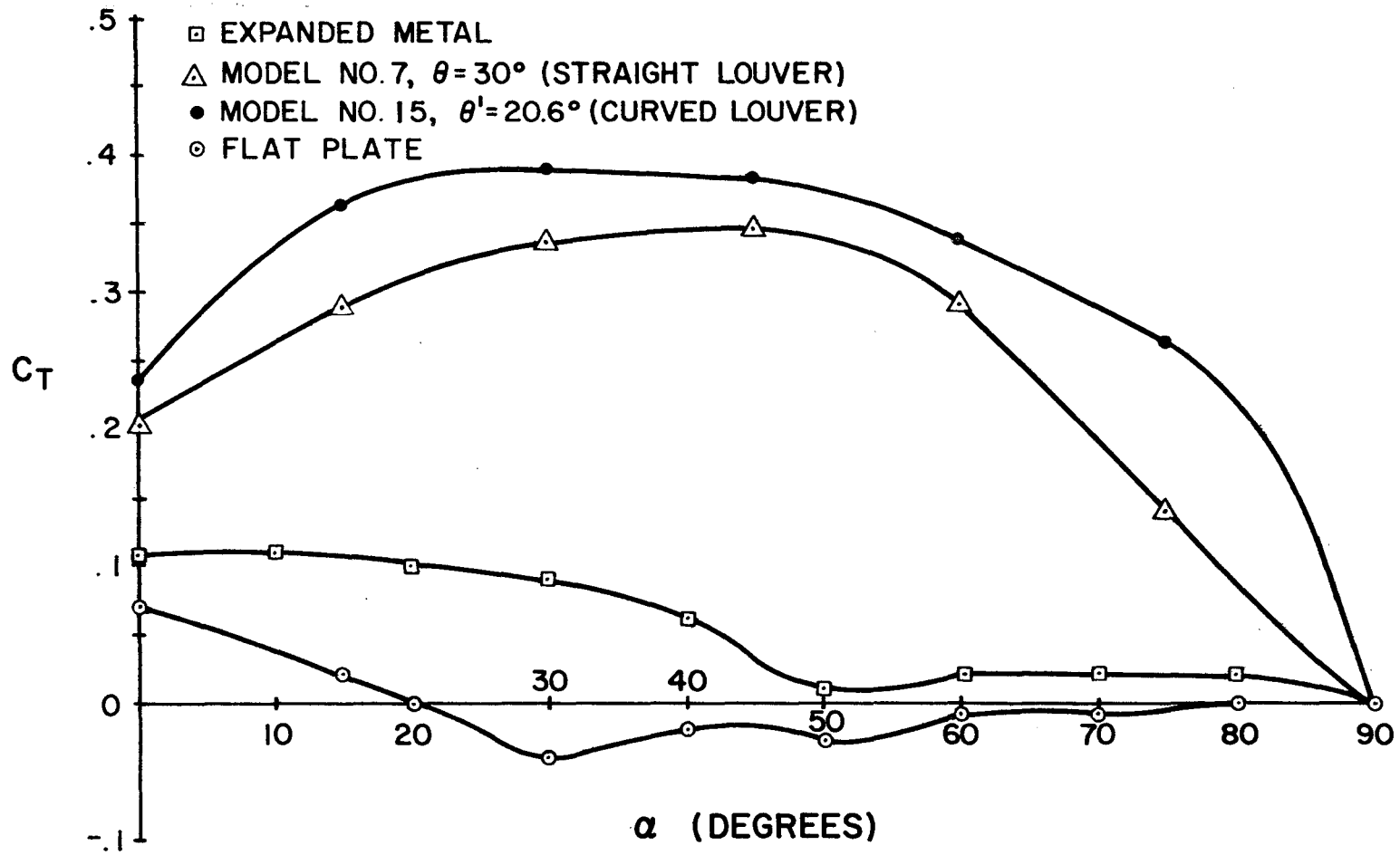

FIGURE 2.3.44 SIDE-FORCE COEFFICIENT VERSUS ANGLE OF ATTACK FOR FOUR BACKGROUND CONFIGURATIONS

on in many cases. Such is the case with flat plates or conventional signs.

Conventional signs. In his test on flat plates, Winter[5] observed that certain flow patterns existed at different ranges of the angle of attack, (refer to Figure 2.4.1). His observations were as follows:

(a) Very small angles of attack -- In this range there was basically the airfoil type of flow. No separation occurred with the flow adhering to the surface.

(b) Angles of attack up to separation -- This was a transition range. The flow was partially detached from the rear or suction side of the plate. The length of the detached area increased as the angle of attack increased. Also observed were strongly developed tip vortices. The vortices were formed by air spilling over the high pressure side (or front) of the plate to the low pressure side (rear). On a sign the tips referred to would be the upper and lower edges of the background.

(c) From separation up to a 90° angle of attack -- In this range the flow was completely separated with no tip vortices present.

Streamers were attached to the models tested in this study, as well as the full-scale sign, and the flow patterns were observed. The same basic patterns as observed by Winter were found to exist with the exception of range (a). The pattern described in range (a) was hardly distinguishable. The flow had some small separations even at the very small angles of attack. This was attributed to the finite thickness of the plates (which was 1/4 inch). Winter's plate models had beveled

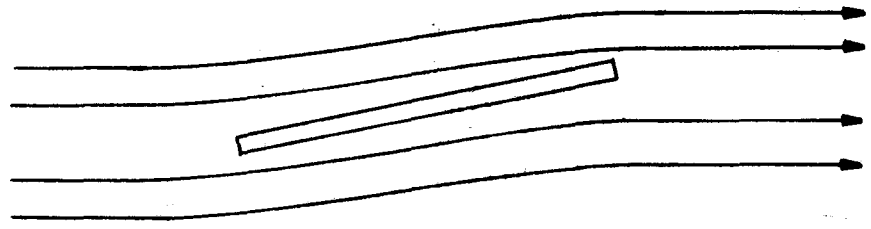

RANGE (a)

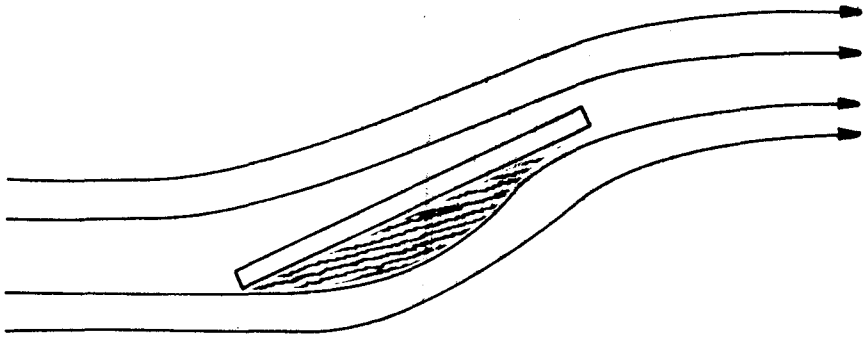

RANGE (b)

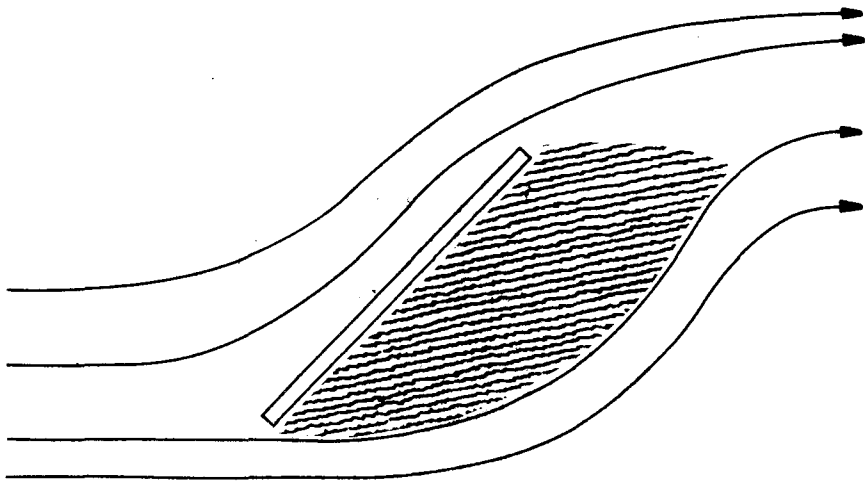

RANGE (c)

FIGURE 2.4.1 FLOW PATTERNS ABOUT FLAT PLATES

edges.

It is significant that this was the only range in which the finite thickness altered the flow pattern. The wind loads in this range are small. Therefore, the edge effects are not considered to be of importance for the thickness ranges of most conventional sign backgrounds.

Range (b) was seen to extend up to about 20°, 30°, and 45° for aspect ratios of 1.4, 1.0, and 0.5, respectively. These points are evident in Figure 2.3.5.

Within range (b) the flow can be considered essentially as divided into two parts, namely, "plate tip flow" and "plate center flow." The "plate tip flow" occurs at the smaller aspect ratios and increasing angles of attack. The "plate center flow" occurs at the larger aspect ratios and is accompanied by partial separation of the flow.

Winter observed that for equal angles of attack there was an increase in the diameter of the tip vortices with decreasing aspect ratio. The vortices were more active on the aft part (or trailing edge) of the plate. The result was an induced transverse flow on the aft part of the suction side. This phenomenon tended to prevent complete separation of the flow, i.e., separation occurred at larger angles of attack. The larger values of the normal force at the smaller aspect ratios are attributed to this phenomenon.

Louvered signs. In considering the development of a means of theoretically predicting the wind forces on the straight louvers, attention was centered on the normal force. The approach used was to determine the normal forces on the various components of the model at

an angle of attack equal to 90°, add them up, then compare the results with the experimental results. Expressions for the component forces were obtained from standard aerodynamic drag (or force) equations. The components consisted of the leading edge drag of the louvers and side plates, windbeam drag, pole drag, viscous drag, and the drag due to the change in momentum of the air as it was deflected by the louvers.

Unfortunately, the theoretical equation proved to be accurate at only the 15° louver angle. The lack of agreement was attributed to the presence of separated flow conditions that existed at the 30° and 45° louver angle configurations. The two different flow patterns are shown in Figure 2.4.2. The flow patterns were determined by observing streamers attached at different points along the louver length and width.

Although theoretical expressions are not available for investigating wind loads at any louver configuration, considerable amounts of experimental data are now available. These data are considered applicable to full-scale signs, provided the louver lengths, widths, and angles of the sign are within the range of values tested. This conclusion is based on the flow patterns that were observed on the models and the nature of the force and moment measurements.

In general, the louvered models were subjected to a combination of two types of flow, namely, flow through the model and flow around the model similar to the flat plate flow. The former type was predominate. This was verified by the absence of well-defined stall or separation points in the data. The absence of any appreciable twisting

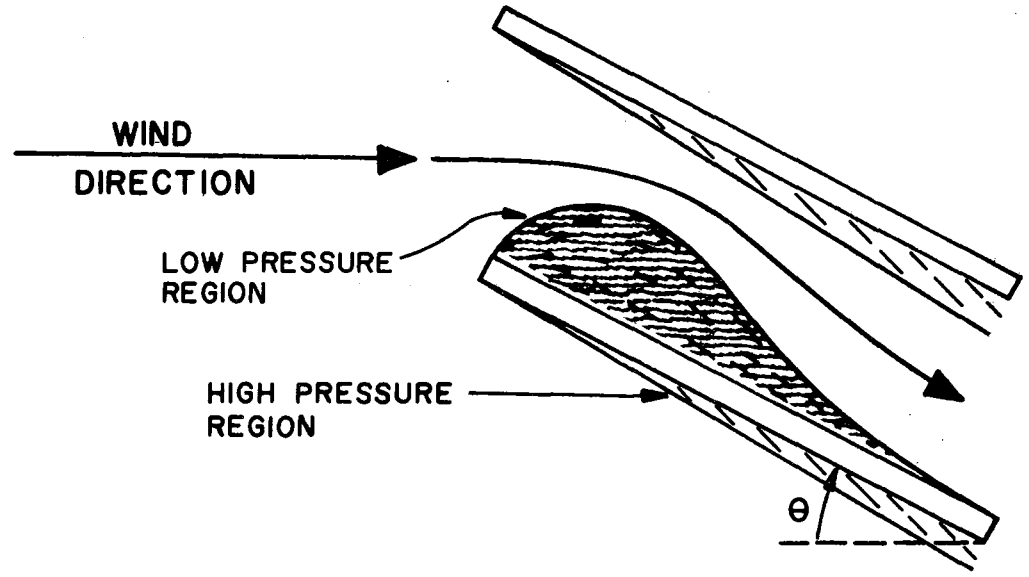

(a) θ=30° AND 45°

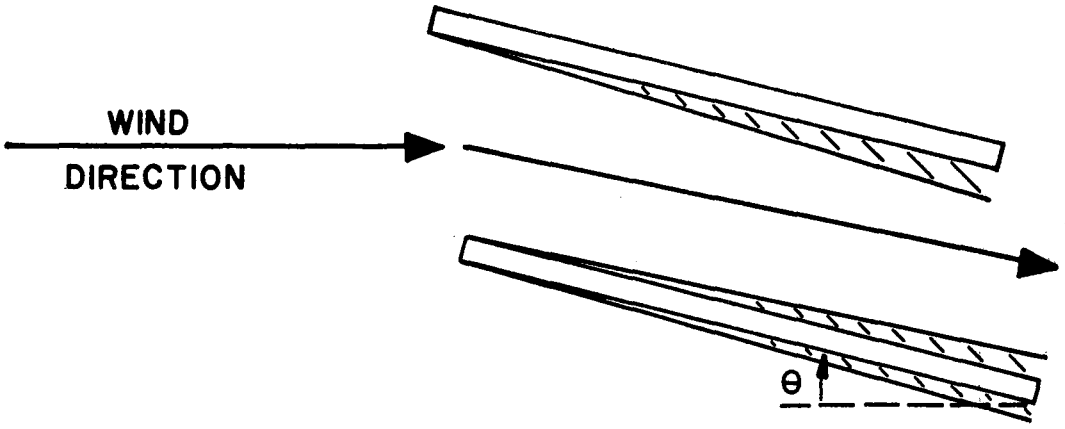

(b) θ=15°

FIGURE 2.4.2 TYPICAL STRAIGHT LOUVER FLOW PATTERN

moment also tends to verify this. It seems reasonable to assume that the flow pattern about larger models would be similar, provided the louver parameters were the same. Similar flow patterns imply similar wind forces, relatively speaking.

Had the flat plate type flow been predominate, the values of the Reynolds number obtained in the tests would not have been large enough to permit the application of the experimental data to full-scale use. The characteristic length in the Reynolds number would then have been the width of the model rather than the width of the louver.

A curved plate configuration was proposed as a means of obtaining a lower drag than the straight or flat plate louvered configuration. The objective of using curved louver plates was to reduce the pressure drag by decreasing the separated flow region which was present for 30° and 45° straight louver plates. Also, curved plates theoretically produce no drag due to a change in the flow direction since the initial and final flow directions are the same.

The theoretical results were similar to the straight louver results. At an effective louver angle (θ') equal to 14.1°, the theory was essentially accurate. However, for effective louver angles of 20.6° and 26.6°, the flow was partially separated and the theory was not applicable.

The experimental data on the curved louver configuration are considered applicable to full-scale signs provided the louver parameters of the sign are within the range of values tested on the models. This conclusion is based on the fact that, in general, the flow patterns were similar to that described for the straight louvers.

Expanded metal. An absence of any substantial wind load reduction in the expanded metal models is attributed mainly to the size and shape of the openings in the material. The boundary layer of air along the surface of the small openings likely retarded air passage through the background. Large louver angles of the models are believed to have produced an effect similar to that shown in Figure 2.4.2(a) on the air that did pass through. As described previously, the drag created by the resulting low pressure region is significant.

CHAPTER 3

A STUDY OF ECONOMIC AND SAFETY ASPECTS OF A SIGN AS A FUNCTION OF THE FREQUENCY OF OCCURRENCE OF DESIGN WINDS

3.1 Introduction

Many factors should be considered in designing an "optimal" sign. For example, one should consider the different types of signs available, the sign material, the location of the sign, the size and color of the letters and sign background, etc. However, the intent of this study was limited to presenting criteria that can be applied in optimizing a sign design when considering its safety aspects (with respect to the motorist) and cost as related to the frequency of occurrence of design winds. The study was constrained to presenting information that can be used in existing AASHO design procedures,[2] with the exception of design wind velocities. In other words, improvements made to the economic and safety aspects of a sign are accomplished by reducing the present design wind velocity rather than changing the sign type, material, location, etc.

A formulation of the problem is included in Section 3.3 in order that one may better understand how the equations were developed and may be used. The "Size" part of Section 3.3 deals with the relation between sign size and frequency of occurrence of design winds. The "Cost" part deals with cost as related to the frequency of occurrence of design winds.

It is important that the meaning of the words "safety" and "size" as used in this study is understood. Safety will refer to the relative

safeness of the sign with respect to the motorist, i.e., the relative hazard that the sign presents to the travelling public. By size is meant the cross-sectional area of those members of the sign whose geometry is dependent on the wind loads. The cross-sectional area of the sign's supports, windbeams, and background are determined according to the magnitude of wind loads. Height and width dimensions of the background are dependent on factors other than wind loads.

The weight or mass of a homogeneous structural member, whose cross-sectional geometry is constant along its length, is directly proportional to the cross-sectional area of the member. Such is the case with most members used in highway signs. The stiffness of a member can be related to its cross-sectional area, but in general is not directly proportional. Hence, as defined, size can be thought of as a measure of the mass and stiffness of the sign structure. In turn, the mass and stiffness of a sign, particularly its supports, are generally regarded as a measure of the sign's relative safeness to the motorist. It is within this context that safety is given dimensions in this study.

It is emphasized that a high degree of uncertainty exists as to the actual relation between mass and stiffness and relative safeness. No attempt was made to relate the two in this study. For example, if the mass and stiffness of a sign structure are reduced by 30% the resulting structure is not necessarily 30% safer. This uncertainty presents a formidable obstruction to the development of specific optimum criteria with regard to safety. Developing criteria when safety and economics are coupled is an even more difficult task. Nevertheless, the information

presented in this study should afford the user with valuable data to aid him in arriving at a more satisfactory design within the boundaries of his particular situation.

The present recurrence interval for the design winds on a sign as specified by AASHO is 50 years. Designing to these low probability winds often results in having larger structures than needed, and thus a greater safety hazard. In some cases, signs have to be removed or replaced within five to ten years after installation for reasons other than wind damage. Another factor to consider when designing a sign is its replacement cost after being blown down. If the replacement cost is small compared with the initial cost, it may be advantageous to reduce the recurrence interval of design winds. These and other factors are considered in this study and are discussed in more detail in Sections 3.3 and 3.4.

The study relies heavily on information obtained from a report by Thom,[10] Chief Climatologist, Office of Climatology, U. S. Weather Bureau. In his report, Thom took the records of 141 open-country stations, with a cumulative total of about 1,700 years of records averaging about 15 years per station, and, through statistical analysis, arrived at distributions of extreme winds in the United States. The data obtained from Thom's report were invaluable.

3.2 Assumptions

In order to conduct this investigation, certain assumptions were necessary. They are listed below along with general comments concerning

their validity. To actually authenticate or disprove these assumptions will require further investigations, both analytically and experimentally.

1. The assumption was made that a sign's design loads consist of wind forces only. For most roadside signs, this assumption is acceptable. However, in the large overhead bridge signs, the live and dead loads (as defined by AASHO) have a larger influence on the size structure required and the assumption would likely be unacceptable in these cases.

2. As a sign is designed for higher probability winds (lower velocities), its size (or mass) and stiffness are reduced. In so doing, the critical wind speed at which resonance occurs may fall below the recommended value as determined in this study. No provisions are made for that possibility, i.e., it was assumed that resonance will not occur below the recommended design wind velocity. The validity of this assumption will depend to a large degree on a particular sign's geometric configuration, including the support spacing, the type of support used, and the type of sign background.

3. With regard to Assumption 2, it was also assumed that the stiffness was such that fatigue will not be a problem. Again, the validity of this assumption depends on the geometric configuration of the sign and the material used.

4. It was assumed that a sign will blow down or experience a structural failure when subjected to the wind velocity for which it was designed. This assumption applies to the present design and to

the reduced design sign, with both types being designed according to AASHO procedures, including safety factors. The validity of this assumption is questionable since the safety factors referred to sometimes reach a value as large as 1.8. However, it was not the purpose of this study to investigate the use of safety factors.

5. It was assumed that the replacement cost, due to a wind load failure, of the currently used sign equals the replacement cost of the reduced design for the same type failure. If a built-in failure mechanism could be incorporated in the reduced design its replacement cost would likely fall below the currently used design and, in turn, enhance the use of the reduced design.

6. It was assumed that the yearly maintenance cost is independent of sign size (as defined previously).

3.3 Formulation of Problem

Size. In Thom's paper, an equation was presented for determining the probability F(X) of a given wind speed being less than X for any given geographical location.

$$F(X) = e^{-[X/\beta]^{-G}} \qquad (3.3.1)$$

In this equation, the value of β and G are found by imposing the boundary conditions:

$$@\ X = V_1,\ F(X) = 0.50$$

and

$$@\ X = V_2,\ F(X) = 0.98$$

These boundary conditions render two equations in terms of β and G and upon solving yield

$$\beta = V_1 \, (.694)^{\left(\frac{\ln \frac{V_1}{V_2}}{-3.54}\right)}$$

and

$$G = -3.54/\ln \left(\frac{V_1}{V_2} \right)$$

where

V_1 = extreme mile wind velocity that occurs during an average 2-year period.

V_2 = extreme mile wind velocity that occurs during an average 50-year period.

The average recurrence interval, R, can be found by the relationship

$$R = 1/[1-F(X)] \qquad (3.3.2)$$

For example, if, for a given ratio V_1/V_2 and a velocity X, the probability F(X) = 0.90, the recurrence interval R would be

$$R = 1/(1 - 0.9) = 10 \text{ years}$$

i.e., one could expect the wind to reach the velocity X once in a mean 10-year period.

Taking the natural logarithm of both sides of Equation 3.3.1. and solving for X yield

$$X = \beta(-\ln F)^{-1/G} \qquad (3.3.3)$$

where

$F = F(X)$

The widely accepted equation for the force per unit area, Q, on a structure due to wind loads is

$$Q = 1/2\ c\rho X^2 \qquad (3.3.4)$$

where c is a constant determined by the shape factor and gust load factor and ρ equals the mass density of the air.

Substituting from Equation 3.3.3 into Equation 3.3.4 yields

$$Q = 1/2\ c\rho\beta^2\ (-\ln F)^{-2/G} \qquad (3.3.5)$$

Thus, for a given structure and V_1/V_2 ratio, it can be seen that the forces or loads on the structures are proportional to $(-\ln F)^{-2/G}$.

The size, or weight, W, of an elastic structure is related to the applied loads and in the present case,

$$W \sim [(-\ln F)^{-2/G}]^f \qquad (3.3.6)$$

(The symbol "$\sim$" means proportional.)

where the exponent f is dependent on the manner in which the structure resists the loads and the type member used. For most roadside sign

configurations, the wind loads are resisted by bending in the supports. Consider a member as shown in Figure 3.3.1.

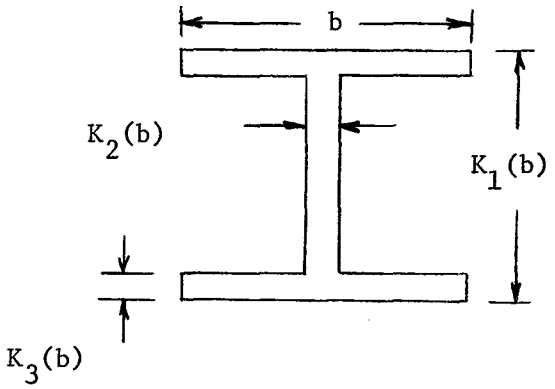

FIGURE 3.3.1 WIDE-FLANGE CROSS SECTION

The cross sectional area A_c is computed as

$$A_c = b^2 (2K_3 + K_1K_2 - 2K_2K_3)$$

and the section modulus z as

$$z = b^3 \left[\frac{K_3}{K_1} (K_1 - K_3)^2 + \frac{K_2}{6K_1} (K_1 - 2K_3)^3\right]$$

The bending stress

$$\sigma_b = \frac{M}{z}$$

where M equals the bending moment. Let

$$\sigma_b = \sigma_D$$

where σ_D is the design stress. Then

$$z = \frac{M}{\sigma_D}$$

If the factors, K_1, K_2 and K_3 remain constant as the moment (M) varies, then z and A_c are proportional to b^3 and b^2, respectively. This is obviously not possible in some cases with available commercial sizes, however, for the purpose of this example, this assumption is made.

The following proportionalities exist:

$$z \sim M$$

therefore,

$$b^3 \sim (-\ln F)^{-2/G}$$

since the moment

$$M \sim Q = (-\ln F)^{-2/G}$$

Then,

$$b^2 \sim [(-\ln F)^{-2/G}]^{2/3} \sim A_c$$

Since the weight/unit length, W, is proportional to the area A_c,

$$W \sim [(-\ln F)^{-2/G}]^{2/3}$$

Thus,

$$f = 2/3$$

In fact, f = 2/3 for any cross section in which the area is proportional to b^2 and the section modulus is proportional to b^3. For instance, a rectangular section in bending as shown in Figure 3.3.2.

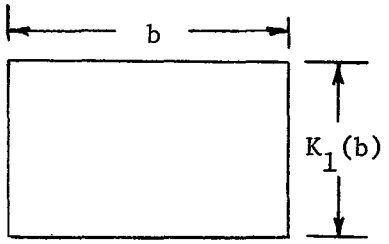

FIGURE 3.3.2 RECTANGULAR CROSS SECTION

would have f = 2/3, provided K_1 remains constant as the cross section is varied.

For members subjected to axial loads, f = 1.0 since the area is directly proportional to the load.

With the factor "f" and Equation 3.3.6, the relative size of a structure as the probability F is varied can now be investigated.

As a general case, let F_p be the probability factor for which the signs in a particular area are being designed. The question is: What percent reduction can one expect in the sign size if the probability factor is reduced to F? If r represents the percent reduction, one gets, using Equation 3.3.6,

$$r = 100\left\{\frac{[(-\ln F_p)^{-2/G}]^f - [(\ln F)^{-2/G}]^f}{[(-\ln F_p)^{-2/G}]^f}\right\}$$

or

$$r = 100\% \left[1 - \left(\frac{\ln F}{\ln F_p} \right)^{-2f/G} \right] \qquad (3.3.7)$$

A relationship between F and R can be obtained from Equation 3.3.2,

$$F = F(X) = \frac{R-1}{R} \qquad (3.3.8)$$

Using this value of F in Equation 3.3.7, one obtains the relation between the percent reduction r and the recurrence interval R

$$r = 100\% \left[1 - \left(\frac{\ln \frac{R-1}{R}}{\ln \frac{R_p-1}{R_p}} \right)^{-2f/G} \right] \qquad (3.3.9)$$

where R_p is the wind recurrence interval for which the signs are presently being designed.

As an example, the curves in Figure 3.3.3 represent a plot of Equation 3.3.9, with the following values used:

R_p = 50 years (i.e., the present sign's design life is 50 years)

f = 0.667 (bending loads)

and V_1/V_2 = 0.20 (G = 2.19)

V_1/V_2 = 0.40 (G = 3.86)

V_1/V_2 = 0.60 (G = 6.92)

V_1/V_2 = 0.80 (G = 15.85)

If, for instance, a sign is in an area where the ratio of V_1/V_2 equals 0.60 and one wishes to redesign to a recurrence interval of 10 years,

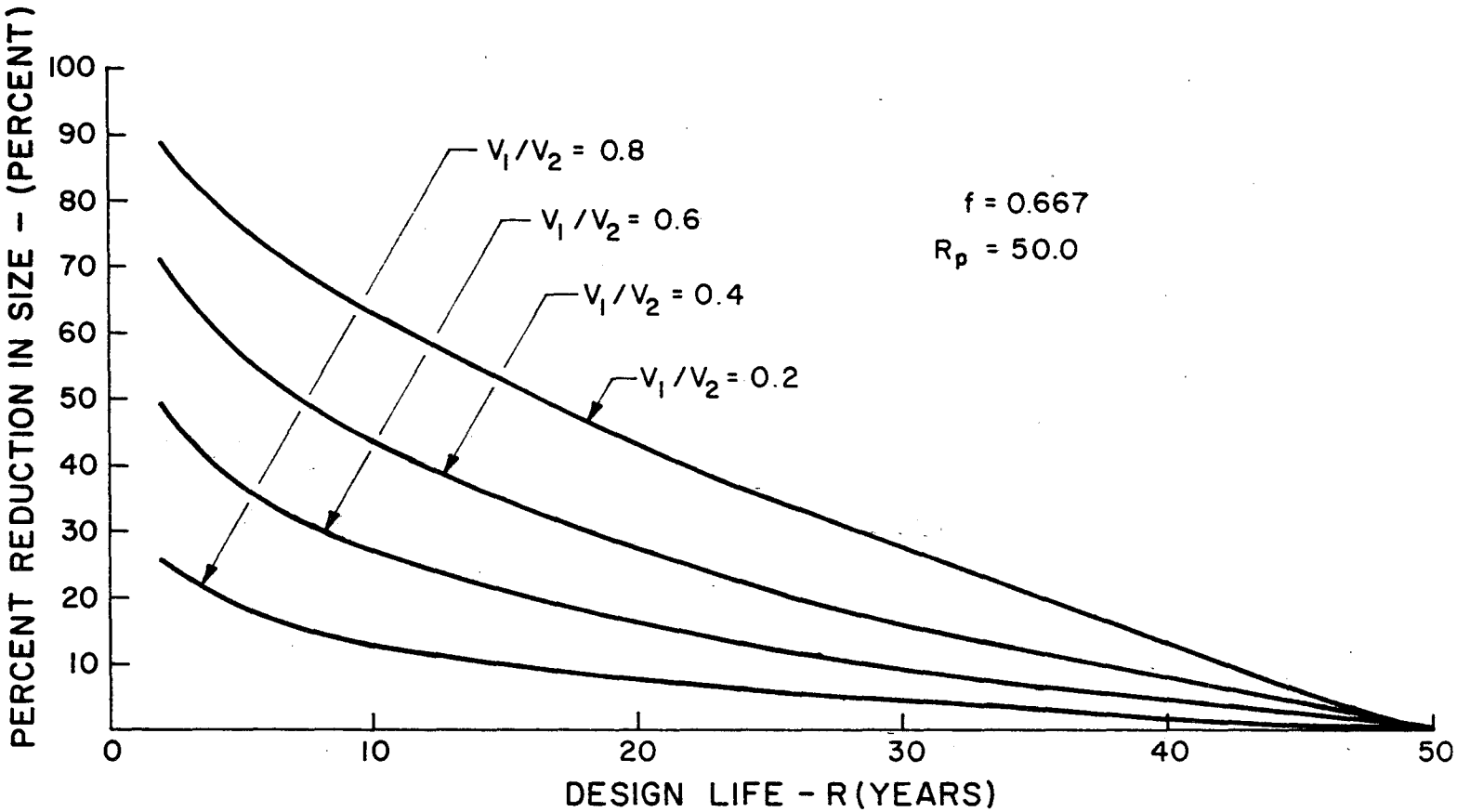

FIGURE 3.3.3 PERCENT CHANGE IN 50-YEAR DESIGN SIZE VERSUS REDUCED DESIGN LIFE

the percent reduction in the 50-year design (size) would be 27.2 percent (refer to Section 3.1 for definition of size).

Cost. It has been shown what reductions in size can be expected as the sign is designed for higher probability winds. The effects on sign cost of designing for higher probability winds will now be considered.

Following is a list of factors considered, in addition to those named in "Size," and an explanation of each:

C_I = initial cost of the sign with reduced design life, i.e., the cost based on the reduced design life R.

C_{Ip} = initial cost of the sign now being used, i.e., the cost based on the present design life R_p. Initial cost includes material, fabrication, and installation cost.

A = useful life of sign - defined as the length of time the sign, whether the present design or the reduced design, will normally remain in place, assuming no wind damage. At the end of its useful life, the sign will either be replaced or removed entirely. Useful life is not to be confused with "design life" or "recurrence interval" R_p as defined previously.

B = Replacement factor - defined as the ratio of the cost required to replace a blown down sign to the initial sign cost.

$$B = \frac{\text{Cost to Replace}}{\text{Initial Cost}}$$

ϕ = Cost function - a function which relates the initial cost of a sign to the size of the sign.

I = Interest rate - used to discount to the present all costs occurring in future periods.

K_p = Maintenance factor - defined as the ratio of the yearly maintenance cost to the sign's initial cost.

$$K_p = \frac{\text{Maintenance Cost Per Year}}{\text{Initial Cost}}$$

K_1 = Salvage factor - defined as the ratio of the salvage value of the sign with reduced design at end of its useful life to its initial cost.

$$K_1 = \frac{\text{Salvage Value of Reduced Design Sign}}{\text{Initial Cost of Reduced Design Sign}}$$

K_2 = Salvage factor of present design

$$K_2 = \frac{\text{Salvage Value of Present Sign}}{\text{Initial Cost of Present Sign}}$$

In order to have a basis for comparison, total sign costs as used in the present research refers to all sign costs incurred during the useful life of a sign. The total cost related to the present design and the reduced design were computed and the results compared to show the percent difference.

Computation of Initial Cost:

Consider the cost function as shown in Figure 3.3.4. It

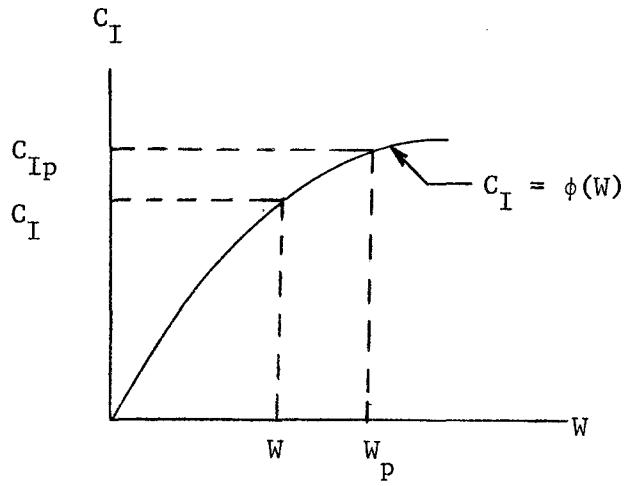

FIGURE 3.3.4 INITIAL COST VERSUS SIZE

can be shown by use of Equation 3.3.9 that

$$\frac{W}{W_p} = 1 - \frac{r}{100}$$

where W_p is the present sign's size and W is the reduced design size. Then

$$W = W_p \left(1 - \frac{r}{100}\right)$$

C_I and C_{Ip} can now be expressed

$$C_I = \phi\left[W_p \left(1 - \frac{r}{100}\right)\right] \qquad (3.3.10)$$

and

$$C_{Ip} = \phi(W_p) \qquad (3.3.11)$$

Computations of Replacement Cost:

C_R and C_{Rp} are now defined as the replacement cost occurring over the useful life of the reduced design and the present design, respectively. Then,

$$C_R = \sum_{J=1}^{A} \frac{P(B)(C_I)}{(1 + I)^J} \qquad (3.3.12)$$

$$C_{Rp} = \sum_{J=1}^{A} \frac{P_p(B)(C_{Ip})}{(1 + I)^J} \qquad (3.3.13)$$

where $P = \frac{1}{R}$ = probability of the reduced wind velocity occurring in any one year, and $P_p = \frac{1}{R_p}$ = probability of the present design wind velocity occurring in any one year.

If these values of P and P_p are substituted into Equation 3.3.12 and 3.3.13, respectively, and the equations are simplified, the following equations are determined.

$$C_R = \frac{B\ C_I}{R} \sum_{J=1}^{A} \frac{1}{(1 + I)^J} \qquad (3.3.14)$$

$$C_{Rp} = \frac{B\ C_{Ip}}{R_p} \sum_{J=1}^{A} \frac{1}{(1 + I)^J} \qquad (3.3.15)$$

Computation of Maintenance Cost:

C_{mp} is defined as the maintenance cost of the sign presently being used. As mentioned earlier, the assumption was made that the

maintenance cost of the reduced design also equals C_{mp}. The quantity C_{mp} is then determined by

$$C_{mp} = \sum_{J=1}^{A} \frac{K_p C_{Ip}}{(1 + I)^J} = K_p C_{Ip} \sum_{J=1}^{A} \frac{1}{(1 + I)^J} \qquad (3.3.16)$$

Computation of Salvage Value:

C_s and C_{sp} are defined, respectively, as the salvage values of the reduced design and the present design, at the end of their useful life. C_s and C_{sp} are then determined by the equations,

$$C_s = K_1 C_I \left[\frac{1}{(1 + I)^A} \right] \qquad (3.3.17)$$

and

$$C_{sp} = K_2 C_{Ip} \left[\frac{1}{(1 + I)^A} \right] \qquad (3.3.18)$$

Computation of Total Cost:

A. Reduced Design. Let C_t denote the total cost of the reduced design occurring over its useful life. Then,

$$C_t = C_I + C_R + C_{mp} - C_s \qquad (3.3.19)$$

Note: The cost involved in salvaging the sign may exceed its salvage value in which case C_s would be negative, which would then result in

an additional cost.

If values from Equation 3.3.10, 3.3.14, 3.3.16, and 3.3.17 are substituted for their equivalents in Equation 3.3.19,

$$C_t = \phi \left[W_p \left(1 - \frac{r}{100}\right) \right] \left[1 + \frac{B}{R} (\Sigma) - \frac{K_1}{(1 + I)^A} \right] + K_p C_{Ip} (\Sigma)$$

where

$$\Sigma = \sum_{J=1}^{A} \frac{1}{(1 + I)^J} = \frac{(1 + I)^A - 1}{I(1 + I)^A}$$

If the relation for C_{Ip} from Equation 3.3.11 is substituted into the above equation, the following relation is obtained.

$$C_t = \phi \left[W_p \left(1 - \frac{r}{100}\right) \right] \left[1 + \frac{B}{R} (\Sigma) - \frac{K_1}{(1 + I)^A} \right]$$

$$+ \phi (W_p) K_p (\Sigma) \qquad (3.3.20)$$

B. Present Design. Let C_{tp} denote the total cost of the present design occurring over its useful life. Then,

$$C_{tp} = C_{Ip} + C_{Rp} + C_{mp} - C_{sp} \qquad (3.3.21)$$

If values from Equations 3.3.11, 3.3.15, 3.3.16, and 3.3.18 are substituted for the equivalent values in Equation 3.3.21,

$$C_{tp} = \phi (W_p) \left[1 + \frac{B}{R_p} (\Sigma) + K_p (\Sigma) - \frac{K_2}{(1 + I)^A} \right] \qquad (3.3.22)$$

A ratio of reduced design to present design cost can now be obtained from Equations 3.3.20 and 3.3.22. If Z denotes this ratio,

$$Z = \frac{C_t}{C_{tp}} \tag{3.3.23}$$

The values of C_t and C_{tp} from Equations 3.3.20 and 3.3.22 substituted into Equation 3.3.23 yield

$$Z = \frac{\phi[W_p\ (1 - \frac{r}{100})]\ [1 + \frac{B}{R}\ (\Sigma) - \frac{K_1}{(1 + I)^A}\ ] + \phi(W_p)\ K_p\ (\Sigma)}{\phi(W_p)\ [1 + \frac{B}{R}\ (\Sigma) + K_p\ (\Sigma) - \frac{K_2}{(1 + I)^A}\ ]} \tag{3.3.24}$$

Thus, for a given cost function ϕ and values of A, B, I, K_p, K_1, K_2, W_p, f, G, and R_p, the ratio Z can be found as a function of the recurrence interval R of the design wind velocity.

If ϕ was of the form $\phi = KW^n$, Equation 3.3.24 could be altered as follows. The term

$$\frac{\phi[W_p\ (1 - \frac{r}{100})]}{\phi(W_p)}$$

would simplify to

$$\frac{K(W_p)^n\ (1 - \frac{r}{100})^n}{K(W_p)^n} = (1 - \frac{r}{100})^n$$

Substituting the above relationship into Equation 3.3.24 yields:

$$Z = \frac{(1 - \frac{r}{100})^n \left[1 + \frac{B}{R}(\Sigma) - \frac{K_1}{(1+I)^A}\right] + K_p(\Sigma)}{1 + \frac{B}{R_p}(\Sigma) + K_p(\Sigma) - \frac{K_1}{(1+I)^A}} \qquad (3.3.25)$$

If the value of r from Equation 3.3.9 is substituted into Equation 3.3.25, the following relation is obtained.

$$Z = \frac{\left(\frac{\ln \frac{R-1}{R}}{\ln \frac{R_p-1}{R_p}}\right)^{-2fn/G} \left[1 + \frac{B}{R}(\Sigma) - \frac{K_1}{(1+I)^A}\right] + K_p(\Sigma)}{1 + \frac{B}{R_p}(\Sigma) + K_p(\Sigma) - \frac{K_2}{(1+I)^A}} \qquad (3.3.26)$$

Thus, Equation 3.3.26 is a special form of Equation 3.3.24 when ϕ is of the form KW^n.

If the percent change in cost is wanted, the following relationship is used:

$$Z_r = (1 - Z)\ 100\% \qquad (3.3.27)$$

where Z is obtained from either Equation 3.3.24 and 3.3.26. It should be noted that a positive Z_r indicates the reduced design cost is less than the present design, and vice-versa.

Next, some examples will be considered. Assume the following

values are given:

V_1/V_2 = 0.60 (G = 6.92)

f = 0.667

R_p = 50 years

B = 0.25

n = 0.50 (i.e., the initial cost varies as the square root of the size).

$K_1 = K_2 = 0$

K_p = 0.025

I = 0.0

The curves of Figure 3.3.5 represent a plot of Equation 3.3.27 (using Z from Equation 3.3.26) for the given values of the parameters and for values of A equal to 5, 10, 20, and 50 years. The portions of the curves above the zero axis represent the percent savings possible in the present design cost as the design life is reduced and the portions below it represent a percent increase.

The curves of Figures 3.3.6, 3.3.7, and 3.3.8 are similar to those in Figure 3.3.5 with the following exceptions:

Figure 3.3.6, I = 0.05

Figure 3.3.7, B = 0.50

Figure 3.3.8, B = 0.50
I = 0.05

Note: "Design Life" as used in the plots and

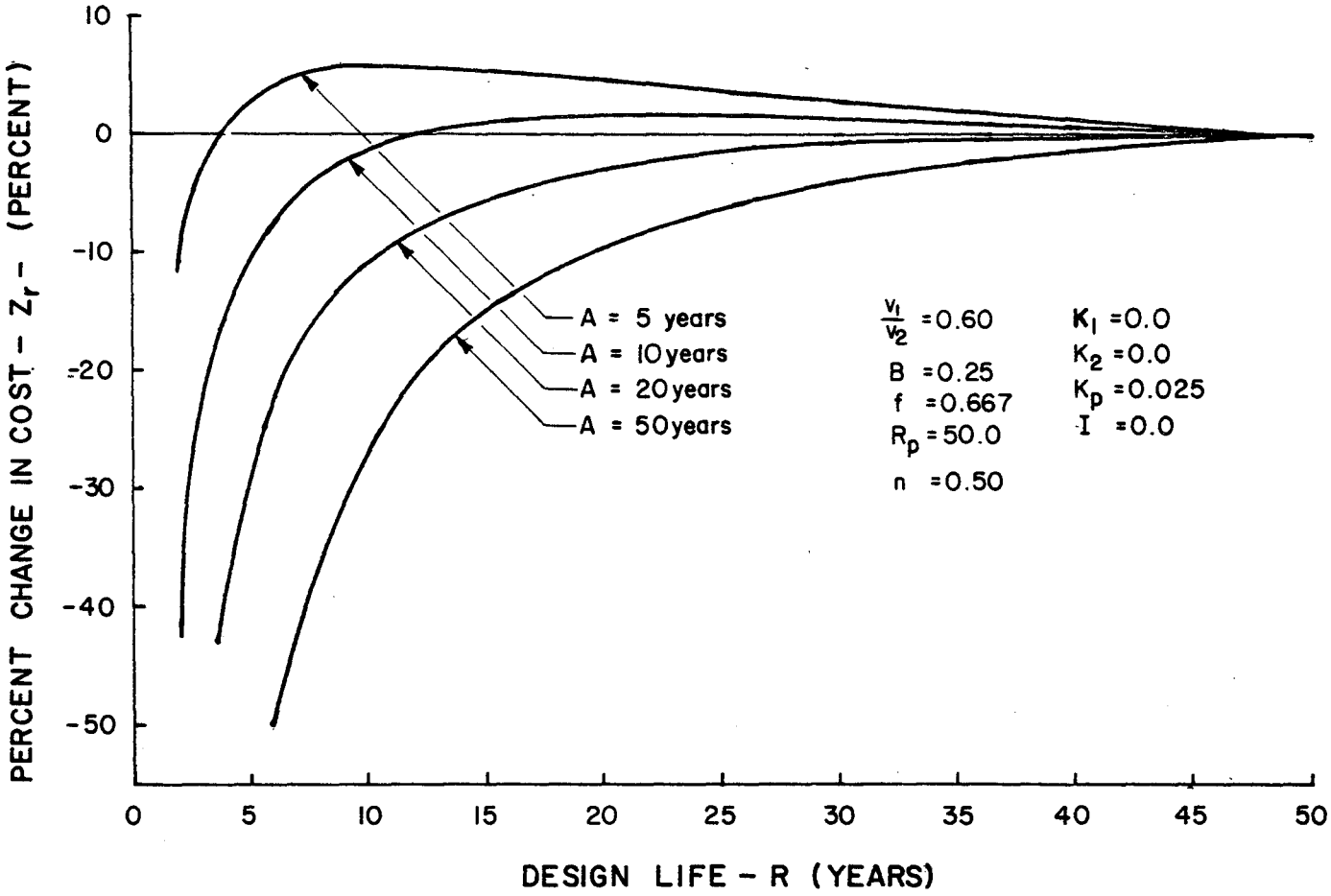

FIGURE 3.3.5 PERCENT CHANGE IN 50-YEAR DESIGN COST VERSUS REDUCED DESIGN LIFE, B=0.25, I=0.0

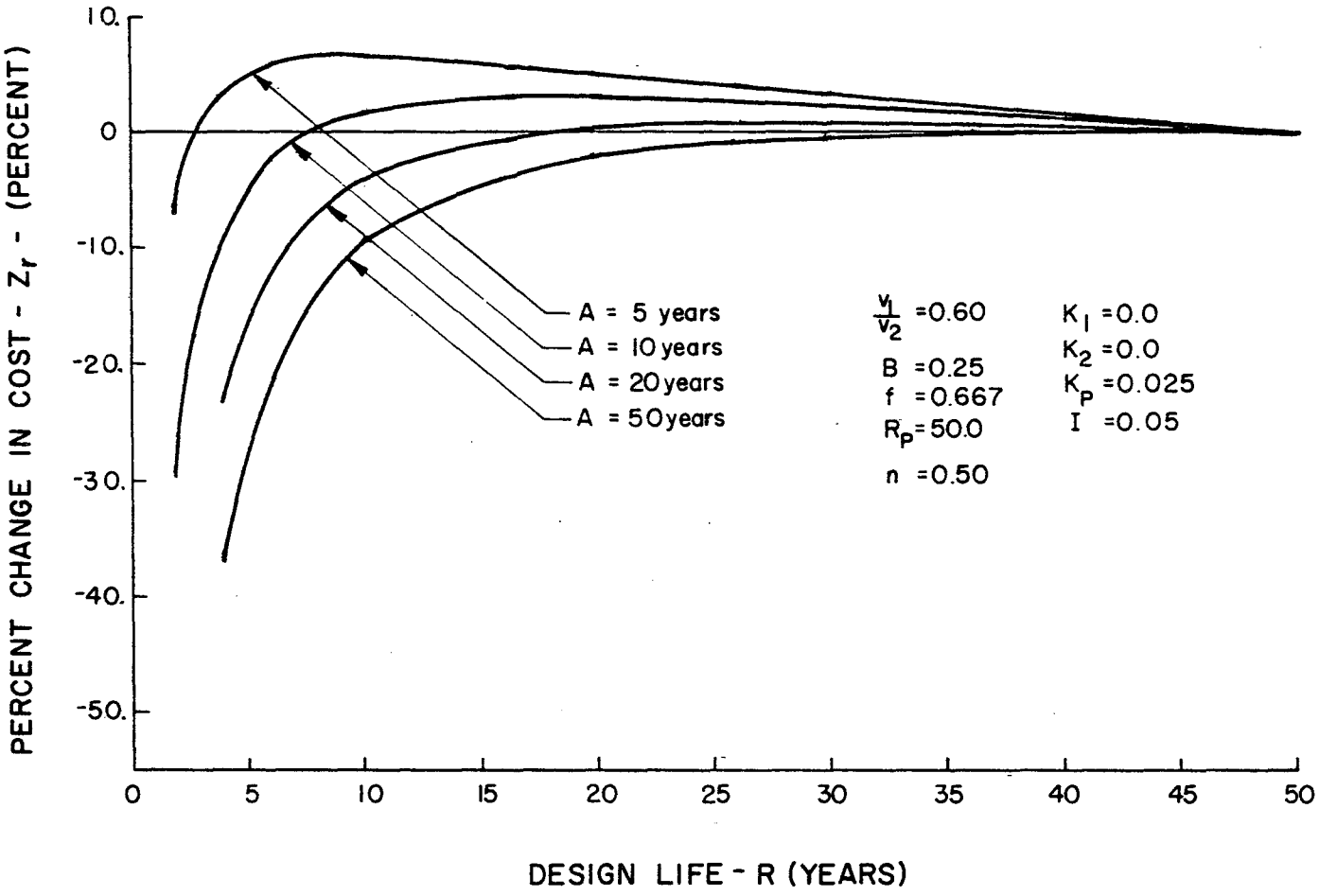

FIGURE 3.3.6 PERCENT CHANGE IN 50-YEAR DESIGN COST VERSUS REDUCED DESIGN LIFE, B=0.25, I=0.05

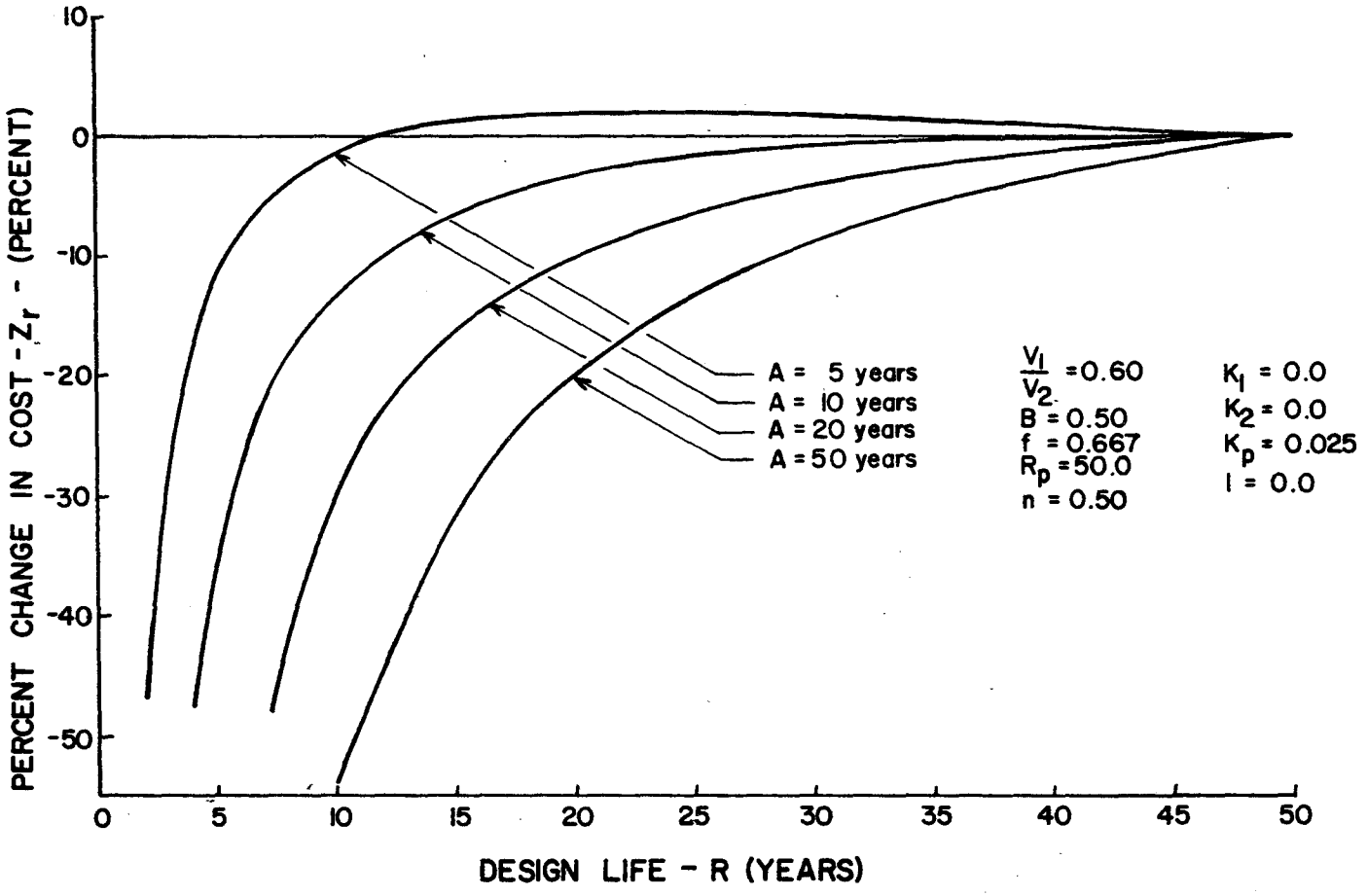

FIGURE 3.3.7 PERCENT CHANGE IN 50-YEAR DESIGN COST VERSUS REDUCED DESIGN LIFE, B=0.50, I=0.0

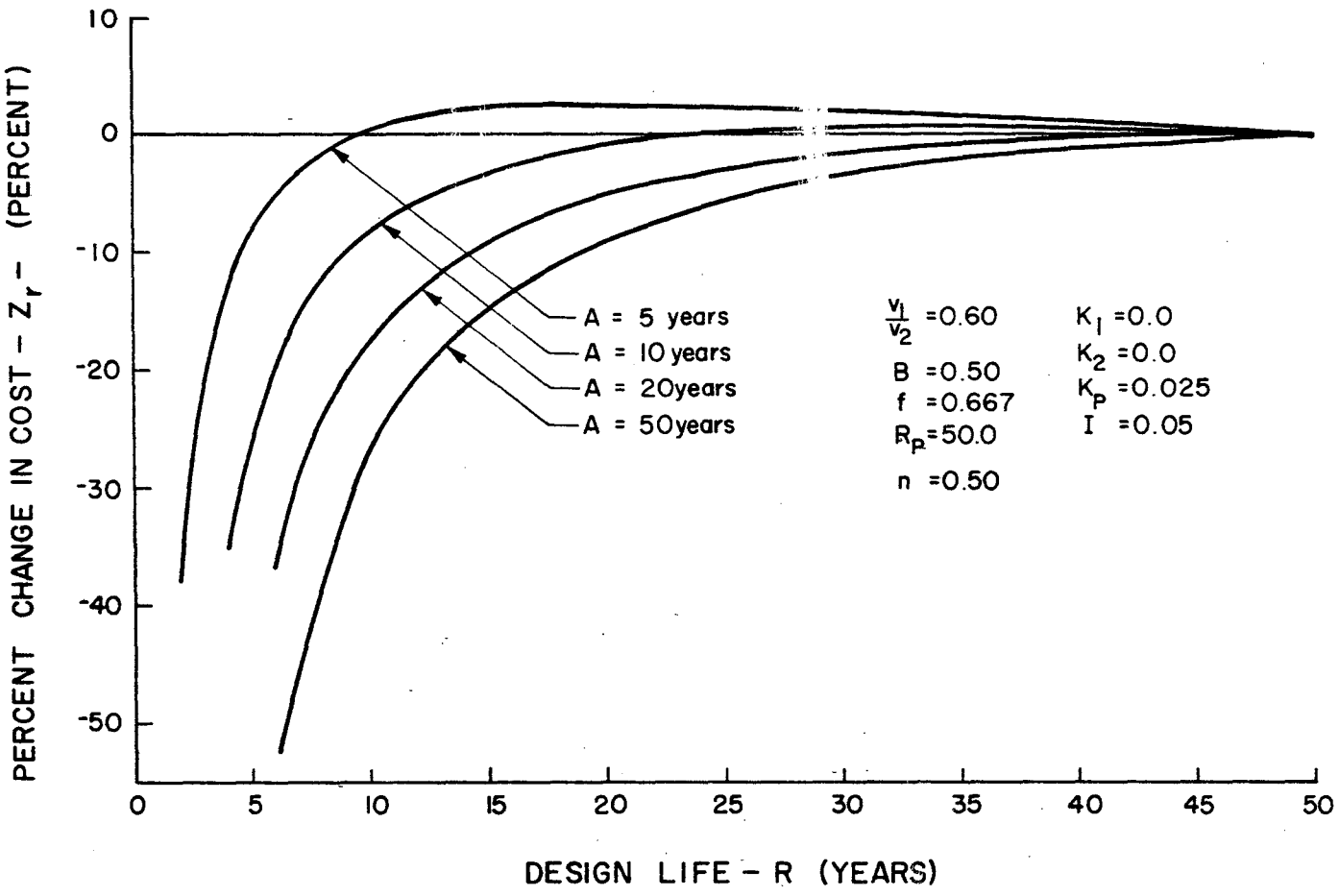

FIGURE 3.3.8 PERCENT CHANGE IN 50-YEAR DESIGN COST VERSUS REDUCED DESIGN LIFE, B=0.50, I=0.05

"recurrence interval of design wind velocity" are one and the same.

3.4 Discussion of Results

Two basic equations were derived in this study whereby the percent change in size (Equation 3.3.9) and cost (Equation 3.3.27) can be computed as a function of the design life (which is equal to the recurrence interval of the design wind velocity), provided certain parameters are available and provided the previously listed assumptions are accepted. Examples of each equation were plotted for selected parameters. The parameters used in the examples were chosen for specific reasons:

1. The 50-year value for the present design life R_p was selected because the design wind speed for signs, as specified by AASHO, has a recurrence interval of 50 years.

2. The factor f = 0.667 was used because most highway signs resist the wind loads by bending in the supports, i.e., the signs are of the cantilever type.

3. A ratio of V_1/V_2 equal to 0.6 was selected because this is representative of a considerable area of the United States (see Figures 2 and 3 of Reference 10).

4. A nonlinear relationship between initial cost and size of the form $\phi = KW^{0.5}$ was used since it is believed that this type of relationship will approximate the actual cost function of most highway signs, especially the larger types of roadside signs. For example, if the mass of reduced design is 80 percent of the present design mass,

the percent reduction in initial cost would be computed as follows:

$$\phi_1 = KW_p^{0.5} = \text{initial cost of present sign}$$

$$\phi_2 = K(0.8W_p)^{.5} = \text{initial cost of reduced sign}$$

$$\text{Therefore, percent reduction in cost} = \frac{KW_p^{0.5} - K(0.8W_p)^{0.5}}{KW_p^{0.5}} \times 100\%$$

$$= [1 - (0.8)^{0.5}] \times 100\%$$

$$= 10.5\%$$

5. A replacement factor, B, equal to 0.25 was used in the belief that it is a reasonable value for the ratio of cost to replace a blown-down sign to initial cost of the sign. The curves of Figures 3.3.7 and 3.3.8, based on B = 0.50, were included for comparative purposes.

6. The particular values of K_1, K_2 and K_p were chosen, again, because it was considered that these values are representative of most signs.

The curves of Figure 3.3.3 show the percent change in size for four different ratios of V_1/V_2 as the design life is reduced. As is evident, the smaller the ratio of V_1/V_2 the larger the reduction in size. Areas along the coastline, where tropical storms are expected to occur on the average of once in a 40 or 50 year period, have the lower V_1/V_2 ratios and could therefore realize substantial reductions in sign size by reducing the 50-year design life to a lower value. In

areas where the average yearly wind speed is not much less than the 50-year wind, the reduction in size would not be as great.

From the curves of Figures 3.3.5, 3.3.6, 3.3.7, and 3.3.8 it can be seen, for certain values of the parameters, that reductions in cost can be realized as the design life is reduced. For example, from Figure 3.3.5, with the useful life "A" equal to five years, a 5.6 percent reduction in cost can be realized if the 50-year design life is reduced to 12 years, provided the parameters used are acceptable. This 12-year design life would be optimum from an economic standpoint, i.e., this is the point of maximum saving. For a 12-year design life, the corresponding reduction in size would be 24.5 percent (from Figure 3.3.3 with $V_1/V_2 = 0.60$). If safety is of primary concern, the same sign could be designed for a 3 3/4-year life (from Figure 3.3.5), with no changes in the 50-year design cost, but with a 41 percent reduction in size (from Figure 3.3.3). The choice would be up to the agency concerned.

Figures 3.3.5, 3.3.6, 3.3.7, and 3.3.8 also show that for certain values of the parameters, the optimum design life is actually the present design life, i.e., 50 years. In fact, for some cases, the optimum design life from an economic standpoint may go beyond the 50-year value. This possibility was not investigated.

Figure 3.3.6 is similar to Figure 3.3.5 except the interest rate "I" equals 5 percent instead of 0 percent. A comparison of Figures 3.3.5 and 3.3.6 shows the effect of discounting to the present, at the rate of 5 percent, all costs which will occur in the future.

Table 3.4.1 summarizes the results of Figures 3.3.5 and 3.3.6 and in addition includes a summary for interest rates of 1.0, 3.0, and 7.0 percent.

The curves of Figures 3.3.7 and 3.3.8 were included for comparative purposes. These curves represent data similar to Figures 3.3.5 and 3.3.6 except the replacement factor B was set equal to 0.50. The effect of increasing B from 0.25 to 0.50 is quite pronounced. It is therefore important, when economizing, to keep the "blown-down" replacement cost small. For more on this matter, see Assumption 4 in Section 3.2.

A computer program was written for use in evaluating Equations 3.3.9 and 3.3.27. This program and the instructions for its use are included in Appendix F.

3.5 Example Problem

Given:

An 8 foot x 16 foot cantilevered sign, as shown in Figure 3.7.1. The sign is located in southeast Texas where the mean two year extreme wind velocity is 50 miles per hour, (see Figure 2 of Reference 10), and the mean 50 year extreme wind velocity is 90 miles per hour (see Figure 3 of Reference 10, or Figure 4 of Reference 2). Thus, V_1/V_2 is 0.56.

The present design life, R_p, is 50 years as specified by AASHO.

Assumptions:

The following assumptions are made on this problem and are based on "best estimates."

1. Initial cost of the present sign C_I including materials,

TABLE 3.4.1 SUMMARY OF EXAMPLE RESULTS

THE OPTIMUM DESIGN VALUES SHOWN ARE BASED ON THE FOLLOWING CONDITIONS:

$V_1/V_2 = 0.60$ $\quad n = 0.50$ $\quad R_p = 50$

$B = 0.25$ $\quad K_1 = K_2 = 0$

$f = 0.667$ $\quad K_p = 0.025$

INTEREST RATE (%)	USEFUL LIFE (YEARS)	OPTIMUM DESIGN					
		ECONOMIC			SAFETY*		
		DESIGN LIFE (YEARS)	COST REDUCTION (%)	SIZE ** REDUCTION (%)	DESIGN LIFE (YEARS)	COST REDUCTION (%)	SIZE ** REDUCTION (%)
0	5	12	5.7	24.5	3.75	0	41.0
	10	22	1.7	14.8	12.0	0	24.5
	20	46	0.02	1.6	43.0	0	3.0
	50	50	0	0	50.0	0	0
1.0	5	10	5.9	27.2	3.50	0	41.8
	10	22	2.0	14.8	10.75	0	26.2
	20	42	0.09	3.3	35.0	0	6.8
	50	50	0	0	50.0	0	0
3.0	5	10	6.3	27.2	3.25	0	42.8
	10	20	2.5	16.4	9.5	0	28.0
	20	34	0.4	7.2	24.0	0	13.4
	50	50	0	0	50.0	0	0
5.0	5	9	6.7	28.7	2.75	0	44.8
	10	18	3.0	18.1	7.75	0	30.9
	20	28	0.9	10.7	18.0	0	18.1
	50	42	0.08	3.3	36.0	0	6.2
7.0	5	9	7.1	28.7	2.50	0	46.2
	10	16	3.5	20.0	6.50	0	33.2
	20	24	1.5	13.4	14.0	0	22.1
	50	32	0.6	8.3	21.5	0	15.0

*Optimum design from safety standpoint is arbitratily defined as the maximum reduction in mass with no increase in present cost.

**From Figure 3.3.3.

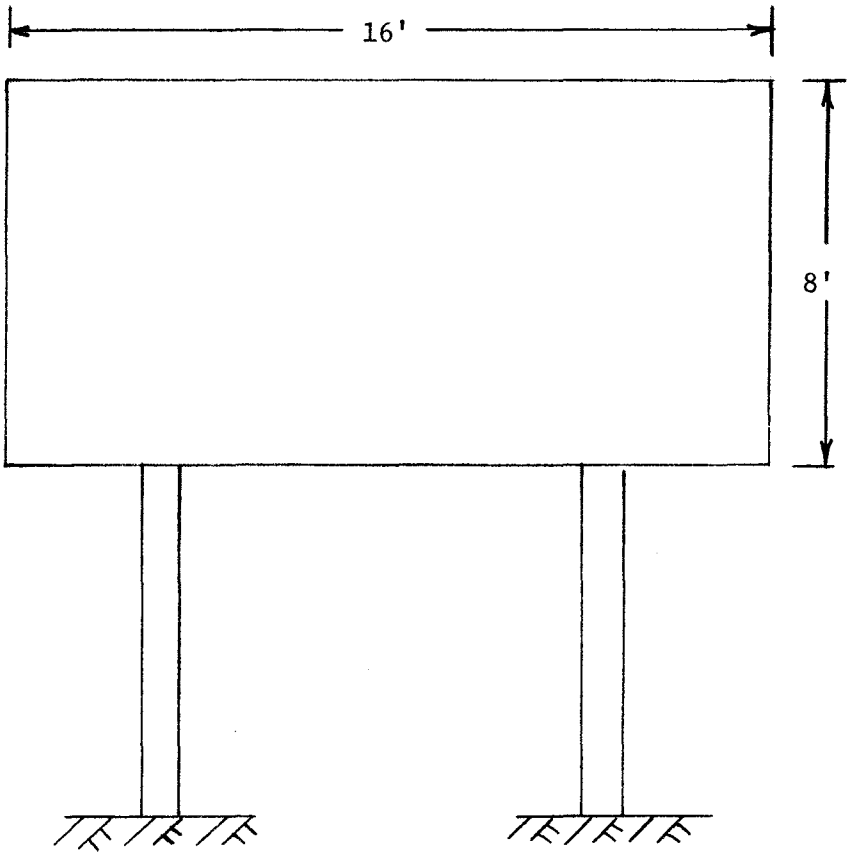

FIGURE 3.7.1 TYPICAL SIGN CONFIGURATION

fabrication and installation, is $10.00 per square foot of sign frontal area.

2. The useful life, A, of the sign is ten years, i.e., within ten years after installation, the entire sign structure will have to be either removed or replaced.

3. The replacement factor, B, is 0.25, i.e., the cost to replace or repair the sign, if blown down, is 25 percent of its initial cost. This factor is assumed to be applicable in both the present design (or 50-year design) as well as the reduced design.

4. The cost function, ϕ, which relates the initial cost of the sign to its size (size as defined in Section 3.1) is equal to $KW^{0.5}$.

5. The interest rate, I, used to discount to the present all costs occurring in future periods is 5 percent.

6. The maintenance factor, K_p, is 0.025, i.e., the yearly maintenance cost of the sign, whether the present size or the reduced size, is equal to 2.5 percent of the 50-year sign's initial cost. Maintenance cost includes those due to painting and mowing around the sign, repairs to the sign background, etc.

7. The salvage factor of the reduced size sign, K_1, and the 50-year size, K_2, is zero, i.e., at the end of the useful life of either type signs, the salvage value is zero.

Required:

Determine an optimum design for this sign based on economic considerations.

Solution:

The values of Table 3.4.1 can be used to obtain the optimum values since they are based on the same conditions that exist in this example. For I = 5 percent and A = 10 years, the optimum life (R), from an economic standpoint, is 18 years. The amount of reduction in present cost (Z_r) is 3 percent, and the reduction in size or mass of the sign structure (r) is 18.1 percent. In order to realize these reductions in the present sign's size and cost, it will be necessary to reduce the size of the members in the sign, whose cross sectional properties depend upon the magnitude of wind loading, by 18.1 percent. This will not always be possible with available commercial sizes. However, if consideration is given to the many different sign configurations that now exist, it is believed that, on the average, the results of the study can be used in practical applications. In those cases where the available member sizes do not meet the requirements of the situation, it may be economically feasible to consider an alternate approach. For example, it may be feasible to make a special order for the required size, or consider different type members (e.g., channel section as opposed to a zee section).

It will now be shown how the 3 percent value for Z_r was determined.

Computation of Initial Cost:

A. Present Design

The initial cost, C_{Ip}, of the present design is

$$C_{Ip} = (\$10.00) \text{ X (frontal area of sign)}$$

$$C_{Ip} = (10)\ (16)\ (8) = \$1{,}280.00$$

Since the cost function ϕ is of the form $KW^{0.5}$, a relation between C_{Ip} and W_p exists, i.e.,

$$C_{Ip} = KW_p^{0.5}$$

Since C_{Ip} and W_p are shown, the value of K can be found.

$$K = \frac{C_{Ip}}{W_p^{0.5}} = \frac{1{,}280.00}{(W_p)^{.5}}$$

B. Reduced Design

The initial cost, C_I, of the reduced design is

$$C_I = KW^{0.5}$$

The reduced size W is found by use of the equation

$$W = (1 - \frac{r}{100})\ (W_p)$$

$$W = (1.000 - .181)\ (W_p) = .819\ W_p$$

Therefore

$$C_I = \frac{1280.}{(W_p)^{0.5}}\ (0.819\ W_p)^{0.5}$$

$$C_I = \$1{,}157.00$$

Computation of Replaced Cost:

The replacement cost of both the present design, C_{Rp}, and the reduced design, C_R, over the useful life A of the sign is

$$C_{Rp} = \frac{BC_{Ip}}{R_p} \sum_{J=1}^{A} \frac{1}{(1 + I)^J} = \frac{(.25)\ (1280)}{50} \left[\frac{(1.00 + 0.05)^{10} - 1}{0.05\ (1.00 + .05)^{10}} \right]$$

$$C_{Rp} = \$49.47$$

$$C_R = \frac{BC_I}{R} \sum_{J=1}^{A} \frac{1}{(1 + I)^J} = \frac{(.25)\ (1157)}{18} \left[\frac{(1.00 + 0.05)^{10} - 1}{0.05\ (1.00 + .05)^{10}} \right]$$

$$C_{Rp} = \$124.22$$

Computation of Maintenance Cost:

The maintenance cost, C_{mp}, for both the present design and the reduced design, over the useful life of the sign, is computed by,

$$C_{mp} = K_p\ C_{Ip} \sum_{J=1}^{A} \frac{1}{(1 + I)^J} = (.025)\ (1280) \left[\frac{(1.00 + 0.05)^{10} - 1}{0.05\ (1.00 + .05)^{10}} \right]$$

$$C_{mp} = \$247.36$$

Computation of Total Cost:

For the present design, the total cost C_{tp} over the useful life of the sign would be,

$$C_{tp} = C_{Ip} + C_{Rp} + C_{mp} - C_{Sp}$$

$$C_{tp} = \$1,280.00 + 49.47 + 247.36 - 0.00$$

$$C_{tp} = \$1,576.83$$

For the reduced design, the total cost C_t on the useful life of the sign would be,

$$C_t = C_I + C_R + C_{mp} - C_s$$

$$C_t = \$1,157.00 + 124.22 + 247.36 - 0.00$$

$$C_t = \$1,528.58$$

The cost reduction, Z_R, is determined by

$$Z_r = \frac{C_{tp} - C_t}{C_{tp}} \times 100\% = \frac{1576.83 - 1528.58}{1576.83} \times 100\%$$

$$Z_r = 3.0\%$$

In this example, the amount of reduction in cost, over the useful life of the two type signs, was small ($1,528.58, as opposed to the present cost of $1,576.83). However, the reduction in size, or mass, of the sign adds considerably to the safety aspects of the sign. If

safety was of more concern than economy, the mass of this sign could be reduced by 30.9 percent with no change in the present cost (see Table 3.4.1).

If the same sign were supported by "braced leg" or "A-frame" type members, greater reductions in the sign's cost and mass could be realized. Consider the following example.

Assume all parameters used in the previous example apply in this case also, with the exception of the factor f. The factor f will have a value somewhere between 0.67 and 1.0 since the sign structure will resist the wind loads by a combination of axial loads in the trussed members and bending moments in the background and windbeams. It is suggested that the following relation be used in computing f for signs of this type:

$$f = \frac{0.667(M_B) + 1.0(M_A)}{M_B + M_A}$$

where

M_B = mass or weight of those members designed primarily for bending loads.

M_A = mass or weight of those members designed primarily for axial loads.

In this example f was assumed to equal 0.85.

The results, obtained by use of the computer program in Appendix F, show that the optimum design life from an economic standpoint for this sign is 14 years. At this design life a 5.6 percent reduction in the 50-year design cost could be realized, along with a 25 percent reduction

in the sign's mass. A 43 percent reduction in mass could be realized with no change in the 50-year cost if the sign were designed for a 5 year life.

CHAPTER 4

CONCLUSIONS AND RECOMMENDATIONS

4.1 Wind Loads on Conventional Signs.

Previous to this study the consensus has been that the current design criteria for highway signs, with regard to wind pressure, were excessive. The results of this study prove otherwise. The close agreement between the results of the full-scale investigations and the model tests in the wind tunnel forms the basis for this conclusion. This close agreement also demonstrates the applicability of conventional sign model data to full-scale signs.

The wind pressure criteria were actually shown to be unconservative, i.e., a sign structure built to the criteria specifications would be under-designed. Inconsistencies were found to exist in the design methods. The shape coefficient as used in the criteria in computing wind pressures has a constant value of 1.3, regardless of the sign's shape (or aspect ratio). The results of this study show the shape coefficient to be dependent on the shape. The coefficient was found to vary from 1.7 for an aspect ratio of 0.5 to 1.5 for an aspect ratio of 1.4. The maximum wind load condition, as specified in the criteria, occurs at an angle of attack of 90 degrees (when the wind direction is normal to the face of the sign). It was shown that the critical wind load condition can occur at angles other than 90 degrees. In these cases the combination of normal force and twisting moment provide the critical condition.

Based on these conclusions, it is recommended that the results of

this conventional sign wind load study be considered in establishing new design criteria for highway signs.

4.2 Conventional Signs Vs. Non-Solid Signs.

It is evident that considerable reductions can be made on the wind loads of a conventional solid background sign by the use of a louvered background. Reductions on the order of 50 percent or greater were obtained. This reduction in wind loads would allow a comparable reduction in the size of the sign supports required, which, in turn, would improve the safety aspects of the structure.

It was also shown that the visibility requirements of a sign can be maintained by the louvered background. The method used in attaching the message to the louvered sign proved to be adequate. The same or a similar type method is recommended in order to minimize the added wind resistance of the message.

It is obvious that the louvered sign cannot be built as cheaply as the conventional sign. However, it is emphasized that the values used in the cost analysis of the louvered signs are, at most, rough estimates. The merits of the louvered sign from a safety standpoint should warrant further consideration, at least for experimental installations.

No one particular louver configuration can be recommended as being the best from an overall standpoint because of the cost factor. In general, the wind loads decrease as the louver angle is decreased. However, because of the smaller louver angle, a greater number of louvers is required to insure a solid appearance. The cost will increase as the

number of louvers increases.

From an aerodynamic standpoint it would appear that the curved louvered model with an effective louver angle of 14.1 degrees is the most desirable. It is desirable if the section properties of the sign support are equal about any axis, e.g., a tubular support. The magnitude of the side force would require that the properties of the sign support members be practically the same in all directions. In commercially available members such as I-beams, wide flange beams, etc., the strong axis section modulus is, on the average, approximately three times the weak axis section modulus. If it is necessary to use this type member the more desirable configuration would be the straight angle louver, with a louver angle equal to 30 degrees and a louver width equal to 2.3 inches.

4.3 Economic and Safety Aspects as a Function of the Frequency of Occurrence of Design Winds.

Two important relationships were derived in this study. The first relates the relative size, or mass, of a sign to the frequency of occurrence of design wind velocities. The second relates the relative cost of a sign to the frequency of occurrence of design wind velocities.

In deriving these relations it was assumed that certain parameters were known, e.g., the replacement cost of a blown-down sign, the useful life of a sign, maintenance cost, and others. Certain overriding assumptions were also made regarding the formulation of the investigation, e.g., it was assumed that a sign will blow down or experience a structural failure when the wind velocity for which it was designed is reached, and others. The value of the information contained in this study will

depend, to a large degree, on the accuracy of the values assigned these parameters and the degree to which the overriding assumptions approximate the actual conditions.

An "average" situation was considered in the study. Values were assigned to the parameters. The values were felt to be representative. If these parameters do, indeed, represent an "average" situation, it is evident that the cost of a sign can be reduced and its safety aspects improved by designing the sign to a lower recurrence interval wind (or lower wind velocity). The current recurrence interval for the design wind velocity is 50 years.

In the "average" situation it was shown that the cost of a sign based on the 50-year recurrence interval could be reduced by as much as 7 percent, if the sign were designed to a nine-year wind velocity. The accompanying reduction in the sign's mass would be 28.7 percent. This would be the optimum design condition from an economic standpoint. If safety was of more concern, the sign could be designed to a 2.5-year wind velocity with no increase in cost, but with a 46.2 percent reduction in mass.

The results of this investigation strongly indicate that the present recurrence interval for the design wind velocity of 50 years is excessive in many instances. It is therefore recommended that the results of this study be considered in establishing new criteria for the recurrence interval of design wind velocities of highway signs.

For future studies, an extension of this investigation should include a consideration of those costs incurred by the motorist for the time the sign is down from wind damage and his costs when colliding with the sign.

Consideration should also be given to the highway department's costs of repairing signs damaged by auto collisions. As the sign's mass is reduced, damage to the colliding auto will likely decrease, but the costs to repair the sign may increase.

REFERENCES

1. Rowan, N. J., Olson, R. M., Edwards, T. C., Gaddis, A. M., Williams, T. G., and Hawkins, D. L., "Impact Behavior of Sign Supports - II," Research Report 68-2, September 1965, Texas Transportation Institute, College Station, Texas.

2. "Specifications for the Design and Construction of Structural Supports for Highway Signs," American Association of State Highway Officials, 917 National Press Building, Washington 4, D. C., 1961.

3. Eiffel, A. G., "Nouvelles Recherches sur la Resistance de 1' Air et la Pression du Vent sur les Hangars de Pirigeables," Paris, 1914, Translated by J. C. Hansaker, Houghton-Mifflin Co., New York.

4. Stanton, T. E., "On the Resistance of Plane Surfaces in a Uniform Current of Air," Minutes of Proceedings of the Institution of Civil Engineers, Volume CLVI, London, 1903-1904, Page 78.

5. Winter, H., "Flow Phenomena on Plates and Airfoils of Short Span," National Advisory Committee for Aeronautics, Technical Memorandum Number 798, Washington, D. C., 1936.

6. Tidwell, D. R. and Ross, H. E. Jr., "Wind Tunnel Tests of Flat Plates," Texas Transportation Institute, Project Number 1068, August 3, 1965 (unpublished).

7. Stanton, T. E., "Experiments on Wind-Pressure," Minutes of Proceedings of the Institution of Civil Engineers, Volume CLXXI, London, 1907-1908, Page 175.

8. Tidwell, D. R. and Samson, C. H., "Wind Tunnel Investigation of Non-Solid Sign Backgrounds," Highway Research Board Record 103, Pages 1-9, 1965.

9. Harlock, J. H., Axial Flow Compressors, Butterworth Scientific Publications, London, 1958, Page 36.

10. Thom, H. C. S., "Distributions of Extreme Winds in the United States," Transactions of the American Society of Civil Engineers, Volume 126, Paper No. 3191, Page 450.

11. Tidwell, D. R. and Samson, C. H., op. cit., Page 3 .

12. Thom, H. C. S., op. cit., Page 451.

13. "Specifications for the Design and Construction of Structural Supports for Highway Signs," op. cit., Page 7.

14. Stanton, T. E., "Experiments on wind Pressures," op. cit., Page 178.

15. "Wind Forces on Structures," Transactions, American Society of Civil Engineers, Volume 126, Part II, 1961, Page 1141.

A P P E N D I X A

LIST OF INSTRUMENTATION

TABLE A-1.1 INSTRUMENTATION, FULL-SCALE STUDIES

DEVICE	DESCRIPTION	LOCATION	TO PROVIDE
ELECTRIC RESISTANCE STRAIN GAGE BRIDGE (NO. 1).	DUAL GAGE PATTERN. TYPE EA-06-200MB-120, 120 OHM, 2.03 GAGE FACTOR. MANUFACTURED BY MICRO MEASUREMENTS, INC.	SEVEN FEET UP FROM FLANGE AT BASE OF POLE.	BENDING MOMENT.
ELECTRIC RESISTANCE STRAIN GAGE BRIDGE (NO. 2).	DUAL GAGE PATTERN. TYPE EA-06-200MB-120, 120 OHM, 2.03 GAGE FACTOR. MANUFACTURED BY MICRO MEASUREMENTS, INC.	ONE FOOT UP FROM FLANGE AT BASE OF POLE.	BENDING MOMENT.
ELECTRIC RESISTANCE STRAIN GAGE BRIDGE (NO. 3).	DUAL GAGE PATTERN. TYPE EA-06-200MB-120, 120 OHM, 2.03 GAGE FACTOR. MANUFACTURED BY MICRO MEASUREMENTS, INC.	SEVEN FEET UP FROM FLANGE AT BASE OF POLE.	BENDING MOMENT.
ELECTRIC RESISTANCE STRAIN GAGE BRIDGE (NO. 4).	DUAL GAGE PATTERN. TYPE EA-06-200MB-120, 120 OHM, 2.03 GAGE FACTOR. MANUFACTURED BY MICRO MEASUREMENTS, INC.	ONE FOOT UP FROM FLANGE AT BASE OF POLE.	BENDING MOMENT.
ELECTRIC RESISTANCE STRAIN GAGE BRIDGE (NO. 5)	90° ROSETTE, TYPE C-6-111-R2A, 120 OHM, 1.99 GAGE FACTOR. MANUFACTURED BY THE BUDD COMPANY.	TWO FEET UP FROM FLANGE AT BASE OF POLE.	TWISTING MOMENT.

TABLE A-1.1 INSTRUMENTATION, FULL-SCALE STUDIES (Continued)

DEVICE	DESCRIPTION	LOCATION	TO PROVIDE
WIND SPEED DETECTOR.	CUP TYPE, MODEL NUMBER T-627/GMQ-12. MANUFACTURED BY RETT COMPANY.	TEST SITE.	WIND SPEED.
WIND DIRECTION DETECTOR.	VANE TYPE, MODEL NUMBER T-628/GMQ-12. MANUFACTURED BY RETT COMPANY.	TEST SITE.	WIND DIRECTION.
WIND SPEED AND DIRECTION AMPLIFIER.	MODEL NUMBER AM-1618A/GMQ-12. MANUFACTURED BY RETT COMPANY.	MOBIL INSTRUMENTATION LABORATORY.	AMPLIFICATION FOR SIGNALS FROM DETECTORS.
OSCILLOGRAPH AMPLIFIER.	HONEYWELL, MODEL 119B1 CARRIER TYPE.	MOBILE INSTRUMENTATION LABORATORY.	AMPLIFICATION FOR STRAIN GAGE SIGNALS.
OSCILLOGRAPH RECORDER.	HONEYWELL, MODEL 1508 VISICORDER.	MOBILE INSTRUMENTATION LABORATORY.	PAPER RECORD OF STRAIN GAGE MEASUREMENTS.
WIND SPEED AND DIRECTION RECORDERS.	ESTERLINE-ANGUS, MODEL AW INK RECORDERS.	MOBILE INSTRUMENTATION LABORATORY.	PAPER RECORD OF WIND SPEED AND DIRECTION.

A P P E N D I X B

FULL-SCALE TEST PROCEDURE

The following procedure was used for the full-size-sign, outdoor wind load studies. The procedure was sub-divided into three parts.

Part A. - Items that were to be completed prior to beginning any actual data acquisition.

Part B. - Items that were to be recorded approximately every hour during data acquisition, or as weather conditions dictate.

Part C. - Items that were to be completed for each run.

Definitions:

Test No. - A number assigned to a particular day of testing. Test numbers were in chronological order.

Run No. - A number assigned to a particular data acquisition run. Run numbers were in chronological order. Normally, the runs were made in groups of 8 (180^{o} in 22.5^{o} increments).

DATA SHEET

Part A

Test No. _____

Date _____

1. Sign aspect ratio (height/width) = _____

2. Names of people working _____

3. Determine actual wind velocity by switching to proper wind speed setting on amplifier box. (Settings are from 0 to 6, 0 to 12, 0 to 30, and 0 to 60 mph.)

   NOTE: It will be necessary to change this initial setting if the wind velocity changes appreciably.

4. Obtain wind direction references by pointing indicator in the 0^{o}, 90^{o}, 180^{o}, and 270^{o} directions and denoting these directions on the wind direction recorder.

COMMENTS:

DATA SHEET

Part B

Test No. ______

1. Time ____________
2. Dry Bulb Temp. ____________ °F
3. Wet Bulb Temp. ____________ °F
4. *Atm. Pressure ____________ " Mercury
5. % Humidity ____________

1. Time ____________
2. Dry Bulb Temp. ____________ °F
3. Wet Bulb Temp. ____________ °F
4. *Atm. Pressure ____________ " Mercury
5. % Humidity ____________

1. Time ____________
2. Dry Bulb Temp. ____________ °F
3. Wet Bulb Temp. ____________ °F
4. *Atm. Pressure ____________ " Mercury
5. % Humidity ____________

1. Time ____________
2. Dry Bulb Temp. ____________ °F
3. Wet Bulb Temp. ____________ °F
4. *Atm. Pressure ____________ " Mercury
5. % Humidity ____________

1. Time ____________
2. Dry Bulb Temp. ____________ °F
3. Wet Bulb Temp. ____________ °F
4. *Atm. Pressure ____________ " Mercury
5. % Humidity ____________

COMMENTS:

*Obtain from Easterwood Airport records at end of day.

DATA SHEET

Part C

Test No. _____

Run No. _____

1. Sign direction = _____ ^{o}

2. Attenuation settings:

   a) Channel 1 _____1. _____.5 _____.2 _____.1 _____.05 _____.01

   b) Channel 2 _____1. _____.5 _____.2 _____.1 _____.05 _____.01

   c) Channel 3 _____1. _____.5 _____.2

   d) Channel 4 _____1. _____.5 _____.2

   e) Channel 5 _____1. _____.5 _____.2 _____.1 _____.05 _____.01

3. Mark channel nos. on visicorder paper.

4. Wind speed setting:

   ____0 to 6 mph,____0 to 12 mph,____0 to 30 mph,____0 to 60 mph.

5. Stamp beginning of run, on each recording paper, with "Start"

   "Test No. ____"
   "Run No. ____".

6. Recorder speed at 0.15 in/sec?

7. Start recorders.

8. Record time of day _____.

9. Stop recorders after 5 minutes running time.

10. Stamp end of run, on each recording paper, with "End"

    "Test No. _____"
    "Run No. _____"

11. Rotate sign 22.5^{o} and repeat Part "C".

A P P E N D I X C

SAMPLE TEST DATA, FULL-SCALE TESTS

1. Sample Data

The raw data shown on the following pages were taken from Test Number 2, Run Number 2. It is typical of the raw data gathered.

Figures C-1.1 and C-1.2 contain the oscillograph records of the strain gage data. The term "channel" is synonymous with "bridge". The data points refer to the sequenced timing marks. These marks were used in correlating the data with the wind speed and direction data, shown in Figures C-1.3 and C-1.4.

The wind speeds could be read directly off the scaled chart for a given range setting. The scale of the wind direction chart was different between the 90^{o} and 180^{o} directions and the 180^{o} and 270^{o} directions, as shown. To account for this, two different scale factors were used. Tests conducted on the equipment indicated that the scale factor for each set of directions was essentially constant, i.e., within the 90^{o} to 180^{o} directions and the 180^{o} to 270^{o} directions.

2. Gust Observations

The plot shown in Figure C-2.1 is a trace of the actual wind velocity recorded during a run of Test Number 5. The curve is typical of the wind speed data and is included to show the magnitude of gust factors that existed. As shown, the maximum positive deviation in the average velocity was 17.2 percent and the maximum negative deviation was 20.7 percent. The gust factor is the maximum positive deviation. Thus, the gust factor was 1.17.

The average velocity was obtained as follows:

(a) The velocity-time curve was integrated until a mile of area was obtained. (The area under the curve has the units of miles).

(b) The time was noted at which the mile of wind occurred.

(c) The average velocity then equals the reciprocal of the time in (b), with "hour" units of time used in place of "second" units.

This is the general procedure used in computing "fastest mile of wind" values. Wind speed records are evaluated over some period of time in order to determine the shortest length of time required for a mile of wind to pass. The reciprocal of this time is the average velocity of the mile of wind. The maximum positive deviation in this average velocity is the gust factor.

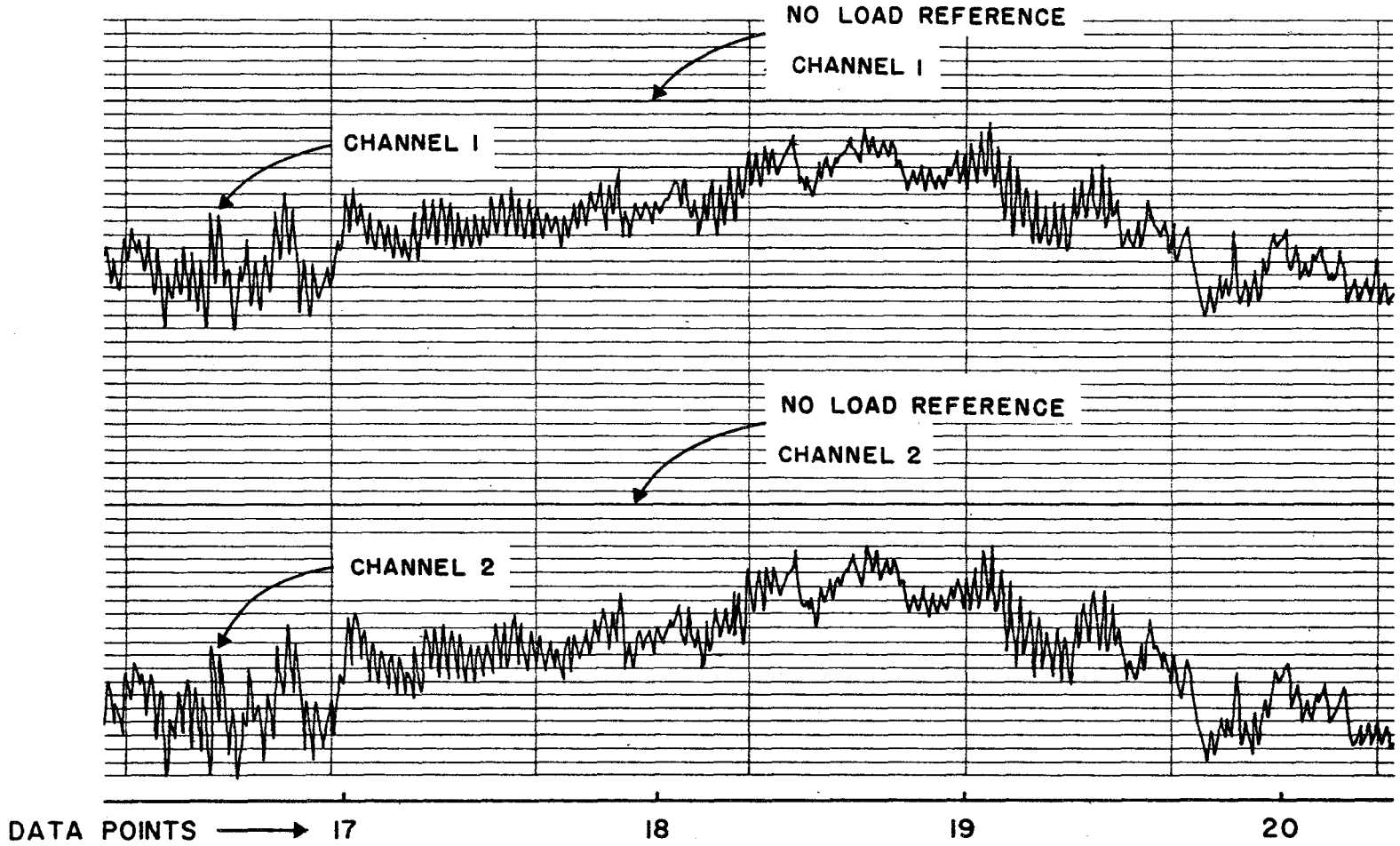

FIGURE C-1.1 OSCILLOGRAPH RECORD, CHANNELS 1 AND 2

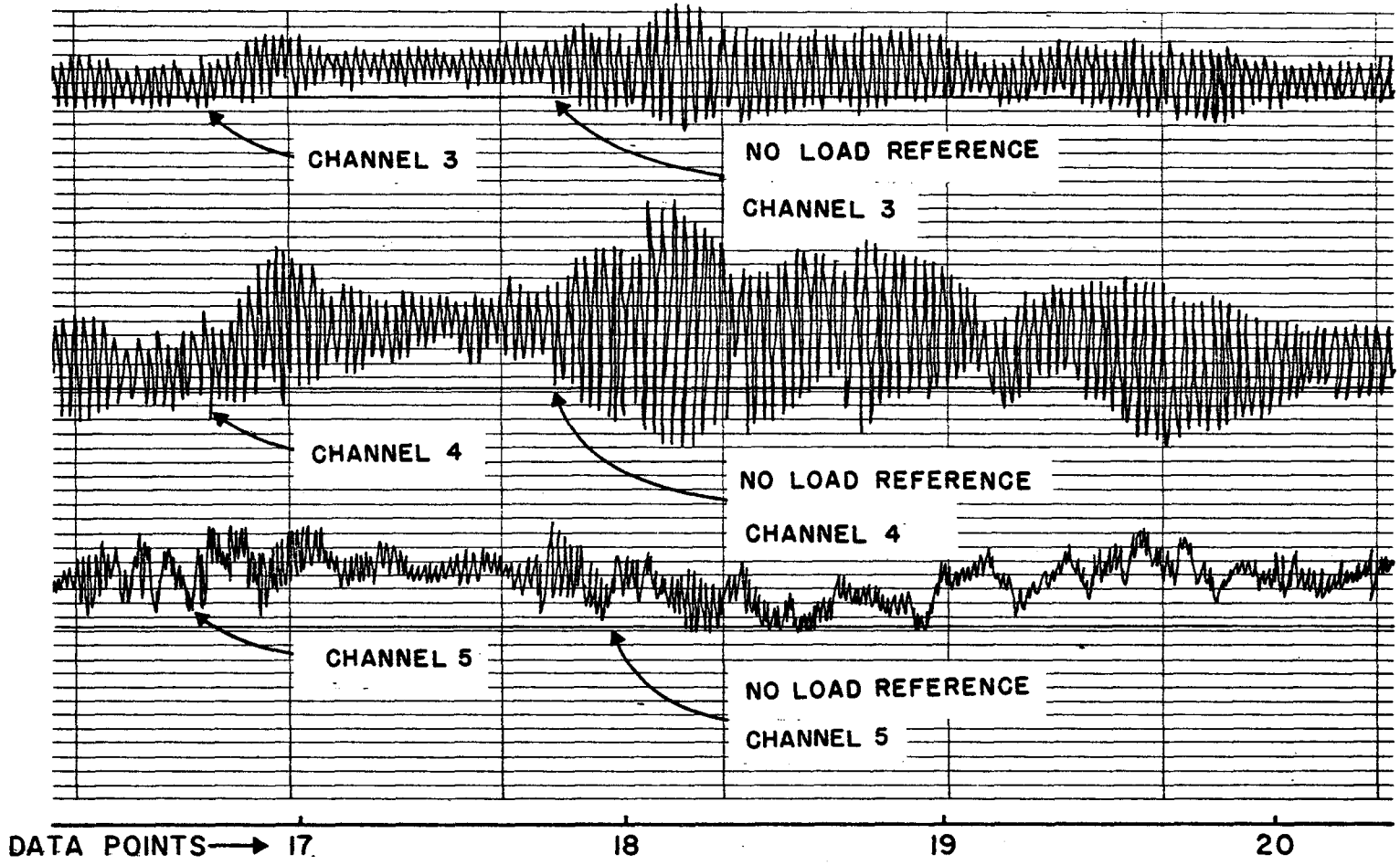

FIGURE C-1.2 OSCILLOGRAPH RECORD, CHANNELS 3, 4, AND 5

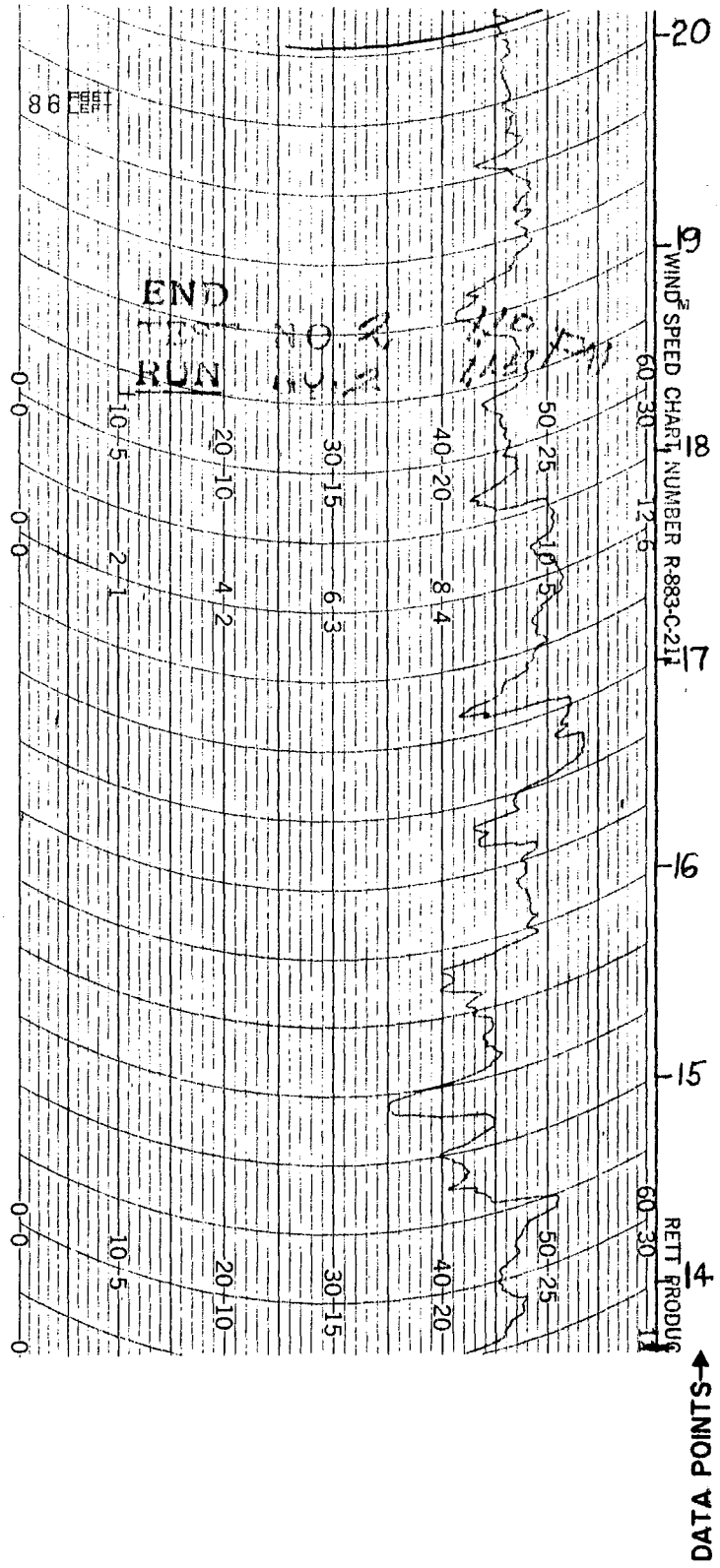

FIGURE C-1.3 WIND SPEED RECORD

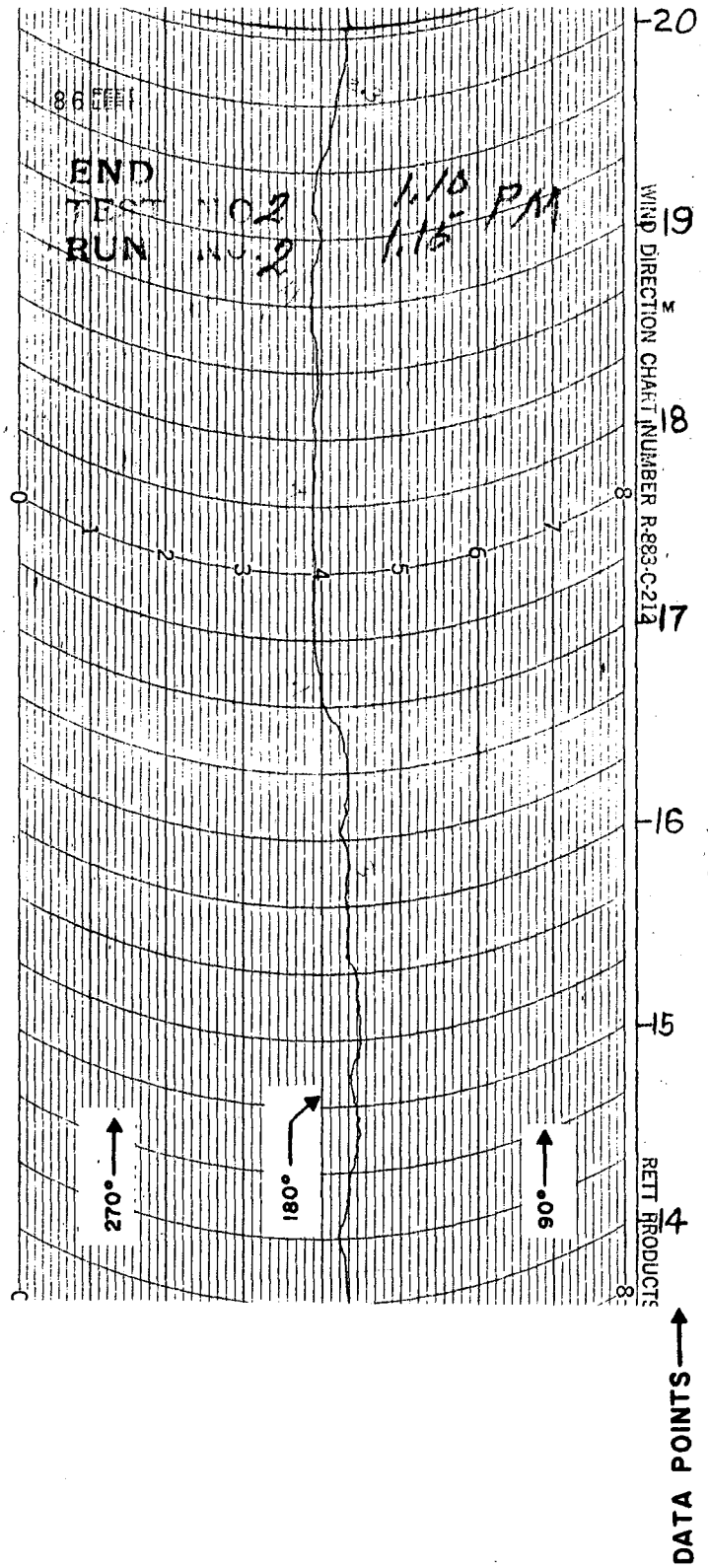

FIGURE C-1.4 WIND DIRECTION RECORD

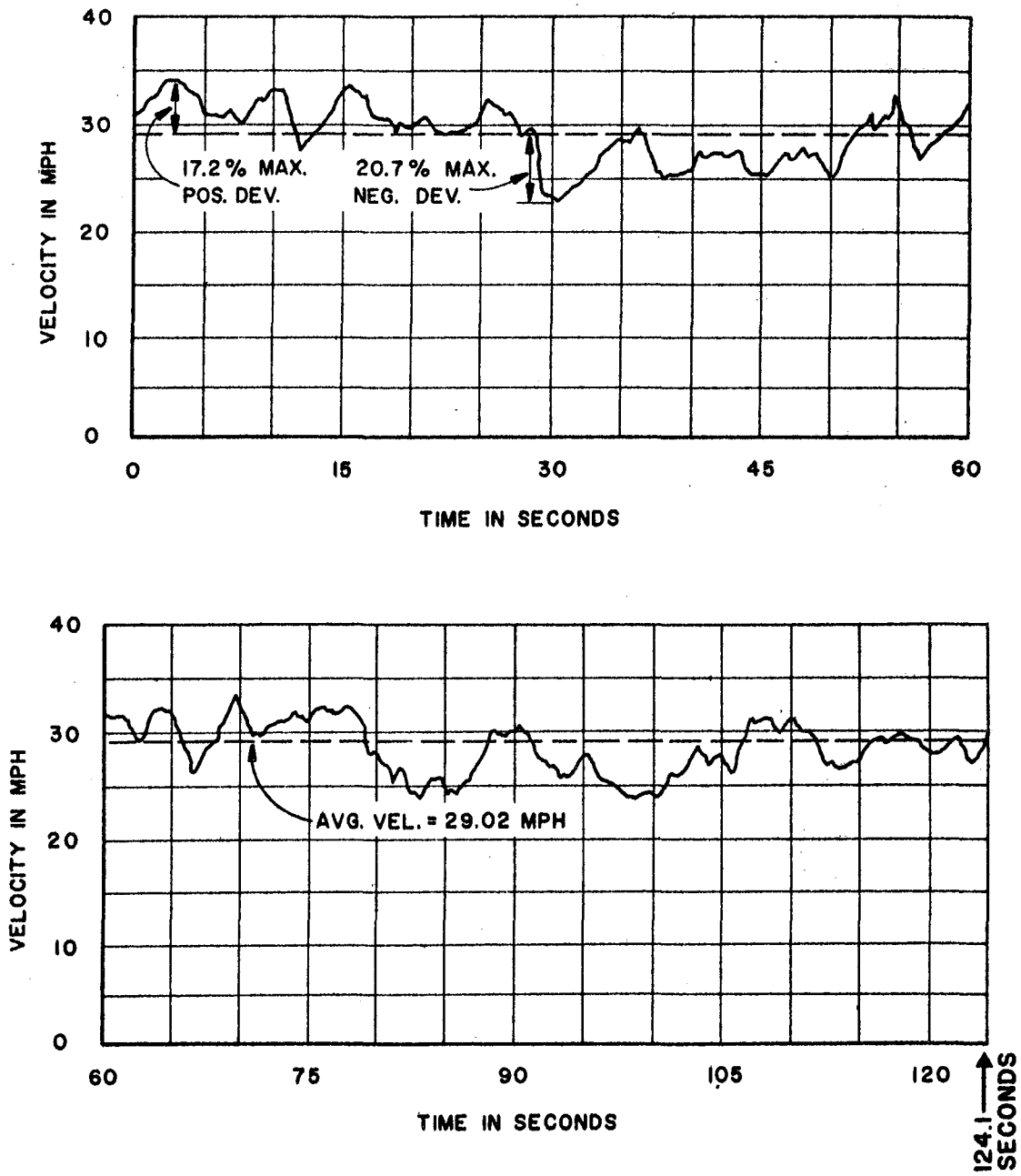

FIGURE C-2.1 OBSERVED GUST FACTORS

A P P E N D I X D

DATA REDUCTION COMPUTER PROGRAM, FULL-SCALE TESTS

1. Formulation

Basically, the program took the raw data from the tests, computed the coefficients and locations of the resultant normal force, and printed the results.

Input consisted of general information about the test (date, etc.), attenuation settings of the oscillograph amplifiers, atmospheric conditions, sign angle, deflections of the oscillograph traces, and the wind's speed and direction.

Most of the equations used in the program have been described in the body of the report. A description of those that were not follows:

Air density, ρ

$$\rho = \frac{(p_A)(70.722) - 0.379\ H_U(2.685 + 0.003537T_A{}^{2.245})}{(53.3)(32.2)(T_A + 459.4)}$$

where,

p_A = Atmospheric pressure (inches of mercury)

H_U = Relative humidity

T_A = Ambient temperature (degrees Fahrenheit)

Location of normal force

Two distances are computed in determining the location of the normal force, namely, the vertical distance L_y from bridge number 1 and the horizontal distance L_z from the center of the sign.

Consider Figure D-1.1. Known are the values of F_N, F_T, M_{TP} , and the bending moment at Bridge 1. M_{TP} is the measured value of the

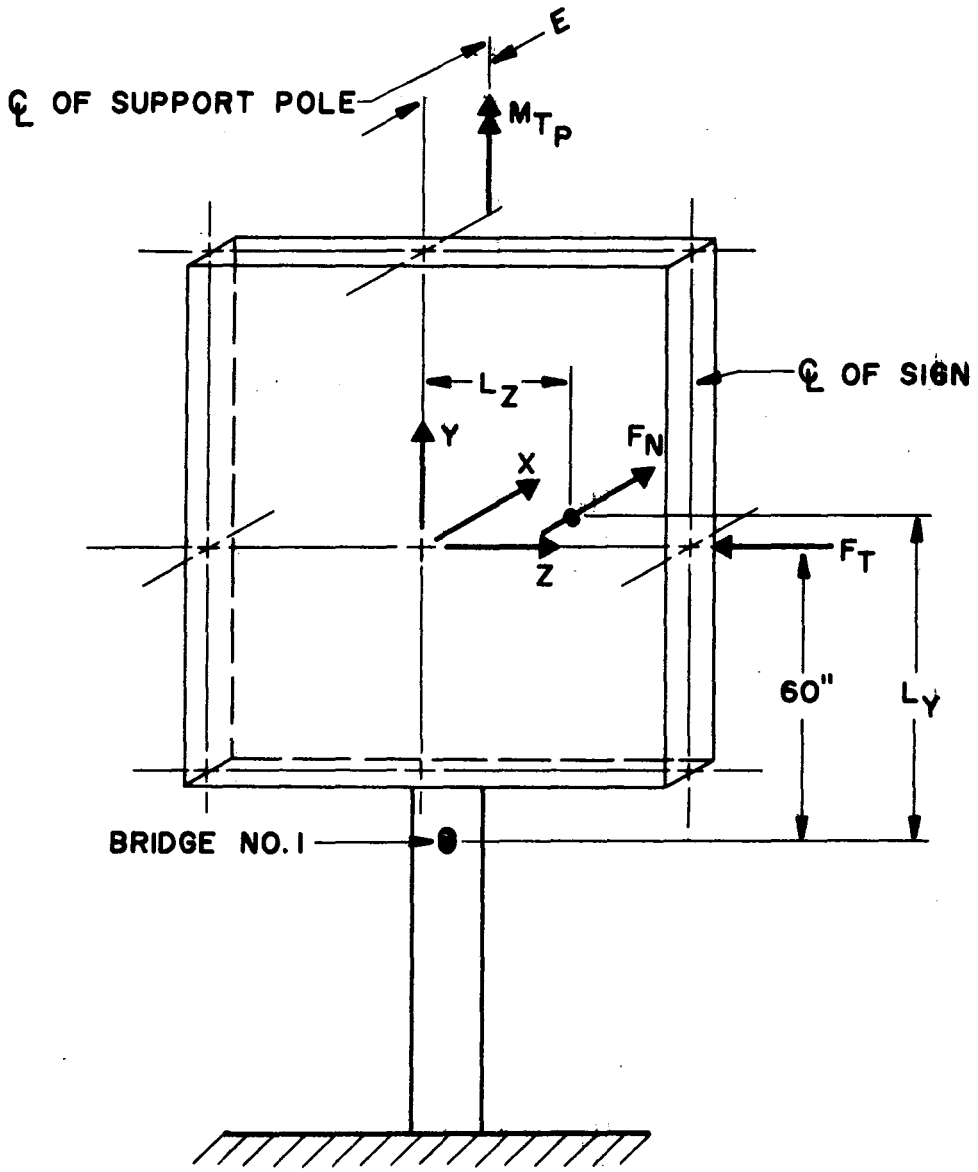

FIGURE D-1.1 LOCATION OF RESULTANT NORMAL FORCE ON FULL-SCALE SIGN

twisting moment on the instrumented support pole. Note that the positive direction of the measured twisting moment is opposite to that set up for the "sign axis" system (Figure 2.2.1). This was not intentional. It was merely due to the wiring of Bridge Number 5, which measures the twisting moment.

If F_T acts along the centerline of the sign, as assumed, the following relations yield the location of F_N :

Summing moments,

$$\sum M_{POLE\ \mathbb{Q}} = M_{TP} = F_N(L_Z) - F_T(E)$$

$$\therefore L_Z = \frac{M_{TP} + F_T(E)}{F_N}$$

where, E = 8.25 inches (Reference Figure 2.1.1)

$$\sum M_{\ BRIDGE\ 1} = M_1 = F_N(L_y)$$

$$\therefore L_y = \frac{M_1}{F_N}$$

where, M_1 = measured bending moment at Bridge 1.

The relation between the notations used in the study and those used in the program are shown on page 200.

The output data were grouped according to the run number. The data computed for each run were outputted according to the magnitude of the angle of attack. This is the reason for the subscripted variables in the program. The data points shown in the output refer to the numbers assigned to the sequenced timing marks on the raw data (See Appendix C).

STUDY NOTATION	COMPUTER NOTATION	DESCRIPTION
P	ADEN	Air Density
V	V(I)	Air Velocity
q	FI	Impact Pressure
θ_w	AW	Wind Angle
θ_s	AS	Sign Angle
α	A(I)	Angle of Attack
F_N	PN	Normal Force
F_S	PS	Side Force
M_T	TQ	Twisting Moment
L_y	VLN(I)	Vertical Location of Normal Force
L_z	VLE(I)	Horizontal Location of Normal Force
C_N	CN(I)	Normal Force Coefficient
C_T	CS(I)	Side Force Coefficient
C_M	CM(I)	Moment Coefficient

2. Fortran IV Listing

```
$IBFTC TEST
      DIMENSION V(100),CN(100),CS(100),CM(100),A(100),NDATAP(100),
     1   VLN(100),VLE(100)
    1 READ(5,100)DATE1,DATE2,DATE3,NT,AR
      WRITE(6,101)NT,DATE1,DATE2,DATE3,AR
      NPAGE = 0
    2 READ(5,102)AT1,AT2,AT3,AT4,AT5
      BSN1 =1680./AT1
      BSN2 =1650./AT2
      BSS1 =2490./AT3
      BSS2 =2526./AT4
      BST =1860./AT5
    3 READ(5,103)RUNN,AS,ATMP,TEMPA,HUMD,NUM
      ADEN = (ATMP*70.722-.379*(HUMD*(2.685+.003537*TEMPA**2.245)))/(53.
     13*32.2*(TEMPA+459.4))
      DO  4 I = 1,NUM
      READ(5,105)DN1,DN2,DS1,DS2,DT,AW,VW,N
      NDATAP(I) = I
      V(I) = VW*1.467
      FI = .5*ADEN*(V(I)**2)*100.
      IF(NT-8)50,51,50
   51 DN1=DN1/10.
      DN2=DN2/10.
      DS1=DS1/10.
      DS2=DS2/10.
      DT=DT/10.
   50 AA=AW-AS
      IF(AA)10,5,5
    5 IF(90.-AA)7,7,6
    6 A(I) = AA
      GO TO 15
    7 IF(270.-AA) 9,9,8
```

```
    8 A(I) = 180. - AA
      GO TO 15
    9 A(I) = AA - 360.
      GO TO 15
   10 IF(90.+AA)12,11,11
   11 A(I) = AA
      GO TO 15
   12 IF(270. + AA)14,13,13
   13 A(I) = -AA - 180.
      GO TO 15
   14 A(I) = 360. + AA
   15 VMN1 = BSN1*(DN1)
      VMN2=(BSN2*(DN2))-(.12096*(FI)*(SIN(A(I))))*(ABS(DN2)/DN2)
      VMS1=BSS1*(DS1)
      VMS2=(BSS2*(DS2))-(.12096*FI*ABS(COS(A(I))))*(ABS(DS2)/DS2)
      PN = (VMN2 - VMN1)/72.
      PS = (VMS2 - VMS1)/72.
      VLN(I) = VMN1/PN
      TQ=BST*(DT)+PS*8.25
      VLE(I) = TQ/PN
      CN(I) = PN/FI
      CS(I) = PS/FI
    4 CN(I) = TQ/(FI*120.)
      L = NUM - 1
   16 DO 18 J=1,L
      JJ = J + 1
      DO 18 K = JJ,NUM
      IF(A(J)-A(K))18,18,17
   17 TEMP = A(K)
      A(K) = A(J)
      A(J) = TEMP
      TEMP = V(K)
      V(K) = V(J)
      V(J) = TEMP
      TEMP = CN(K)
```

```
      CN(K) = CN(J)
      CN(J) = TEMP
      TEMP = CS(K)
      CS(K) = CS(J)
      CS(J) = TEMP
      TEMP = CM(K)
      CM(K) = CM(J)
      CM(J) = TEMP
      KTEMP = NDATAP(K)
      NDATAP(K) = NDATAP(J)
      NDATAP(J) = KTEMP
      TEMP = VLN(K)
      VLN(K) = VLN(J)
      VLN(J) = TEMP
      TEMP = VLE(K)
      VLE(K) = VLE(J)
      VLE(J) = TEMP
   18 CONTINUE
      NPAGE = NPAGE + 1
      WRITE(6,106)NPAGE,NT,RUNN
      LINES = 7
      DO 23 M = 1,NUM
      WRITE(6,107)NDATAP(M),A(M),V(M),CN(M),CS(M),CM(M),VLN(M),VLE(M)
      LINES = LINES + 1
      IF(NPAGE - 1)19,19,20
   19 NLINE = 55
      GO TO 21
   20 NLINE = 60
   21 IF(NLINE - LINES)22,22,23
   22 WRITE(6,108)
      NPAGE = NPAGE + 1
      WRITE(6,106)NPAGE,NT,RUNN
      LINES = 7
   23 CONTINUE
      WRITE(6,108)
      IF(N-1)3,2,24
```

```
 24 NPAGE = NPAGE + 1
    WRITE(6,109)NPAGE,NT
    IF(N-2)25,25,1
 25 WRITE(6,108)
100 FORMAT(3A6,2X,I2,2X,F3.1)
101 FORMAT(1HI,4X,24HFULL-SIZE SIGN WIND DATA/5X,9HTEST NO. ,I2/5X,7HD
   1ATE - ,3A6/5X,15HASPECT RATIO = ,F3.1)
102 FORMAT(5F5.0)
103 FORMAT(7X,A3,4F10.0,7X,I3)
105 FORMAT(5F6.2,2F10.0,29X,I1)
106 FORMAT(89X,9HPAGE NO. ,I2,/43X,9HTEST NO. ,I3,/43X,9HRUN  NO. ,A3/
   1/5X,78HDATA  ANGLE OF   WIND   NORMAL FORCE SIDE FORCE    MOMENT
   2  DISTANCE DISTANCE/5X,75HPOINT  ATTACK  VELOCITY COEFFICIENT  COE
   3FFICIENT COEFFICIENT    LN       LE/12X,16H(DEG.)  (FT/SEC),40X,14
   4H(IN.)    (IN.)//I
107 FORMAT(6X,I2,2(4X,F5.1),5X,F6.3,7X,F6.3,6X,F6.3,6X,F5.1,4X,F5.1)
108 FORMAT(1H1)
109 FORMAT(89X,9HPAGE NO. ,I2//5X,26HEND OF DATA FROM TEST NO. ,I2)
    STOP
    END
```

3. Sample Output

TEST NO. 2
RUN NO. 2

DATA PCINT	ANGLE CF ATTACK (DEG.)	WIND VELCCITY (FT/SEC)	NORMAL FCRCE CCEFFICIENT	SIDE FCRCE CCEFFICIENT	MCMENT CCEFFICIENT	DISTANCE LN (IN.)	DISTANCE LE (IN.)
4	12.C	22.4	C.543	-C.C93	C.032	74.5	7.1
2C	13.9	33.4	1.368	-C.C09	-C.C85	6C.7	-7.5
6	15.C	23.5	C.475	-C.C97	C.024	86.6	6.C
2	15.2	25.2	C.986	-C.C74	-C.C53	69.8	-6.5
5	15.4	24.8	C.691	-C.C71	-C.C28	74.7	-4.8
1	18.3	27.C	C.641	-C.C73	-C.C13	68.C	-2.4
19	18.4	32.7	C.627	-C.C58	-C.C67	6C.8	-12.7
18	18.7	33.C	C.933	-C.C49	-C.C93	58.C	-12.C
9	21.7	28.8	1.227	-C.C33	-C.C8C	62.6	-7.8
3	21.7	23.5	C.919	-C.C73	-C.C15	68.6	-2.C
17	22.1	33.4	1.171	-C.C7C	-C.122	59.4	-12.5
12	22.5	32.C	1.151	-C.C11	-C.1C4	64.2	-1C.9
7	23.6	25.4	C.992	-C.C54	-C.C43	69.7	-5.2
8	3C.1	22.9	1.318	-C.C24	-C.C34	65.7	-3.1
1C	37.3	24.6	1.C34	-C.C25	-C.CC6	69.7	-C.7
14	37.3	34.9	2.C55	-C.C17	-C.C58	48.8	-3.4
16	38.4	35.1	1.326	-C.C22	-C.C45	67.2	-4.C
15	39.5	31.5	1.88C	-C.C16	-C.C63	52.5	-4.C
11	41.6	22.4	1.457	-C.CC6	-C.C28	1C1.9	-2.3
13	47.9	22.4	2.6C3	-C.C12	-C.C62	57.C	-2.8

A P P E N D I X E

DATA REDUCTION COMPUTER PROGRAM, WIND-TUNNEL TESTS

1. Formulation

This program was written initially to evaluate the wind-tunnel tests of the louvered models. It was also used to evaluate the flat plate data.

Input consisted of general information about the model and the raw data from the wind tunnel tests.

The program transformed the recorded actions, which were in the "wind tunnel" axes (Figure 2.1.21), to the "sign" axes (Figure 2.2.1), computed the coefficients and the normal force locations, and printed out the results. The transformation matrix is shown below.

$$\begin{bmatrix} F_N \\ F_T \\ F_L \\ \hline M_R \\ M_P \\ M_T \end{bmatrix} = \left[\begin{array}{ccc|ccc} \cos\psi & -\sin\psi & 0 & & & \\ \sin\psi & \cos\psi & 0 & & 0 & \\ 0 & 0 & 1 & & & \\ \hline 0 & 0 & 0 & \cos\psi & \sin\psi & 0 \\ 0 & 0 & -E & -\sin\psi & \cos\psi & 0 \\ -E\sin\psi & -E\cos\psi & 0 & 0 & 0 & 1 \end{array}\right] \begin{bmatrix} D \\ S \\ L \\ M_r \\ M_p \\ M_y \end{bmatrix}$$

In computing the location of the normal force resultant, the following assumptions were made. Refer to Figure E-1.1.

(a) The lift force F_L (if existant) acts through the center of the sign, as shown.

(b) The side force F_T acts through the center of the sign, as shown.

The results indicated that these assumptions were acceptable, i.e., the rolling moment M_R was found to be negligible.

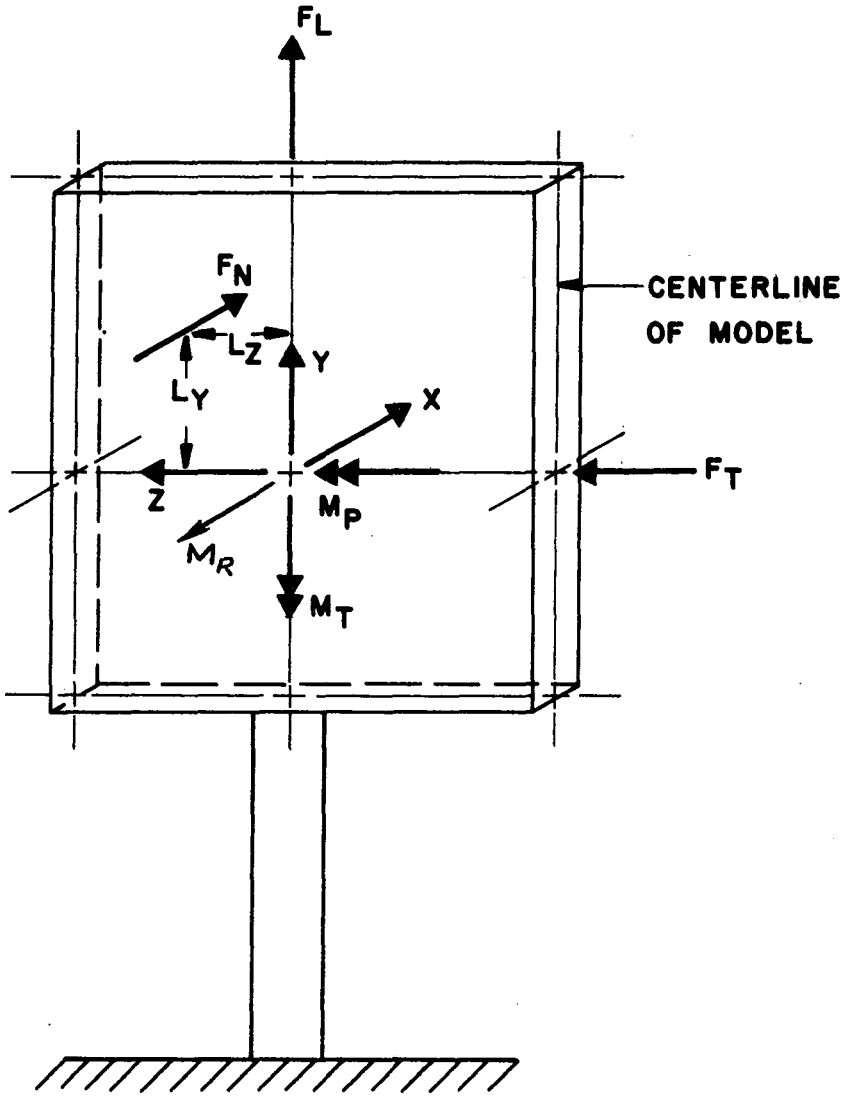

FIGURE E-I.I LOCATION OF RESULTANT NORMAL FORCE ON MODELS

Summing moments,

$$\sum M_{yy} = M_R = 0$$

$$\sum M_{yy} = M_T = F_N(L_Z)$$

$$\therefore L_Z = \frac{M_T}{F_N}$$

$$\sum M_{ZZ} = M_P = F_N(L_y)$$

$$\therefore L_y = \frac{M_P}{F_n}$$

The relation between the notations used in the study and those used in the program are shown on the following page. The units of the output were in the "pound-feet-second-degree" system.

STUDY NOTATION	PROGRAM NOTATION	DESCRIPTION
E	E	Distance from center of support to center of sign or model
ψ	PSI	Rotation angle
α	ALPHA	Angle of attack
F_N	BN	Normal Force
F_T	BT	Side Force
F_L	BL	Lift Force
M_T	BMY	Twisting Moment
M_R	BMR	Rolling Moment
M_P	BMP	Pitching Moment
C_N	CN	Normal Force Coefficient
C_T	CT	Side Force Coefficient
C_L	CL	Lift Force Coefficient
C_{MT}	CMY	Twisting Moment Coefficient
C_{MR}	CMR	Rolling Moment Coefficient
C_{MP}	CMP	Pitching Moment Coefficient
L_Z	VLZ	Horizontal Location of Normal Force
L_y	VLY	Vertical Location of Normal Force
q	Q	Impact Pressure

2. Fortran IV Listing

```
$IBFTC MAIN
      PI = 3.1415927
      WRITE(6,1)
    1 FORMAT(1H1)
    2 READ(5,3)C,B,DD,VFS,Q,N,OLL,THETA,NS
    3 FORMAT(5F10.0,I5,2F10.0,I5)
      DEN = Q*C*B
       I = 0
    4 READ(5,5)VL,D,E,Y,VMP,VMR,VMY,PSI,H
    5 FORMAT(7F10.0,2F5.2)
      E = E/12.
      DI = 1.2*Q*H*DD
      D = D - DI
      PSI = (PSI/180.)*PI
      BN = (D*COS(PSI) - Y*SIN(PSI))
      BT = (D*SIN(PSI) + Y*COS(PSI))
      BL = YL
      BMY = (-E*D*SIN(PSI) -E*Y*COS(PSI) + VMY)
      BMR = (VMR*COS(PSI) + VMP*SIN(PSI))
      BMP = (-E*VL - VMR*SIN(PSI) + VMP*COS(PSI))
      CN = BN/DEN
      CT = BT/DEN
      CL = BL/DEN
      CMY = BMY/(DEN*C)
      CMR = BMR/(DEN*C)
      CMP = BMP/(DEN*C)
      VLZ = BMY/BN
      VLY = BMP/BN
      I = I + 1
      IF(I-1)6,6,11
    6 WRITE(6,7)NS
    7 FORMAT(25X,9HSIGN NO. ,I3,//)
```

```
      WRITE(6,8)
    8 FORMAT(5X,5HWIDTH,2X,6HHEIGHT,3X,3HVFS,5X,1HQ,5X,4HTEST,3X,6HLOUVE
     1R,3X,6HLOUVER/42X,5HWIDTH,4X,5HANGLE//)
      WRITE(6,9)C,B,VFS,Q,N,OLL,THETA
    9 FORMAT(5X,F5.3,3X,F5.3,2X,F5.1,2X,F5.2,3X,I3,4X,F6.4,3X,F6.4//)
      WRITE(6,10)
   10 FORMAT(5X,58HALPHA    CN      CT      CL      CMY     CMR     CMP     LZ
     1    LY//)
   11 PSI = (PSI/PI)*180.
      ALPHA = 90. - PSI
      WRITE(6,12)ALPHA,CN,CT,CL,CMY,CMR,CMP,VLZ,VLY
   12 FORMAT(5X,F5.1,8(2X,F5.2))
      IF(N-1)2,2,4
      STOP
```

3. Sample Output

WIDTH	HEIGHT	VFS	Q	TEST	LOUVER WIDTH	LOUVER ANGLE
2.610	1.305	123.0	18.00	13	0.	0.

ALPHA	CN	CT	CL	CMY	CMR	CMP	LZ	LY
90.0	1.45	0.01	0.	-0.00	-0.	-0.03	-0.01	-0.05
75.0	1.44	-0.00	0.	-0.04	-0.00	-0.01	-0.08	-0.02
60.0	1.35	0.00	0.	-0.07	-0.01	-0.02	-0.13	-0.04
45.0	1.67	-0.02	0.	-0.15	-0.01	-0.01	-0.24	-0.02
30.0	1.04	0.01	0.	-0.16	0.00	0.00	-0.40	0.00
15.0	0.45	0.02	0.	-0.08	0.00	0.00	-0.47	0.00
0.	-0.01	0.04	0.	0.02	-0.00	0.	-3.53	-0.
-15.0	-0.49	0.05	0.	0.10	-0.01	0.00	-0.55	-0.01
-30.0	-1.18	0.04	0.	0.23	-0.01	0.00	-0.50	-0.01
-45.0	-1.63	0.01	0.	0.22	-0.01	0.01	-0.35	-0.01
-60.0	-1.29	-0.01	0.	0.08	-0.01	0.02	-0.16	-0.04
-75.0	-1.33	-0.02	0.	0.05	-0.01	0.02	-0.10	-0.04
-90.0	-1.31	-0.00	0.	0.01	0.00	0.03	-0.02	-0.07

A P P E N D I X F

COMPUTER PROGRAM, ECONOMIC STUDY

1. Description

This program was written to evaluate equations 3.3.9 and 3.3.27 for given values of the various parameters. The flow chart and the Fortran IV listing follow the list of computer notations.

The computer notations are related to the symbols used in the study as follows:

Study Notation	Computer Notation
n	VN
f	F
R_p	RP
B	B
V_1/V_2	RATIO
K_p	VKP
K_1	VK1
K_2	VK2
I	VI
A	A
G	GAMMA
R	R
r	ZRE
Z_R	ZRED

The program, as shown, is set up to furnish the data contained in Figures 3.3.3, 3.3.5 and 3.3.6 and similar data for values of "VI" equal to 1.0%, 3.0% and 7.0%. However, the program can easily be

altered for any given situation.

A page of output from this particular program is also included. Note in the first group of numbers of the print-out, the value of "VI" appears as -0.01. This is not to say that the interest rate was a negative 1.0%. The -0.01 is used for the purposes of incrementing the interest rate in the program and where -0.01 appears in the output the true value is actually zero.

2. Flow Diagram

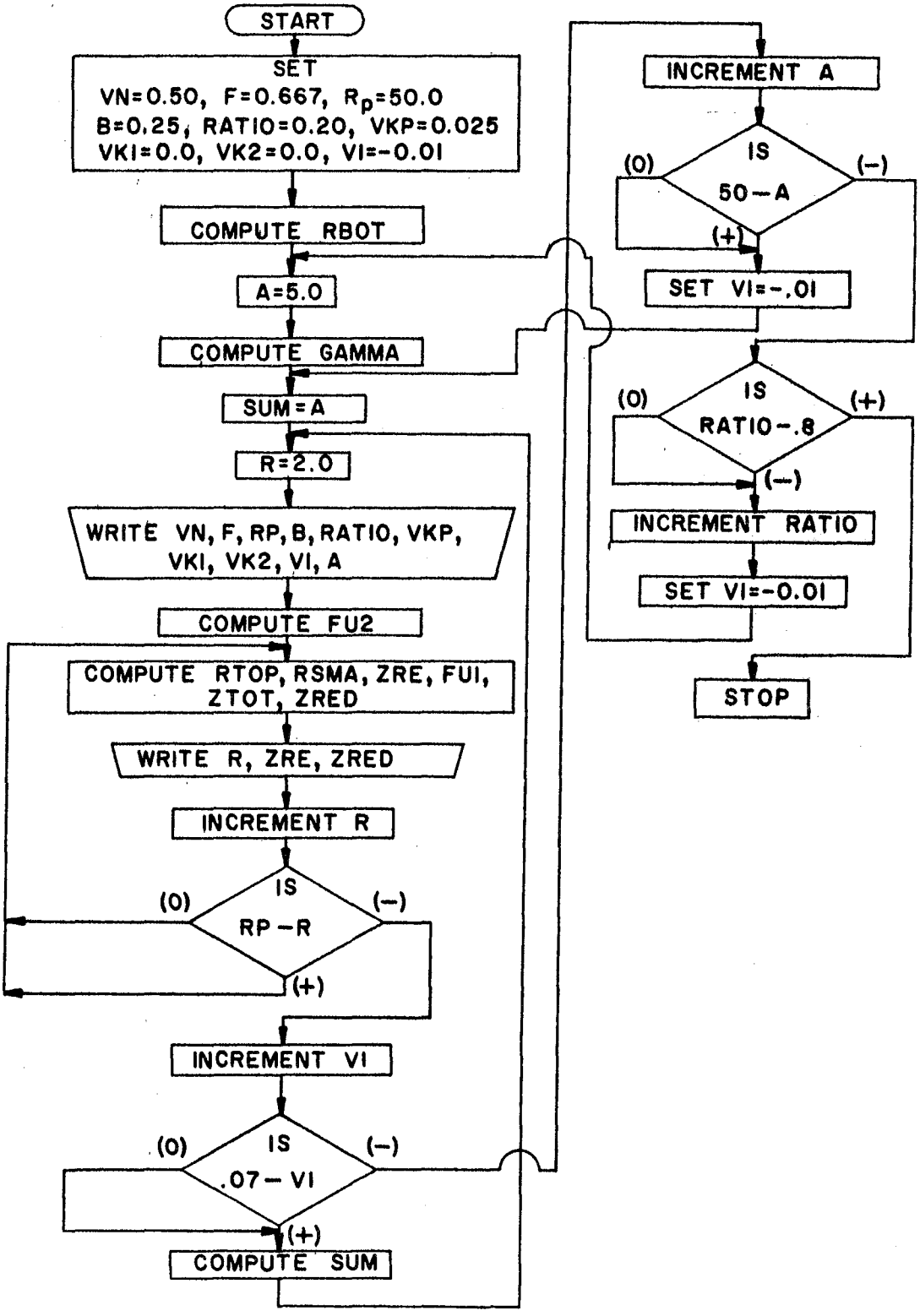

3. Fortran IV Listing

```
$IBFTC MAIN
      WRITE(6,52)
      VN = 0.50
      F = 0.66667
      RP = 50.0
      B=0.25
      RATIO = 0.20
      VKP=0.025
      VK1 = 0.0
      VK2 = 0.0
      VI = -0.01
      RBOT = -ALOG((RP-1.)/RP)
   10 A = 5.0
      GAMMA = -3.54/ALOG(RATIO)
    1 SUM = A
    2 R = 2.0
      WRITE(6,50)VN,F,RP,B,RATIO,VKP,VK1,VK2,A,VI
      FU2 = 1. + (1./RP)*B*SUM + VKP*SUM - VK2*(1./((1.+VI)**A))
    3 RTOP = -ALOG((R-1.)/R)
      RSMA = (RTOP/RBOT)**(-2.*F/GAMMA)
      ZRE=100.*(1.-RSMA)
      FU1 = 1. + (1./R)*B*SUM + (1./((RSMA)**VN))*VKP*SUM - VK1*(1./((1.
     1+ VI)**A))
      ZTOT = 100.*((RSMA)**VN)*(FU1/FU2)
      ZRED = (100. - ZTOT)
      WRITE(6,51)R,ZRE,ZRED
      R = R + 2.
      IF(RP - R)4,3,3
    4 VI = VI + 0.02
      IF(.07 - VI)6,5,5
    5 SUM = (((1.+VI)**A)-1.)/(VI*(1.+VI)**A)
      GO TO 2
```

```
 6 A = A + 5.0
   IF(50.-A)8,7,7
 7 VI = -0.01
   GO TO 1
 8 IF(RATIC-.8)9,9,11
 9 RATIO=RATIO+0.2
   VI=-0.01
   GO TO 10
50 FORMAT(//20X,3HVN=,F4.1,3X,2HF=,F4.2,3X,3HRP=,F5.1,3X,2HB=,F4.2,
  13X,6HRATIO=,F3.1,3X,4HVKP=,F6.3/20X,4HVK1=,F4.1,3X,4HVK2=,F4.1,3X,
  22HA=,F5.1,3X,3HVI=,F5.2,//)
51 FORMAT(10X,2HR=,F7.3,15X,5HZRE =,F9.3,15X,5HZRED=,F9.3)
52 FORMAT(1H1)
11 STOP
   END
```

4. Sample Output

```
          VN= 0.5    F=0.67    RP= 50.0    B=0.25    RATIO=0.2    VKP= 0.025
          VK1= 0.    VK2= 0.     A=  5.0    VI=-0.01

R=   2.000          ZRE =   88.272          ZRED=   40.738
R=   4.000          ZRE =   80.013          ZRED=   38.106
R=   6.000          ZRE =   73.647          ZRED=   35.192
R=   8.000          ZRE =   68.172          ZRED=   32.407
R=  10.000          ZRE =   63.255          ZRED=   29.831
R=  12.000          ZRE =   58.736          ZRED=   27.454
R=  14.000          ZRE =   54.519          ZRED=   25.251
R=  16.000          ZRE =   50.543          ZRED=   23.200
R=  18.000          ZRE =   46.765          ZRED=   21.279
R=  20.000          ZRE =   43.154          ZRED=   19.471
R=  22.000          ZRE =   39.686          ZRED=   17.761
R=  24.000          ZRE =   36.343          ZRED=   16.139
R=  26.000          ZRE =   33.111          ZRED=   14.594
R=  28.000          ZRE =   29.978          ZRED=   13.117
R=  30.000          ZRE =   26.933          ZRED=   11.704
R=  32.000          ZRE =   23.968          ZRED=   10.346
R=  34.000          ZRE =   21.077          ZRED=    9.039
R=  36.000          ZRE =   18.253          ZRED=    7.780
R=  38.000          ZRE =   15.491          ZRED=    6.563
R=  40.000          ZRE =   12.787          ZRED=    5.386
R=  42.000          ZRE =   10.136          ZRED=    4.245
R=  44.000          ZRE =    7.534          ZRED=    3.138
R=  46.000          ZRE =    4.980          ZRED=    2.063
R=  48.000          ZRE =    2.469          ZRED=    1.018
R=  50.000          ZRE =    0.             ZRED=    0.
```